August 2016

Synthesis of Hydrofluorocarbon Ethers and New Amorphous Fluoropolymers with Cyclic Fluorocarbon Ether Units

Xiaolin Liu
Clemson University, xliu6@g.clemson.edu

SYNTHESIS OF HYDROFLUOROCARBON ETHERS AND NEW AMORPHOUS FLUOROPOLYMERS WITH CYCLIC FLUOROCARBON ETHER UNITS

A Dissertation
Presented to
the Graduate School of
Clemson University

In Partial Fulfillment
of the Requirements for the Degree
Doctor of Philosophy
Materials Science and Engineering

---

by
Xiaolin Liu
August 2016

Accepted by:
Joseph S. Thrasher, Ph.D., Committee Chair
Marek W. Urban, Ph.D.
Gary C. Lickfield, Ph.D.
Stephen H. Foulger, Ph.D.

ABSTRACT

The main focus of this work is the synthesis of hydrofluorocarbon ethers (HFEs). New synthetic methods and new HFEs were successfully developed. In Chapter 1, new HFEs were synthesized with tetrafluoroethylene (CF_2=CF_2, TFE) as new engineered fluids. The fluorinated olefins' addition to alcohols is a more conventional approach to HFEs, and in our group a synthetic method consists of three steps was attempted:

a. radical addition of tetrafluoroethylene (TFE) to 2,2-dimethyl-1,3-dioxolane compound; b. hydrolysis of the fluorinated dioxolane compound to make a diol; c. TFE addition to the diol under ionic condition.

The following two chapters cover the synthesis of several other HFEs with a strong Lewis acid. Especially the one-step synthesis of sevoflurane starting from hexafluoroisopropanol (HFIP) and difluoromethane (R32) with SbF_5 as catalyst gives 95+% yield which is very attractive to industry, meanwhile the catalysts can be recycled for multiple reactions. Several other existing or new HFEs were also synthesized by using the same method. The products were identified with NMR spectroscopy and gas chromatography/mass spectrometry.

Another cyclic hydrofluorocarbon ether compound 2,2,5,5-tetrafluoro-2,5-dihydrofuran (M1) was synthesized as a monomer for the development of new amorphous fluoropolymers. M1 has been successfully copolymerized with several perfluoro olefins including CF_2=CF_2 (TFE), CF_3CF=CF_2 (HFP), and SF_5CF=CF_2 (MSF_5). And the materials were characterized and analyzed by NMR spectroscopy, attenuated total reflectance-infrared spectroscopy (ATR-IR), thermalgravimetric analysis/mass spectrometry

(TGA/MS), scanning electron microscopy/energy dispersive X-ray spectroscopy (SEM/EDX), gel permeation chromatography (GPC) and static light scattering (SLS).

Along the work of the polymerization of M1, more chemistry has been explored on M1 and several crystal structures were solved, which will be further discussed in Chapter 5 and Chapter 6. In the crystal structures, a variety of short distance contacts of Ag---Ag, Ag---O, H---F, O---F, O-Cl, and F---F, were observed. Two other bissulfonyl chloride compounds were synthesized and in the structure of these two -SO_2Cl containing molecules, Cl---O and F---F short contacts were observed and considered as halogen bonding.

DEDICATION

I would like to dedicate this work to my mother Chunxia Tian, my father Jingde Liu, my brother Xiangyu Liu and my husband Steven Belina for their support and love in my life.

ACKNOWLEDGEMENTS

It is very fortunate for me to have Dr. Joseph Thrasher as my academic advisor that I am able to grow up to an independent, initiative and passionate researcher. I would also like to thank Dr. Andrej Matsnev for his advisement and encouragement during this course of work as a scientist and a friend.

I must thank Dr. Colin McMillen, Dr. Haijun Qian, Dr. Stephen Foulger, Dr. Marek Urban, Dr. Gary Lickfield, Dr. Bill Bauknight, Dr. Richard Fernandez, and Dr. Changqing Lu for their help and advice on this work. I must also thank Dr. Christopher Huebner for the help with TGA/MS, and my coworkers Mingzhe Jiang for his assistance with SLS measurement, Chen Liu and Siyan Qing for the help with part of the synthetic work, and Longyu Hu for the help with AFM analysis.

TABLE OF CONTENTS

Page

Table of Contents (Continued)

Page

Table of Contents (Continued)

Page

Table of Contents (Continued)

Page

Table of Contents (Continued)

Page

Table of Contents (Continued)

Page

Table of Contents (Continued)

Page

Table of Contents (Continued)

Page

LIST OF TABLES

Page

List of Tables (Continued)

Page

LIST OF FIGURES

Page

List of Figures (Continued)

Page

List of Figures (Continued)

Page

List of Figures (Continued)

Page

List of Figures (Continued)

Page

List of Figures (Continued)

Page

LIST OF SCHEMES

Page

LIST OF REPORTS

Page

ABBREVIATIONS

3M	3M Company
3P	Bis(pentafluoropropionyl) Peroxide
AIBN	Azobisisobutyronitrile
ATR-IR	Attenuated Total Reflectance
BPO	Benzoyl Peroxide
C4	Perfluoro-1,4-butanedisulfonyl Dichloride
C6	Perfluoro-1,6-hexanedisulfonyl Dichloride
CFC	chlorofluorocarbon
DMSO	Dimethyl sulfoxide
DMF	Dimethyl formamide
DPO	Disilver Perfluoro-oxodiacetate
DPO-H2O	Crystal of DPO Prepared from H2O
DPO-THF	Crystal of DPO Prepared from THF
DSC	Differential Scanning Calorimetry

DTBP	Di-tert-Butyl Peroxide
DuPont	E. I. du Pont de Nemours and Company
ETFE	poly(ethene-co-tetrafluoroethene)
Formal	1,1,1,3,3,3-hexafluoro-2-[[2,2,2-trifluoro-1-(trifluoromethyl) ethoxy]methoxy]-propane
GC-MS	Gas Chromatography-Mass Spectroscopy
GPC	Gel Permeation Chromatography
HCFC	Hydrochlorofluorocarbon
HFC	Hydrofluorocarbon Ether
HFC-134a	1,1,1,2-Tetrafluoroethane, CF3CH2F
HFC-227ea	1,1,1,2,3,3,3-Heptafluoropropane, CF3CFHCF2
HFE	Hydrofluorocarbon Ether
HFIP	Hexafluoroisopropanol
HFMOP	1,1,1,3,3,3-Hexafluoro-2-methoxy-propane
HFP	Hexafluoropropene
M1	2,2,5,5-Tetrafluoro-2,5-Dihydrofuran
MSF5	Trifluorovinylsulfur Pentafluoride, SF5CF=CF2

Poly(M1-*co*-HFP)	Copolymer of M1 and HFP
Poly(M1-co-MSF_5)	Copolymer of M1 and MSF_5
Poly(M1-*co*-TFE)	Copolymer of M1 and TFE
MALDI-TOF	Matrix-assisted Laser Desorption-Time of Fly
NMR	Nuclear Magnetic Rasonance
PCTFE	Polychlorotrifluoroethylene
PDD	Perfluoro-2,2-dimethyl-1,3-dioxole
PFA	Perfluoroalkoxy Alkane
PFC	Perfluorocarbon
PFCB	Perfluorocyclobutyl Polymer
POA	Perfluoro-oxodiacetic Acid
PTFE	Polytetrafluoroethylene
PVDF	Polyvinylidene
R32	Difluoromethane
SDS	Safety Data Sheet
SEM/EDX	Scanning Electron Microscopy/Energy-dispersive X-ray spectroscopy

SLS	Static Light Scattering
SS	Stainless Steel
STA	Silver Trifluoroacetate
TFE	Tetrafluoroethylene
TGA	Thermal Gravitational Analysis
TGA/MS	Thermal Gravitational Analysis/Mass Spectroscopy
UV	Ultraviolet
UV/vis	Ultraviolet-visible spectroscopy
XRD	X-ray Diffraction

CHAPTER ONE

INTRODUCTION

1.1 INTRODUCTION

Hydrofluorocarbon ethers (HFEs) are a family of compound having a general but not limited formula of R_f-O-R_h, in which R_f is a perfluorocarbon segment and R_h is a hydrocarbon segment. In recent years, hydrofluoro ethers (HFEs) have largely attracted the attention of researchers' due to their potential of being replacement of ozone depleting and/or global warming substances like chlorofluorocarbons (CFCs), hydrochlorofluoro carbons (HCFCs), hydrofluorocarbons (HFCs), and perfluorocarbons (PFCs).[1] The introduction of an oxygen atom into the structure to segregate the perfluorocarbon and hydrocarbon segments in the molecules largely reduces the atmospheric lifetimes of the materials, thereby yielding a low global warming potential, while maintaining the desired properties of inflammability, low toxicity, volatility, thermal stability and chemical inertness.[2] In recent years, they have been widely used in pharmaceuticals,[3] Li battery co-solvents,[4] and replacements for CFCs, HCFCs, HFCs, and PFCs in various industries.[5] More alternatives and new synthetic methods still need to be developed to improve the performance of every aspect and enrich the HFE family.

The synthesis methods of HFEs used so far are mainly the addition of fluoroolefins to alcohols,[6] alkylation of acyl fluorides,[7] and other molecular modifications. Recently an interesting work by Friesen revealed an unexpected degradation of HFE materials followed by alkylation of tertiary amines. [8]

1.2 HYDROFLUOROCARBON ETHERS (HFEs) AS ENGINEERED FLUIDS

The 3M Company (3M) has developed several HFEs with the commercial name Novec™ Engineered Fluids: Novec™ 7100 is $(CF_3)_2CFCF_2OCH_3/CF_3CF_2CF_2CF_2OCH_3$; Novec™ 7200 is $CF_3)_2CFCF_2OC_2H_5$/ $CF_3CF_2CF_2CF_2OC_2H_5$; Novec™ 7500 is $CF_3CF_2CF_2CF(OC_2H_5)CF(CF_3)_2$ and Novec™ 7600 is $CF_3CHFCF_2CH(CH_3)OCF_2CHFCF_3$. Their boiling points range from 61 to 131 °C. Both a wider temperature range of boiling points for HFEs and more alternatives of zero toxicity are needed. Especially new HFEs containing the $–CF_2H$ group are expected to have shorter or more limited atmospheric lifetimes, which is highly preferred according to the study on α,ω-dialkoxyfluoropolyethers by Wu and Navarrini.[7a, 9]

1.3 PHARMACUTICAL APPLICATION OF HFEs

The thermal stability and physical properties of alkanes and ethers were largely altered or improved by substituting hydrogen with fluorine in the molecules, and a class of fluorinated alkanes and ethers were first tested out in several industrial laboratories.[10] Several of these classes of compounds were discovered to have an anesthetic effect in mammals.[11] In clinic practice, more characteristics are required such as low toxicity, solubility in blood and tissue, speed of action, recover time, stability to the absorbents etc.[12] The fluorinated ethers enflurane ($ClHFCCF_2OCHF_2$, 2-chloro-1,1,2-trifluoroethyl-difluoromethyl ether), isoflurane ($CF_3CHClOCHF_2$, 1-chloro-2,2,2-trifluoroethyl difluoromethyl ether), sevoflurane [$(CF_3)_2CHOCH_2F$, fluoromethyl 2,2,2-trifluoro-1-trifluoromethyl ethyl ether] and desflurane ($CF_3CHFOCHF_2$, 1,2,2,2-tetrafluoroethyl difluoromethyl ether) are currently in clinical practice after hundreds of fluorinated

compounds have been tested for this application.[13] Sevoflurane is one of the most widely used anesthetics, and an exclusive study of the synthetic methods to this compound has been carried out. One industrial synthesis consists of three steps starting with hexafluoroisopropanol (HFIP) (Scheme 1.1).[11, 14] Easier and more economic synthetic methods are always attractive to both academic and industry.

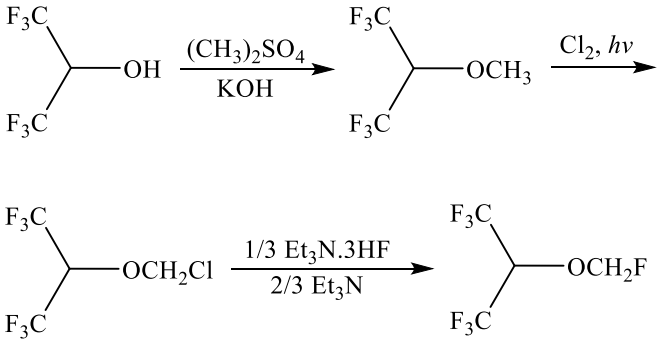

Scheme 1.1. Industrial synthesis of sevoflurane

Other methods were also developed over time,[14a, 15] and many other sevoflurane derivatives and reactions were also prepared in order to enrich this catalog of materials.[16]

1.4 FLUOROCARBONETHER LINKAGE IN FLUOROPOLYMERS

Not only are the small molecules of HFEs attractive, the fluoropolyethers have also been developed as low temperature fluids, coating materials, sealants etc.[17] The flexibility of fluoropolyalkanes is largely improved by the introduction of ether linkages in the structure. Another special type of perfluoropolymers with ether linkages exists called amorphous fluoropolymers, which have outstanding properties.

The class of amorphous fluoropolyethers usually consist of a cyclic unit and a linear unit on the backbone of the molecular chain, which has comparable thermal and chemical stability to other fluoropolymers such as poly(tetrafluoroethylene) (PTFE), poly(ethylene-*co*-tetrafluoroethylene) ETFE, perfluoroalkoxy resins (PFA), poly(chlorotrifluoroethylene) (PCTFE), and poly(vinylidene fluoride) (PVDF). In addition, these polymers have unique properties like intrinsic micro-porosity, transparency at UV range, low refractive index, reasonable solubility in fluorinated organic solvents (e.g., perfluorohexane, perfluorobenzene, perfluorooctane) at room temperature, and low dielectric constant. The properties of these materials make them suitable for many applications such as gas separation, microlithography, fiber cladding, anti-reflective coating, and hydrophobic coating or mixing.[18]

The first class of amorphous fluoropolymers was developed in the 1970's-1980's by DuPont and was called Teflon® AF,[19] which is a copolymer of TFE and perfluoro-2,2-dimethyl-1,3-dioxole (PDD).[20] Asahi Glass also prepared Cytop®[21] at the same time, and Solvay Solexis patented Hyflon® AD in the 1990's (see **Error! Reference source not found.**). [22]

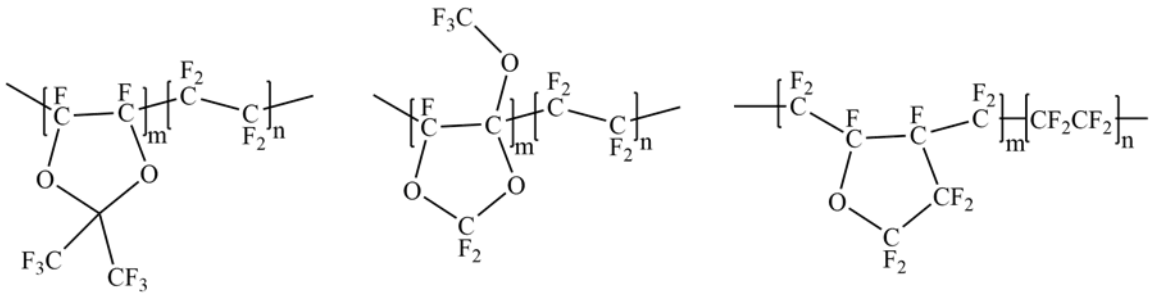

Figure 1. 1 Commercial amorphous fluoropolymers.

To enrich and further develop the family of amorphous fluoropolymer, as well as reduce the environmental impact of solvent usage in the polymerization, many more monomers and new synthesis methods have been studied. Okamoto and his coworkers synthesized several new perfluoro dioxolanes and their polymers.[23]

The perfluoro dioxoles were studied mostly by DuPont as researchers there developed the first materials, and new synthetic routes to such monomers were also developed by Navarrini.[24] To reduce the cost of the polymerization in organic solvent and the corresponding environmental effects, supercritical CO_2 was used in the polymerization as an environmentally friendly solvent.[25] Even though such polymers have excellent properties, they have fatal drawbacks because they are extremely expensive to synthesize and their solubility is very limited, as they only dissolve in fluorinated solvents, which are also quite expensive to use. To improve the solubility of amorphous fluoropolymers, hydrocarbon cyclic units were introduced into the structure. The resulting copolymers can also be dissolved in regular organic solvents.[26] Currently, partially fluorinated amorphous fluoropolymers are still under development. Another type of amorphous fluoropolymer

that stands out is perfluorocyclobutyl polymer (PFCB) that is made from aromatic trifluorovinyl ether monomers by thermal cyclopolymerization.[27]

1.5 SHORT CONTACTS INVOLVED IN F AND SILVER ATOMS

During the work, short distance interactions of halogen-halogen (Cl, F), halogen-oxygen, and silver-silver atoms were also observed and studied in several crystal structures obtained.

A variety of Ag---Ag contacts have been observed in the past few decades. Not only do argentophilic interactions exist between pairs of silver atoms, but they are also presented in multinuclear units, chains, or even layers.[28] Silver (I) compounds have been used to construct various supramolecular structures, especially Ag (I) organics have shown a wide variety of structures of 2D or 3D networks.[29]

Silver (I) carboxylates often form oligomers and give interesting long range structures that are complexed with donor ligands.[30] Most of the time, the supramolecular isomerism have solvents in the structures and the solvents used can be good tools to manipulate the packing of the structures.[31] Li and Du reviewed the role of solvents in supramolecular systems in 2011.[32]

Silver trifluoroacetate is a commonly used building block in the study of Ag networks or complex formations. The presence of silver atoms often shows argentophilic

phenomena and helps with supramolecular network assembly in crystal structures.[33] Lots of research has been carried out regarding the organosilver (I) framework, and interestingly the single crystal structure of silver trifluoroacetae has long been left without being properly solved. In 1972, the single crystal of $CF_3C(O)OAg$ was solved, and unfortunately, a more detailed report was not filed.[34] We revised the work and prepared specimen for single crystal X-ray analysis.

In terms of halogen-halogen interactions, Desiraju, et al. recommended a definition of the halogen bonding (XB) in 2013, and it states that: '*A halogen bond occurs when there is evidence of a net attractive interaction between an electrophilic region associated with a halogen atom in a molecular entity and a nucleophilic region in another, or the same, molecular entity.*'[35].

The reason why XB attracts more and more attention from scientists is the wide growing range applications in pharmaceutical chemistry and self-assembling materials[36], especially when fluorine is introduced into the organic molecules, the structures and the chemical and biological properties can be significantly altered when compared to the non-fluorinated molecules[37]. Fluorine is known as the most electronegative element having the least polarizability among the halogen atom, and whether it can be a XB donor or not has been long debated[38]. In the case of H---F contacts, it has been widely accepted as a type of hydrogen bonding;[39] however, in XB several theories exist to explain the formation mechanism of XB among which σ-hole theory is most widely used. The halogen atom X acts as electrophilic XB donor to the nucleophile XB acceptor (lewis base), and on the outmost side of the halogen along the axis, a positive electrostatic potential area exists,

which is termed as σ-hole[40]. The electrostatic potential is considered as the driving force of the XB formation along with some contribution of induction and dispersion interactions[41].

The X···O, X···N, X···S, X···Se interactions were discussed long ago, where X =F, Cl, Br, I. It has been shown that they are electrostatic in nature[42]. The halogen-halogen (X···X) bonding is classified as a special type of halogen bonding. The nature of X···X has been believed to be specific attractive forces, however, the debating never stopped[43]. In bihalogens (X_a···X_a) or hetero-halogens (X_a···X_b) bonding, one halogen atom acts as halogen bonding donor having a positive electrostatic potential area or σ-hole interacting with the electron rich area on the other halogen atom as halogen bonding acceptor[44]. Generally the more polarizable the halogen is, the stronger the halogen bonding is, and therefore the strength of XB increases in the order F < Cl < Br < I. In the case of fluorine, the interaction is very weak compared to other XBs[38a, 45].

In the geometry of X···X, the interaction is very weak but highly directional. There are mainly two types, type I and type II contacts (Error! Reference source not found.)[42b, HYPERLINK \l "_ENREF_91" \o "Ramasubbu, 1985 #12" 46]. The cause of the geometries has been believed to be their chemical difference,[47] and both experimental and some computational studies have been carried out based on the strong analogies between XB and corresponding hydrogen bonding[39b, 41].

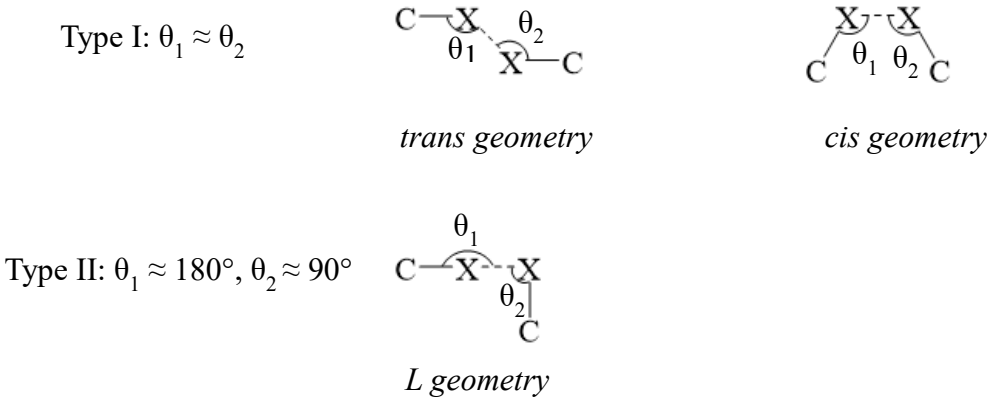

Figure 1. 2 Type I and type II halogen---halogen bonding.

Two perfluorinated disulfonyl dichloride compounds were synthesized for fuel cell applications. Crystals of good quality were obtained and analyzed by single crystal X-ray and short distance F---F and Cl---O interactions were observed in the structures.

1.6 REFERENCES

1. (a) WMO (World Meterorological Organization), *Scientific Assessment of Ozone Depletion: 2010*, Global Ozone Research and Monitoring Project-Report No. 52, p 516, Geneva, Switzerland, 2011; (b) Burkholder, J. B.; Cox, R. A.; Ravishankara, A. R. Atmospheric Degradation of Ozone Depleting Substances, Their Substitutes, and Related Species. *Chem. Rev.* **2015**, *115*, 3704-59; (c) Good, D. A.; Francisco, J. S. Atmospheric Chemistry of Alternative Fuels and Alternative Chlorofluorocarbons. *Chem. Rev.* **2003**, *103*, 4999-5023.
2. (a) Owens, J. G. Low GWP Alternatives to HFCs and PFCs; in Proceedings of the 1999 Taipei International Conference on Atmospheric Protection: Taipei, Taiwan,

1999; also available at Owens, J. G. Low GWP Alternative to HFCs and PFCs, 3M Specialty Materials, St. Paul, MN USA. http://solutions.3maustria.at/3MContentRetrievalAPI/BlobServlet?lmd=1310648569000&assetId=1273689616858&assetType=MMM_Image&blobAttribute=ImageFile; (b) Tsai, W. T. Environmental risk assessment of hydrofluoroethers (HFEs). *J. Hazard. Mater.* **2005**, *119*, 69-78; (c) Sekiya, A.; Misaki, S. The Potential of Hydrofluoroethers to Replace CFCs, HCFCs and PFCs. *J. Fluorine Chem.* **2000**, *101*, 215-221.

3. Gilbert, E. E.; Veldhuis, B. Hexafluoroisopropyl Ethers as Anesthetics. U.S. Patent 3,346,448, Oct. 10, 1967.

4. (a) Achiha, T.; Nakajima, T.; Ohzawa, Y.; Koh, M.; Yamauchi, A.; Kagawa, M.; Aoyama, H. Electrochemical Behavior of Nonflammable Organo-Fluorine Compounds for Lithium Ion Batteries. *J. Electrochem. Soc.* **2009**, *156*, A483-A488; (b) Lamanna, W. M.; Bulinski, M. J.; Castello, M. G.; Dahn, J. R.; Flynn, R. M.; Wang, Y.; Li, J.; Moshurchak, L. Fluorinated Compounds for Use in Lithium Battery Electrolytes. U.S. Patent 8,435,679 B2, May 7, 2013; (c) Nagasubramanian, G.; Fenton, K. Reducing Li-ion safety hazards through use of non-flammable solvents and recent work at Sandia National Laboratories. *Electrochimica. Acta* **2013**, *101*, 3-10.

5. Drakesmith, F. G.; Powell, R. L.; Chambers, R. D.; Grievson, B. Process for Fluorinating Ethers. U.S. Patent 4,736,045 A, Apr. 5, 1988.

6. (a) Crawford, J. W. C. Preparation of Alkyl 1,1,2,2-Tetrafluoroethyl Ethers. *J. Chem. Soc. C* **1967**, 2395-2396; (b) Coffman, D. D.; Raasch, M. S.; Rigby, G. W.; Barrick, P. L.; Hanford, W. E. Addition Reactions of Tetrafluoroethylene. *J. Org. Chem.* **1949**, *14*, 747-753.

7. (a) Wu, M.; Navarrini, W.; Avataneo, M.; Venturini, F.; Sansotera, M.; Gola, M. α,ω-Dialkoxyfluoropolyethers a Promising Class of Hydrofluoroether (HFE). *Chemistry Today* **2011**, *29*, 67-71; (b) Sheppard, W. A. α-Fluorinated Ethers. I. Aryl Fluoroalkyl Ethers. *J. Org. Chem.* **1964**, *29*, 1-11; (c) Aldrich, P. E.; Sheppard, W. A. α-Fluorinated Ethers. II. Alkyl Fluoroalkyl Ethers. *J. Org. Chem.* **1964**, *29*, 11-15.

8. Jelier, B. J.; Howell, J. L.; Montgomery, C. D.; Leznoff, D. B.; Friesen, C. M. A convenient route to tetraalkylammonium perfluoroalkoxides from hydrofluoroethers. *Angew. Chem.* **2015**, *54*, 2945-2949.

9. Wu, M.; Navarrini, W.; Spataro, G.; Venturini, F.; Sansotera, M. An Environmentally Friendly Class of Fluoropolyether: α,ω-Dialkoxyfluoropolyethers. *Appl. Sci.* **2012**, *2*, 351-367.

10. (a) Jones, W. G. M. Inhalation Anesthetics of the Organofluorine Class. In *Preparation, Properties, and Industrial Applications of Organofluorine Compounds;* Bank, R. E., Ed.; Ellis Horwood Linited: Chichester, 1982; pp 157-192; (b) Halpern, D. F. Fluorinated Inhalation Anesthetics. In *Organofluorine Chemistry: Principles and Commercial Applications*; Banks, R. E.; Smart, B. E.; Tatlow, J. C., Eds.; Plenum Press: New York, 1994; pp 543-554.

11. Regan, B. M.; Long, J. C. Method of Anesthesia. U.S. Patent 3,683,092, Aug 8, 1972.

12. Eger, E. I., II. Characteristics of Anesthetic Agents Used for Induction and Maintenance of General Anesthesia. *Am. J. Health Syst. Pharm.* **2004,** *61 (Suppl. 4), S3-S10.*

13. Terrell, R. C. The Invention and Development of Enflurane, Isoflurane, Sevoflurane, and Desfluran. *Anesthesiology* **2008,** *108*, 531-533.

14. (a) Kudzma, L. V.; Huang, C. G.; Lessor, R. A.; Rozov, L. A.; Afrin, S.; Kallashi, F.; McCutcheon, C.; Ramig, K. Diisopropylethylamine Mono (Hydrogen Fluoride) for Nueclophilic Fluorination of Sensitive Substrates: Synthesis of Sevoflurane. *J. Fluorine Chem.* **2001,** *111*, 11-16; (b) Croix, L. S. Fluorinated Isopropyl Derivatives. U.S. Patent 3,911,024, Oct. 7, 1975.

15. (a) Prakash, G. K. S.; Ledneczki, I.; Chacko, S.; Olah, G. A. Direct Electrophilic Monofluoromethylation. *Org. Lett.* **2008,** *10*, 557-560; (b) Ramakrishna, K.; Behme, C.; Schure, R. M.; Bieniarz, C. A Safe and Efficient Process for the Synthesis of the Inhalation Anesthetic Sevoflurane. *Org. Process Res. Dev.* **2000,** *4*, 581−584.

16. (a) Ramig, K. Synthesis and Reactions of Fluoroether Anesthetics. *Synthesis* **2002,** *17*, 2627–2631; (b) Rozov, L. A.; Lessor, R. A.; Kudzma, L. V.; Ramig, K. The Fluoromethyl Ether Sevoflurane as a Fluoride Source in Halogen-Exchange Reactions. *J. Fluorine Chem.* **1998,** *88*, 51-54.

17. (a) Howell, J. L.; Shtarov, A. B.; Thrasher, J. S.; Waterfeld, A.; Murata, K.; Friesen, C. M.; Pérez, E. W. Synthesis of new linear perfluoroalkyl polyethers starting from diols and tetrafluoroethylene. *Lubr. Sci.* **2010,** *23*, 61-80; (b) Hanford, W. E.; Rigby, G. W. Polyfluoro Organic Ethers and the Preparation. U.S. Patent 2,469,274, Oct. 15, 1946; (c) Koshikawa, H.; Tarumi, Y.; Shiono, M. Perfluoroether elastomer for wide fluid and temperature capabilities. *Sealing Tech.* **2006,** *2006*, 7-12; (d) Woo, E. J.; Lehman, G. K. Perfluoroether Release Coatings for Organic Photoreceptors. U.S. Patent 5,723,242, Mar. 3, 1998; (e) Jones, W. R. J.; Bierschenk, T. R.; Juhlke, T. J.; Kawa, H.; Lagow, R. J. The Preparation of New Perfluoro Ether Fluids Exhibiting Excellent Thermal-Oxidative Stabilities. *Ind. Eng. Chem. Res.* **1988,** *27*, 1497-1502.

18. (a) Prabhakar, R. S.; Freeman, B. D.; Roman, I. Gas and Vapor Sorption and Permeation in Poly(2,2,4-trifluoro-5-trifluoromethoxy-1,3-dioxole-co-tetrafluoroethylene). *Macromolecules* **2004,** *37*, 7688-7697; (b) Jesorka, A.; Shaali, M. Lithographic Pattern Development Process for Amorphous Fluoropolymer. U.S. Patent Appl. 20140065551 A1, Mar. 6, 2014; (c) Khang, D.; Lee, H. H. Sub-100 nm Patterning with an Amorphous Fluoropolymer Mold. *Langmuir* **2004,** *20*, 2445-2448.

19. Hung, M.-H.; Resnick, P. R. Thermal Rearrangement of Fluorinated Dioxoles. *J. Am. Chem. Soc.* **1990,** *112*, 9672-9674.

20. (a) Teng, H. Overview of the Development of the Fluoropolymer Industry. *Appl. Sci.* **2012,** *2*, 496-512; (b) Resnick, P. R. Polymers of Fluorinated Dioxoles. U.S. Patent 3,978,030, Aug. 31, 1976; (c) Squire, E. N. Perfluorodioxole and Its Polymers. U.S. Patent 4,399,264 A, Aug. 16, 1983; (d) Squire, E. N. Perfluorodioxole and Its Polymers. U.S. Patent 4,558,141, Dec. 10, 1985..

21. Ino, T.; Shinohara, T.; Sakane, Y. Process for Molding Amorphous Perfluororesin and Optical Elements. EP Patent 2,199,051A1, Jun. 23, 2010.

22. Navarrini, W.; Tortelli, V.; Colaianna, P.; Abusleme, J. A. Perfluorodioxoles, the Preparation Process Thereof, and Homopolymers and Copolymers Therefrom. U.S. Patent 5,646,223 A, Jul. 8, 1997.

23. (a) Liu, W.; Koike, Y.; Okamoto, Y. Synthesis and Radical Polymerization of Perfluoro-2-methylene-1,3-dioxolanes. *Macromolecules* **2005,** *38*, 9466-9473; (b) Yang, Y.; Mikeš, F.; Yang, L.; Liu, W.; Koike, Y.; Okamoto, Y. Investigation of homopolymerization rate of perfluoro-4,5-substituted-2-methylene-1,3-dioxolane derivatives and properties of the polymers. *J. Fluorine Chem.* **2006,** *127*, 277-281.

24. (a) Navarrini, W.; Bragante, L. Process for the Dehalogenation of 1,3-Dioxolanes. U.S. Patent 5,245,054 A, Sep. 14, 1993; (b) Navarrini, W.; Fontana, S. Process for Preparing 1,3-Dioxoles. U.S. Patent 5,296,617 A, Mar. 22, 1994; (c) Russo, A.; Navarrini, W. Perfluoro-4-methyl-1,3-dioxole: a new monomer for high-Tg amorphous fluoropolymers. *J. Fluorine Chem.* **2004,** *125,* 73-78; (d) Avataneo, M.; Navarrini, W.; De Patto, U.; Marchionni, G. Novel perfluoropolyethers containing 2,2,4-trifluoro-5-trifluoromethoxy-1,3-dioxole blocks: synthesis and characterization. *J. Fluorine Chem.* **2009,** *130,* 933-937.

25. (a) Romack, T. J.; DeSimone, J. M. Synthesis of Tetrafluoroethylene-Based, Nonaqueous Fluoropolymers in Supercritical Carbon Dioxide. *Macromolecules* **1995,** *28,* 8429-8431; (b) Kendall, J. L.; Canelas, D. A.; Young, J. L.; DeSimone, J. M. Polymerizations in Supercritical Carbon Dioxide. *Chem. Rev.* **1999,** *99,* 543-563; (c) Michel, U.; Resnick, P.; Kipp, B.; DeSimone, J. M. Copolymerization of Tetrafluoroethylene and 2,2-Bis(trifluoromethyl)-4,5-difluoro-1,3-dioxole in Supercritical Carbon Dioxide. *Macromolecules* **2003,** *36,* 7107-7113; (d) Wood, C. D.; Michel, U.; Rolland, J. P.; DeSimone, J. M. New fluoropolymer materials. *J. Fluorine Chem.* **2004,** *125,* 1671-1676.

26. Feiring, A. E.; Crawford, M. K.; Farnham, W. B.; Feldman, J.; French, R. H.; Junk, C. P.; Leffew, K. W.; Petrov, V. A.; Qiu, W.; Schadt, F. L., III; Tran, H. V.; Zumsteg, F. C. New Amorphous Fluoropolymers of Tetrafluoroethylene with Fluorinated and Non-Fluorinated Tricyclononenes. Semiconductor Photoresists for Imaging at 157 and 193 nm. *Macromolecules* **2006,** *39,* 3252-3261.

27. Smith, D. W. Jr.; Babb, D. A.; Shah, H. V.; Hoeglund, A.; Traiphol, R.; Perahia, D.; Boone, H. W.; Langhoff, C.; Radler, M. Perfluorocyclobutane (PFCB) polyaryl ethers: verstatile coatings materials. *J. Fluorine Chem.* **2000,** *104*, 109-117.

28. Schmidbaur, H.; Schier, A. Argentophilic interactions. *Angew. Chem. Int. Ed.* **2015,** *54*, 746-784.

29. (a) Hau, S. C.; Tam, D. Y.; Mak, T. C. Organosilver(I) framework assembly with trifluoroacetate and enediyne-functionalized alicycles. *Acta Crystallogr., Sect. B: Struct. Sci.* **2014,** *70*, 37-46; (b) Crundwell, G.; Cantalupo, S.; Foss, P. D. C.; McBurney, B.; Kopp, K.; Westcott, B. L.; Updegraff Iii, J.; Zeller, M.; Hunter, A. D. Molecular and electronic structure of several 2,3-dithienylquinoxalines and their 2:1 complexes with silver(I) nitrate. *Open J. Inorg. Chem.* **2014,** *04*, 10-17; (c) Li, B.; Zang, S. Q.; Ji, C.; Hou, H. W.; Mak, T. C. W. Syntheses, Structures, and Properties of Silver–Organic Frameworks Constructed with 1,1′-Biphenyl-2,2′,6,6′-tetracarboxylic Acid. *Cryst. Growth Des.* **2012,** *12*, 1443-1451; (d) Serpe, A.; Artizzu, F.; Marchiò, L.; Mercuri, M. L.; Pilia, L.; Deplano, P. Argentophilic Interactions in Mono-, Di-, and Polymeric Ag(I) Complexes withN,N′-Dimethyl-piperazine-2,3-dithione and Iodide. *Cryst. Growth Des.* **2011,** *11*, 1278-1286.

30. Djordjevic, B.; Schuster, O.; Schmidbaur, H. A Cyclic Hexamer of Silver Trifluoroacetate Supported by Four Triphenylphosphine Sulfide Template Molecules. *Inorg. Chem.* **2005,** *44*, 673-676.

31. Yin, P.; Zhang, J.; Li, Z.; Qin, Y.; Cheng, J.; Zhang, L.; Lin, Q.; Yao, Y. Supramolecular Isomerism and Various Chain/Layer Substructures in Silver(I)

Compounds: Syntheses, Structures, and Luminescent Properties. *Cryst. Growth Des.* **2009,** *9,* 4884-4896.

32. Li, C. P.; Du, M. Role of solvents in coordination supramolecular systems. *Chem. Commun.* **2011,** *47,* 5958-72.

33. (a) Sun, D.; Cao, R.; Bi, W.; Weng, J.; Hong, M.; Liang, Y. Syntheses and characterizations of a series of silver-carboxylate polymers. *Inorg. Chim. Acta* **2004,** *357,* 991-1001; (b) Whitcomb, D. R.; Rajeswaran, M. Designing silver carboxylate polymers: Crystal structures of silver-acetyl-benzoate and silver-1,2-benzenedicarboxylate monomethyl ester. *Polyhedron* **2006,** *25,* 1747-1752; (c) Effendy; Marchetti, F.; Pettinari, C.; Pettinari, R.; Skelton, B. W.; White, A. H. Synthesis and structural characterization of adducts of silver(I) carboxylate salts AgX (X=CF3COO, CH3COO) with ER3 (E=P, As; R=Ph, cy, o-tolyl) and oligodentate aromatic bases derivative of 2,2′-bipyridyl, L, AgX:PR3:L (1:1:1). *Inorg. Chim. Acta* **2007,** *360,* 1451-1465; (d) Whitcomb, D. R.; Rajeswaran, M. Unusual silver coordination by mono-carboxylate utilization of a poly-carboxylate anion, solid-state structures of silver-tetrachlorophthalate with phthalazine and amine ligands. *Inorg. Chim. Acta* **2008,** *361,* 1357-1362; (e) Chen, H. T.; Lin, H. L.; Chen, I. G.; Kuo, C. Conducting silver networks based on electrospun poly(methyl methacrylate) and silver trifluoroacetate. *Appl. Mater. Interfaces* **2015,** *7,* 9479-85.

34. Griffin, R. G. Single Crystal Study of the 19F Shielding Tensors of a Trifluoromethyl Group. *J. Chem. Phys.* **1972,** *57,* 2147.

35. Desiraju, G. R.; Ho, P. S.; Kloo, L.; Legon, A. C.; Marquardt, R.; Metrangolo, P.; Politzer, P.; Resnati, G.; Rissanen, K. Definition of the Halogen Bond. *Pure Appl. Chem.* **2013,** *85*, 1711-1713.

36. Wang, C.; Danovich, D.; Mo, Y.; Shaik, S. On The Nature of the Halogen Bond. *J. Chem. Theory Comput.* **2014,** *10*, 3726-3737.

37. (a) Nayak, S. K.; Reddy, M. K.; Row, T. N. G.; Chopra, D. Role of Hetero-Halogen (F···X, X = Cl, Br, and I) or Homo-Halogen (X···X, X = F, Cl, Br, and I) Interactions in Substituted Benzanilides. *Cryst. Growth Des.* **2011,** *11*, 1578-1596; (b) Chopra, D.; Row, T. N. G. Role of Organic Fluorine in Crystal Engineering. *Cryst. Eng. Comm.* **2011,** *13*, 2175.

38. (a) Metrangolo, P.; Murray, J. S.; Pilati, T.; Politzer, P.; Resnati, G.; Terraneo, G. The fluorine atom as a halogen bond donor, viz. a positive site. *Cryst. Eng. Comm.* **2011,** *13*, 6593; (b) Metrangolo, P.; Murray, J. S.; Pilati, T.; Politzer, P.; Resnati, G.; Terraneo, G. Fluorine-Centered Halogen Bonding: A Factor in Recognition Phenomena and Reactivity. *Cryst. Growth Des.* **2011,** *11*, 4238-4246; (c) Chopra, D. Is Organic Fluorine Really "Not" Polarizable? *Cryst. Growth Des.* **2012,** *12*, 541-546.

39. (a) Schneider, H. Hydrogen bonds with fluorine. Studies in solution, in gas phase and by computations, conflicting conclusions from crystallographic analyses. *Chem. Sci.* **2012,** *3*, 1381; (b) Wolters, L. P.; Bickelhaupt, F. M. Halogen Bonding versus Hydrogen Bonding: A Molecular Orbital Perspective. *Chemistry Open* **2012,** *1*, 96-105.

40. (a) Pavan, M. S.; Durga Prasad, K.; Row, T. N. Halogen Bonding in Fluorine: Experimental Charge Density Study on Intermolecular F...F and F...S Donor-acceptor Contacts. *Chem. Commun.* **2013,** *49*, 7558-7560; (b) Clark, T.; Hennemann, M.; Murray, J. S.; Politzer, P. Halogen bonding: the sigma-hole. Proceedings of "Modeling interactions in biomolecules II", Prague, September 5th-9th, 2005. *J. Mol. Model.* **2007,** *13*, 291-296.

41. Stone, A. J. Are halogen bonded structures electrostatically driven? *J. Am. Chem. Soc.* **2013,** *135*, 7005-7009.

42. (a) Awwadi, F. F.; Willett, R. D.; Peterson, K. A.; Twamley, B. The Nature of Halogen···Halogen Synthons: Crystallographic and Theoretical Studies. *Chem. Eur. J.* **2006,** *12*, 8952 - 8960; (b) Bent, H. A. Structural Chemistry of Donor-acceptor Interactions. *Chem. Rev.* **1968,** *68*, 587-648; (c) Politzer, P.; Murray, J. S.; Clark, T. Halogen bonding: an electrostatically-driven highly directional noncovalent interaction. *Phys. Chem. Chem. Phys.* **2010,** *12*, 7748-7757.

43. (a) Hathwar, V. R.; Row, T. N. G. Nature of Cl···Cl Intermolecular Interactions via Experimental and Theoretical Charge Density Analysis: Correlation of Polar Flattening Effects with Geometry. *J. Phys. Chem. A* **2010,** *114*, 13434-13441; (b) Desiraju, G. R.; Parthasarathy, R. The Nature of Halogen-Halogen Interactions: Are Short Halogen Contacts Due to Specific Attractive Forces or Due to Close Packing of Nonspherical Atoms? *J. Am. Chem. Soc.* **1989,** *111*, 8725-8726; (c) Yang, M. K. Optical properties of Teflon® AF amorphous fluoropolymers. *J. Micro/Nanolith. MEMS MOEMS* **2008,** *7*, 033010-1-033010-9.

44. Dikundwar, A. G.; Row, T. N. G. Evidence for the “Amphoteric” Nature of Fluorine in Halogen Bonds: An Instance of Cl···F Contact. *Cryst. Growth Des.* **2012,** *12*, 1713-1716.

45. (a) Donald, K. J.; Wittmaack, B. K.; Crigger, C. Tuning σ-Holes Charge Redistribution in the Heavy (Group 14) Analogues of Simple and Mixed Halomethanes Can Impose Strong Propensities for Halogen Bonding. *J. Phys. Chem. A* **2010,** *114*, 7213–7222; (b) Politzer, P.; Lane, P.; Concha, M. C.; Ma, Y.; Murray, J. S. An Overview of Halogen Bonding. *J. Mol. Model.* **2007,** *13*, 305-311.

46. Ramasubbu, N.; Parthasarathy, R.; Murray-RustI, P. Angular Preferences of Intermolecular Forces around Halogen Centers: Preferred Directions of Approach of Electrophiles and Nucleophiles around the Carbon-Halogen Bondla. *J. Am. Chem. Soc.* **1985,** *108*, 4308-4314.

47. Metrangolo, P.; Resnati, G. Type II halogen...halogen contacts are halogen bonds. *IUCrJ* **2014,** *1*, 5-7.

CHAPTER TWO

SYNTHESIS OF NEW HFEs AS ENGINEERED FLUIDS BY TFE ADDITION

2.1 INTRODUCTION

In recent years, hydrofluoro ethers (HFEs) have largely attracted attention of researchers due to their potential of being replacement of ozone depleting and/or global warming substances like chlorofluorocarbons (CFCs), hydrochlorofluoro carbons (HCFCs), hydrofluorocarbons (HFCs), and perfluorocarbons (PFCs).[1] HFEs normally have a structure of R_f-O-R_h, (R_f is perfluorocarbon segment and R_h is a hydrocarbon segment). The introduction of an oxygen atom into the structure to segregate the perfluorocarbon and hydrocarbon segments in the molecules largely reduced the atmospheric lifetime of the materials, thereby yielding a low global warming effect, while maintaining the desired properties of inflammability, low toxicity, volatility, thermal stability and chemical inertness.[2] In recent years, they have been widely used in pharmaceuticals,[3] Li battery co-solvents,[4] and replacements for CFCs, HCFCs, HFCs, and PFCs in various industries.[5] More alternatives and new synthetic methods still need to be developed to improve the performance of every aspect and enrich the HFE family.

The synthesis methods of HFEs used so far are mainly the addition of fluoroolefins to alcohols,[6] alkylation of acyl fluorides,[7] and other molecular modifications. Recently an interesting publication by Friesen and others[8] reveals an unexpected degradation of HFEs materials that also gives alkylation of tertiary amines.

The 3M Company (3M) has developed several HFEs with commercial name Novec™ Engineered Fluids: Novec™ 7100 is $(CF_3)_2CFCF_2OCH_3/CF_3CF_2CF_2CF_2OCH_3$; Novec™ 7200 is $CF_3)_2CFCF_2OC_2H_5/ CF_3CF_2CF_2CF_2OC_2H_5$; Novec™ 7500 is $CF_3CF_2CF_2CF(OC_2H_5)CF(CF_3)_2$ and Novec™ 7600 is $CF_3CHFCF_2CH(CH_3)OCF_2CHFCF_3$. Their boiling points range from 61 to 131 °C. Both a wider temperature range boiling points for HFEs and more alternatives of zero toxicity are needed. Especially new HFEs containing $–CF_2H$ group are expected to have shorter or more limited atmospheric lifetimes, which is highly preferred according to a study on α,ω-dialkoxyfluoropolyethers by Wu and Navarrini.[7a, 9]

In our laboratory, we extended the work by Cirkva and Paleta[10] by using tetrafluoroethylene ($CF_2=CF_2$, TFE) instead of the other perfluoroolefins to limit the number of carbon atoms in the molecule. In addition, TFE was further added to the diol product to make a fluorinated ether compound with two $-CF_2H$ groups.[11]

2.2 RESULTS AND DISCUSSION

TFE is well known as a deflagrant, and its use is often avoided, especially in academic laboratories.[12] In the addition reaction of TFE to the starting material 2,2-dimethyl-1,3-dioxolane under radical conditions, TFE tends to form longer chains of up to 10 units at the active site, which is not desired. A restriction on the number of carbon atoms in HFEs makes the precursor **1** desirable (see Scheme 2.1).

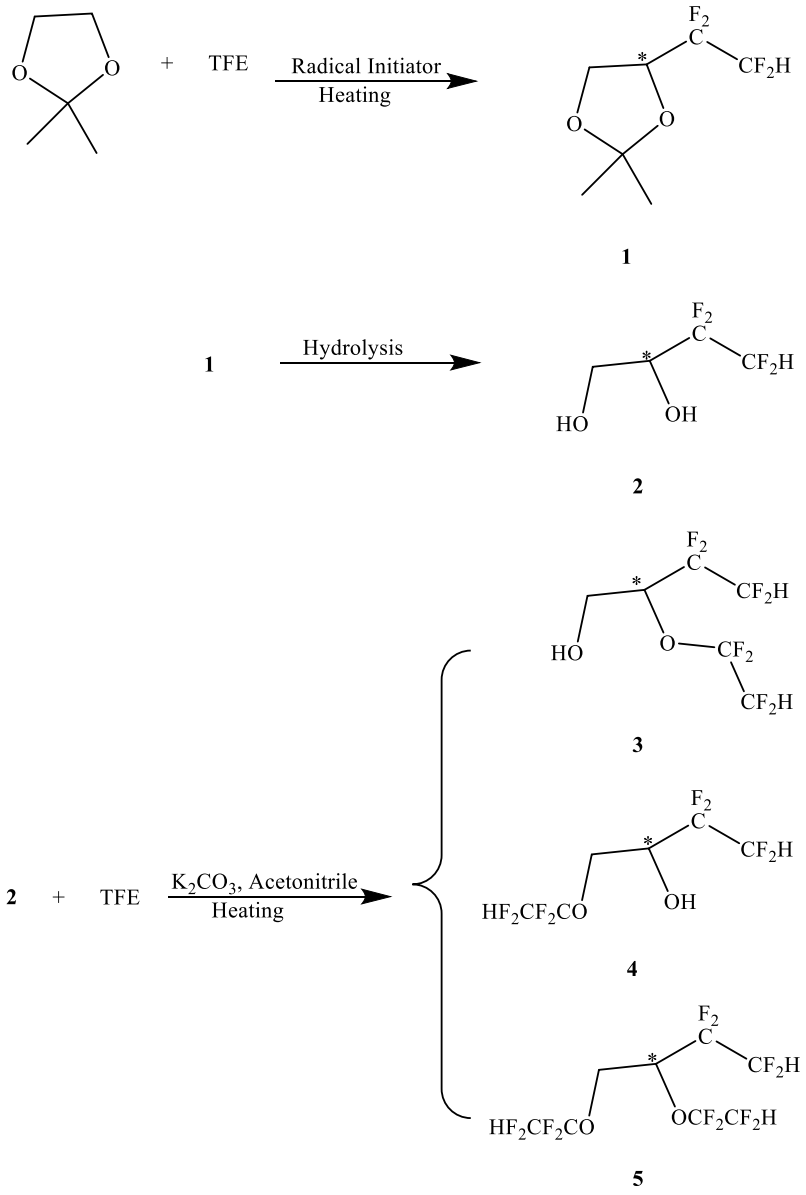

Scheme 2.1. Synthesis of new HFEs by TFE addition method.

In order to drive the reaction towards the direction of compound **1**, a large excess amount of the starting dioxolane (5 molar equivalents) was used to lower the chances of getting long -CF_2CF_2- chains. Under these reaction conditions, the primary product was the desired addition of one molecule of TFE to give 4-tetrafluoroethyl-2,2-dimethyl-1,3-dioxolane (**1**) accompanied by trace amounts of the analogous compound resulting from the addition of two molecules of TFE to the same reaction center. The NMR spectra of compound **1** are shown in **Error! Reference source not found.**, **Error! Reference source no t found.**, and Figure 2.3. The carbon atom where the molecule of TFE is inserted in compound **1**, as shown in Scheme 2.1 becomes a chiral center after the insertion of one molecule of TFE, and this causes the signals in the NMR spectra to become more complicated than normal, especially the ^{19}F NMR spectrum, as the CF_2 fluorine atoms on both the α- and β- carbon atoms with respect to the chiral carbon atom become diastereotopic. This is also true for compound **2** and compound **3**, and the chemical shifts and coupling constants fall in the expected range compare with several compounds of similar structures reported before.[10, 13] GC/MS was used to analyze each compound to further confirm the structure elucidation as shown in Figure 2.4, Figure 2.8, and Figure 2.12.

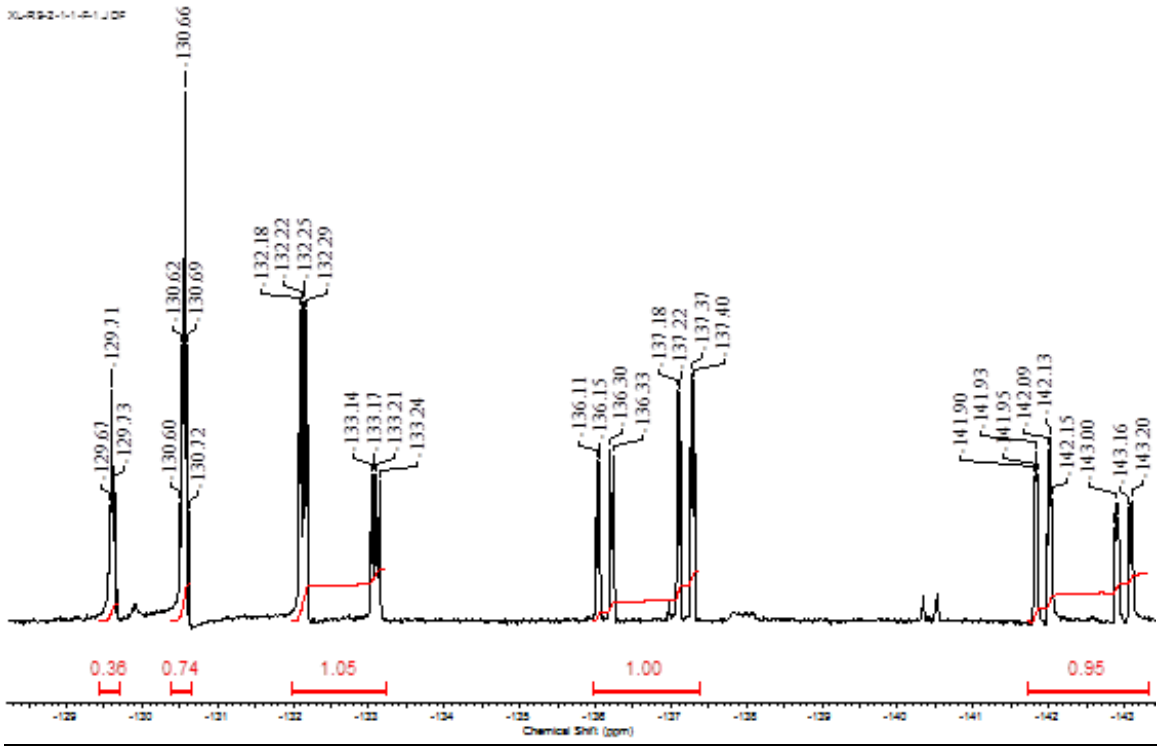

Figure 2. 1 ^{19}F NMR spectrum of compound 1 in acetone-d6.

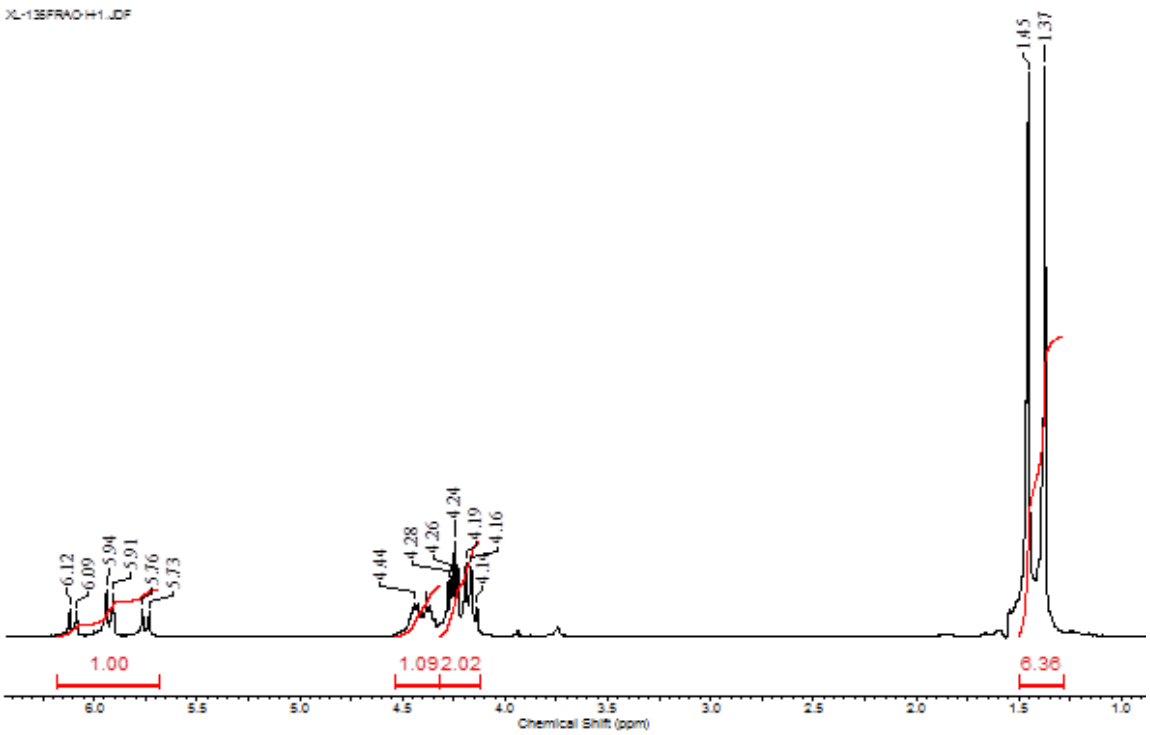

Figure 2. 2 ^{1}H NMR spectrum of compound 1 in acetone-d6.

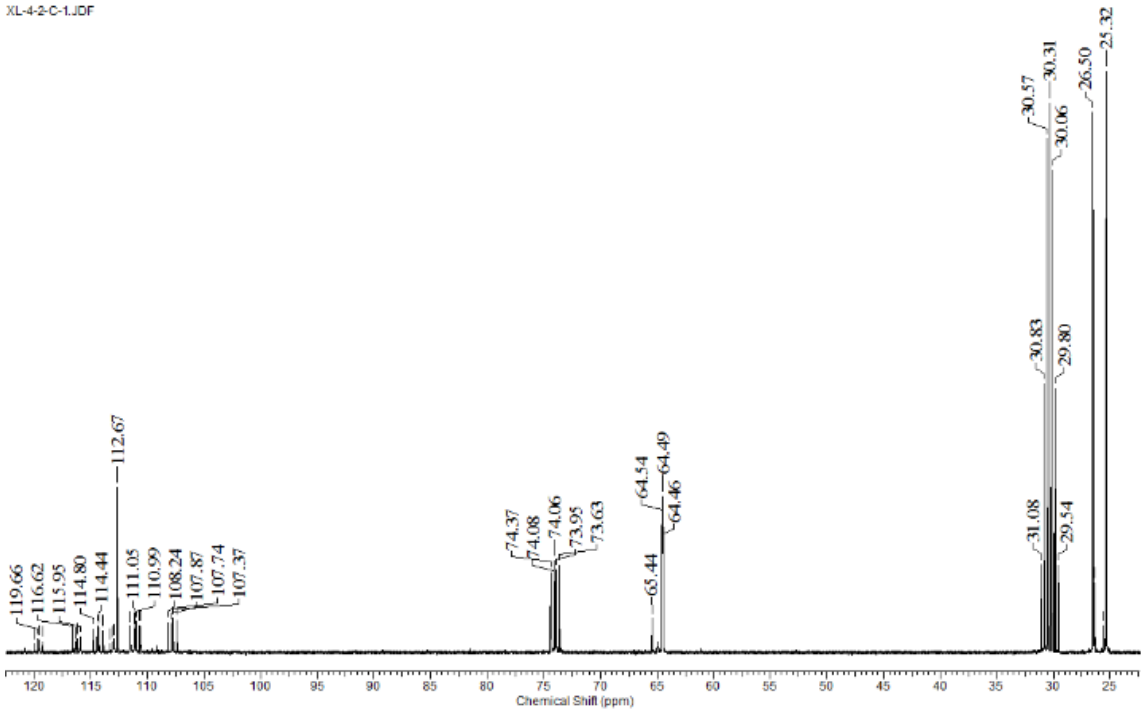

Figure 2.3. ^{13}C NMR spectrum of compound **1** in acetone-d6.

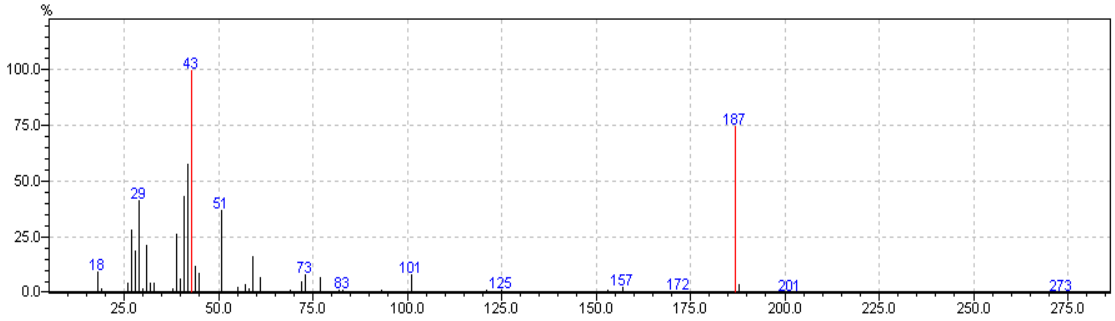

Figure 2.4. Mass spectrum of compound **1**.

Next, as shown in Scheme 2.1, the hydrolysis of compound **1** in refluxing acidic methanol gave compound **2** fairly effectively in 90+% yield. Furthermore, any unreacted compound **1** can be recycled along with the solvent for the next hydrolysis procedure. The two -CF_2- groups in compound **2** also gave two sets of AB patterns in ^{19}F NMR spectrum as shown in Figure 2.5. The coupling constant of $^2J_{FF}$ is 302.6 Hz and $^2J_{HF}$ = 52.6 Hz for CF_2H fluorine atoms, and $^2J_{FF}$ = 268.7 Hz for CF_2 fluorine atoms.

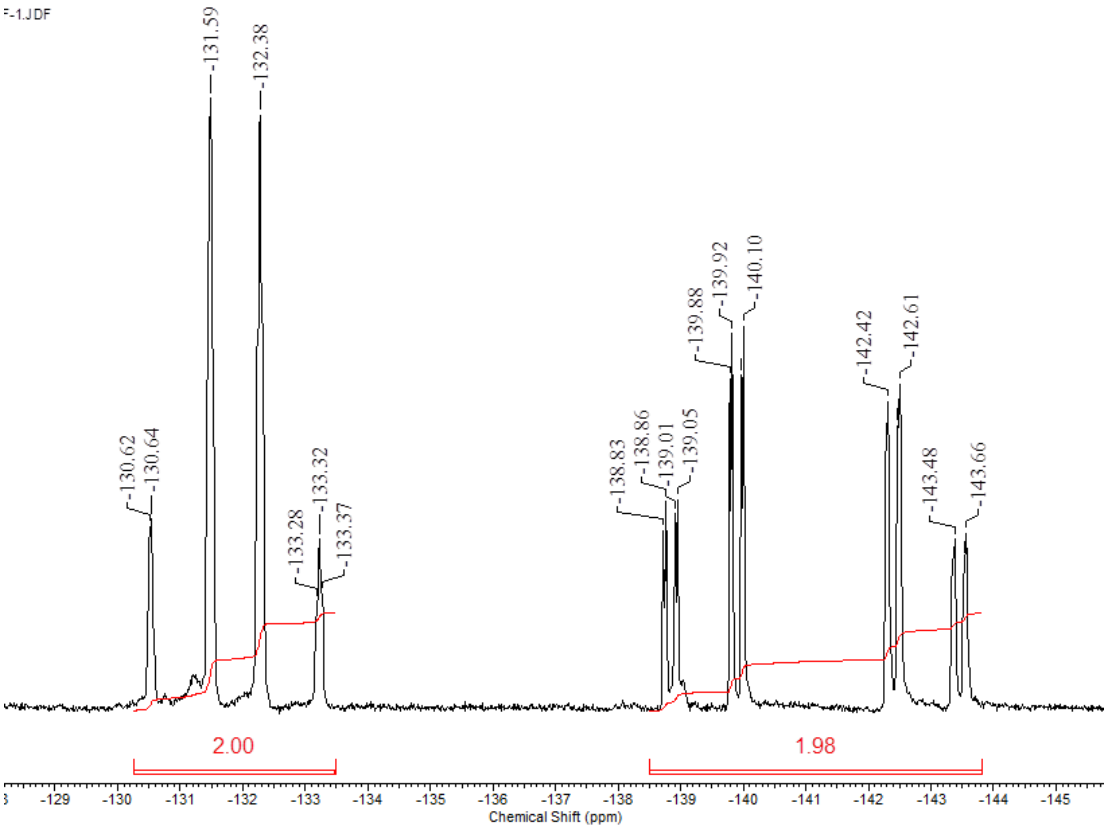

Figure 2.5. ^{19}F NMR spectrum of compound **2**.

In the ^1H spectrum of compound **2,** as shown in Figure 2.6, the proton peak of the CF_2H group is split into a triplet of triplet by the two fluorine atoms on the same carbon

atom and the other two fluorine atoms on the adjacent carbon atom. The proton on the CH group is split by the protons of CH_2 group and the fluorine atoms of CF_2 groups, which gives a complicated pattern. The CH_2 protons have an AB spin system, and the peaks are split by the CH proton into a doublet.

In the ^{13}C NMR spectrum of compound **2** as shown in Figure 2.7, the carbon peaks of both CF_2 are split into triplet of triplet by the fluorine atoms on the carbon and the fluorine atoms from the adjacent carbon. The carbon peak of CH is split into a doublet of doublet by the two fluorine atoms on the adjacent carbon.

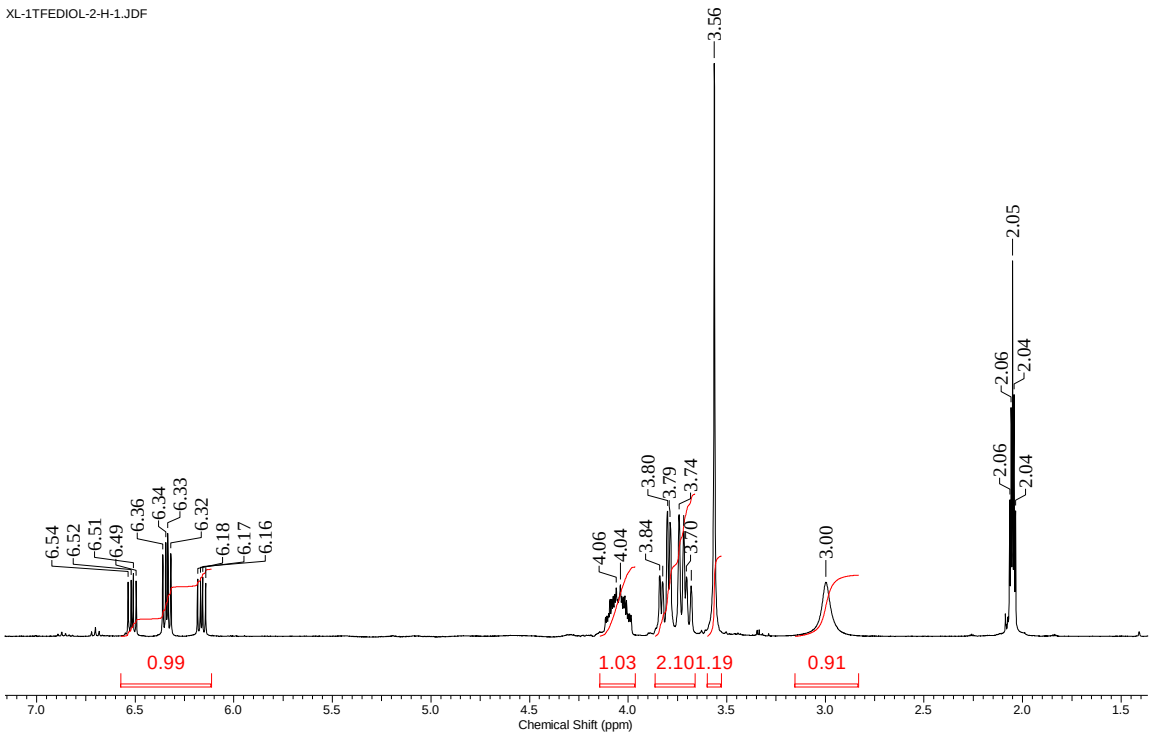

Figure 2.6. ^1H NMR spectrum of compound **2**.

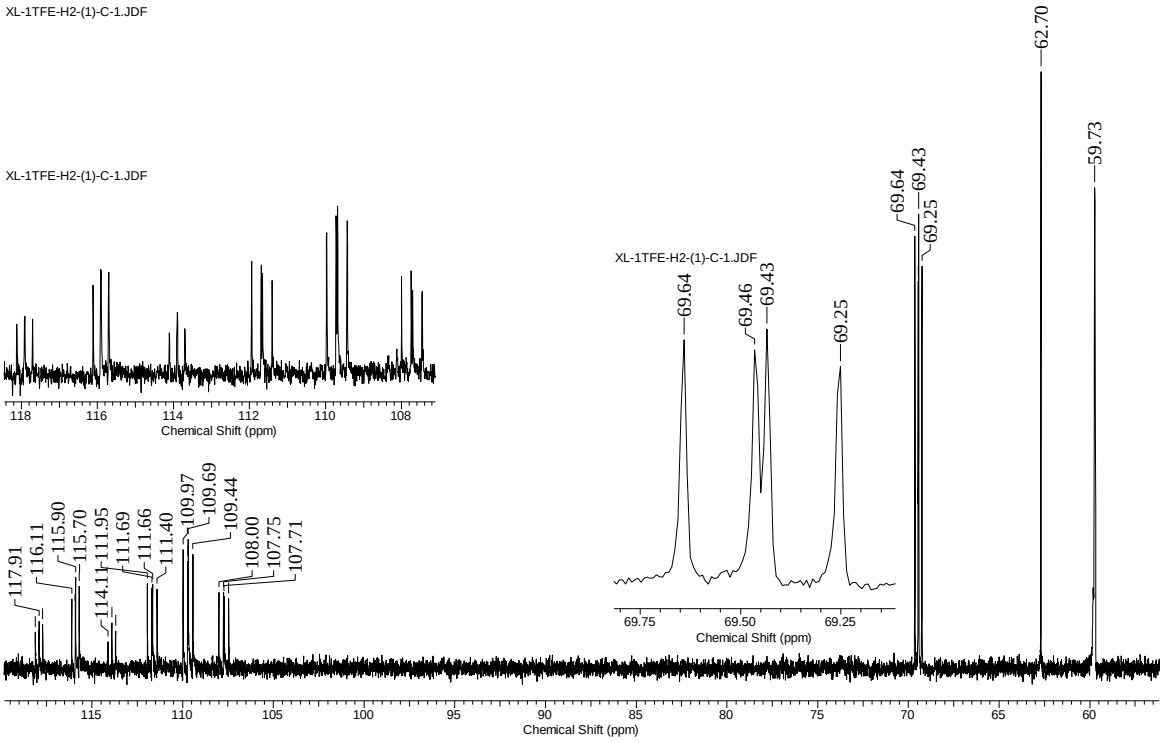

Figure 2.7. ^{13}C NMR spectrum of compound **2**.

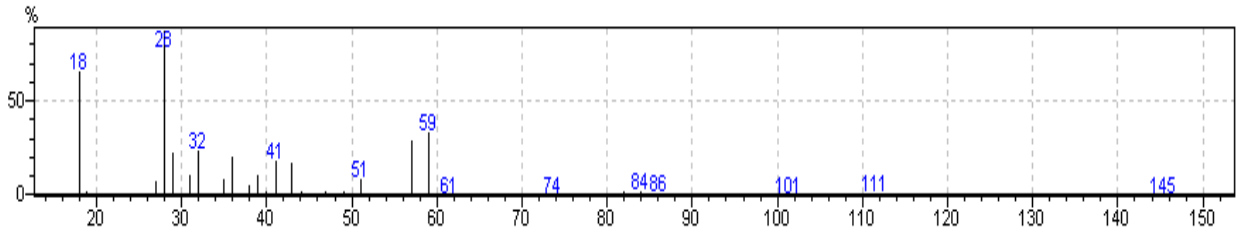

Figure 2.8. Mass spectrum of compound **2**.

Further addition of TFE to the alcohol groups was performed under basic conditions. Only compound **3** was synthesized by this method, and compound **4** and **5** were not observed. The selectivity of the TFE addition to one of the -OH groups over the other can be explained that the increased acidity of the -OH group closer to the chiral carbon

center versus the other -OH group due to the presence of electron withdrawing -CF_2CF_2H group. Again, addition of TFE to both –OH groups in compound **2** was not observed, and the yield of compound **3** was very low. The yield of compound **3** can be improved by using DMSO instead of acetonitrile as solvent; however, the product and DMSO formed an azeotrope over a large temperature range, which made it very difficult to separate the product compound **3** in a pure form. Nevertheless, the NMR spectra and mass spectra are shown in Figure 2.9-2.12. The spectra of compound **3** are even more complicated the those of compound **1** and compound **2** due to the addition of one more molecule of TFE to the -OH group adjacent to the chiral carbon center. In ^{19}F NMR spectrum of compound **3**, the -OCF_2- fluorine atoms give an AB pattern at -87.64 ppm and -90.45 ppm with a coupling constant $^2J_{FF}$ = 144.7 Hz. The CF_2H fluorine peaks are split by the proton on the same carbon atom and have a coupling constant $^2J_{HF}$ = 52 Hz.

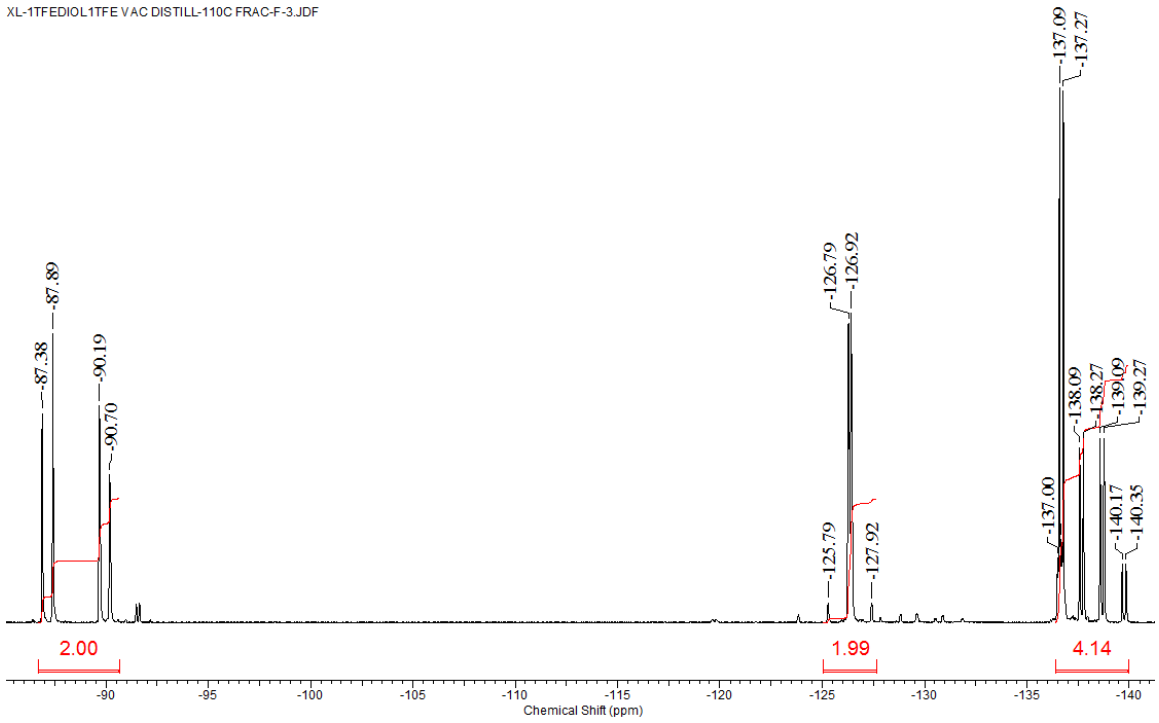

Figure 2.9. ^{19}F NMR spectrum of compound **3** in $CDCl_3$.

In ^{1}H NMR spectrum of compound 3 shown in Figure 2.10, both protons of -CF_2H are split into a triplet by the fluorine atoms on the same carbon atom and further split by the CF2 fluorine atoms of the adjacent carbon atom. The two protons of CH_2 group give

an AB pattern and the peaks are further split by CH proton. The CH proton has a quite complicated pattern due to splitting by multiple NMR active nuclei.

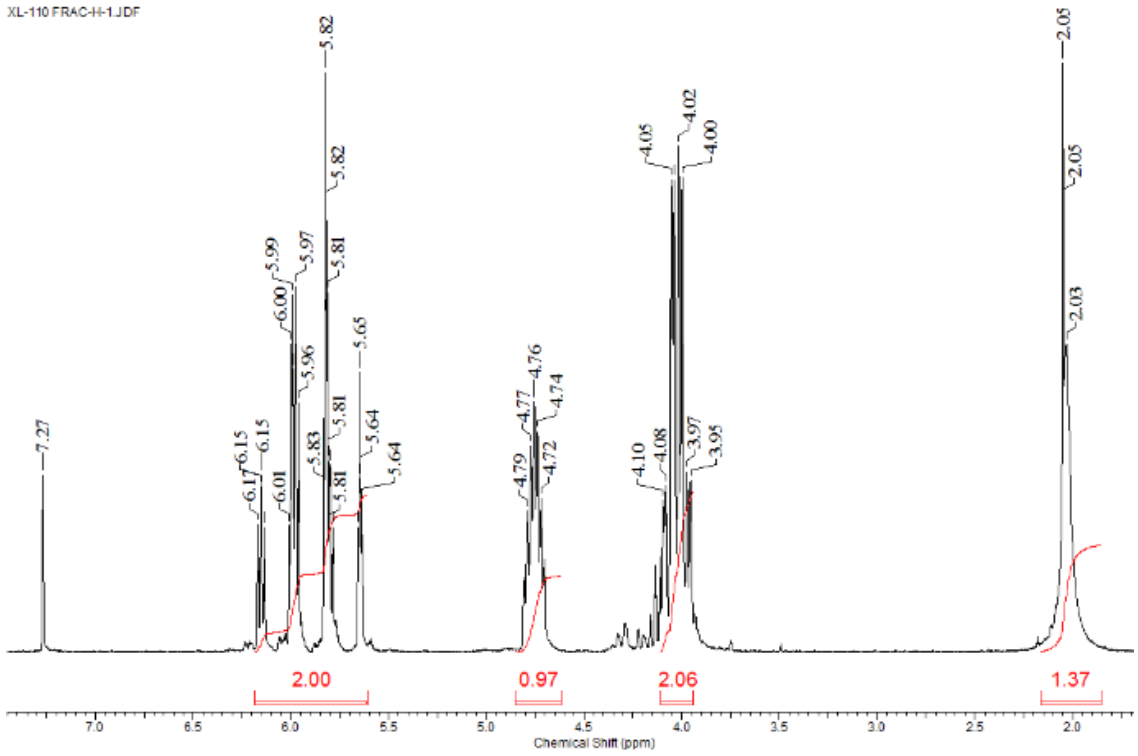

Figure 2.10. ^{1}H NMR spectrum of compound **3** in $CDCl_3$.

The carbon peaks in ^{13}C NMR spectrum of compound **3** are shown in Figure 2.11, and the carbon atoms carrying fluorine atoms have very distinguishable J_{CF} coupling constant range of 250-275 Hz.

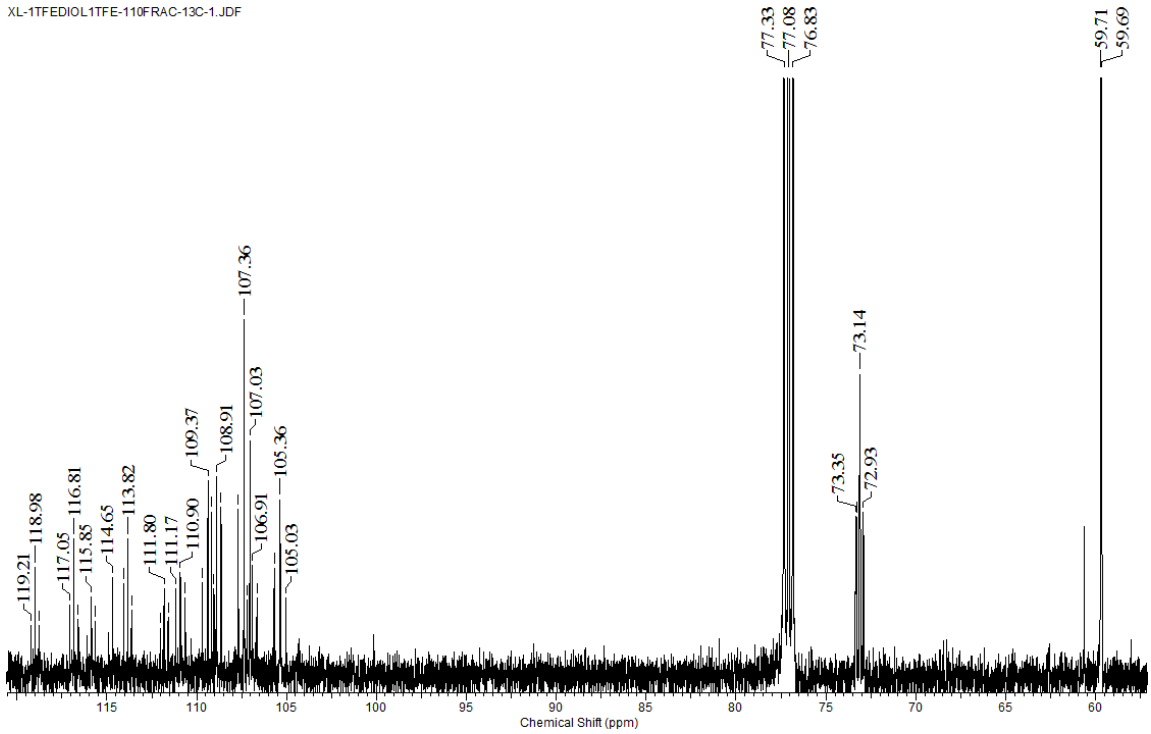

Figure 2.11 ^{13}C NMR spectrum of compound **3** with proton decoupling in $CDCl_3$.

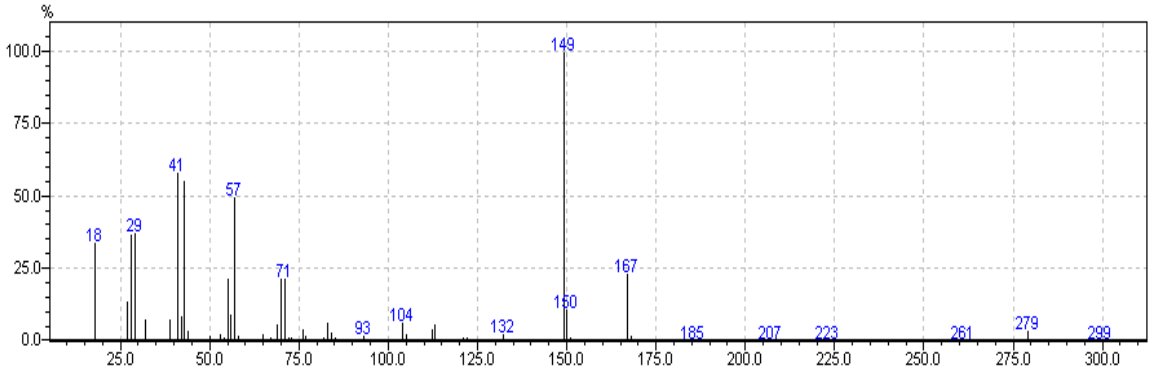

Figure 2.12. Mass spectrum of compound **3**.

2.3 CONCLUSION AND FUTURE WORK

The addition of TFE to the dioxolane compound under radical conditions was quite successful, and this can be an effective approach to new fluorinated alcohol. The fluorinated alcohols are very useful building blocks for synthesizing a variety of fluorinated compounds and further molecular modification. Unfortunately, the further addition of TFE under anionic conditions to the diol compound was not very successful in this case.

2.4 EXPERIMENTAL

2.4.1 Reagents and synthetic equipment

2,2-Dimethyl-1,3-dioxolane and DMSO were purchased from Alfa Aesar; acetonitrile was purchased from Mallinckrodt Baker; di-tert-butyl peroxide (DTBP) was purchased from Merck; and KOH and K_2CO_3 were purchased from Sigma Aldrich. Acetone-d_6, D_2O, and $CDCl_3$ were purchased from Cambridge Isotope Laboratories, Inc. These chemicals were used without further purification. TFE stabilized with limonene was available from laboratory stock and it was filtered through silica gel to remove residue limonene before use.[12c, 14] Stainless steel cylinders (75-, 300-, or 500-mL capacities) were purchased from Hoke®; valves were purchased from Swagelok®.

2.4.2 Instrumentation.

NMR spectroscopic data was collected on a multinuclear JOEL ECX-300 Spectrometer. The frequency is 300 MHz for ^1H, 282.78 MHz for ^{19}F and 75.57 MHz for ^{13}C respectively. Multiplicity is as follows: s (singlet), d (doublet), t (triplet), m (multiplet), dd (doublet of doublet), td (triplet of doublet), tt (triplet of triplet), tm (triplet of multiplet).

The internal standard of ^{19}F NMR spectroscopy is $CClF_3$ (0.00 ppm). GC/MS data was collected on a SHIMADZU GCMS-QP5000 instrument.

*2.4.3 Synthesis of 4-tetrafluoroethyl-2,2-dimethyl-1,3-dioxolane (**1**)*

An amount of 102.13 g (1 mol) 2,2-dimethyl-1,3-dioxolane and 2.44 g DTBP initiator were added to a 500 mL stainless steel cylinder equipped with a Swagelok® valve. The cylinder was then degassed on the vacuum line at liquid nitrogen temperature. The cylinder was cooled to liquid nitrogen temperature, and an amount of 20.0 g (0.2 mol) TFE was condensed into the cylinder on a vacuum line. The reaction mixture was warmed to room temperature and then heated at 70-75 °C for 4 days, over which time approximately 99% of the TFE was consumed. The product was purified by fractional distillation giving an approximate boiling point of compound **1** as 135-136 °C, and any unreacted 2,2-dimethy-1,3-dioxolane was recycled for use in the next run.

NMR chemical shifts of compound **1**:

^{19}F NMR chemical shifts:

δ_8 = -130.19 ppm, -132.71 ppm (AB system, $^2J_{FF}$ = 268.7 Hz, $^3J_{FF}$ = 9.9 Hz); δ_9 = -136.76 ppm, -142.55 ppm (AB system, $^2J_{FF}$ = 302.6 Hz, $^2J_{HF}$ = 52.6 Hz, $^3J_{FF}$ = 6.6 Hz).

^1H NMR chemical shifts:

δ_9 = 5.93 ppm (tdd, $^2J_{HF}$ = 52.6 Hz, $^3J_{HF}$ = 9.6 Hz); δ_5 = 4.41 ppm (dddd, $^3J_{HF}$ = 19.3 and 6.5 Hz,); δ_2 = 4.21 ppm (AB, $^2J_{HH}$ = 9.3 Hz, $^3J_{HH}$ = 4.5 Hz); δ_6 = 1.45 ppm (s); δ_7 = 1.37 ppm (s).

^{13}C NMR chemical shifts:

δ_2 = 112.67 ppm (s); δ_4 = 64.49 ppm (m); δ_5 = 74.06 ppm (m); δ_6 = 26.50 ppm (s); δ_7 = 25.32 ppm (s); δ_8 = 111.09 ppm (tdd, J_{CF} = 246.4 Hz, $^2J_{CF}$ = 37.6 Hz, $^2J_{CF}$ = 4.3 Hz); δ_9 = 116.30 ppm (tdd, J_{CF} = 249.8 Hz, $^2J_{CF}$ = 27.5 Hz, $^2J_{CF}$ = 2.2 Hz).

Mass spectrum of compound **1**, m/z (relative intensity, %):

201 (0.03) $[M-H]^+$, 187 (75.0) $[M-CH_3]^+$, 172 (1.1) $[M-2CH_3]^+$, 157 (2.9) $[M-CH_3OCH_2]^+$, 101 (8.2) $[CF_2CF_2H/M-CF_2CF_2H]^+$, 83 (1.8) $[CF2CCH_2O]^+$, 73 (8.2) $[CFHCCHO]^+$, 51 (37.1) $[CF_2H]^+$, 43 (100.0) $[CH_2CHO]^+$, 29 (41.5) $[CF]^+$.

*2.4.4 Synthesis of 3,3,4,4-tetrafluoro-1,2-butanediol (**2**).*

A mixture of 20.20 g (0.1 mol) compound **1**, 64.00 g (2 mol) methanol, and 2.5 g concentrated hydrochloric acid were mixed and refluxed for 12 h with stirring. The completion of the reaction was confirmed by ^{19}F NMR spectroscopy. The solvent was vacuum transferred away from the bulk product mixture on a vacuum line leaving a viscous product mixture behind. The resulting diol product **2** was then purified by distillation under vacuum yielding 90+% of the desired product. The boiling point of compound 2 at atmospheric pressure is 195-196 °C.

NMR chemical shifts of compound **2**:

^{19}F NMR chemical shifts:

δ_5 = -131.11 ppm, -132.85 ppm (AB system, $^2J_{FF}$ = 273.0 Hz); δ_6 = -139.47 ppm, -143.04 ppm (AB system, $^2J_{FF}$ = 302.6 Hz, $^2J_{HF}$ = 55.9 Hz).

^{1}H NMR chemical shifts:

δ_6 = 6.33 ppm (tdd, $^2J_{HF}$ = 53.0 Hz, $^3J_{HF}$ = 7.9 Hz, $^3J_{HF}$ = 4.8 Hz); δ_2 = 4.05 ppm (ddt, $^3J_{HF}$ = 6.5 Hz); δ_3 = 3.76 ppm (AB, $^2J_{HH}$ =12.0 Hz, $^3J_{HH}$ = 3.8 Hz).

^{13}C NMR chemical shifts:

δ_2 = 69.45 ppm (dd, $^2J_{CF}$ = 25.9 Hz); δ_3 = 59.73 ppm (s); δ_5 = 115.90 ppm (tt, J_{CF} = 253.4 Hz, $^2J_{CF}$ = 25.0 Hz); δ_6 = 109.69 ppm (td, J_{CF} = 248.6 Hz, $^2J_{CF}$ = 31.7 Hz). The peak at 62.70 ppm belongs to trace amount of $HOCH_2CH_2OH$ generated as a byproduct from the reaction.

Mass spectrum of compound **2**, m/z (relative intensity, %):

145 (0.9) $[M\text{-}OH]^+$, 111 (1.1) $[M\text{-}CF_2H]^+$, 101 (1.1) $[CF_2CF_2H]^+$, 74 (0.7) $[CF_2CC]^+$, 61 (0.8)$[HOCH_2CH_2OH]^+$, 59 (33.9) $[OCH_2CH_2O]^+$, 51 (9.3) $[CF_2H]^+$, 32 (24.7) $[CFH]^+$, 28 (100.0) $[CO]^+$.

*2.4.5 Synthesis of 3,3,4,4-tetrafluoro-2-(1,1,2,2-tetrafluoroethyoxy)butan-1-ol (**3**).*

An amount of 32.7 g compound **2**, 2.3 g K_2CO_3 and 80 mL acetonitrile were added to a 300 mL stainless cylinder. Then 30 g TFE was condensed into the cylinder on a vacuum line. The reactor vessel was heated up at 40-60 °C overnight. The products were separated by column chromatography with hexane and ethyl acetate. The yield of the product **3** was only about 6%, and most of the starting material remained unreacted. When DMSO was used as solvent instead of acetonitrile, the yield increased to 25%; however, purification was made difficult because of the formation of an azeotrope between compound **3** and DMSO over a large temperature range.

NMR chemical shifts of compound **3**:

^{19}F NMR chemical shifts:

δ_2 = -87.64 ppm, -90.45 ppm (AB system, $^2J_{FF}$ = 144.7 Hz); δ_3 = -137.64 ppm, -139.72 ppm (AB system, $^2J_{FF}$ = 305.8 Hz, $^2J_{HF}$ = 52.3 Hz); δ_7 = -126.29 ppm, -127.22 ppm (AB system, $^2J_{FF}$ = 282.8 Hz); δ_8 = -137.18 ppm, (d, $^2J_{HF}$ = 52.3 Hz).

^{1}H NMR chemical shifts:

δ_3 = 5.82 ppm, (tm, $^2J_{HF}$ = 53.0 Hz); δ_4 = 4.76 ppm, (m, $^3J_{HF}$ = $^3J_{HH}$ = 5.2 Hz); δ_5 = 4.07 ppm, 3.99 ppm (AB, $^2J_{HH}$ = 12.7 Hz, $^3J_{HH}$ = 5.5 Hz); δ_8 = 5.98 ppm, (tm, $^2J_{HF}$ = 52.6 Hz).

^{13}C NMR chemical shifts:

δ_2 = 116.81 ppm, (tt, J_{CF} = 273.5 Hz, $^2J_{CF}$ = 28.8 Hz); δ_3 = 113.82 ppm, (tt, J_{CF} = 255.3 Hz, $^2J_{CF}$ = 26.9 Hz); δ_4 = 73.14 ppm, (t, $^2J_{CF}$ = 26.9 Hz); δ_5 = 59.70 ppm, (m, $^3J_{CF}$ = 2.9 Hz); δ_7 = 108.91 ppm, (tt, J_{CF} = 251.4 Hz, $^2J_{CF}$ = 33.6 Hz); δ_8 = 107.36 ppm, (tt, J_{CF} = 251.4 Hz, $^2J_{CF}$ = 41.3 Hz).

Mass spectrum of compound **3**, m/z (relative intensity, %):

261 (0.1) $[M-H]^+$, 223 (0.2) $[M-HF_2]^+$, 207 (0.3) $[M-2F-OH]^+$, 185 (0.1) $[M-HF_4]^+$, 167 (23.2) $[M-H_3F_4O]^+$, 150 (11.0), 149 (100.0), 93 (1.9) $[CH_2CHOCF_2]^+$, 71 (21.9) $[OCH_2CHOC]^+$, 57 (49.8) $[OCCHO]^+$, 41 (58.0) $[CCHO]^+$, 29 (37.6) $[CHO]^+$.

2.5 REFERENCES

1. (a) WMO (World Meteorological Organization), *Scientific Assessment of Ozone Depletion: 2010*, Global Ozone Research and Monitoring Project-Report No. 52, p 516, Geneva, Switzerland, 2011; (b) Burkholder, J. B.; Cox, R. A.; Ravishankara, A. R. Atmospheric Degradation of Ozone Depleting Substances, Their Substitutes, and Related Species. *Chem. Rev.* **2015**, *115*, 3704-59; (c) Good, D. A.; Francisco,

J. S. Atmospheric Chemistry of Alternative Fuels and Alternative Chlorofluorocarbons. *Chem. Rev.* **2003**, *103*, 4999-5023.

2. (a) Owens, J. G. Low GWP Alternatives to HFCs and PFCs; in Proceedings of the 1999 Taipei International Conference on Atmospheric Protection: Taipei, Taiwan, 1999; also available at Owens, J. G. Low GWP Alternative to HFCs and PFCs, 3M Specialty Materials, St. Paul, MN USA. http://solutions.3maustria.at/3MContentRetrievalAPI/BlobServlet?lmd=1310648569000&assetId=1273689616858&assetType=MMM_Image&blobAttribute=ImageFile; (b) Tsai, W. T. Environmental risk assessment of hydrofluoroethers (HFEs). *J. Hazard. Mater.* **2005**, *119*, 69-78; (c) Sekiya, A.; Misaki, S. The Potential of Hydrofluoroethers to Replace CFCs, HCFCs and PFCs. *J. Fluorine Chem.* **2000**, *101*, 215-221; (d) Owens, J. G. Hydrofluoroethers. In *Handbook for Critical Cleaning, 2nd edn.*; Kanegsberg, B.; Kanegsberg, E., Eds.; CRC Press: Boca Raton, FL, **2011**; *Vol. 1*, pp 115-129;

3. Gilbert, E. E.; Veldhuis, B. Hexafluoroisopropyl Ethers as Anesthetics. U.S. Patent 3,346,448, Oct. 10, 1967.

4. (a) Achiha, T.; Nakajima, T.; Ohzawa, Y.; Koh, M.; Yamauchi, A.; Kagawa, M.; Aoyama, H. Electrochemical Behavior of Nonflammable Organo-Fluorine Compounds for Lithium Ion Batteries. *J. Electrochem. Soc.* **2009**, *156*, A483-A488; (b) Lamanna, W. M.; Bulinski, M. J.; Castello, M. G.; Dahn, J. R.; Flynn, R. M.; Wang, Y.; Li, J.; Moshurchak, L. Fluorinated Compounds for Use in Lithium Battery Electrolytes. U.S. Patent 8,435,679 B2, May 7, 2013; (c) Nagasubramanian,

G.; Fenton, K. Reducing Li-ion safety hazards through use of non-flammable solvents and recent work at Sandia National Laboratories. *Electrochimica. Acta* **2013**, *101*, 3-10.

5. Drakesmith, F. G.; Powell, R. L.; Chambers, R. D.; Grievson, B. Process for Fluorinating Ethers. U.S. Patent 4,736,045 A, Apr. 5, 1988.

6. (a) Crawford, J. W. C. Preparation of Alkyl 1,1,2,2-Tetrafluoroethyl Ethers. *J. Chem. Soc. C* **1967**, 2395-2396; (b) Coffman, D. D.; Raasch, M. S.; Rigby, G. W.; Barrick, P. L.; Hanford, W. E. Addition Reactions of Tetrafluoroethylene. *J. Org. Chem.* **1949**, *14*, 747-753.

7. (a) Wu, M.; Navarrini, W.; Avataneo, M.; Venturini, F.; Sansotera, M.; Gola, M. α,ω-Dialkoxyfluoropolyethers a Promising Class of Hydrofluoroether (HFE). *Chemistry Today* **2011**, *29*, 67-71; (b) Sheppard, W. A. α-Fluorinated Ethers. I. Aryl Fluoroalkyl Ethers. *J. Org. Chem.* **1964**, *29*, 1-11; (c) Aldrich, P. E.; Sheppard, W. A. α-Fluorinated Ethers. II. Alkyl Fluoroalkyl Ethers. *J. Org. Chem.* **1964**, *29*, 11-15.

8. Jelier, B. J.; Howell, J. L.; Montgomery, C. D.; Leznoff, D. B.; Friesen, C. M. A convenient route to tetraalkylammonium perfluoroalkoxides from hydrofluoroethers. *Angew. Chem.* **2015**, *54*, 2945-9.

9. Wu, M.; Navarrini, W.; Spataro, G.; Venturini, F.; Sansotera, M. An Environmentally Friendly Class of Fluoropolyether: α,ω-Dialkoxyfluoropolyethers. *Appl. Sci.* **2012**, *2*, 351-367.

10. Cirkva, V.; Paleta, O. Radical Addition Reactions of Fluorinated Species. Part 7. Highly Selective Two-Step Synthesis of 1-(Polyfluoroalkyl)ethane-1,2-diols; Regioselectivity of the Additions of Methylated 1,3-Dioxolanes to Perfluoroolefins. *J. Fluorine Chem.* **1999**, *94*, 141-156.

11. (a) Marchionni, G.; Silvani, R.; Fontana, G.; Malinverno, G.; Visca, M. Hydrofluoropolyethers. *J. Fluorine Chem.* **1999**, *95*, 41-50; (b) Marchionni, G.; Bassi, M.; Fontana, G.; Maccone, P.; Ajroldi, G. Some Physical Chemical Properties of α,ω-dihydroperfluoropolyethers. *J. Fluorine Chem.* **1999**, *98*, 41-54.

12. (a) Shiflett, M. B.; Yokozeki, A. Process for Separation of Tetrafluoroethylene from Carbon Dioxide Using Ionic Liquids. U.S. Patent 8,313,558 B2, Nov. 20, 2012; (b) Bramer, D. J. V.; Shiflett, M. B.; Yokozeki, A. Safe Handling of Tetrafluoroethylene. U.S. Patent 5,345,013, Sep. 6, 1994; (c) Hercules, D. A.; DesMarteau, D. D.; Fernandez, R. E.; Clark, Jr., J. L.; Thrasher, J. S. Evolution of Academic Barricades for the Use of Tetrafluoroethylene (TFE) in the Preparation of Fluoropolymers. In *Handbook of Fluoropolymer Science and Technology*, Smith, Jr., D. W.; Iacono, S. T.; Iyer, S. S., Eds.; JohnWiley & Sons, Inc.: Hoboken, NJ, 2014, Chapter 18; pp 413-431.

13. Chernykh, Y.; Hlat-Glembová, K.; Klepetářová, B.; Beier, P. Development of PhSCF2CF2SiMe3 as a Tandem Anion and Radical Tetrafluoroethylene Equivalent: Preparation of Tetrafluoroethyl-Substituted Alcohols and Tetrafluorotetrahydropyrans. *Eur. J. Org. Chem.* **2011**, *2011*, 4528-4531.

14. (a) Hals, L. J.; Reid, T. S.; Smith, G. H. Process of Making Perfluoro Olefins. U.S. Patent 2,668,864, Feb. 9, 1954; (b) Lazerte, J. D.; Hals, L. J.; Reid, T. S.; Smith, G. H. Pyrolyses of the Salts of the Perfluoro Carboxylic Acids. *J. Am. Chem. Soc.* **1953**, *75*, 4525–4528.

CHAPTER THREE

ONE STEP SYNTHESIS OF SEVOFLURANE WITH STRONG LEWIS ACIDS

3.1 INTRODUCTION

The development of inhalation anesthetics has a long history.[1] The fluoro-organic anesthetics stemmed from the development of refrigerants. The thermal stability and physical properties of alkanes and ethers were largely altered or improved by substituting hydrogen by fluorine in the molecules, and a class of fluorinated alkanes and ethers were first tested out in several industrial laboratories.[2] Several of these compounds were discovered to have an anesthetic effect in mammals.[3] In clinic practice, more characteristics are required such as low toxicity, solubility in blood and tissue, speed of action, recover time, stability to the absorbents etc.[4]

The fluorinated ethers enflurane ($ClHFCCF_2OCHF_2$, 2-chloro-1,1,2-trifluoroethyl-difluoromethyl ether), isoflurane ($CF_3CHClOCHF_2$, 1-chloro-2,2,2-trifluoroethyl difluoromethyl ether), sevoflurane [$(CF_3)_2CHOCH_2F$, fluoromethyl 2,2,2-trifluoro-1-trifluoromethyl ethyl ether] and desflurane ($CF_3CHFOCHF_2$, 1,2,2,2-tetrafluoroethyl difluoromethyl ether) are currently in clinical practice after hundreds of fluorinated compounds have been tested for this application.[5] Sevoflurane is one of the most widely used anesthetics, and an exclusive study of the synthetic methods to this compound has been carried out. One industrial synthesis consists of three steps starting with

hexafluoroisopropanol (HFIP) (Scheme 1.1).[3, 6] Easier and more economic synthetic methods are always attractive to both academic and industry.

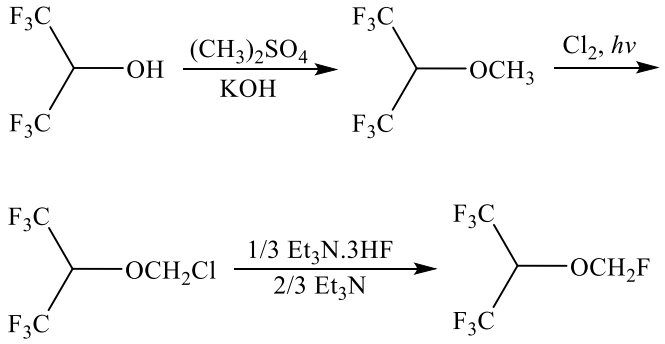

Scheme 3.2. Industrial synthesis of sevoflurane

Other methods were also developed over time,[6a, 7] and many other sevoflurane derivatives and reactions were also prepared in order to enrich this catalog.[8] In Christe's work, the use of strong Lewis acids along with anhydrous HF to convert CF_3OH to either the trifluoromethyloxonium salt $CF_3OH_2^+MF_6^-$or the ether CH_3OCF_3 by introducing CH_3F was reported.[9] Inspired by this work, HFIP and difluoromethane (CH_2F_2, R32) were reacted over a strong Lewis acid (SbF_5, TaF_5, NbF_5, $SbCl_5$, TiF_4) and anhydrous HF, and sevoflurane was synthesized in one step with 95+% yield when the Lewis acid was SbF_5.

Due to restrictions on the use of flammable chemicals in the production plant and difficulty in loading solid catalysts, etc., a preliminary process design was also carried out by varying the ratio of the reagents and catalysts. R32 falls in categories 1,2 of flammable aerosols, which should be used with caution in a chemical plant. The catalysts used are preferred in a liquid form, and SbF_5 and $SbCl_5$ are both liquids under normal condition

while the other catalysts that were used are solids at room temperature. The catalysts are also very easily hydrolyzed and generate hydrogen fluoride when they react with moisture, which might make the large scale loading process even more difficult in a chemical plant.

3.2 RESULTS AND DISCUSSION

Sevoflurane has a formula of $(CF_3)_2CHOCH_2F$, and we initially came up with two ways of assembling the molecule in the presence of strong Lewis acid, namely Method A and Method B as shown in Scheme 3.3.

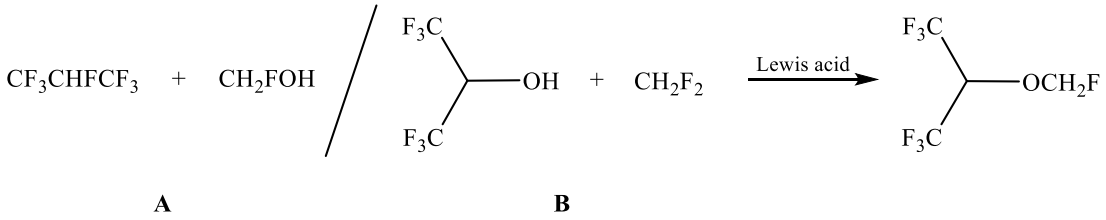

Scheme 3.3. Two ways of assembling sevoflurane

Method **A** requires CH_2FOH, which exists in an equilibrium in the presence of a molar excess amount of HF (eq 3.1). Most of the alcohols having one or more than one fluorine atoms on the alpha carbon are not stable and experience HF elimination, and thus a large excess of HF would help to drive the equilibrium towards the alcohol form.[9]

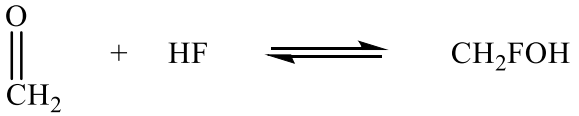

(3.1)

One source of formaldehyde (CH_2O) used was trioxane, which could be depolymerized and release three molar equivalents of CH_2O equilibrating to CH_2FOH in

the presence of HF without producing water (Scheme 3.4). The strong Lewis acid chosen was antimony pentafluoride (SbF_5), which was loaded into a stainless steel reaction cylinder in a dry box. Trioxane was sublimated prior to use, and when it was loaded in the dry box along with SbF_5, heavy white smoke was generated exothermically. It was possible that when the trioxane came in contact with SbF_5, it was vigorously depolymerized into CH_2O. In future experiments, trioxane was instead transferred into the cylinder on a vacuum line over time. The hydrofluorocarbon CF_3CHFCF_3 (HFC-227ea) and HF were then condensed into the cylinder on the vacuum line (Scheme 3.5). The reaction was warmed up to 70-90 °C above the melting point of trioxane over 2 days; however, no desired reactions took place according to the NMR spectroscopy, and 95+% of the HFC-227ea starting material and some black solid were recovered from each trial regardless of the amount of HF used in the reaction (catalytic amount or excess amount).

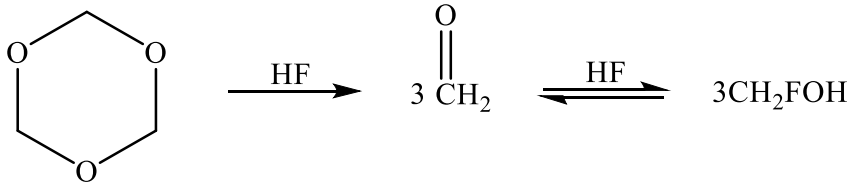

Scheme 3.4. Trioxane as CH_2O source

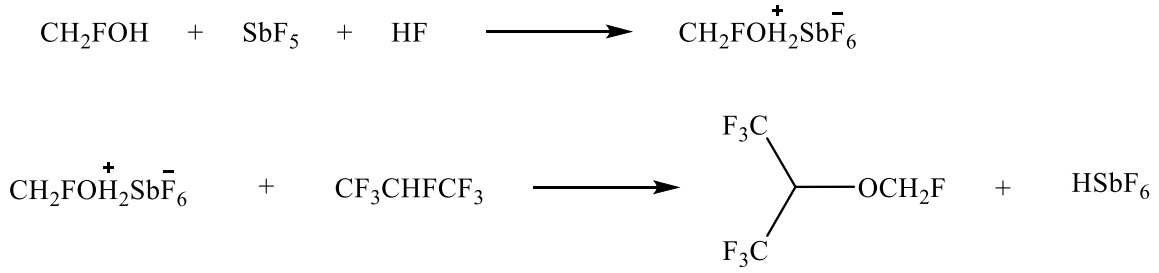

Scheme 3.5. Proposed mechanism of method A

Since Method **A** did not take place, we turned to Method **B** (Scheme 3.3). To examine the formation of the oxonium salt in the proposed Mechanism 1 (Scheme 3.6), equivalent moles of HFIP, HF and SbF_5 were loaded into a perfluoroalkoxy resin (PFA) tube, and when the mixture was kept at room temperature, a milky white solid precipitated out. The mass balanced agreed with the mechanism; however, the crystal structure of the solid was not obtainable, therefore, solid evidence to confirm the formation of the oxonium salt was still lacking. The reaction between SbF_5 and R32 at room temperature was also tested, and no reaction products were observed and the R32 was fully recovered. More advanced analysis method such as neutron diffraction is needed to determine the mechanism of this reaction. In both Mechanisms 1 and 2, a C-F bond of CH_2F_2 must be activated to form an electrophilic carboncation which was attacked by the nucleophilic oxygen of HFIP.

In our group, SbF_5 was chosen to be a starting material as it is one of the strongest Lewis acids knowns and it was available in large quantity in laboratory stock.[10]

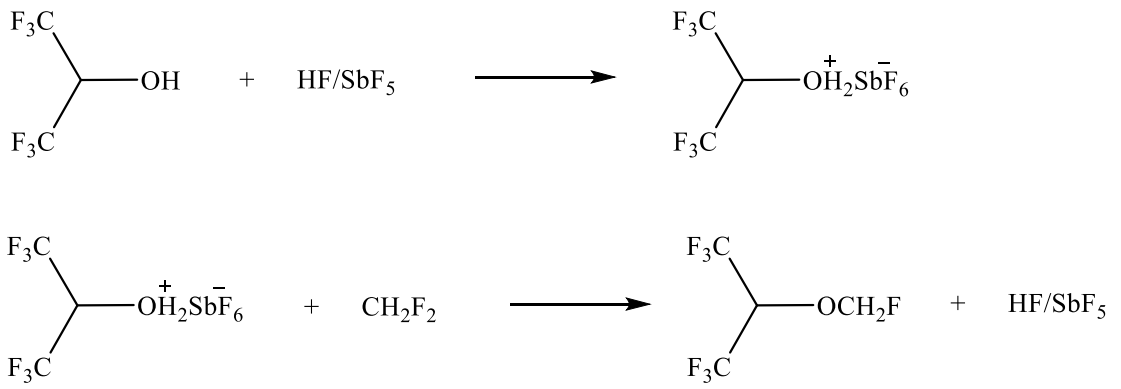

Mechanism 1

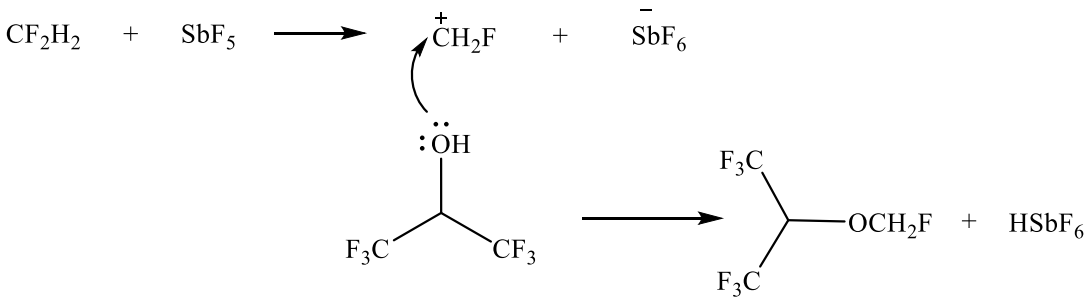

Mechanism 2

Scheme 3.6. Proposed mechanisms of synthesis of sevoflurane with Lewis acids

First, we attempted to only use SbF_5, R32 and HFIP without treating the SbF_5 with HF; however, SbF_5 always carries some HF in it due to trace hydrolysis of the chemical. When HF is in presence, it combines with SbF_5 to form $HSbF_6$, which is a super acid.[10-11] Therefore, it is not certain what kind of role HF plays in these reactions with SbF_5, and it is hard to decide whether it is the Lewis acid or the super-acid that kicks off the reaction.

As shown in Table 3.1, SbF_5 (15.7 mmol), HFIP (15.7 mmol) and R32 (18.1 mmol) were used in equimolar ratio in reaction cycle # 1B-C1. The reaction did not take place at

room temperature; therefore, the mixture was warmed up to 50 °C for 48 h. Upon workup of the reaction, the desired product sevoflurane [$(CF_3)_2CHOCH_2F$] along with a major byproduct 1,1,1,3,3,3-hexafluoro-2-[[2,2,2-trifluoro-1-(trifluoromethyl) ethoxy]methoxy]-propane [$(CF_3)_2CHOCH_2OCH(CF_3)_2$, formal] and a minor byproduct 1,1,1,3,3,3-hexafluoro-2-methoxy-propane [$(CF_3)_2CHOCH_3$, HFMOP] were identified by multinuclear NMR (^1H, ^{19}F) spectroscopy and gas chromatography/mass spectrometry (see Figure 3.1-3.9).

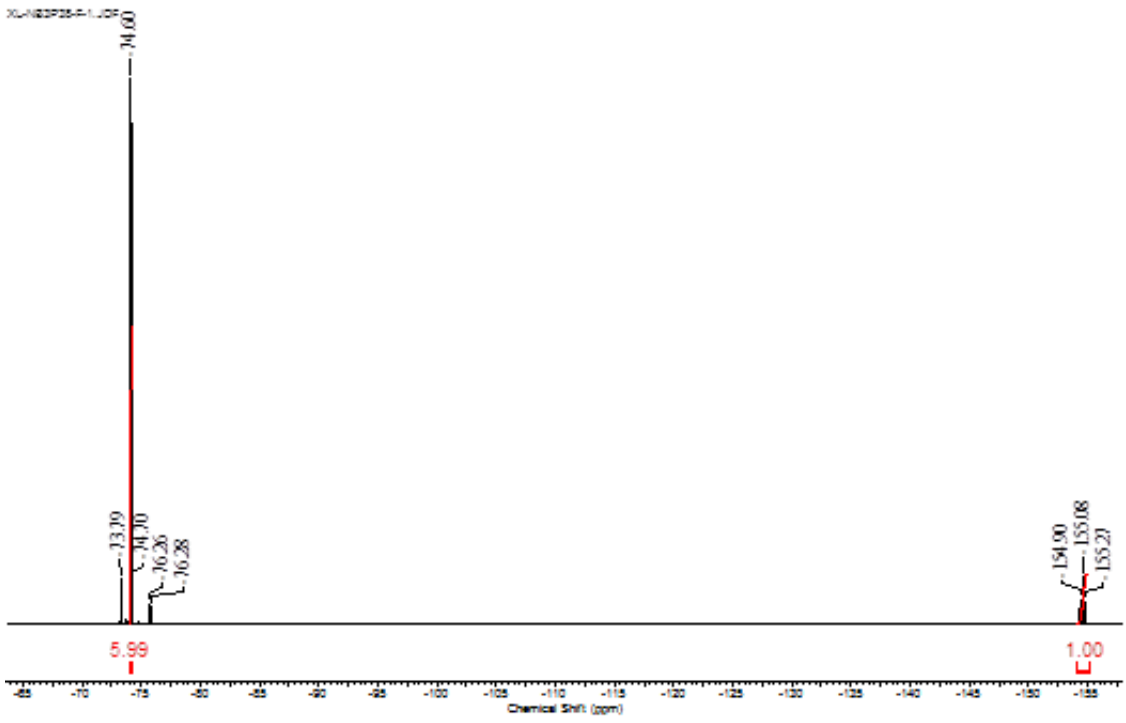

Figure 3. 1 ^{19}F NMR spectrum of the product mixture of 1B-C7.

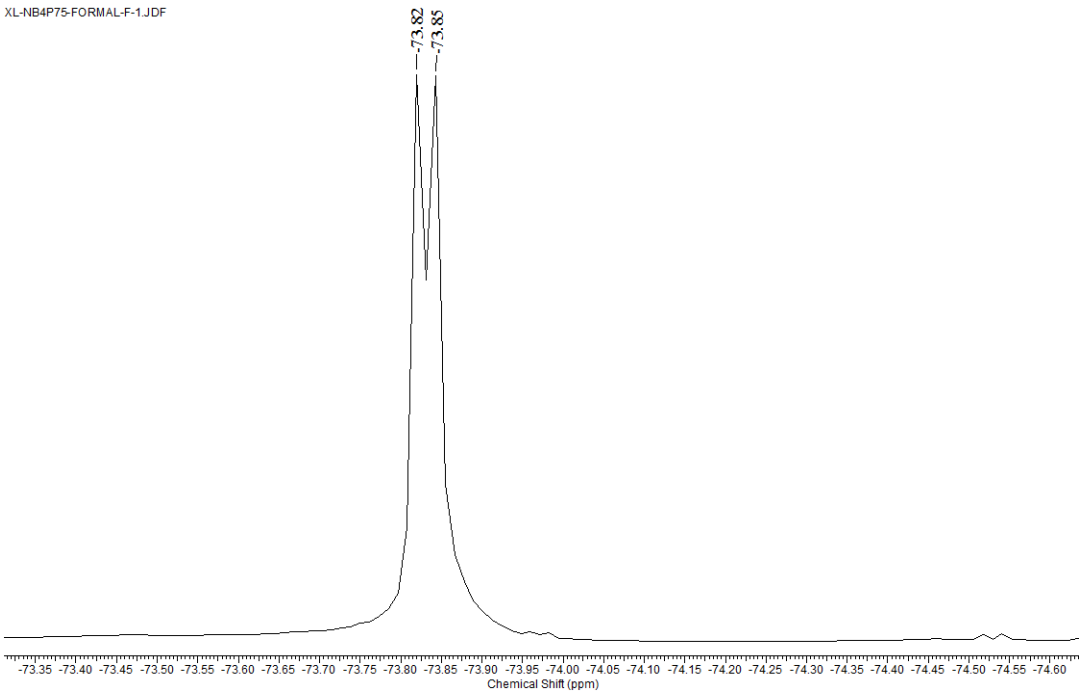

Figure 3. 2 ^{19}F NMR spectrum of formal.

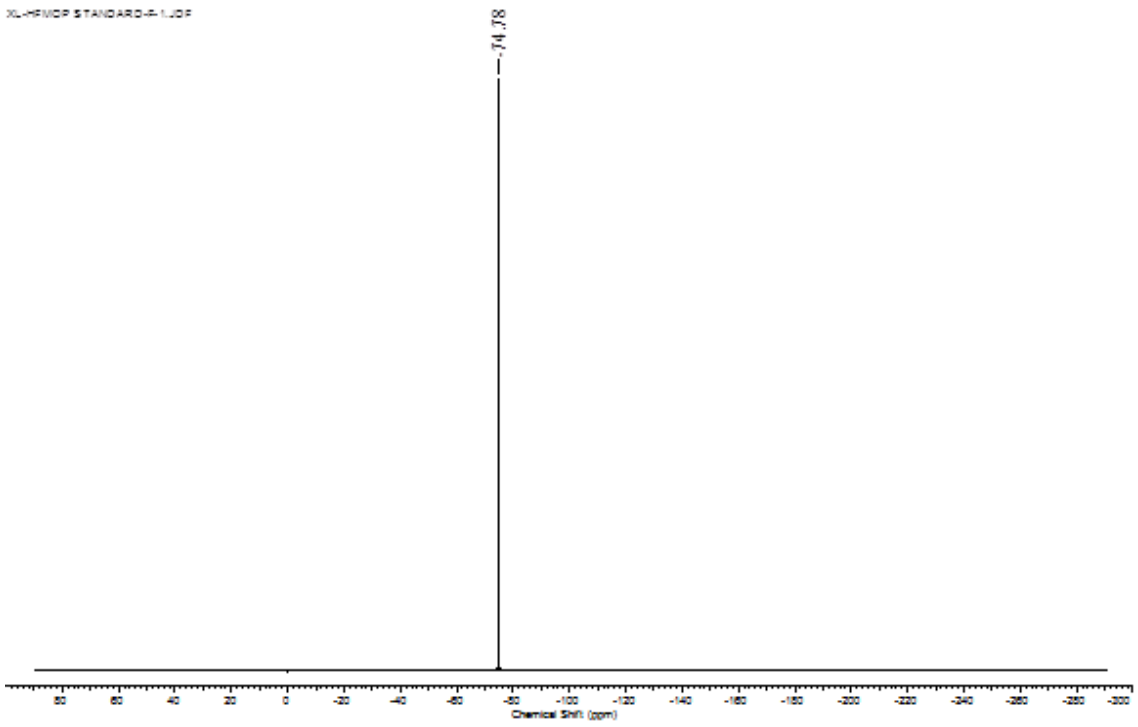

Figure 3.3. ^{19}F NMR spectrum of commercial HFMOP.

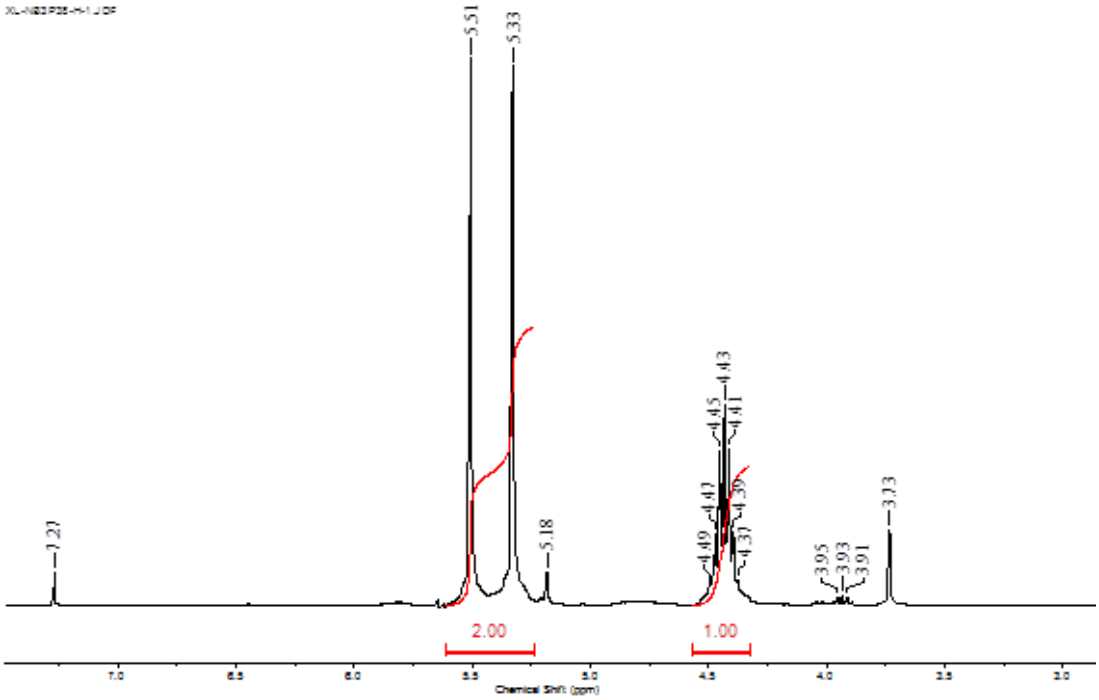

Figure 3.4. ^{1}H NMR spectrum of the product mixture of 1B-C7.

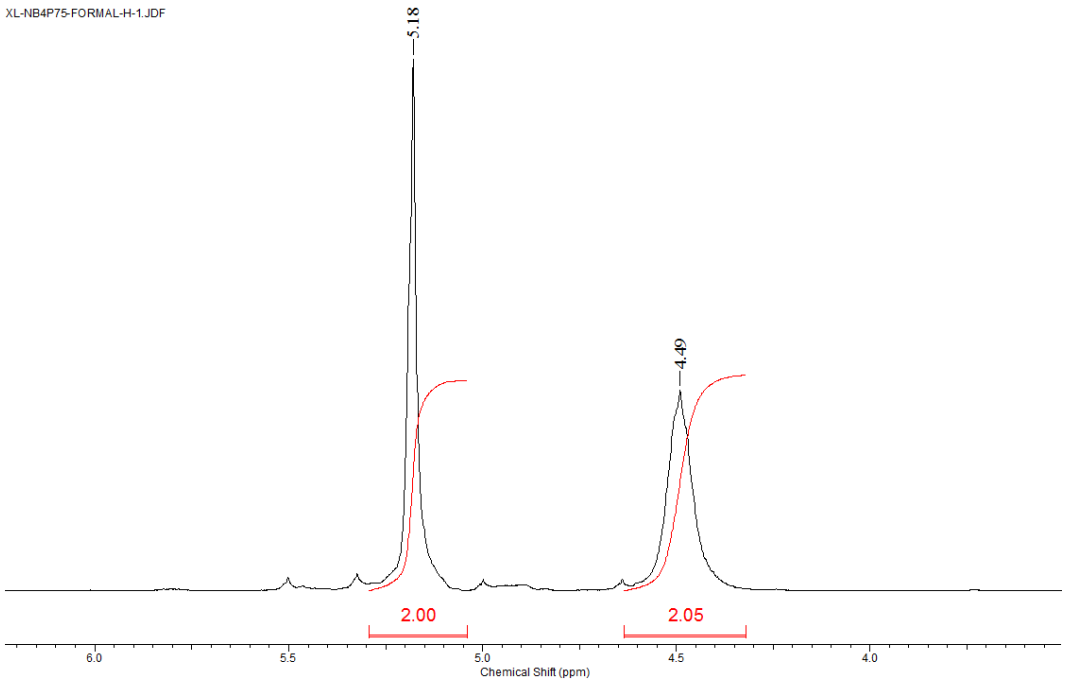

Figure 3.5. ^{1}H NMR spectrum of formal.

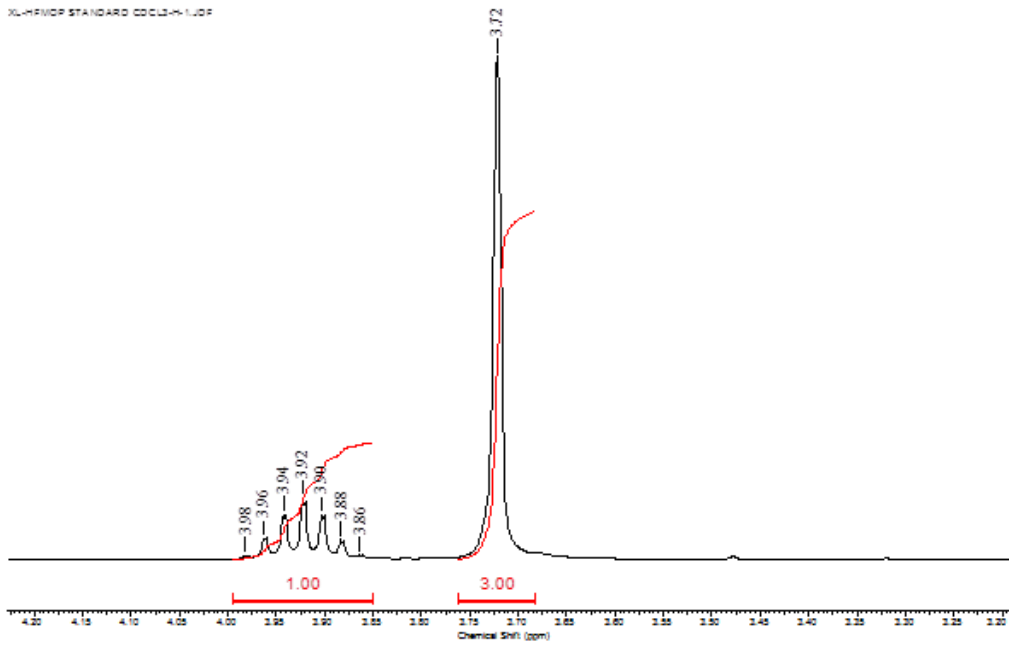

Figure 3.6. ^{1}H NMR spectrum of commercial HFMOP.

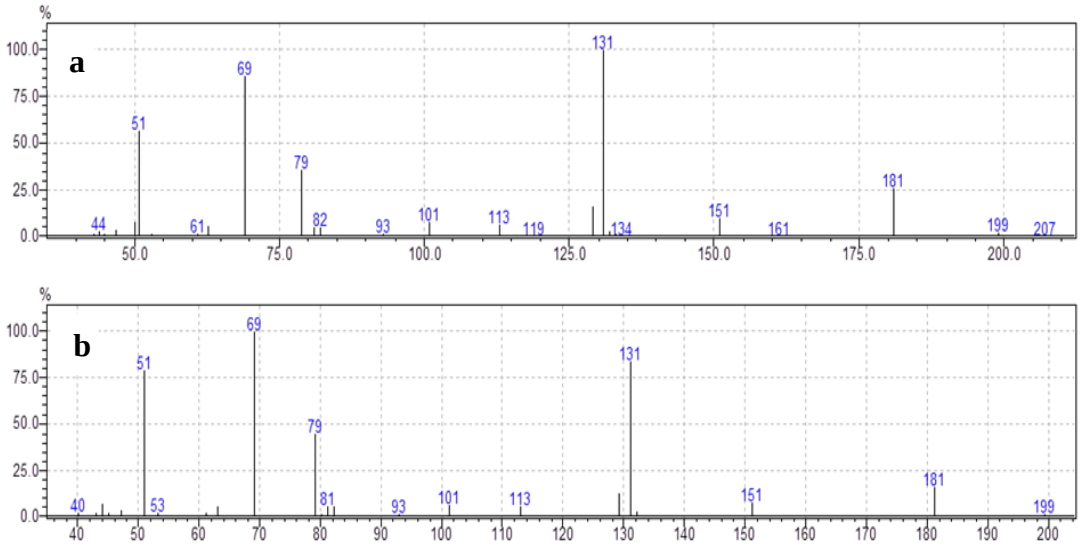

Figure 3.7. a. Mass spectrum of commercial sevoflurane. b. Mass spectrum of synthesized sevoflurane. GC retention time: 17.175 min.

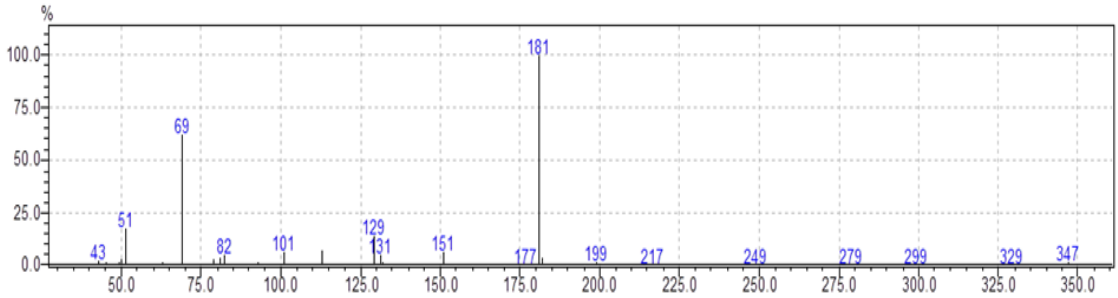

Figure 3.8. Mass spectrum of formal. GC retention time: 27.433 min.

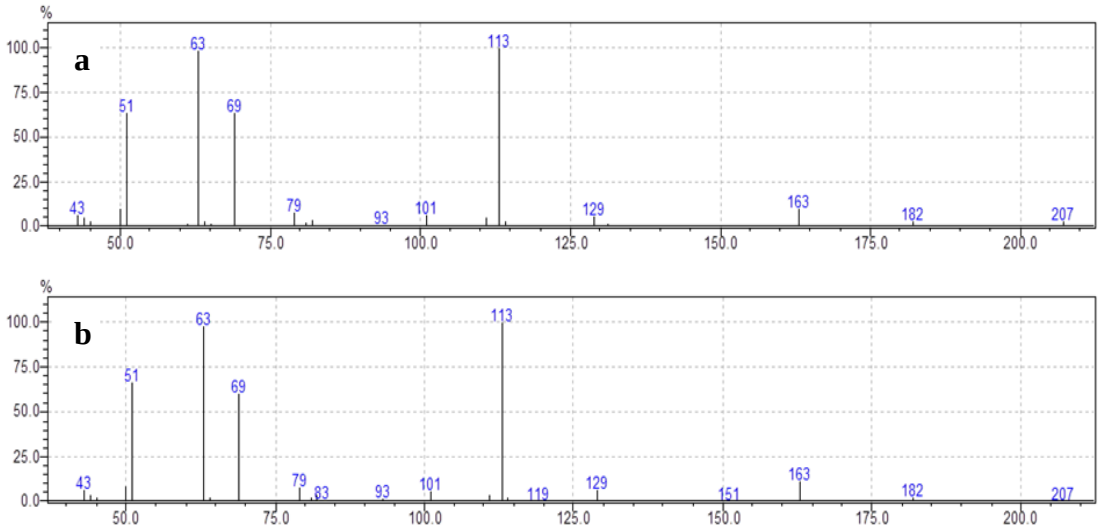

Figure 3.9. a. Mass spectrum of commercial HFMOP. b. Mass spectrum of HFMOP from sevoflurane synthesis. GC retention time: 16.842 min.

It was also discovered that the catalyst salt remaining in the cylinder could be recycled for multiple time. As shown in Table 3.1, the same catalyst remaining from reaction cycle 1B-C1 was used for six more reactions with varying ratios of HFIP to R32 in order to increase the yield of sevoflurane and avoid the formation of the byproducts.

Table 3.1. Reaction Summary of Sevoflurane Synthesis with SbF_5

# of Reactor	SbF_5 (mmol)	HF (mmol)	HFIP (mmol)	Cat (g)	Cycle#	HFIP (mmol)	R32 (mmol)	V (mL)	Temp (°C)	Time (hr)	Yield (%)
1B	15.7	0	15.7	6.0	1B-C1	n/a	18.1	75	50	48	n/a
				6.0	1B-C2	15.8	58.5	75	50-70	n/a	n/a
				5.2	1B-C3	15.4	19.0	75	90	n/a	48
				5.1	1B-C4	0	24.0	75	50-60	100	trace
				5.0	1B-C5	0	32.9	75	50-60	48	0
				5.3	1B-C6	23.8	30	75	55-85	100	27
				4.9	1B-C7	9.0	93.3	75	60-65	16	95+
2B	19.4	19.6	19.6	7.4	2B-C0			75	r.t.		0
				7.9	2B-C1	50.0	54.4	75	55	48	56
				7.4	2B-C2	50.0	51.0	75	60	16	54
				6.2	2B-C3	10.0	64.4	75	50-60	16	99
				6.7	2B-C4	50.0	60.8	75	60-65	16	48
				5.4	2B-C5	9.5	95.4	75	60-65	16	95+

Note: The cycle # means the reactions using the same batch of catalyst (cat) salt in the same reactor. For example, the cat salt in 1B-C1 was continued to be used in 1B-C2. The mass of cat shown in this table is the amount of cat remaining in the cylinder after the reaction. For example, there is 6.0 g cat salt remaining after reaction 1B-C1. Reactions cycle #1B-C1 to #1B-C7 are shown under #1B.

In the reactions under #2B in Table 3.1, cycle #2B-C0 was only for the preparation of the oxonium salt, and one molar equivalent of HF was added. This mixture was used as the catalyst for the following reactions #2B-C1 to #2B-C5.

From all of the reactions under #1B and # 2B, it became obvious that when R32 is used in a large molar excess over HFIP, and meanwhile HFIP is used at about half of the molar amount of SbF_5, the reaction cycles #1B-C7, #2B-C3 and #2B-C5 gave 95+% yield of sevoflurane. The product mixture contained a very high portion of sevoflurane (see **Error! Reference source not found.** and Figure 3.4). The yield of sevoflurane was c alculated by the integration in ^{19}F and ^{1}H NMR spectra versus the mass of the product mixture. One can also observe from the data presented in Table 3.1 and Table 3.5 that the mass of the remaining SbF_5 catalyst decreases after being used more and more, and eventually the mass of the remaining salt remains steadily.

After the successful synthesis of sevoflurane in one step in high yield, it was desirable to ascertain what the exact structure of the SbF_5 catalyst is. Several analytical techniques were used to look for the answer. The Lewis acid SbF_5 was loaded into a reaction cylinder inside a dry box as a liquid, while the catalysts that were taken out of the cylinder after reactions were milky white or slightly brown powders. When the powder was exposed to the moisture, it quickly turned into liquid and hydrolyzed, and when put in contact with water or organic solvents such as acetone, it released white smoke vigorously. The white smoke was probably HF being generated.

The powder taken after the reactions under #B was analyzed by X-ray powder diffraction (XRD). Since the powder was sealed in the cavity of the sample holder with a

layer of amorphous Kapton® tape, the graph had an uneven baseline. It was found that the pattern of the SbF_5-based catalyst matched the pattern of $H_3O^+SbF_6^-$, which has a cubic crystal system (see Figure 3.10-3.11).

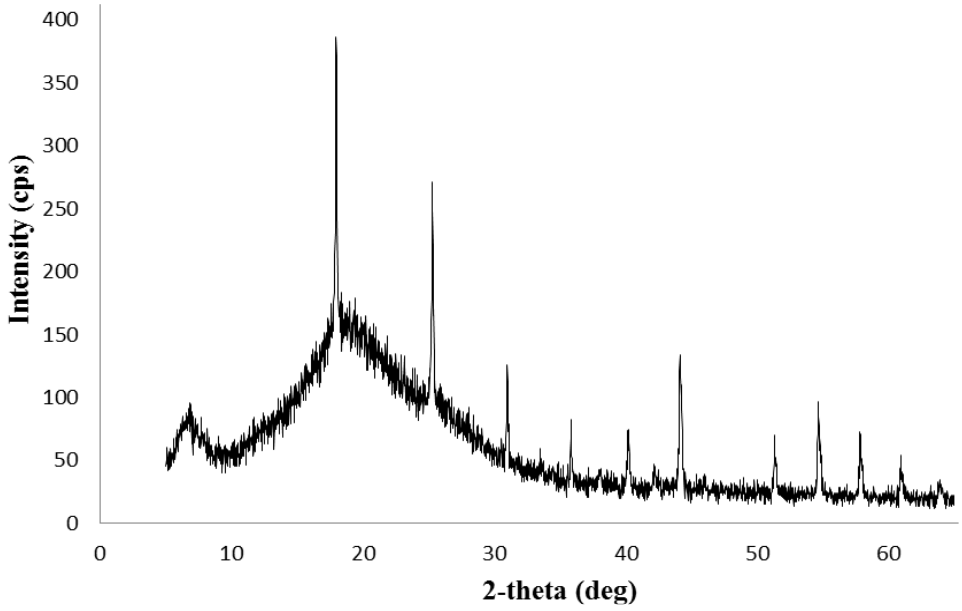

Figure 3.10. XRD of SbF_5-based catalyst after #2B reactions.

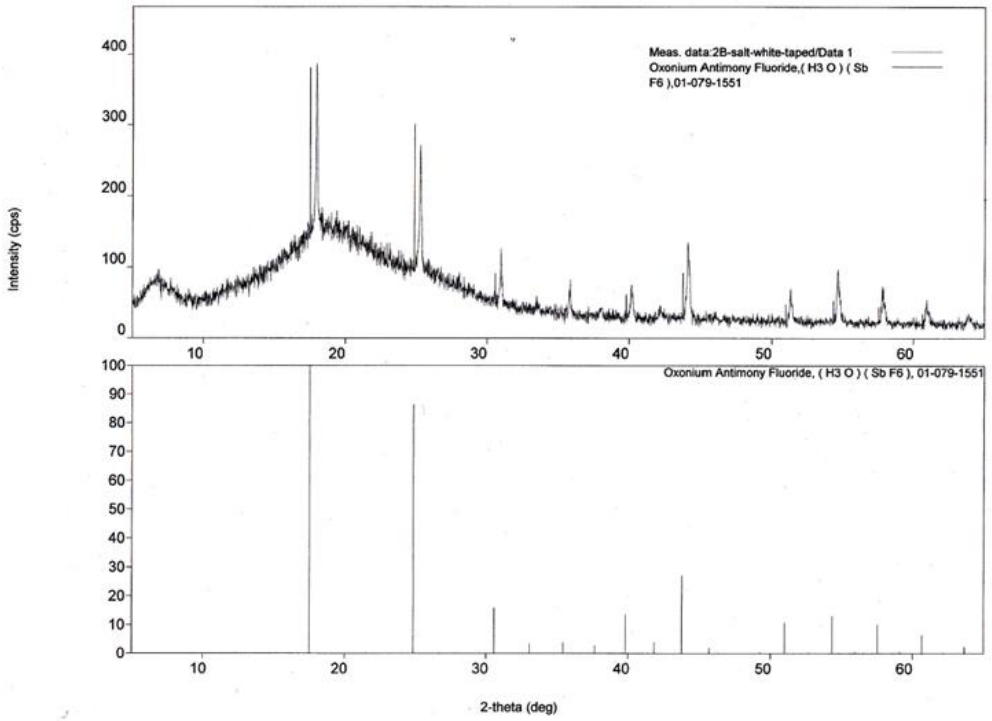

Figure 3.11 XRD comparison of SbF_5-based catalyst and H_3OSbF_6.

Table 3.2. XRD of SbF_5-based Catalyst after #2B Reactions

Peak No.	2-θ (deg)	d (Å)	Height (cps)	Size (ang.)
1	6.43(6)	13.73(13)	81(6)	19.0(6)
2	19.97(6)	4.442(13)	103(7)	9.09022
3	17.944(9)	4.939(2)	188(11)	869(149)
4	25.274(6)	3.5209(8)	144(9)	869(107)
5	30.975(5)	2.8847(5)	63(6)	1290(174)
6	35.80(2)	2.5063(16)	27(4)	719(166)
7	40.17(3)	2.2432(14)	34(5)	561(85)
8	44.114(6)	2.0512(3)	94(8)	671(58)
9	51.312(9)	1.7791(3)	44(5)	1003(193)
10	54.621(5)	1.67885(13)	71(7)	783(65)
11	57.864(9)	1.5922(2)	40(5)	598(57)
12	60.939(10)	1.5190(2)	29(4)	788(105)

The peaks of the catalyst are slightly shifted to the right side of the $H_3O^+SbF_6^-$ peaks[12] by 0.434 2-θ degrees (Table 3.2). According to Bragg's Law:

$$n\lambda = 2d \cdot \sin\theta \tag{3.2}$$

In Equation 3.2, n is a positive integer, λ is the wavelength of X-ray, d is the distance between the planes of the lattice and θ is the incident angle between the X-ray and the plane. The value of θ in SbF_5 catalyst is larger than that of $H_3O^+SbF_6^-$, which means the lattice size of SbF_5-based catalyst is smaller than that of $H_3O^+SbF_6^-$.

The SbF_5-based catalyst was also analyzed with SEM/EDX (see Figure 3.12-3.13); six specimens were taken and compared (see Report 1). The sample appeared to be some white spherical particles with rough surface. The sample may be hydrolyzed on the surface during the transportation from the sample preparation bench to the vacuum chamber due to the lack of protection of the catalyst from moisture in the air. The samples were prepared on carbon tape; therefore, the value of carbon should not be taken into consideration due to the interference of the carbon tape. It was found that, more fluorine atoms were present than was needed to account for only having SbF_5 remaining in the catalyst, which means the another fluorine source, such as HF or HFIP, could be part of the catalyst. The average formula of the catalyst calculated was $SbF_{7.4}O_{3.2}C_x$. One possible conclusion as sor the identity of the catalyst would be $H_2F^+SbF_6^-$, which should have a slightly smaller size than $H_3O^+SbF_6^-$ and very close to the Sb to F ratio 1:7 in the average formula. Regardless of which of the aforementioned mechanisms is correct, one molar equivalent of HF is

generated; therefore, the remaining catalyst after the reactions could be combined with HF. For example, in sample 1, the ratio of Sb to F is 1:10, while only five F atoms are needed to maintain SbF_5. A good amount of oxygen was also presence in each sample, which is likely formed from hydrolysis. Since the composition of elements present in each sample varies largely, it is difficult to come up with a definitive formula for the catalyst.

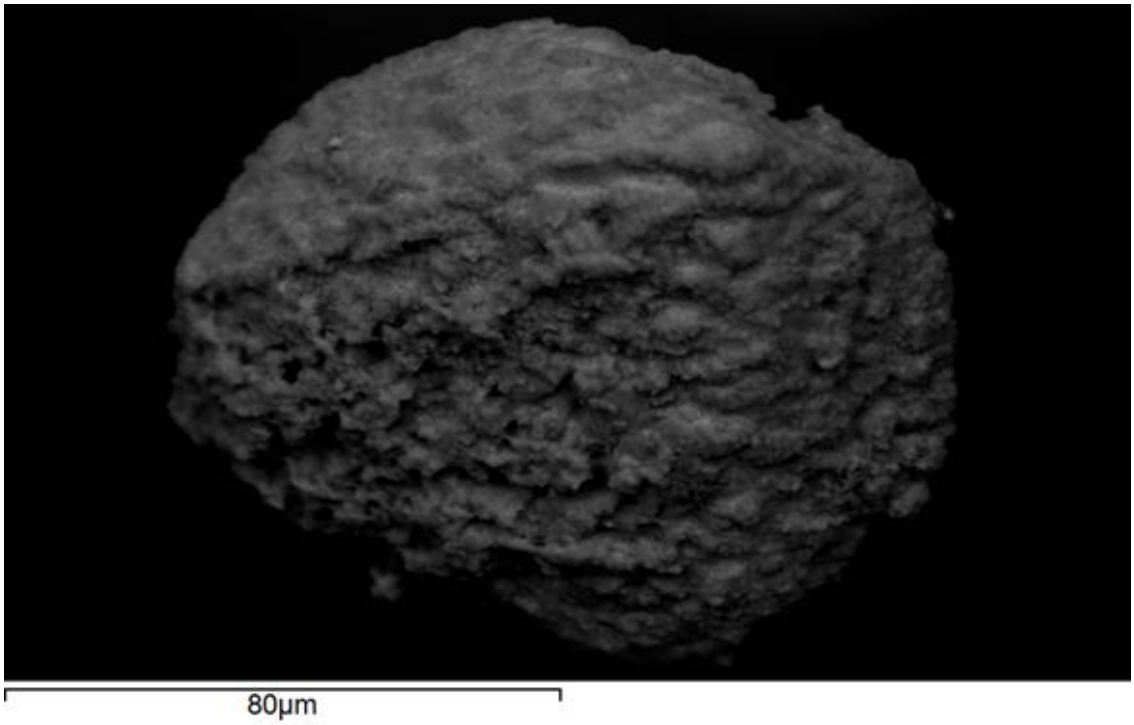

Figure 3.12. SEM of SbF_5-based catalyst.

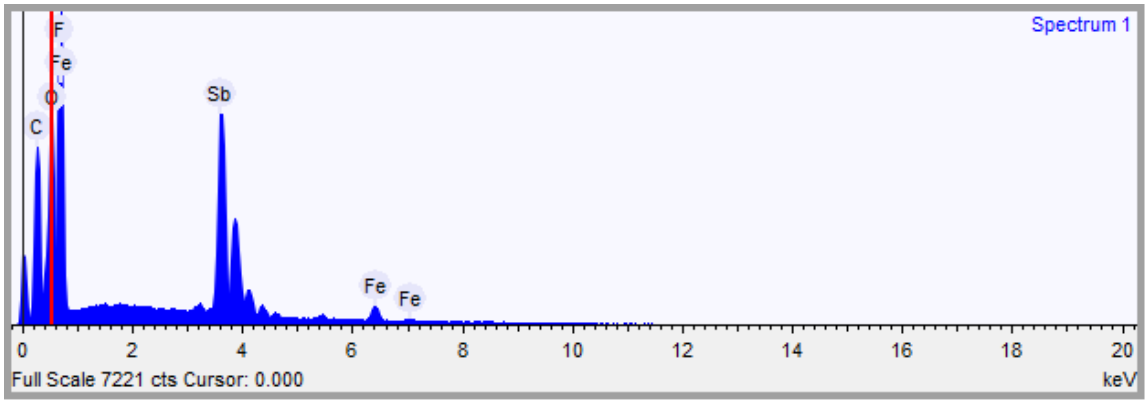

Figure 3.13. EDX of SbF5-based catalyst.

Besides SbF_5, several other strong Lewis acids including $SbCl_5$, TaF_5, NbF_5, TiF_4, SbF_3, $AlCl_xF_y$, BF_3 were used in additional attempts to prepare sevoflurane. The Lewis acids $SbCl_5$, TaF_5, NbF_5, and $HTiF_5$ gave the desired product sevoflurane but in much lower yield when compared to that obtained with the SbF_5-based catalyst at the same molar ratio of reagents. A higher temperature was required as the acidity of the Lewis acid catalyst decreased. For example, a temperature range of 50-100 °C is required to prepare sevoflurane with SbF_5 or SbF_5-based catalysts, while the reactions with $SbCl_5$, TaF_5, NbF_5 and $HTiF_5$ only take place at a relatively higher temperature 100-160 °C (see Table 3.1, 3.3 and Table 3.5). According to our experiments, the yield of sevoflurane with TaF_5 (22%) was lower than the yield of sevoflurane with $HTaF_6$ (51%), while the same was true for NbF_5 (27%) and $HNbF_6$ (45%) reactions (Table 3.3). The experiments of $HTaF_6$ (Cycle# Ta2-C0 and # Ta2-C1) and $HNbF_6$ (Cycle# Nb2-C0 and #Nb2-C1) were carried out by Dr. Andrej Matsnev in the research group.

Table 3.3. Synthesis of Sevoflurane with Lewis Acids other than SbF_5

Reactor#	Catalyst Preparation		Cycle#	Reaction Conditions					
	Lewis Acid (mmol)	HF (mmol)		HFIP (mmol)	R32 (mmol)	V (mL)	Temp (°C)	Time (hr)	Yield (%)
SCl1	17.8 ($SbCl_5$)	0	SCl1-C1	16.7	71.9	75	100	16	5
Ta1	2.6 (TaF_5)	0	Ta1-C1	6	57	75	110 - 120	16	22
Ta2	19.0 (TaF_5)	19.0	Ta2-C0	0	0	75	r.t.	16	n/a
			Ta2-C1	9.5	55	75	120-130	16	51
Nb1	4.4 (NbF_5)	0	Nb1-C1	4.8	25.2	75	120	16	27
Nb2	19.0 (NbF_5)	19.0	Nb2-C0	0	0	75	r.t.	16	n/a
			Nb2-C1	10	55	75	120-130	16	45
Ti1	7.9 (TiF_4)	7.9	Ti1-C0	0	0	75	r.t.	16	n/a
			Ti1-C1	7.9	106.0	75	110-160	1 week	17

The remaining catalyst from reaction #Ta1 cycle #Ta1-C1 was also analyzed with XRD (see Figure 3.14 and

Table 3.4), and a comparison was done with the XRD results of the SbF_5-based catalyst (see Figure 3.15), which reveals a high similarity of the structures of the two catalysts.

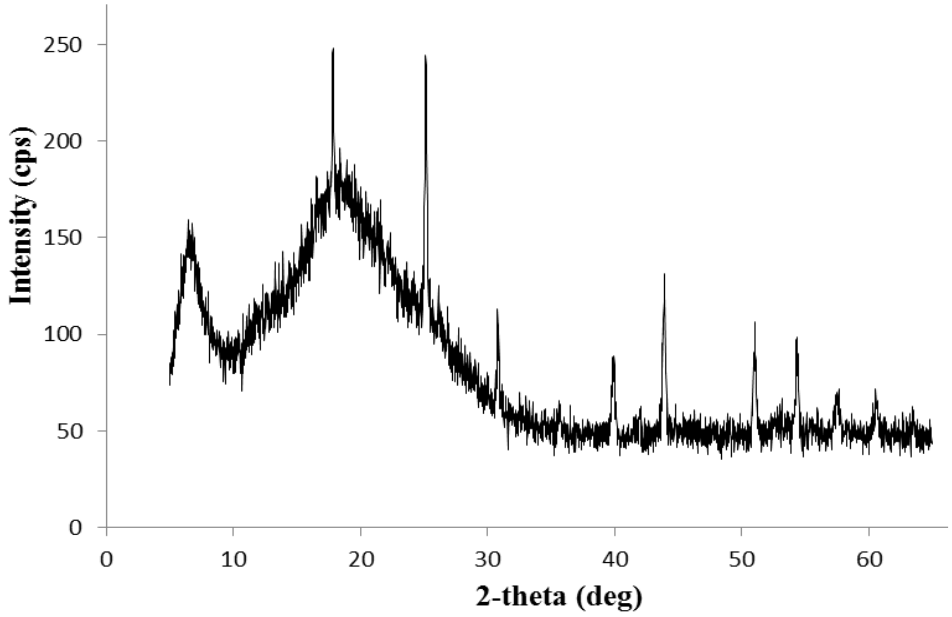

Figure 3.14. XRD of TaF_5-based catalyst after reaction.

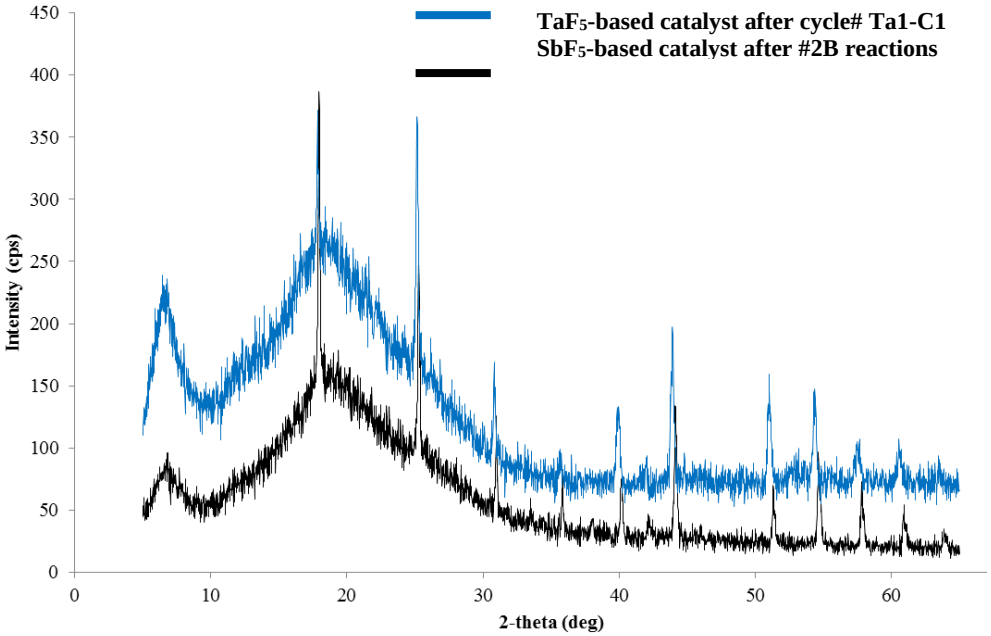

Figure 3.15. XRD results comparison of SbF_5-based catalyst and TaF_5-based catalyst.

Table 3.4. XRD of TaF_5-based Catalyst

No.	2-theta (deg)	d (ang.)	Height (cps)	Size (ang.)
1	6.44(8)	13.72(16)	29(3)	57
2	17.851(15)	4.965(4)	59(5)	746
3	25.146(18)	3.539(2)	106(7)	503
4	30.828(15)	2.8981(14)	40(4)	847
5	39.90(3)	2.2576(17)	27(3)	333
6	43.83(2)	2.0639(9)	57(5)	396
7	51.02(3)	1.7885(9)	36(4)	408
8	54.309(16)	1.6878(5)	39(4)	516

The Lewis acid TiF_4 was the exception of all the effective Lewis acids. When TiF_4 was used without HF treatment prior the reaction, no reaction was observed even at 175 °C. However, in reaction cycle # Ti1-C0, when TiF_4 was treated with one molar equivalent of HF prior to use, reaction took place in cycle # Ti1-C1 at 110-160 °C. Although the yield of sevoflurane was only 17%, it appears evident that HF is necessary to kick off the reaction, at least in the case of TiF_4, which makes Mechanism 1 more likely to be the correct reaction mechanism (Scheme 3.6). The same strategy was attempted with BF_3, and unfortunately no reaction was observed with or without HF treatment of BF_3 prior to use.

When the strong Lewis acids used in this project were combined with one molar equivalent of HF, they form a solid super-acids.[10] Considering the fact that the perfluorinated sulfonic acid resin Nafion®-H is a super acid,[13] if such material can perform as a catalyst in this synthesis, it will be much easier to handle the system for industry. However when Nafion®-H pellets were used as a catalyst, no reaction took place at 80-100 °C.

Based on an overview of the data, a range of the acidity should exists in which the reaction can take place, and higher temperatures might be needed with the less reactive Lewis acids. However, a further survey of additional catalysts and conditions was not carried out. Instead a preliminary process design was investigated in order to find reaction conditions suitable for a potential industrial process. Such a process requires as low as possible molar excess of the Lewis acid catalysts as well as their recyclability due to both the expense and handling difficulties of the catalysts. And although large molar excesses of R32 could readily be recycled based on its boiling point being greatly different from that of sevoflurane, concern did exist on the part of our sponsor with respect to the flammability of R32. On the other hand, R32 is used as a refrigerant, usually in blends, although Daikin has proposed to use this material as a single-component refrigerant.[14]

Various reactants ratios and pressures were tried out for reactions from #1 to #8 as shown in Table 3.5 in Section 3.4.14. It was expected that a higher pressure might result in higher yield of sevoflurane, however, increasing the pressure of the reaction did not improve the yield of sevoflurane nor did it have any other impacts on the process. For instance, in reaction cycle # 4-C1 and #6-C2, the catalysts were prepared in the same way, and the ratio of SbF_5:HFIP:R32 was 2:1:3.4. The initial pressure of #4-C1 was 628.9 psi and 368.5 psi for #6-C2; however, the yield of sevoflurane was 44% in #4-C1 and 69% in #6-C2.

The reaction normally took several hours to complete. Under the same conditions, some reactions were stopped in 3 h, and they had lower yields of sevoflurane when compared with those runs that went for a longer time. For example, reaction cycle #2-C2,

#2-C3 and #2-C4 were carried out under similar reaction conditions, except that #2-C4 had a much shorter reaction time. The yield of sevoflurane in #2-C4 was 44%, while the yield of sevoflurane was 51% for #2-C2 and 68% for #2-C3. Although considerable human errors could occur during the running and workup of these reactions, the results were quite reproducible.

3.3 CONCLUSION AND FUTURE WORK

The goal of the project was accomplished in that sevoflurane was successfully synthesized in one step with very high yield by using a strong Lewis acid (SbF_5) or its combination with anhydrous HF as catalyst. This method largely reduced the complexity of the current industrial synthetic methods. Besides the Lewis acids attempted in the above work, another Lewis acid AsF_5 will also be attempted to prepare sevoflurane. If the reaction could be carried out with deuterium fluoride (DF), neutron diffraction might be an option to gain more information, especially on the role DF plays in the system. In terms of process design, if a continuous flow control experiment would have been carried out, the dynamics of the reaction could have been studied in much better detail.

3.4 EXPERIMENTAL

3.4.1 Reagents and synthetic equipment

Antimony pentafluoride (SbF_5) and difluoromethane (CH_2F_2, R32) were purchased from SynQuest; tantalum pentafluoride (TaF_5) and niobium pentafluoride (NbF_5) were purchased from STEM Chemical; titanium tetrafluoride (TiF_4) was purchased from Alfa Aesar; chlorine (Cl_2) was purchased from Specialty Gases of America; hexafluoroisopropanol (HFIP) was purchased from Oakwood Chemical; HFMOP and

sevoflurane were provided by Piramal Enterprises; antimony trichloride ($SbCl_3$) was purchased from Sigma-Aldrich Corporation; HF was purchased from Air Products & Chemicals, Inc. Deuterated chloroform was purchased from Cambridge Isotope Laboratories, Inc.. The chemicals were used without further purification. Stainless steel cylinders (75-mLcapacity) were purchased from Hoke®, while, valves were purchased from Swagelok®.

3.4.2 Instrumentation.

NMR spectroscopic data was collected on a multinuclear JOEL ECX-300 Spectrometer. The frequency is 300 MHz for ^{1}H, 282.78 MHz for ^{19}F and 75.57 MHz for ^{13}C respectively. Multiplicities are as follows: s (singlet), d (doublet), t (triplet), m (multiplet), dd (doublet of doublet), td (triplet of doublet), tt (triplet of triplet), tm (triplet of multiplets), and sep (septet). The internal standard for ^{19}F NMR spectroscopy is CF_3Cl (0.00 ppm). GC/MS data was collected on a SHIMADZU GCMS-QP5000 instrument. XRD data was collected on an Ultima IV X-Ray Diffractometer. SEM/EDX data was collected on a Hitachi TM 3000 tabletop Scanning Electron Microscope. ATR-IR spectra were collected on a Thermo Scientific Nicolet iS5 diamond ATR spectrometer.

GC column information: Restek Rxi®-5HT column, 30m, 0.25 mm i.d., 0.25 μm.

GC/MS method: Initial Temperature: 250 °C. Interface Temperature: 250 °C. Control Mode: Split. Column Inlet Pressure: 94.8 kPa. Column Flow: 0.5 mL/min. Linear Velocity: 13.6 cm/sec. Split Ratio: 20. Total Flow: 13.3 mL/min. Oven Temperature Program: 35 °C ramp to 50 °C at a rate of 5 °C/min, and isothermal at 50 °C for 30 min. Ramp from 50 °C to 290 °C at a rate of 30 °C/min.

3.4.3 General preparation of Lewis acid catalysts.

The Lewis acid catalysts used were SbF_5, TaF_5, NbF_5, TiF_4, and $SbCl_5$. They treated with one molar equivalent of anhydrous HF before use. However, SbF_5, TaF_5, NbF_5 can also be used directly without HF treatment, and $SbCl_5$ was used neat without any HF treatment in all cases. After treatment with one molar equivalent of anhydrous HF, the Lewis acids SbF_5, TaF_5, NbF_5, TiF_4 are thought to exist in the form of $HSbF_6$, $HTaF_6$, $HNbF_6$ and $HTiF_5$ respectively.[10-11]

3.4.4 General synthetic method.

To a 75-mL stainless steel (SS) cylinder containing catalyst loaded in the dry box, HFIP and R32 were condensed into the cylinder on the vacuum line at liquid nitrogen temperature. The cylinder was well sealed, and its contents heated up to 50 ~ 160 °C. The reaction can be worked up with two procedures as described below, and the remaining catalyst in the reactor can be reused or recycled for multiple reactions.

Work up procedure: After the reaction was stopped by cooling down to room temperature, the volatile materials including excess R32, unreacted HFIP, HF and products were condensed on bulk 10 wt% K_2CO_3 soln in a second cylinder in order to scrub the HF generated from the reaction. This second cylinder was warmed up to room temperature on a shaker for 30 min, and then carefully opened in a fume hood in order to release the pressure of excess R32. The remaining liquid phase at the bottom of the cylinder was pipetted out, and this bottom phase was the products phase, which was analyzed by NMR spectroscopy and GC/MS.

3.4.5 Synthesis of sevoflurane with SbF_5.

To a 75-mL stainless steel cylinder, 3.4 g (15.7 mmol) SbF_5 was loaded in a dry box. A quantity of 1.5 g (9.0 mmol) HFIP and 4.9 g (93.3 mmol) R32 were then transferred on vacuum line into the cylinder being held at liquid nitrogen temperature. The cylinder was heated up to 60-65 °C overnight. After the reaction was worked up, the products phase was analyzed by NMR spectroscopy, showing a yield of 95+% sevoflurane. Trace amounts of formal and HFMOP were generated as byproducts.

3.4.6 Synthesis of sevoflurane with $HSbF_6$.

To a 75-mL stainless steel cylinder containing 4.6 g (19.4 mmol) catalyst prepared from SbF_5, a quantity of 1.7 g (10 mmol) HFIP and 3.4 g (64.4 mmol) R32 were transferred on vacuum line into the cylinder being held at liquid nitrogen temperature. The cylinder was heated up to 50-65 °C for 16 hrs. After the reaction was worked up, the product phase was analyzed by NMR spectroscopy, showing a yield of 95+% sevoflurane. Trace amounts of formal and HFMOP were generated as byproducts.

^{19}F NMR chemical shifts:

$(CF^a_3)_2CHOCH_2F^b$: δ_a = -74.60 ppm (s), δ_b = -155.08 ppm (t, $^2J_{HF}$ = 52.6 Hz)

$(CF^a_3)_2CHOCH_2OCH(CF_3)_2$: δ_a = -73.84 ppm (d, $^3J_{HF}$ = 8.5 Hz)

Commercial $(CF^a_3)_2CHOCH_3$: δ_a = -74.78 ppm (s)

^{1}H NMR chemical shifts:

$(CF_3)_2CH^aOCH^b_2F$: δ_a = 4.43 ppm (sep, $^3J_{HF}$ = 5.9 Hz), δ_b = 5.42 ppm (d, $^2J_{HF}$ = 53.7 Hz)

$(CF_3)_2CH^aOCH^b_2OCH(CF_3)_2$: δ_a = 4.49 ppm (s), δ_b = 5.18 ppm (s).

Commercial $(CF_3)_2CH^aOCH^b{}_3$: δ_a = 3.92 ppm (sep, $^3J_{HF}$ = 5.9 Hz), δ_b = 3.72 ppm (s)

Mass spectra, m/z (relative intensity, %):

$(CF_3)_2CHOCH_2F$: 199 (2.51) $[M-H]^+$, 181 (18.8) $[M-F]^+$, 151 (9.2) $[CF_3CHCF_3]^+$, 131 (84.2) $[M-CF_3/CF_3CCF_2]^+$, 113 (6.5) $[CF_3CHCF/CF_2CHCF_2]^+$, 101 (7.0) $[CF_3CHF]^+$, 93 (1.7) $[CF_3CC]^+$, 81 (6.0) $[CF_3C]^+$, 79 (46.9) $[CF_2CHO]^+$, 69 (100.0) $[CF_3]^+$.

$(CF_3)_2CHOCH_2OCH(CF_3)_2$: 347 (1.8) $[M-H]^+$, 279 (0.8) $[M-CF_3]^+$, 181 (100.0) $[M-CF_3CH(CF_3)O]^+$, 151 (6.5) $[CF_3CHCF_3]^+$, 82 (5.2) $[CF_3CH]^+$, 69 (65.5) $[CF_3]^+$.

$(CF_3)_2CHOCH_3$: 182 (3.5) $[M]^+$, 163 (10.3) $[M-F]^+$, 129 (6.1) $[CF_3CH(O)CF/CF_2CH(O)CF_2]^+$, 113 (100.0) $[CF_3CHCF/CF_2CHCF_2]^+$, 101 (6.6) $[CF_3CHF]^+$, 93 (1.6) $[CF_3CC]^+$, 79 (8.3) $[CF_2CHO]^+$, 69 (64.2) $[CF_3]^+$.

3.4.7 Synthesis of $SbCl_5$

An amount of 3 g $SbCl_3$ was added to a 500-mL, three-necked flask. The flask was equipped with a magnetic stir bar and a condenser that was cooled with dry ice and an n-propanol slush bath and topped with a bubbler. Chlorine gas was slowly passed above the solid at room temperature with stirring.[15] The Cl_2 gas flow was stopped after all of the solid turned to a yellow colored liquid. The total mass increased to 3.5 g, and the yield of $SbCl_5$ was 89%. The liquid was used without further purification.

3.4.8 Synthesis of sevoflurane with $SbCl_5$.

An amount of 5.3 g (17.8 mmol) $SbCl_5$ prepared by treating $SbCl_3$ with Cl_2 at room temperature was loaded to a 75-mL stainless steel cylinder, and the cylinder was degassed on the vacuum line. To this cylinder, 2.8 g (16.7 mmol) HFIP and 3.7 g (71.9 mmol) R32

were condensed on the vacuum line. The cylinder was warmed up to 100 °C overnight. The yield of sevoflurane was 5%, and the main byproduct was formal.

3.4.9 Synthesis of sevoflurane with TaF_5 without HF treatment.

To a 75-mL stainless steel cylinder, 0.7 g (2.6 mmol) TaF_5 was loaded in the dry box, and 1 g (6 mmol) HFIP and 3.0 g (57 mmol) difluoromethane (R32) were transferred on vacuum line at liquid nitrogen temperature. The contents of the cylinder were heated up to 110-120 °C for overnight. After the reaction being worked up, the products phase was analyzed by NMR spectroscopy, showing a yield of 22% sevoflurane. A trace amount of formal was generated as a byproduct**.**

3.4.10 Synthesis of sevoflurane with $HTaF_6$.

To a 75-mL stainless steel cylinder containing 5.6 g (19 mmol) $HTaF_6$, 1.6 g (9.5 mmol) HFIP and 2.9 g (55 mmol) difluoromethane (R32) were transferred on vacuum line at liquid nitrogen temperature. The contents of the cylinder were heated up to 120-130 °C overnight. After the reaction being worked up, the product phase was analyzed by NMR spectroscopy, showing a yield of 51% sevoflurane. 4% formal, and 1 % HFMOP.

3.4.11 Synthesis of sevoflurane with NbF_5

To a 75-mL stainless steel cylinder, 0.8 g (4.4 mmol) NbF_5 was loaded in the dry box, and 0.8 g (4.8 mmol) HFIP and 1.3 g (25.2 mmol) R32 were condensed into the cylinder on the vacuum line at liquid nitrogen temperature. The contents of the cylinder were heated up to 120-130 °C overnight. After the reaction being worked up, the product

phase was analyzed by NMR spectroscopy, showing a yield of 26% sevoflurane and 6% formal.

3.4.12 Synthesis of sevoflurane with $HNbF_6$

To a 75-mL stainless steel cylinder containing 3.9 g (19 mmol) $HNbF_6$, 1.7g (10 mmol) HFIP and 2.9g (55 mmol) difluoromethane (R32) were transferred on vacuum line at liquid nitrogen temperature. The contents of the cylinder were heated up to 120-130 °C overnight. After the reaction being worked up, the product phase was analyzed by NMR spectroscopy, which showed a yield of 45% sevoflurane and 3% formal.

3.4.13 Synthesis of sevoflurane with $HTiF_5$.

To a 75-mL stainless steel cylinder containing 1.9g (7.9 mmol) $HTiF_5$, 1.3g (7.9 mmol) HFIP and 5.5g (106 mmol) difluoromethane (R32) were transferred on vacuum line at liquid nitrogen temperature. The contents of the cylinder were heated up to 110 °C for 1 week, then 160 °C overnight. After the reaction was worked up, the product phase was analyzed with NMR spectroscopy, showing a yield of 17% sevoflurane, 12 % formal, and 3% HFMOP.

3.4.14 Process design for sevoflurane production

The synthesis of sevoflurane was performed with various molar ratios of the starting materials in order to find out the best conditions for having reasonable yield with the lowest use of a catalyst and an excess of R32 (see Table 3.6). The procedure of each reaction was following the general procedure. The pressure was calculated from PV = nRT, in which V is the volume of the reaction cylinder, n is the mole of R32, and T is the reaction temperature. The pressure was not monitored by pressure gauge.

Table 3.5. Preliminary Process Design of Sevoflurane Synthesis with SbF_5

#	SbF_5 (mmol)	HF (mmol)	HFIP (mmol)	Cat Salt (g)	Cycle #	HFIP (mmol)	R32 (mmol)	V (mL)	Temp (°C)	Initial Pressure (psi)	Time (hr)	Yield (%)
1	10.2	12.5	10.1	3.8	1-C0	0	0	10	rt	0		0
				4.2	1-C1	10.1	9.7	10	60	473	12	32
				3.3	1-C2	5.1	15.6	10	60	716	12	49
				3.1	1-C3	2.7	10	10	50	434	12	<30
				3.1	1-C4	2.7	11.2	10	60	498	12	<30
2	6.4	8	6.4	2.3	2-C0		0	30	rt	0		0
				1.9	2-C1	6.4	34.2	30	60	476.0	12	66
				1.7	2-C2	3.2	32.7	30	50	428.9	12	51
				1.5	2-C3	3.2	31.3	30	60	424.0	12	68
				1.4	2-C4	3.3	34.8	30	70	485.1	3	44
				1.4	2-C5	6.4	57.3	30	87	847.8	3	69
				1.3	2-C6	3.2	34.4	30	85	500.5	3	<1%
3	10.0	12.5	10	3.8	3-C0	0	0	10	rt	0	16	0
				3.4	3-C1	10.1	10.8	10	60	525.6	12	37
				n/a	3-C2	5.1	14.4	10	50	641.7	12	n/a
4	8.3	7	8.3	3.0	4-C0	0	0	10	rt	0	16	0
				3.1	4-C1	4.2	14.0	10	60	628.9	3	44
6	37.2	23.9	37.2	14.7	6-C0	0	0	75	rt	0	16	0
				13.8	6-C1	18	108	75	70	634.2	16	89
				12.9	6-C2	19.6	65	75	70	368.5	21	69
				12.9	6-C3	18.1	110.	75	70	623.1	3	57
7	20.3	20	20	8.4	7-C0	0	0	75	rt	0	16	0
				7.7	7-C1	40	144	75	80	865.5	16	73
				n/a	7-C2	5	10	75	80	57.1	16	40
8	6.3	4.0	calcd	2.1	8-C0	0	0	75	rt	0	16	0
				2.0	8-C1	18.4	99.6	75	83	588.5	20	66
				1.9	8-C2	25	175.	75	85	1055.5	16	59
				1.6	8-C3	25	175.	75	95	1085.0	16	69
				1.6	8-C4	25	175.	75	85	1055.5	16	60
Note: For example, Cycle# 1-C0 to #1-C4 were carried out in the same cylinder #1 and the catalyst												

Table 3.6. Selected Sevoflurane Synthesis Reactions with Various Starting Material Ratios

SbF_5-based CAT/HFIP	R32/HFIP	Yield of Sevo (%)
2.04	10.04	95
2.01	3.08	49
2.00	3.37	44
1.94	6.44	100
1.02	1.23	48
1.00	5.32	66
0.39	1.09	56
0.25	7.00	69
0.01	10.70	34

3.4.15 SEM/EDX analysis of the catalysts

The powder sample was carefully scattered on the aluminum sample holder which was covered with a layer of dark carbon tape. The sample holder was quickly installed in the vacuum chamber, then vacuum was applied to the chamber. The formula of the catalyst was calculated from the six specimens analyzed with EDX. The average formula of the catalyst is $SbF_{7.4}O_{3.2}C_x$.

Report 1. SEM/EDX Report of SbF_5-based Catalyst on TM-3000.

Acquisition conditions

Acquisition time (s) 30.0 Process time 5

Accelerating voltage (kV) 15.0

Summary results

Sample 1				
Element	Weight %	Weight % σ	Atomic %	# of atoms
Carbon	17.296	0.202	30.983	6.564
Oxygen	12.005	0.179	16.145	3.421
Fluorine	41.757	0.317	47.291	10.019
Antimony	26.707	0.200	4.720	1.000
Sample 2				
Carbon	17.508	0.249	32.279	5.595
Oxygen	15.867	0.238	21.961	3.807
Fluorine	33.999	0.434	39.63	6.869
Antimony	31.716	0.282	5.769	1.000
Sample 3				
Carbon	16.867	0.208	30.484	5.839
Oxygen	12.926	0.192	17.537	3.359
Fluorine	40.922	0.281	46.758	8.956
Antimony	29.285	0.208	5.221	1.000
Sample 4				
Carbon	8.813	0.206	18.953	2.211
Oxygen	13.499	0.194	21.794	2.542
Fluorine	37.275	0.339	50.679	5.911
Antimony	40.413	0.281	8.574	1.000
Sample 5				
Carbon	12.886	0.2	25.568	3.619
Oxygen	14.303	0.188	21.304	3.016
Fluorine	36.721	0.3	46.064	6.521
Antimony	36.09	0.237	7.064	1.000
Sample 6				
Carbon	14.104	0.231	27.734	3.949

Oxygen	14.868	0.22	21.949	3.125
Fluorine	34.825	0.346	43.295	6.165
Antimony	36.203	0.271	7.023	1.000

3.4.16 XRD analysis of the catalysts

A silicon zero background sample holder with a shallow cavity in the center where the powder sample can be analyzed was used. The powder catalyst was loaded to the cavity in the dry box and protected with a layer of Kapton® tape. The Kapton® tape prevented the sample from being in contact with the moisture in the air. Each sample was analyzed from 5° to 65° at a rate of 1°/min at room temperature.

3.5 REFERENCES

1. Khan, K. S.; Hayes, I.; Buggy, D. J. Pharmacology of anaesthetic agents II: inhalation anaesthetic agents. *Contin. Educ. Anaesth. Crit. Care Pain* **2013,** *14*, 106-111.

2. (a) Jones, W. G. M. Inhalation Anesthetics of the Organofluorine Class. In *Preparation, Properties, and Industrial Applications of Organofluorine Compounds;* Bank, R. E., Ed.; Ellis Horwood Linited: Chichester, 1982; pp 157-192; (b) Halpern, D. F. Fluorinated Inhalation Anesthetics. In *Organofluorine Chemistry: Principles and Commercial Applications*; Banks, R. E.; Smart, B. E.; Tatlow, J. C., Eds.; Plenum Press: New York, 1994; pp 543-554.

3. Regan, B. M.; Long, J. C. Method of Anesthesia. U.S. Patent 3,683,092, Aug 8, 1972.

4. Eger, E. I., II. Characteristics of Anesthetic Agents Used for Induction and Maintenance of General Anesthesia. *Am. J. Health Syst. Pharm.* **2004,** *61 (Suppl. 4), S3-S10.*

5. Terrell, R. C. The Invention and Development of Enflurane, Isoflurane, Sevoflurane, and Desfluran. *Anesthesiology* **2008,** *108*, 531-533.

6. (a) Kudzma, L. V.; Huang, C. G.; Lessor, R. A.; Rozov, L. A.; Afrin, S.; Kallashi, F.; McCutcheon, C.; Ramig, K. Diisopropylethylamine Mono (Hydrogen Fluoride) for Nueclophilic Fluorination of Sensitive Substrates: Synthesis of Sevoflurane. *J. Fluorine Chem.* **2001,** *111*, 11-16; (b) Croix, L. S. Fluorinated Isopropyl Derivatives. U.S. Patent 3,911,024, Oct. 7, 1975.

7. (a) Prakash, G. K. S.; Ledneczki, I.; Chacko, S.; Olah, G. A. Direct Electrophilic Monofluoromethylation. *Org. Lett.* **2008,** *10*, 557-560; (b) Ramakrishna, K.; Behme, C.; Schure, R. M.; Bieniarz, C. A Safe and Efficient Process for the Synthesis of the Inhalation Anesthetic Sevoflurane. *Org. Process Res. Dev.* **2000,** *4*, 581−584.

8. (a) Ramig, K. Synthesis and Reactions of Fluoroether Anesthetics. *Synthesis* **2002,** *17*, 2627–2631; (b) Rozov, L. A.; Lessor, R. A.; Kudzma, L. V.; Ramig, K. The Fluoromethyl Ether Sevoflurane as a Fluoride Source in Halogen-Exchange Reactions. *J. Fluorine Chem.* **1998,** *88*, 51-54.

9. Christe, K. O.; Hegge, J.; Hoge, B.; Haiges, R. Convenient access to trifluoromethanol. *Angew. Chem. Int. Ed.* **2007,** *46*, 6155-6158.

10. Sohn, J. R. Recent Advances in Solid Superacids. *J. Ind. Eng. Chem.* **2004,** *10*, 1-15.

11. Culmann, J. C.; Fauconet, M.; Jost, R.; Sommer, J. Fluoroanions and cations in the HF–SbF_5 superacid system. A ^{19}F and ^{1}H NMR study. *New J. Chem.* **1999,** *23*, 863-867.

12. Larson, E. M.; Abney, K. D.; Larson, A. C.; Eller, P. G. Structure of Oxonium Hexafluoroantimonate(V). *Acta Cryst.* **1991,** *B47*, 206-209.

13. (a) Yamato, T.; Hideshima, J. C.; Suehiro, K.; Tashiro, M.; Prakash, G. K. S.; Olah, G. A. Organic Reactions Catalyzed by Solid Superacids. Perfluorinated Sulfonic Acid Resin (Nafion-H) Catalyzed Ring Closure Reaction of 2,3-Diaminobiphenyls. A Preparative Route to Carbazoles. *J. Org. Chem.* **1991,** *56*,

6248-6250; (b) Abid, M.; Savolainen, M.; Landge, S.; Hu, J.; Prakash, G. K. S.; Olah, G. A.; Torok, B. Synthesis of Trifluoromethyl-Imines by Solid Acid/Superacid Catalyzed Microwave Assisted Approach. *J. Fluorine Chem.* **2007,** *128*, 587-594.

14. Taira, S. Refrigerating Apparatus. U.S. Patent 6,718,777 B1, Apr. 13, 2004.

15. Patnaik, P. In *Handbook of Inorganic Chemicals*. McGraw-Hill: New York, 2002; p 50.

CHAPTER FOUR

SYNTHESIS OF OTHER HFES WITH SUPER-ACID SYSTEMS

4.1 INTRODUCTION

Organic fluorine compounds have attracted a lot of attention because the addition of one fluorine atom can affect the chemical and thermal properties of a molecule significantly. The approach of C-F bond activation is just as good as C-F bond formation toward building a variety of organo fluorine molecules as reviewed by Amii and Uneyama in 2009.[1] More methods of C-F activation have been reported and summarized by Shen and coworkers in 2015.[2]

The C-F bond is the strongest single bond that carbon can form, and the C-F bond energy increases as the degree of fluorination of the carbon atom increases (C-F BDE: 109.0 kcal/mol for CH_3F, 119.5 kcal/mol for CH_2F_2, 127.4 kcal/mol for CHF_3, 130.5 kcal/mol for CF_4).[3] Activation of a C-F bond or defluorination of a fluorocarbon is not easy to achieve. Much of the effort in this direction has involved in the use of metallic catalysts such as nickel, titanium, and rhodium.[4] Silicon based compounds were also used due to their high fluorine affinity.[5] Recently, the use of nonmetal systems has emerged in the area of C-F bond activation.[2, 4d] Nova and his coworkers reported examples of C-F bond activation via nucleophilic attack of coordinated ligands.[6]

The emergence of C-F bond activation methodology by the use of strong main-group Lewis acids provides a powerful tool of synthesizing various building blocks.[5a, 7] In

this approach, it is believed that the activation of the C-F bond is via heterolytic fluoride abstraction by strong Lewis acids.

Following the work discussed in Chapter 2, the same method was applied to the synthesis other fluorinated isopropyl derivatives. The HFCs used were 1,1,1,2-tetrafluoroethane, CF_3CH_2F (HFC-134a) and 1,1,1,2,3,3,3-heptafluoropropane, CF_3CFHCF_3 (HFC-227ea) instead of R32. It was of interest to find out which C-F bond in these two HFCs is favored during the C-F bond activation by a Lewis acid or super acid. Sevoflurane was also used to react with 1,1,1,3,3,3-hexafluoro-2-isopropanol (HFIP) to prepare the compound formal $[(CF_3)_2CHOCH_2OCH(CF_3)_2]$.

4.2 RESULTS AND DISCUSSION

Formal is the main byproduct in the synthesis of sevoflurane with R32 as discussed in Chapter 2. In order to collect more information about the molecule formal, sevoflurane was used to react with HFIP over SbF_5 based catalyst (see Table 4.1). An excess amount of HFIP was used to ensure the conversion of sevoflurane to formal, and the yield of formal was 99% as shown in Table 4.1, in reaction cycle# 2B-C8 and #2B-C9. The results of NMR spectroscopy and gas chromatography/mass spectrometry (GC/MS) agreed with the former results as shown in the Experimental Section of Chapter 3 (see **Error! Reference source not found.**, Figure 3.5 and Figure 4.3-4.3).

Table 4.1. Synthesis Summary of Formal

Reactor #	SbF_5 based Cat (g)	Cycle #	Sevo (mmol)	HFIP (mmol)	$V_{reactor}$ (mL)	Temp (°C)	Time (hr)	Yield of Formal (%)
2BEx	2.2	2B-	10	10	75	90	48	n/a
	4.5	2B-	5.4	5.4	75	100	16	n/a
	2.7	2B-	5.4	27.2	75	70	48	99
	2.4	2B-	5.4	26.4	75	70	16	99
	0.4	2B-	10.4	111.3	75	70-80	100	34

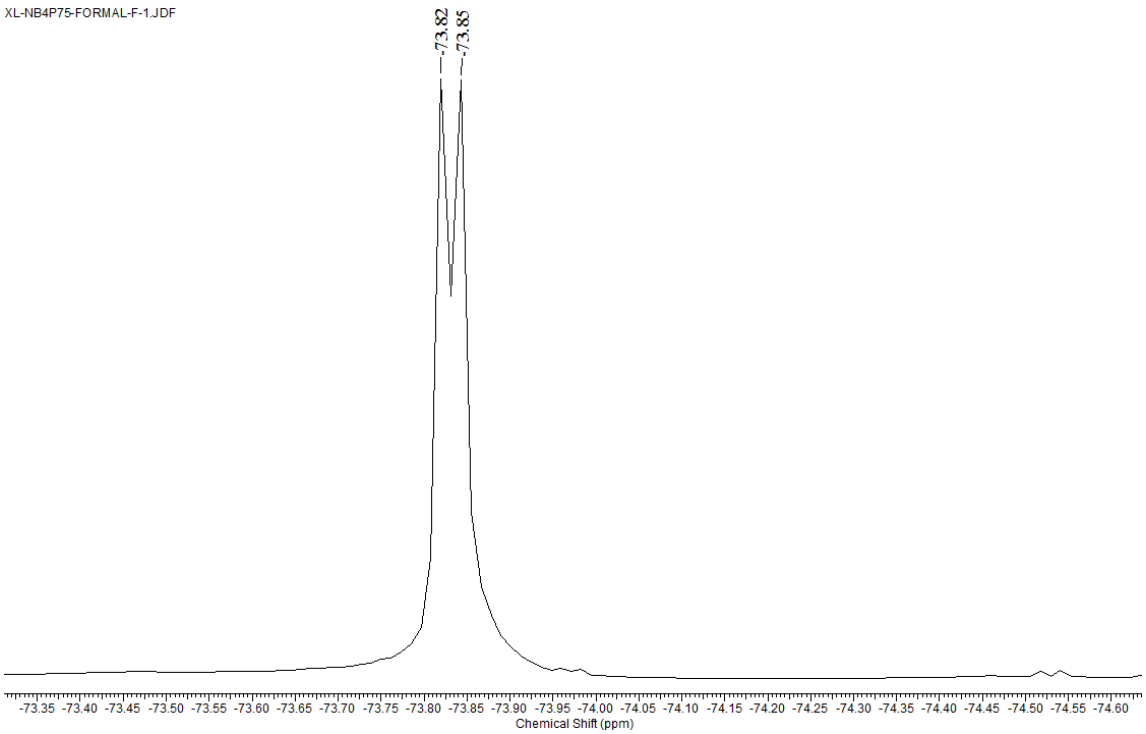

Figure 4.3. ^{19}F NMR spectrum of formal in $CDCl_3$.

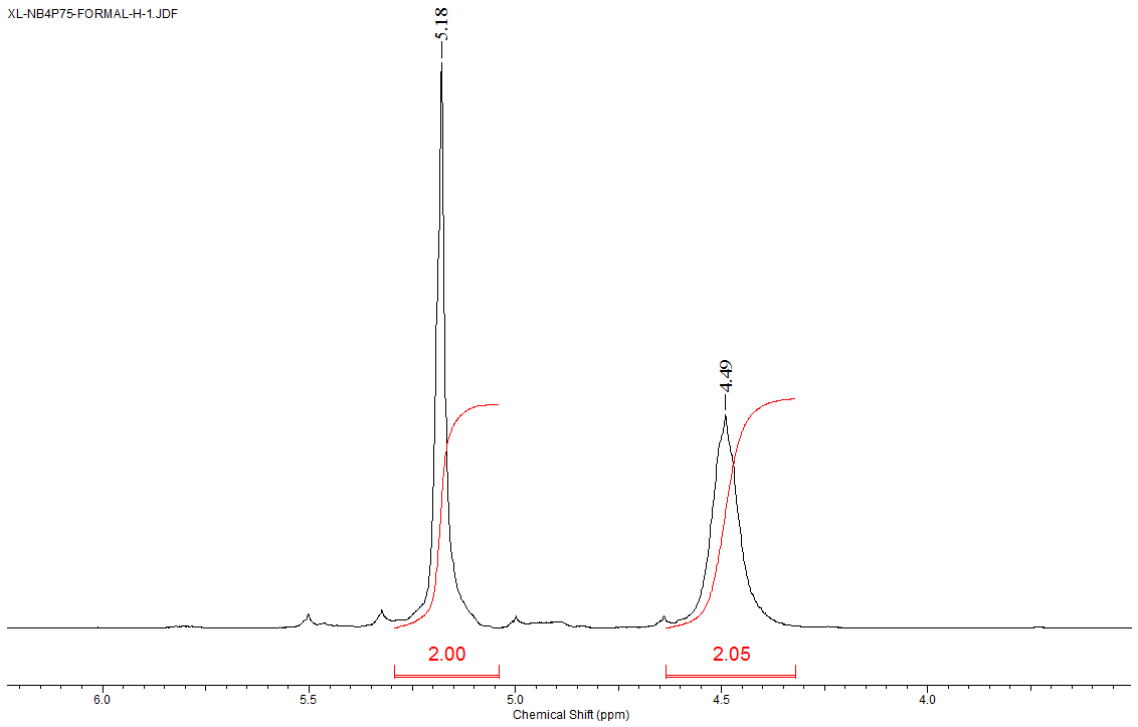

Figure 4.4. ^{1}H NMR spectrum of formal in $CDCl_3$.

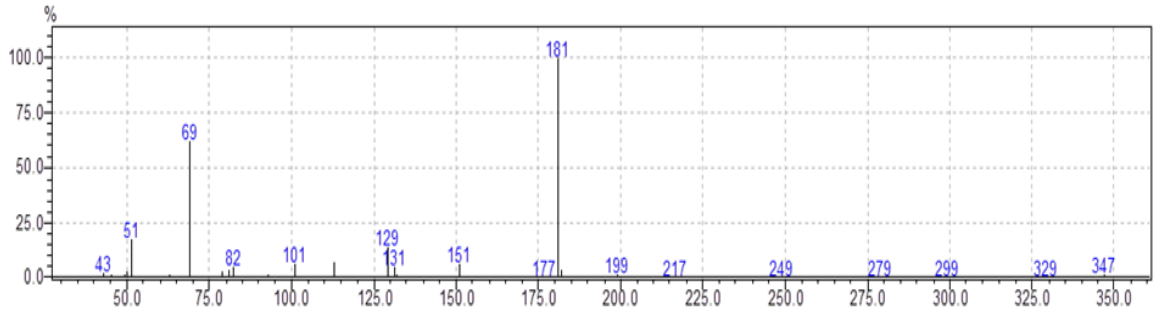

Figure 4.5. Mass spectrum of formal. GC retention time: 27.433 min.

Formal was also found to be one of the byproducts produced in the industrial sevoflurane synthetic methods reported in several US patents.[8] The reaction took place at around 70 °C, which is close to the reaction temperature required in the synthesis of sevoflurane with SbF_5-based catalysts. The yield of compound formal decreased to 34%

when a catalytic amount of the SbF_5-based catalyst was used in reaction cycle# 2B-10, even though the molar ratio of HFIP to sevoflurane was nearly 11:1. If the quantity of catalyst is increased, and the molar ratio of sevoflurane to HFIP is 5:1, such as in reaction cycle# 2B-C8 and cycle# 2B-C9, the yield of formal was 99%, which again is significantly higher than that obtained in reaction cycle# 2B-10. The catalyst can be used over and over again; however, the quantity of catalyst required to obtain a high yield of formal is more than a catalytic amount when using this method.

Under similar conditions to those used in reaction cycle# 2B-8 or cycle# 2B-9, the yield of compound formal was 95% when TaF_5 was used as catalyst. The TaF_5-based catalyst remaining from the preparation of formal was analyzed with SEM/EDX (see Figure 4.6-4.5 and Report 2).

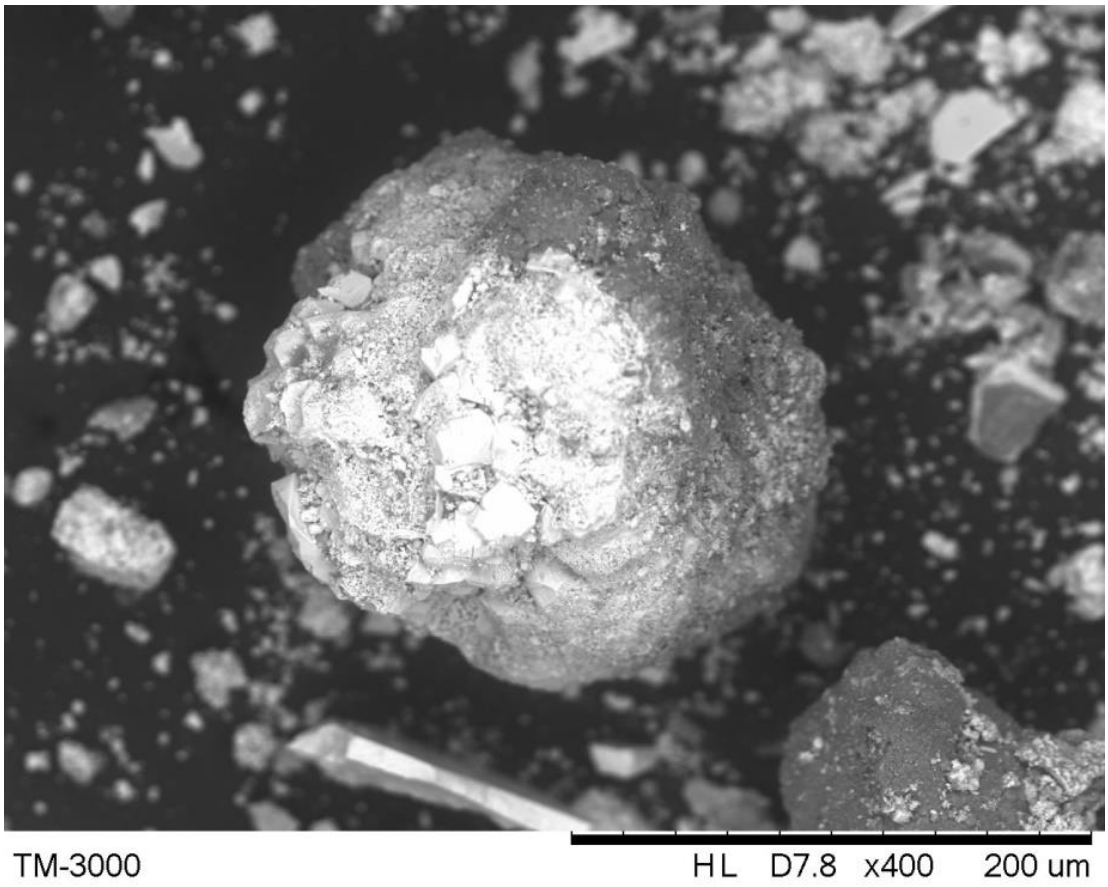

Figure 4.6. SEM of TaF_5-based catalyst recovered from formal preparation with $TaF_5 \cdot KF$.

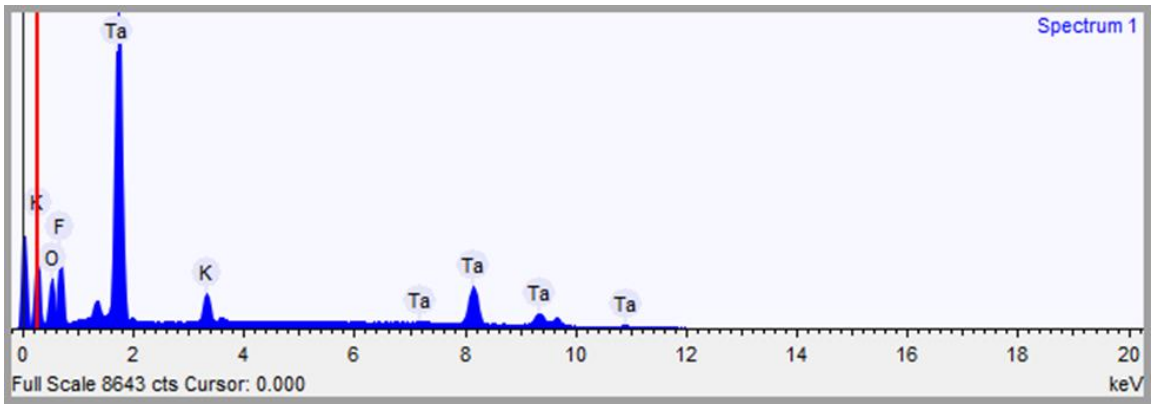

Figure 4.7. EDX of TaF_5-based catalyst recovered from formal preparation with $TaF_5 \cdot KF$.

In order to protect the glass vessel used, one molar equivalent of potassium fluoride (KF) was added to absorb HF generated from the reaction. Therefore, the fluorine from KF was taken into consideration in the EDX results. The percentage of the elements varied largely from sample to sample, especially the percentage of fluorine atoms, which made it difficult to come up with a constant formula for the catalyst. It might be difficult to get a homogeneous catalyst from the reaction due to the presence of HF and potential moisture; the HF will also combine with both KF and TaF_5.

The reactions of HFIP with HFCs other than R32 or sevoflurane required much higher reaction temperatures in the range of 120-205 °C (see Table 4.2). Mostly the yield of the products was very low, and sometimes only trace amount of the products were collected. Usually in the first few batch reactions in reaction sequence (i.e., reuse of the same catalyst) had higher yields than the latter reactions. Eventually the catalysts became ineffective.

Table 4.2. Reaction of HFIP with HFCs other than R32

#	SbF_5 [TaF_5] (mmol)	HF (mmol)	CAT Salt (g)	Cycle#	HFIP (mmol)	CF_3CH_2F ($CF_3CF_2CF_3$) [CF_3CHFCF_3] (mmol)	V (ml)	Temp (°C)	Time (hr)	Mix (g)
H	21.8	23.0	4.4	H1-C0			75	rt	16	n/a
			4.7	H1-C1	9.2	80.3	75	90	48	No
			4.7	H1-C2	8.0	92.8	75	130-155	48	0.35
			4.7	H1-C3	6.0	59.8	75	120-160	168	0.39
			4.5	H1-C4	5.5	(34)	75	200-205	48	trace
			4.4	H1-C5	3.3	(23.6)	75	200-205	72	No
H	16.2	0	3.5	H2-C1	16.2	[42.4]	150	80	16	No
			4.6	H2-C2	16.2	[50.0]	150	120-150	16	1.0
			4.5	H2-C3	16.2	[51.2]	150	113-127	48	Trace
			3.5	H2-C4	16.2	[59.3]	150	135-157	72	Trace
			3.2	H2-C5	8.1	[125.4]	150	135	24	Trace
			3.2	H2-C6	4.3	[42.3]	150	150-170	168	No
H	[0.4]	0	0.11	H3-C1	1.7	[24.2]	75	150-170	16	trace

The first HFC used other than R32 and sevoflurane was CF_3CH_2F (HFC-134a). In reactions cycle# H1-C1, the reaction did not take place at 90 °C. Higher temperature was applied in reaction cycle# H1-C2 and cycle# H1-C3, and the yield of the main product $(CF_3)_2CHOCF_2CH_2F$ was 28%. The compound was identified by ^{19}F and ^{1}H NMR spectroscopy (Figure 4.8-4.7).

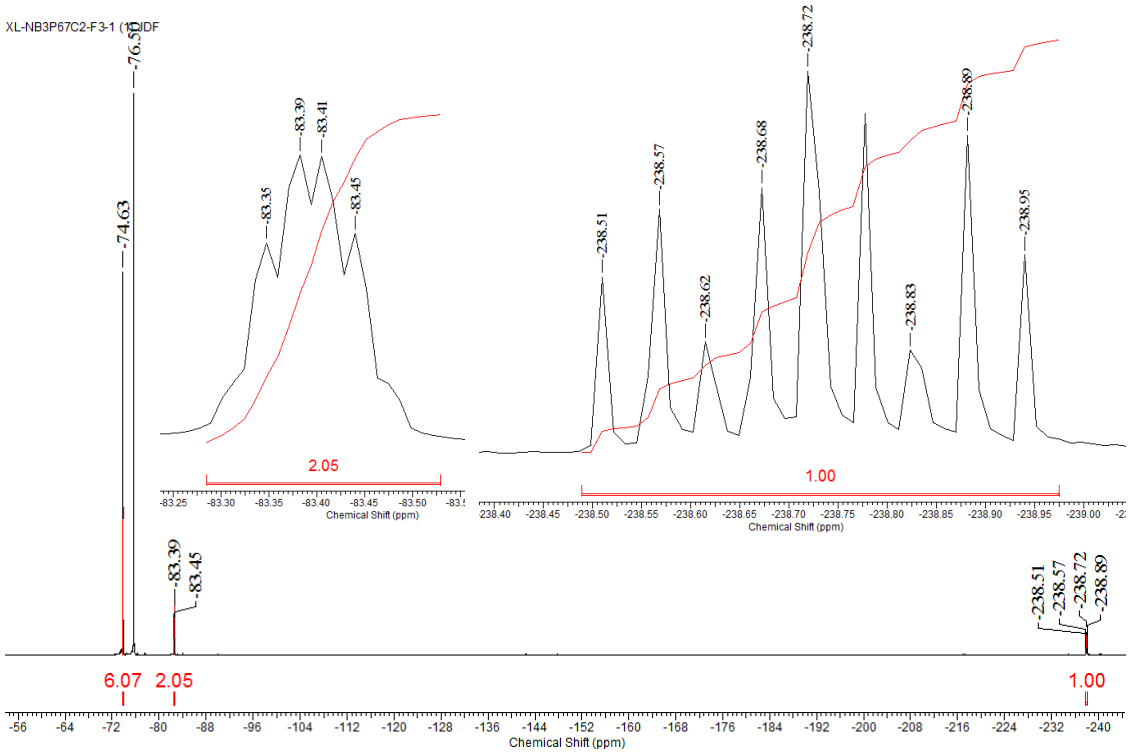

Figure 4.8. ^{19}F NMR spectrum of $(CF_3)_2CHOCF_2CH_2F$ in acetone-d_6.

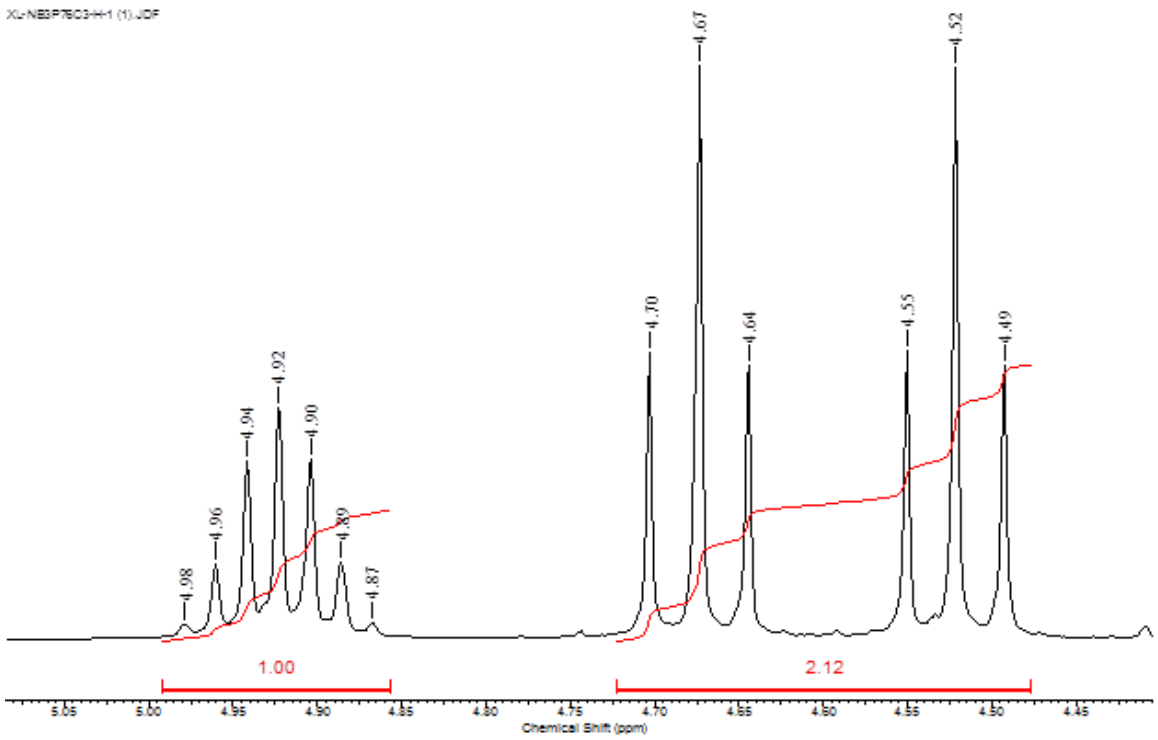

Figure 4.9. ^{1}H NMR spectrum of of $(CF_3)_2CHOCF_2CH_2F$ in acetone-d_6.

Most of the starting materials remained unreacted. In the ^{19}F NMR spectrum, the CF_3 fluorine peak at -74.63 ppm is split by a proton on the adjacent carbon and the $^{3}J_{HF}$ is 6.6 Hz which is expected. The CF_2 fluorine peak at -83.40 ppm is split by both fluorine atom and two protons on the adjacent carbon. The coupling constant $^{3}J_{HF}$ and $^{3}J_{FF}$ have values of 5.7 Hz and 9.9 Hz, respectively, which close in this case. The fluorine peak of -CH_2F is split into a triplet of triplet by the two protons on the same carbon atom and the two fluorine atoms on the adjacent carbon. The $^{2}J_{HF}$ coupling constant is 42.4 Hz, which is commonly observed in organo fluorine compounds and the $^{3}J_{FF}$ coupling constant is 17.0 Hz. In the ^{1}H NMR spectrum of $(CF_3)_2CHOCF_2CH_2F$, the CH proton is split into a septet by the six fluorine atoms on the two adjacent CF_3 groups. The coupling constant $^{3}J_{HF}$ is 6.0

Hz, which corresponds to the value measured in the ^{19}F NMR spectrum. The proton peak of -CH_2F group is split into a doublet of triplet by the fluorine atom on the same carbon atom and the two fluorine atoms on the adjacent carbon atom, which gives $^2J_{HF}$ = 45.0 Hz and $^3J_{HF}$ = 9.0 Hz fall in the expected range.

In the reaction with R-134a, had C-F bond activation taken place at the CH_2F group, $(CF_3)_2CHOCH_2CF_3$ would have been the expected product, however, no evidence was observed for this compound in the product mixture. Therefore, only a C-F bond in the -CF_3 group in HFC-134a was activated, thereby leaving the -CH_2F group untouched. Thus, in R-134a, under the conditions tried, the -CF_3 is preferred over the -CH_2F group for C-F bond activation.

After reaction cycles # H1-C2 and # H1-C3, perfluoropropane ($CF_3CF_2CF_3$) was introduced into the reaction cylinder with the same batch of catalyst for reaction cycle# H1-C4 in order to see if any reaction would occur. The reaction temperature was raised up to 205 °C, and no reaction was observed to occur with $CF_3CF_2CF_3$. However, a trace amount of another product namely $(CF_3)_2CHOCH_2CH_3$ was discovered. This compound appears to be the defluorinated residue of $(CF_3)_2CHOCF_2CH_2F$ from reaction cycle# H1-C3. It was identified by multinuclear NMR spectroscopy and GC/MS as shown in Figure 4.10-4.12.

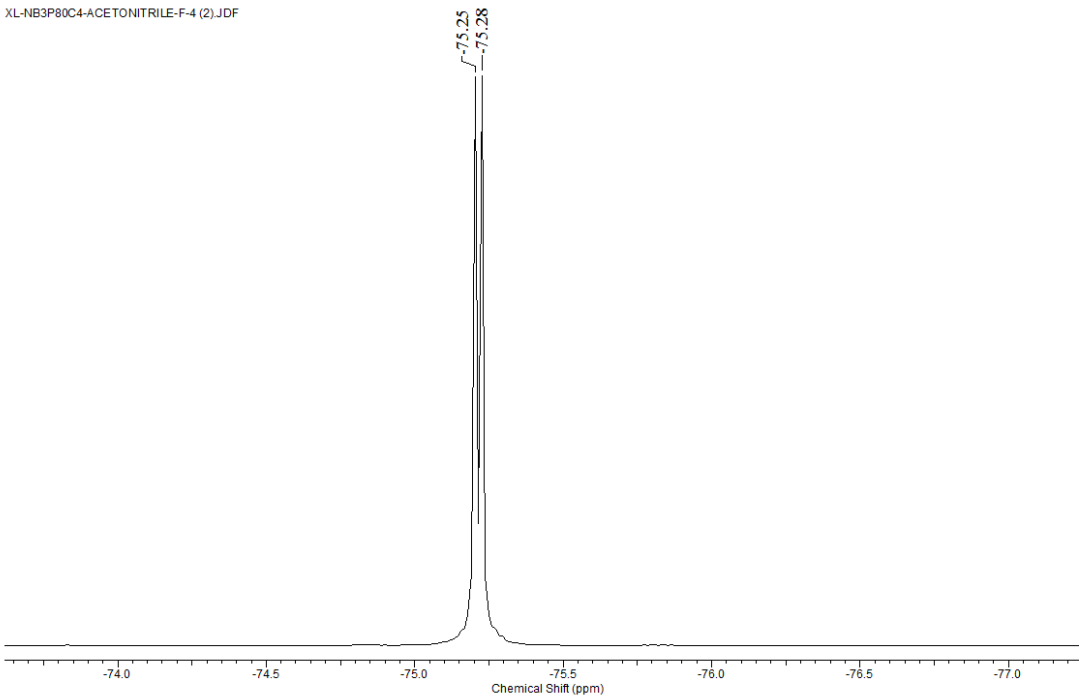

Figure 4.10. ^{19}F NMR spectrum of $(CF_3)_2CHOCH_2CH_3$ in acetonitrile-d_3.

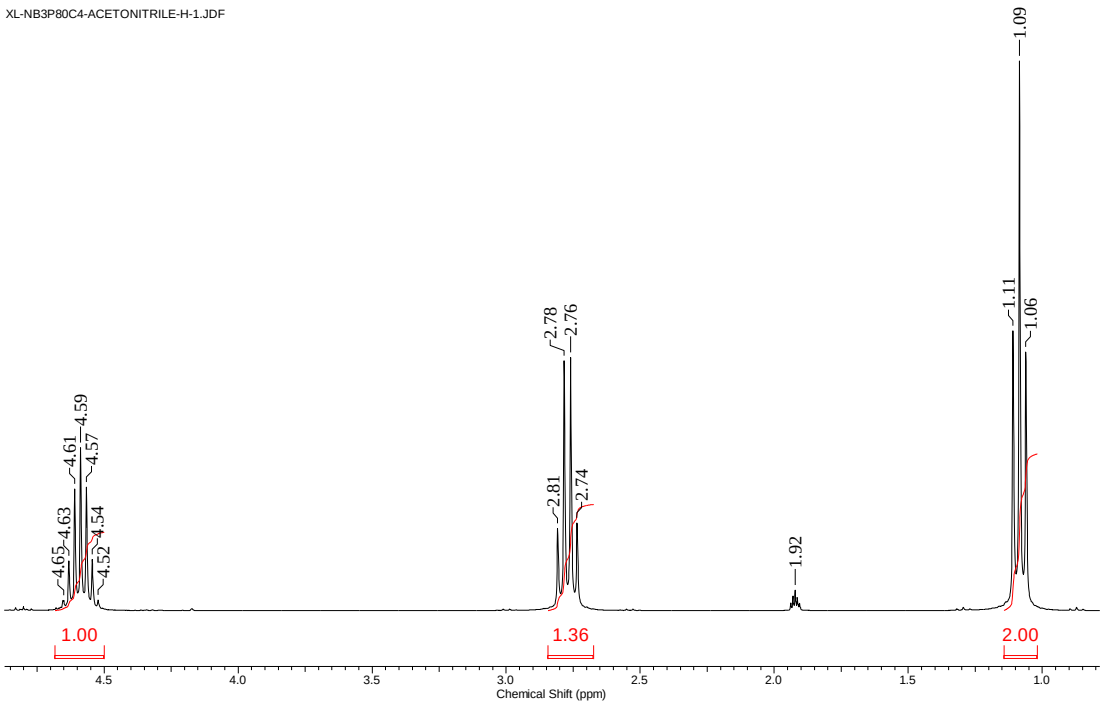

Figure 4.11. ^{1}H NMR spectrum of $(CF_3)_2CHOCH_2CH_3$ in acetonitrile-d_3.

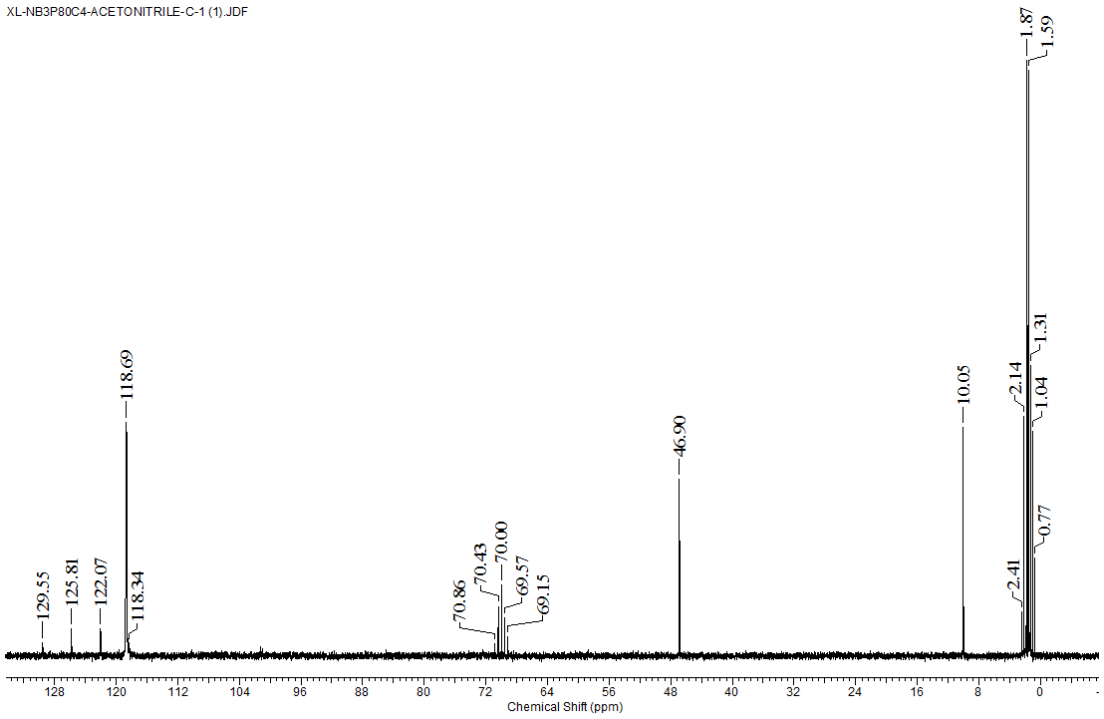

Figure 4.12. ^{13}C NMR spectrum of $(CF_3)_2CHOCH_2CH_3$ with proton decoupling in acetonitrile-d_3.

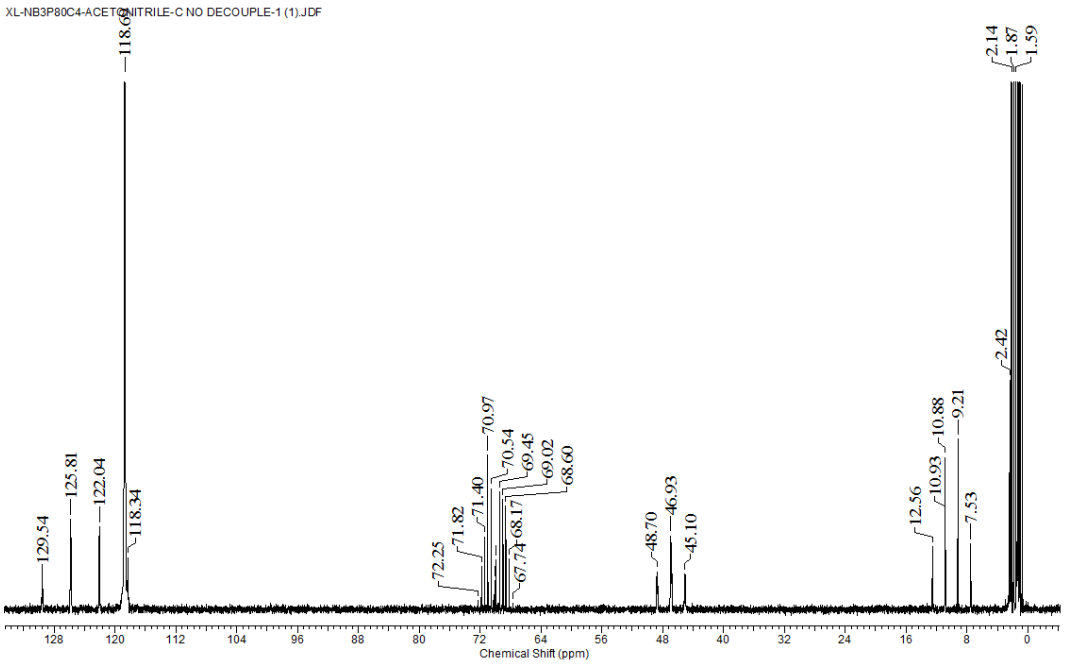

Figure 4.13. ^{13}C NMR spectrum of $(CF_3)_2CHOCH_2CH_3$ without proton decoupling in acetonitrile-d_3.

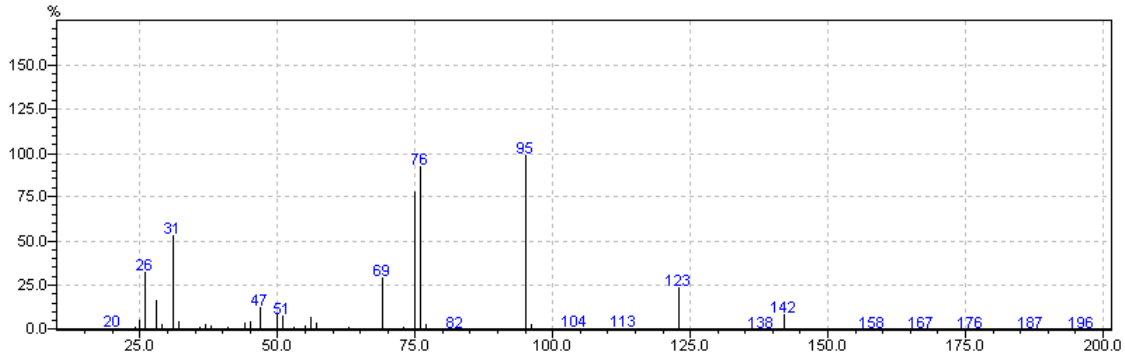

Figure 4.14. Mass spectrum of $(CF_3)_2CHOCH_2CH_3$.

The fluorine peak of CF_3 at -75.23 ppm is split into a doublet by the proton on the adjacent CH with a coupling constant of $^3J_{HF}$ = 6.6 Hz, which is expected. In the ^1H NMR spectrum of $(CF_3)_2CHOCH_2CH_3$, the proton peak of the CH hydrogen atom is split into a

septet by the fluorine atoms of CF_3 groups. The ethyl group has a common A_2X_3 spin system, in which the CH_2 proton peak is split into a quartet by CH_3 protons and the CH_3 proton peak is split into a triplet by CH_2 protons. The ^{13}C NMR analysis was carried out with and without proton decoupling capability of the instrument to further confirm the structure of the molecule. In the ^{13}C NMR spectrum with proton decoupling, the two carbons of the ethyl group give two singlet at 46.90 ppm and 10.05 ppm. The carbon peak of CH group is split into a septet by the fluorine atoms on the adjacent CF_3 groups with a $^2J_{CF}$ coupling constant 32.5 Hz. The carbon signal of CF_3 group appear to be a quartet with a large J_{CF} coupling constant 282.5 Hz. In the ^{13}C NMR spectrum without proton decoupling, the peaks of the carbon atoms carrying protons are split into a doublet of septets for the CH carbon atom, a triplet for the CH_2 carbon atom and quartet for the CH_3 carbon atom respectively. The J_{HC} values fall into the expected range of 120-150 Hz.

The defluorination of fluorocarbons has been reported by several groups in the past, and metallic elements were involved such as calcium, lithium, and nickel.[9] Silicon containing compounds were used in some reactions to assist the C-F bond cleavage with success.[4b, 10] The reaction vessel used in this study is made of 304 stainless steel, which consists of Ni, Cr, Mo, Fe, Mn, C, P, and S, and this means the environment of the interior surface of the cylinder is quite complicated. The source of hydrogen for the observed reduction could be either HFIP and/or perhaps residual moisture contained in the HFIP.

When CF_3CFHCF_3 (HFC-227ea) was used as the reactant in reaction # H2 (see Table 4.2), a C-F bond of either terminal -CF_3 group was expected to be activated; however,

no evidence of $(CF_3)_2CHOCF_2CHFCF_3$ was observed in the NMR spectra[11] of the product mixture from the reaction (see Figure 4.15-4.14).

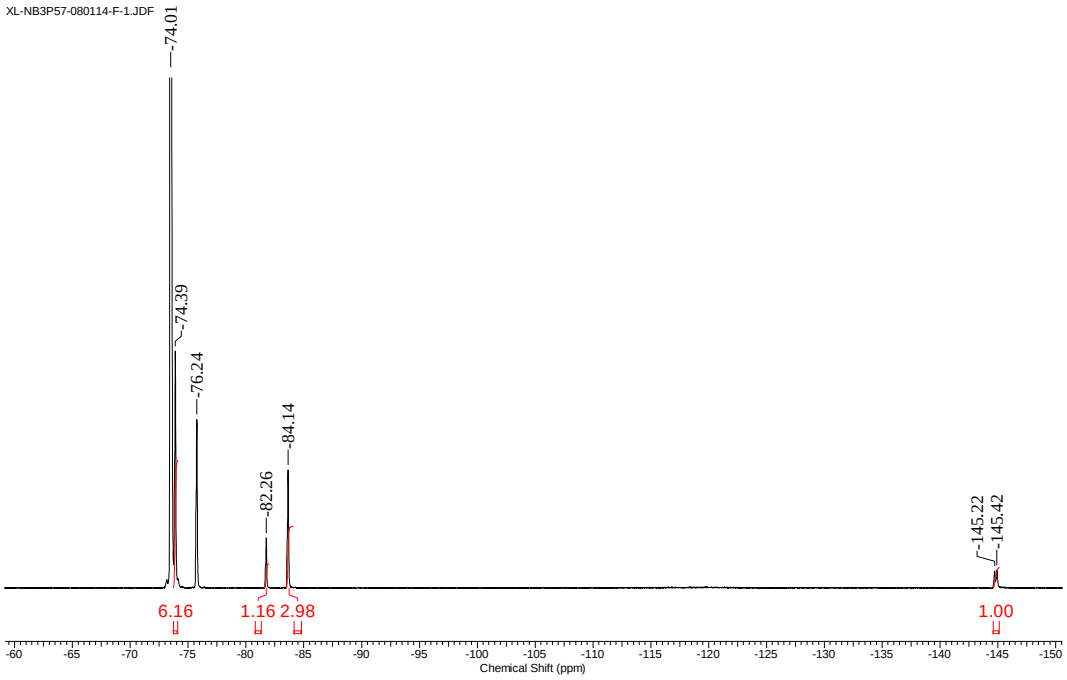

Figure 4.15. ^1H NMR spectrum of the products mixture in $CDCl_3$.

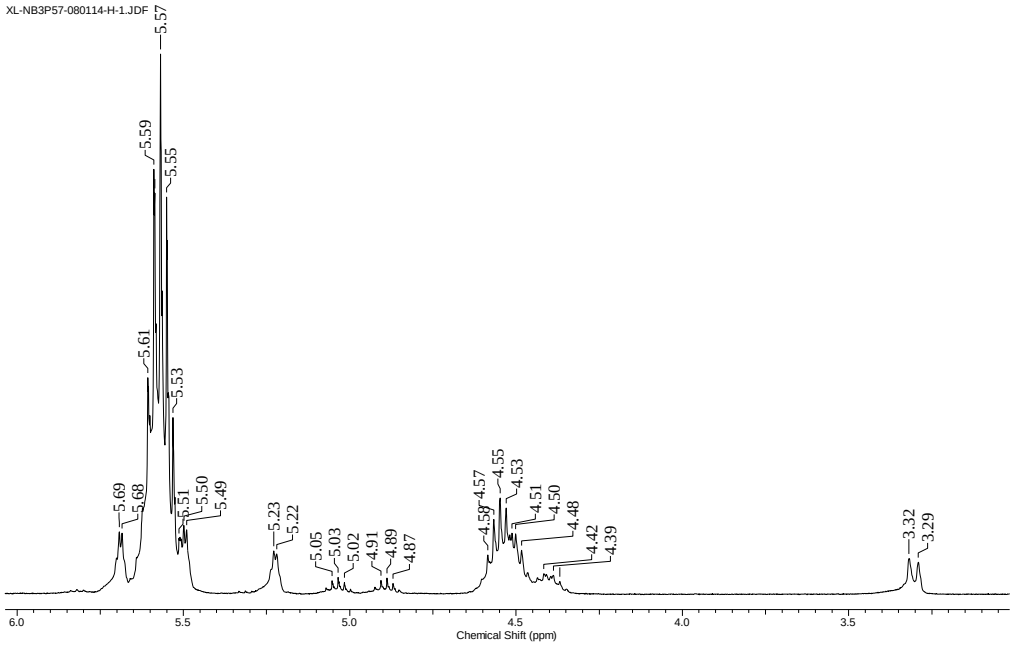

Figure 4.16. ^{1}H NMR spectrum of the products mixture in $CDCl_3$.

If $(CF_3)_2CHOCF_2CHFCF_3$ were formed, four different sets of fluorine peaks should be observed and due to the chirality of the carbon atom of CHF group, complicated spin systems for the signals of the CF_2 and CF_3 groups are expected. However, no such system is observed in the ^{19}F NMR spectrum of the product mixture. The peak at -145.32 ppm that is split into a doublet with a coupling constant of 56.6 Hz should belong to the CHF fluorine. The peak at -76.24 ppm belongs to residue starting material HFIP in the mixture.

The main product was separated and identified by NMR spectroscopy and GC/MS (see, Figure 4.17-Figure 4.21) as $(CF_3)_2CHOC(O)OCH(CF_3)_2$, which was not expected. This compound has been reported in several patents.[12] A doublet with a $^{3}J_{HF}$ coupling

constant of around 6 Hz is expected in the ^{19}F NMR spectrum; however, this signal appears to be a broaden singlet.

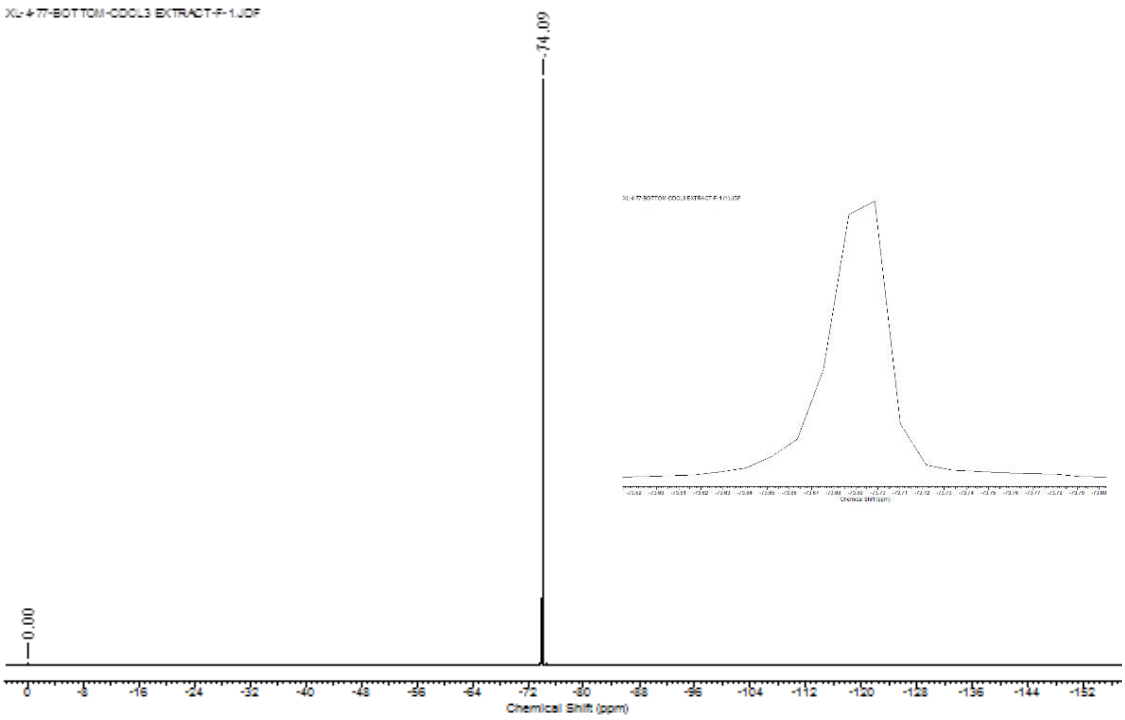

Figure 4.17. ^{19}F NMR spectrum of $(CF_3)_2CHOC(O)OCH(CF_3)_2$ in $CDCl_3$.

In the ^{1}H NMR spectrum, which is shown in Figure 4.18, the peak for the CH proton at 5.57 ppm is split into a septet with a $^{3}J_{HF}$ coupling constant of 5.5 Hz. The structure of the main product can not be confirmed only by ^{1}H and ^{19}F NMR spectroscopy, because $(CF_3)_2CHOCH(CF_3)_2$ is also expected to have very similar patterns in both ^{1}H and ^{19}F NMR spectra with those of $(CF_3)_2CHOC(O)OCH(CF_3)_2$.

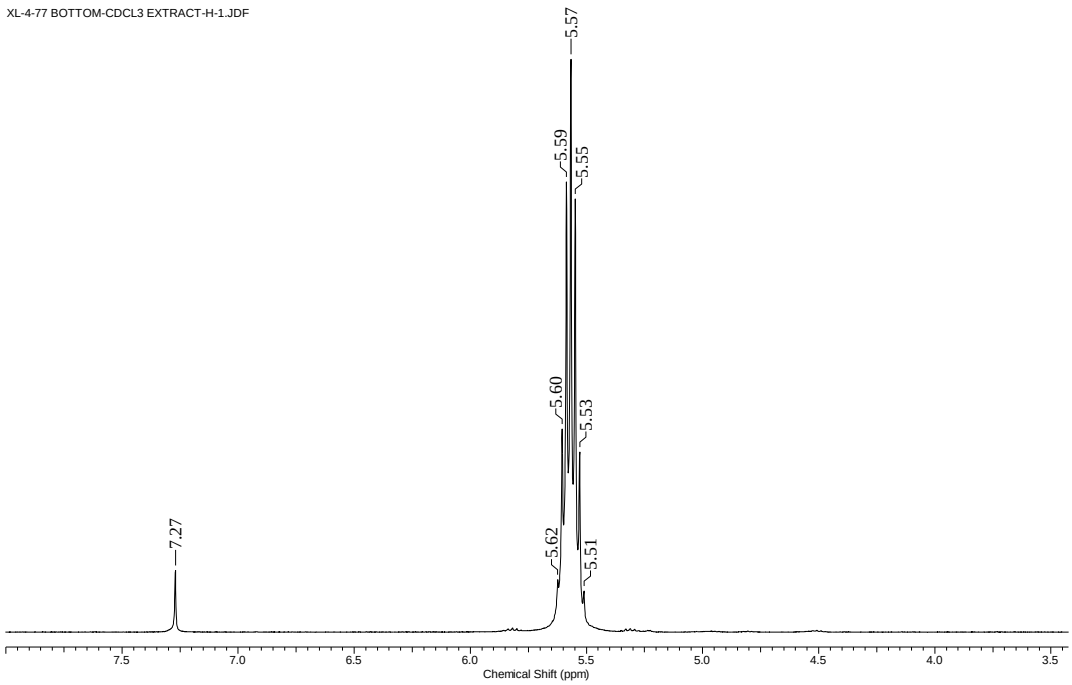

Figure 4.18. ^{1}H NMR spectrum of $(CF_3)_2CHOC(O)OCH(CF_3)_2$ in $CDCl_3$.

What helped with final structural determination was ^{13}C NMR and GC/MS experiments on the main product. In ^{13}C NMR spectrum of the main product with proton decoupling capability, as shown in Figure 4.17, the resonance of the carbon peak of the CF_3 group is split into a quartet at 119.69 ppm with a J_{CF} coupling constant 281.8 Hz, and the carbon peak of the CH group is split into a septet at 71.87 ppm ($^{2}J_{CF}$ = 35.4 Hz) by the CF_3 fluorine atoms. Another carbon signal shows up at 151.69 ppm as a singlet, which means this carbon does not carry any fluorine atoms. In order to find out if protons are carried on this carbon, ^{13}C NMR experiment without proton decoupling was carried out. Besides the expected split of CH carbon by one proton, the signal at 151.70 ppm appears to be a triplet with a coupling constant of 5.3 Hz. In the mass spectra of the main product,

the fragment 195 $[(CF_3)_2CHOC(O)]^+$ indicates the presence of a carbonyl group in the structure.

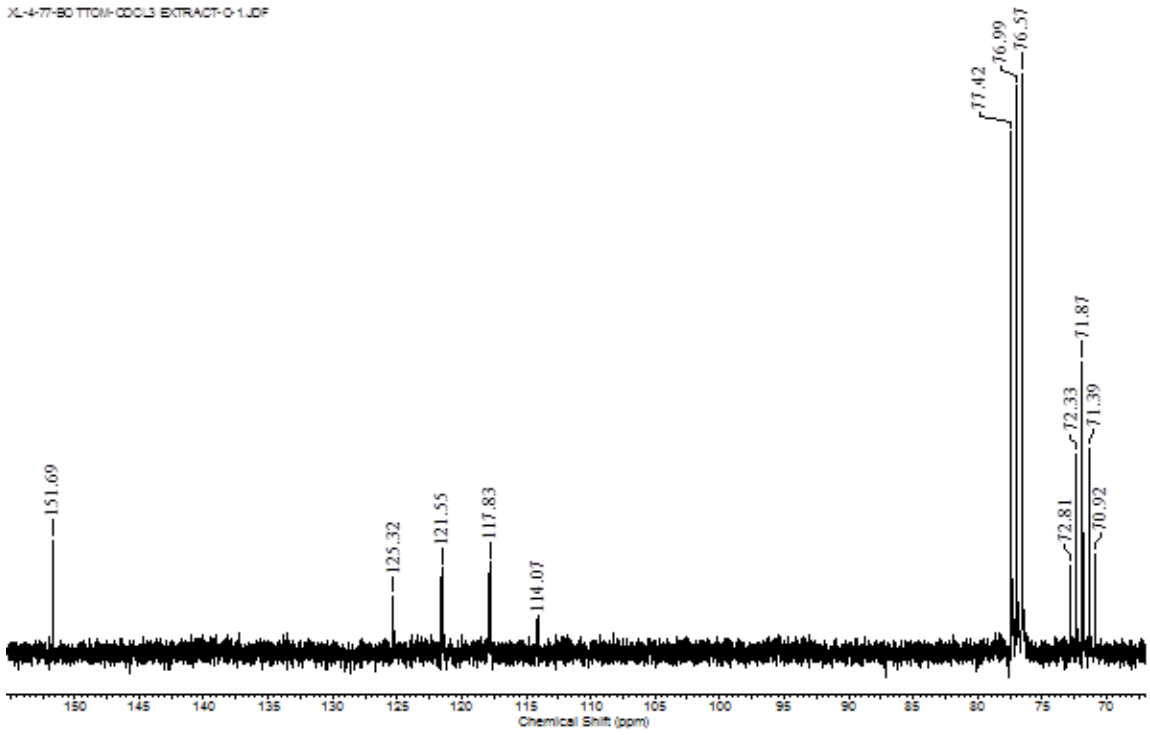

Figure 4.19. ^{13}C NMR spectrum of $(CF_3)_2CHOC(O)OCH(CF_3)_2$ with proton decoupling.

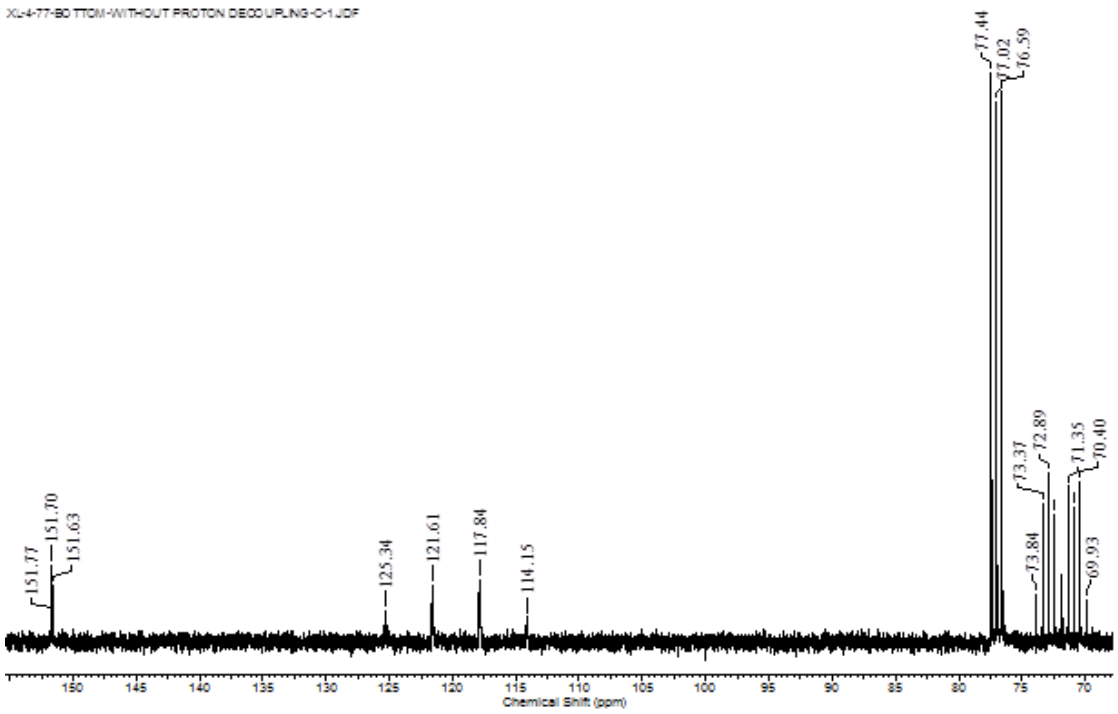

Figure 4.20. ^{13}C NMR spectrum of $(CF_3)_2CHOC(O)OCH(CF_3)_2$ without proton decoupling.

The other byproducts were possibly $(CF_3)_2CHOCH(CF_3)_2$ (see Figure 4.22) and $(CF_3)_2CHOCF_2CFHCF_2OCH(CF_3)_2$ (see Figure 4.23) according to the NMR spectra of the product mixture (Figure 4.15-Figure 4.16) and the GC/MS results. The parent ions of both $(CF_3)_2CHOCH(CF_3)_2$ and $(CF_3)_2CHOCF_2CFHCF_2OCH(CF_3)_2$ were not observed in their mass spectra; however, the fragments of each molecule following the loss of a CF_3 group was caught by the detector. The byproducts were not purified due to the small portion of each produced in the reaction. Further proof of the identities of the byproducts is needed. The Lewis acid TaF_5 was also used as catalyst in cycle# H3-C1, and only trace amounts of the products were collected at higher reaction temperature 150-170 °C (Table 4.2).

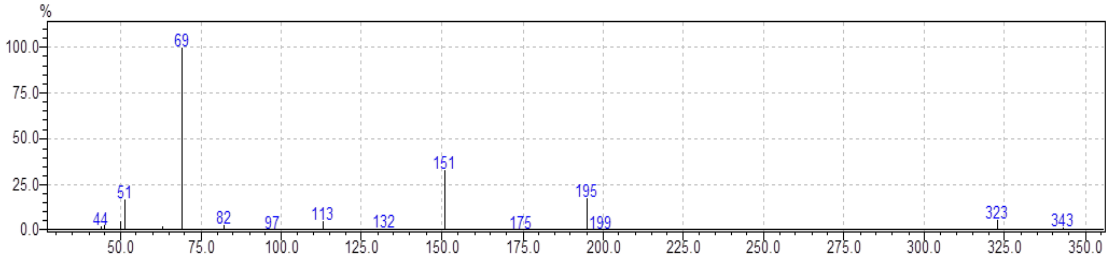

Figure 4.21. Mass spectroscopy of $(CF_3)_2CHOC(O)OCH(CF_3)_2$. Retention time: 17.608 min.

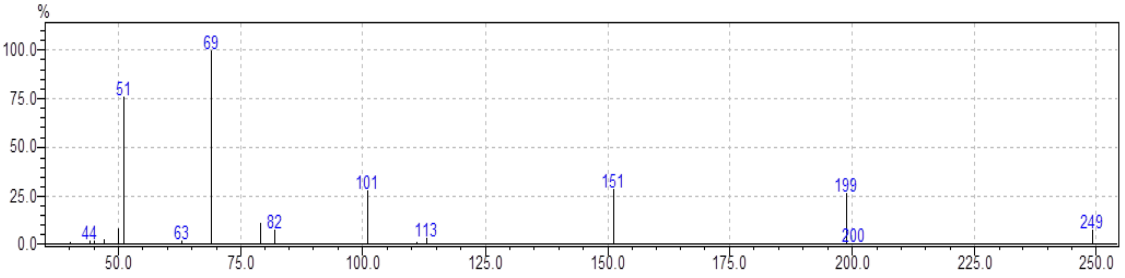

Figure 4.22. Mass spectroscopy of $(CF_3)_2CHOCH(CF_3)_2$. Retention time 15.800 min.

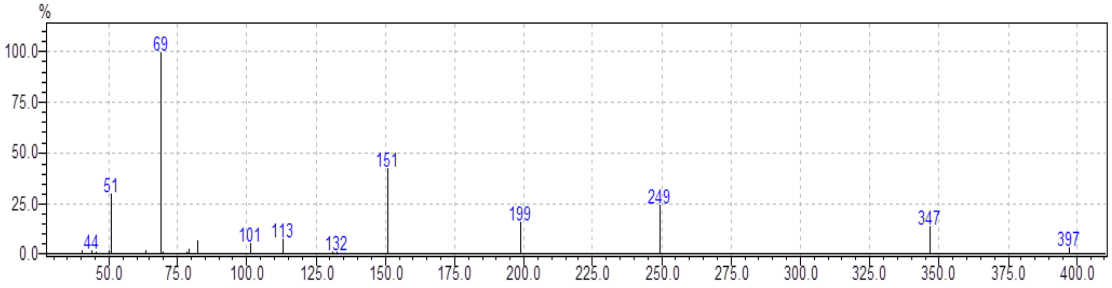

Figure 4.23. Mass spectroscopy of $(CF_3)_2CHOCF_2CHFCF_2OCH(CF_3)_2$. Retention time 20.758 min.

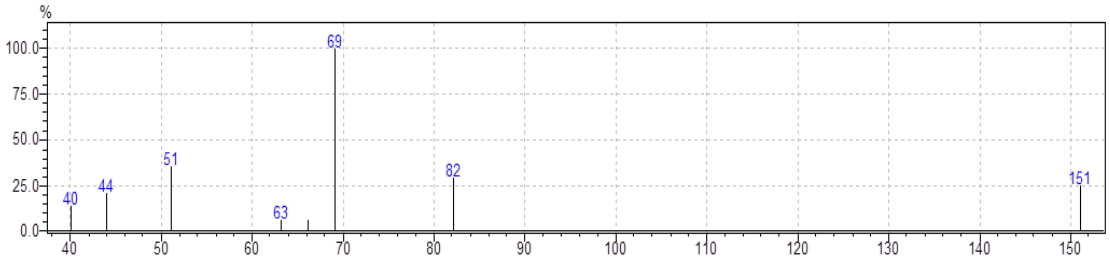

Figure 4.24. Mass spectroscopy of CF_3CFHCF_3. Retention time 13.958 min.

4.3 CONCLUSION AND FUTURE WORK

Several more HFEs were synthesized with the same method and the catalogue of HFEs can certainly be enriched in the future. C-F bond activation appears to occur in various circumstances in the presence of strong Lewis acid catalysts. One way to resurrect catalysts might be to treat the ineffective catalysts with fluorine gas, which will be attempted in the future.

4.4 EXPERIMENTAL

4.4.1 Reagents and synthetic equipment

Antimony pentafluoride (SbF_5) was purchased from SynQuest; tantalum pentafluoride (TaF_5) was purchased from STEM Chemical; hexafluoroisopropanol (HFIP) was purchased from Oakwood Chemical; sevoflurane were provided by Piramal Enterprises; HF was purchased from Air Products & Chemicals, Inc; CF_3CH_2F (HFC-134a) and CF_3CFHCF_3 (HFC-227ea) were taken from laboratory stock. These chemicals were used without further purification. Stainless steel cylinders (10-, 30-, 75- and 150-mL capacities) were purchased from Hoke®; valves were purchased from Swagelok®.

4.4.2 Instrumentation

NMR spectroscopic data was collected on a multinuclear JOEL ECX-300 spectrometer. The frequencies are 300 MHz for ^{1}H, 282.78 MHz for ^{19}F and 75.57 MHz for ^{13}C respectively. Multiplicities are as follows: s (singlet), d (doublet), t (triplet), m (multiplet), dd (doublet of doublet), ds (doublet of septet), td (triplet of doublet), tt (triplet of triplet), tm (triplet of multiplets), sep (septet), qt (quartet of triplet). The solvents used for NMR spectroscopy were $CDCl_3$, acetone-d_6, acetonitrile-d_3, which were purchased from Cambridge Isotope Laboratories, Inc.. The internal standard for ^{19}F NMR spectroscopy is CF_3Cl (0.00 ppm). GC/MS data were collected on a SHIMADZU GCMS-QP5000 instrument; XRD data were collected on a Ultima IV X-Ray diffractometer; and SEM/EDX data were collected on a Hitachi TM 3000 tabletop Scanning Electron Microscope.

GC column information: Restek Rxi®-5HT column, 30m, 0.25 mm i.d., 0.25 um.

GC/MS method: Initial Temp.: 250 °C. Interface Temp.: 250 °C. Control Mode: Split. Column Inlet Pressure: 94.8 kPa. Colum Flow: 0.5 mL/min. Linear Velocity: 13.6 cm/sec. Split Ratio: 20. Total Flow: 13.3 mL/min. Oven Temp. Program: 35 °C ramp to 50 °C at a rate of 5 °C/min, and isothermal at 50 °C for 30 min. Ramp from 50 °C to 290 °C at a rate of 30 °C/min.

4.4.3 General work up procedure

After the reaction was stopped and cooled down to room temperature, the volatile materials including excess HFCs, unreacted HFIP, HF and products were condensed on bulk 10 wt% K_2CO_3 soln in a second cylinder in order to scrub the HF generated from the

reaction. This second cylinder was warmed up to room temperature on a shaker for 30 min, and then carefully opened in a fume hood in order to release the pressure of HFCs. The remaining liquid phase at the bottom of the cylinder was pipetted out, and this bottom phase was the products phase, which was analyzed by NMR spectroscopy and GC/MS.

4.4.4 Synthesis of formal

To a three-necked flask equipped with a magnetic stir bar, 0.06 g (1.0 mmol) KF, and 0.20 g (0.72 mmol) TaF_5 were loaded in a dry box. Sevoflurane 0.15 g (0.75 mmol) and HFIP 0.66 g (3.9 mmol) were injected into the flask while using a fume hood. The flask was heated up to 55 °C overnight, yielding 95+ % formal.

Or to a 75-mL stainless steel cylinder containing 2.2 g SbF_5-based catalyst, 1.09 g (5.5 mmol) sevoflurane and 4.56 g (27.1 mmol) HFIP were transferred on the vacuum line. The reaction mixture was warmed up to 70 °C and held at that temperature for 2 days. Upon work-up of the reaction, the formal $(CF_3)_2CHOCH_2OCH(CF_3)_2$ was isolated in 99 % yield.

NMR chemical shifts of formal:

^{19}F NMR chemical shifts:

$(CF^a_3)_2CHOCH_2OCH(CF_3)_2$: δ_a = -73.84 ppm (d, $^3J_{HF}$ = 8.5 Hz)

$(CF_3)_2CH^aOCH^b_2OCH(CF_3)_2$: δ_a = 4.49 ppm (s), δ_b = 5.18 ppm (s).

Mass spectrum of formal, m/z (relative intensity, %):

347 (1.8) $[M-H]^+$, 279 (0.8) $[M-CF_3]^+$, 181 (100.0) $[M-CF_3CH(CF_3)O]^+$, 151 (6.5) $[CF_3CHCF_3]^+$, 82 (5.2) $[CF_3CH]^+$, 69 (65.5) $[CF_3]^+$.

4.4.5 SEM/EDX analysis of the TaF_5-based catalyst after the synthesis of formal

The powder sample was carefully scattered on the aluminum sample holder which was covered with a layer of dark carbon tape. The sample holder was quickly installed in the vacuum chamber, then vacuum was applied to the chamber. The catalyst appears to be particles with both rough edges and surface. The formula of the catalyst was calculated from the atomic % of the elements in the six specimens analyzed with EDX. The average formula of the catalyst is $TaF_{3.6}O_{2.8}K_{0.3}$.

Report 2. SEM/EDX with TM 3000 of the Solid Recovered from Formal Preparation with TaF_5.KF.

Acquisition conditions

Acquisition time (s) 45.0 Process time 5

Accelerating voltage (kV) 15.0

Summary results

Sample 1				
Element	Weight %	Weight %	Atomic %	
Oxygen	13.273	0.2	31.365	2.727154
Fluorine	25.901	0.23	51.544	4.481697
Potassium	5.782	0.073	5.59	0.486045
Tantalum	55.044	0.235	11.501	1
Sample 2				
Oxygen	14.588	0.281	36.942	2.748456
Fluorine	21.268	0.317	45.356	3.374451
Potassium	4.113	0.094	4.262	0.31709
Tantalum	60.03	0.338	13.441	1
Sample 3				
Oxygen	15.407	0.202	37.16	3.001131
Fluorine	23.243	0.232	47.211	3.812874
Potassium	3.289	0.061	3.246	0.262155
Tantalum	58.061	0.242	12.382	1
Sample 4				
Oxygen	15.597	0.221	41.62	2.746107
Fluorine	18.353	0.247	41.243	2.721233
Potassium	1.814	0.061	1.98	0.130641
Tantalum	64.237	0.271	15.156	1

4.4.6 Reaction of Hexafluoroisopropanol with CF_3CH_2F (HFC-134a)

To a 75-mL stainless steel cylinder equipped with a Swagelok valve and containing 5.0 g $HSbF_6$, 1.33 g (7.9 mmol) HFIP and 9.47 g (92.8 mmol) HFC-134a were condensed

on a vacuum line. The reaction mixture was heated up to 130 °C and held at that temperature for 2 days, then heated up to 155 °C for 2 h. The products and unreacted starting material were condensed into another cylinder containing 10 wt% K_2CO_3 soln to strip off any HF, and the bottom phase (0.35 g) was collected and analyzed directly with NMR spectroscopy without further separation. The yield of the main product $(CF_3)_2CHOCF_2CH_2F$ was 28%.

^{19}F NMR chemical shifts:

$(CF^a_3)_2CHOCF^b_2CH_2F^c$: δ_a = -74.63 ppm (d, $^3J_{HF}$ = 6.6 Hz), δ_b = -83.40 ppm (td, $^3J_{HF}$ = 5.7 Hz, $^3J_{FF}$ = 9.9 Hz), δ_c = -238.72 ppm (tt, $^2J_{HF}$ = 42.4 Hz, $^3J_{FF}$ = 17.0 Hz).

^{1}H NMR chemical shifts:

$(CF_3)_2CH^aOCF_2CH^b_2F$: δ_a = 4.93 ppm (sep, $^3J_{HF}$ = 6.0 Hz), δ_b = 4.61 ppm (dt, $^2J_{HF}$ =45.0 Hz, $^3J_{HF}$ = 9.0 Hz)

4.4.7 Synthesis of 2-ethoxy-1,1,1,3,3,3-hexafluoropropane.

To the cylinder containing the solid left from section 4.4.6, 0.92 g (5.5 mmol) HFIP and 6.37 g (33.9 mmol) perfluoropropane were condensed on the vacuum line. The cylinder was warmed up to 200-205 °C and held at this temperature for 2 days, and the same work up procedure was used on this product. A very small amount of the product was collected and analyzed with NMR spectroscopy. It was identified as $(CF_3)_2CHOCH_2CH_3$.

^{19}F NMR chemical shifts:

$(CF^a_3)_2CHOCH_2CH_3$: δ_a = -75.23 ppm (d, $^3J_{HF}$ = 6.6 Hz).

^{1}H NMR chemical shifts:

$(CF_3)_2CH^aOCH^b{}_2CH^c{}_3$: δ_a = 4.61 ppm (sep, $^3J_{HF}$ = 6.5 Hz), δ_b = 2.79 ppm (q, $^3J_{HH}$ = 7.2 Hz), δ_c = 1.10 ppm (t, $^3J_{HH}$ = 7.2 Hz).

^{13}C NMR chemical shifts with proton decoupling:

$(C^aF_3)_2C^bHOC^cH_2CH^d{}_3$: δ_a = 123.94 ppm (q, J_{CF} = 282.5 Hz), δ_b = 70.00 ppm (sep, $^2J_{CF}$ = 32.5 Hz), δ_c = 46.90 ppm (s), δ_d = 10.05 ppm (s).

^{13}C NMR chemical shifts without proton decoupling:

$(C^aF_3)_2C^bHOC^cH_2CH^d{}_3$: δ_a = 123.94 ppm (q, J_{CF} = 282.5 Hz), δ_b = 70.00 ppm (dsep, J_{CH} = 147.4 Hz, $^2J_{CF}$ = 32.5 Hz), δ_c = 46.93 ppm (tm, J_{CH} = 138.0 Hz, $^2J_{CH}$ = 3.6 Hz), δ_d = 10.05 ppm (qt, J_{CH} = 127.2 Hz, $^2J_{CH}$ = 3.6 Hz).

Mass spectrum of $(CF_3)_2CHOCH_2CH_3$, m/z (relative intensity, %):

$(CF_3)_2CHOCH_2CH_3$: 196 (0.4) $[M]^+$, 142 (7.7) $[M\text{-}2F\text{-}CH_3\text{-}H]^+$, 123 (23.2) $[M\text{-}HF_3\text{-}CH_3]^+$, 113 (1.2) $[CF_3CHCF/CF_2CHCF_2]^+$, 104 (1.4) $[CFCCFOC_2]^+$, 95 (97.5) $[C5OF]^+$, 76 (100.0) $[C5O]^+$, 69 (30.5) $[CF_3]^+$, 31 (54.1) $[CF]^+$.

4.4.8 Reaction of Hexafluoroisopropanol with CF_3CFHCF_3 (HFC-227ea)

To a 75-mL stainless steel cylinder, 3.5 g SbF_5 was loaded in the dry box. The cylinder was degassed on a vacuum line at liquid nitrogen temperature. Quantities of 2.72 g HFIP and 8.5 g HFC-227ea were condensed into the cylinder. The reaction mixture was warmed up to 120 °C and held at this temperature overnight, then 150 °C for 1 h to finish the reaction. After the reaction was worked up, a bottom phase of 1 g was collected. The main product was identified by NMR spectroscopy and GC/MS as $(CF_3)_2CHOC(O)OCH(CF_3)_2$.

^{19}F NMR chemical shifts:

$(CF^a_3)_2CHOC(O)OCH(CF_3)_2$: δ_a = -74.09 ppm (s).

^{1}H NMR chemical shifts:

$(CF_3)_2CH^aOC(O)OCH(CF_3)_2$: δ_a = 5.57 ppm (s, $^3J_{HF}$ = 5.5 Hz).

^{13}C NMR chemical shifts with proton decoupling:

$(C^aF_3)_2C^bHOC^c(O)OCH(CF_3)_2$: δ_a = 119.69 ppm (q, J_{CF} = 281.8 Hz), δ_b = 71.87 ppm (s, $^2J_{CF}$ = 35.4 Hz), δ_c = 151.69 ppm (s).

^{13}C NMR chemical shifts without proton decoupling:

$(C^aF_3)_2C^bHOC^c(O)OCH(CF_3)_2$: δ_a = 119.73 ppm (q, J_{CF} = 281.8 Hz), δ_b = 71.87 ppm (dsep, J_{CH} = 152.5 Hz, $^2J_{CF}$ = 36.3 Hz), δ_c = 151.70 ppm (t, $^3J_{HC}$ = 5.3 Hz).

Mass spectrum, m/z (relative intensity, %):

$(CF_3)_2CHOC(O)OCH(CF_3)_2$: 343 (2.1) $[M-F]^+$, 323 (6.3) $[M-HF-F]^+$, 195 (18.4) $[(CF_3)_2CHOC(O)]^+$, 151 (33.3) $[CF_3CHCF_3]^+$, 132 (1.2) $[CF_3CHCF_2]^+$, 113 (5.5) $[CF_3CHCF/CF_2CHCF_2]^+$, 97 (0.6) $[CF_3CO]^+$, 82 (4.1) $[CF_3CH]^+$, 69 (100.0) $[CF_3]^+$.

$(CF_3)_2CHOCH(CF_3)_2$: 249 (8.7) $[M-CF_3]^+$, 199 (27.8) $[(CF_3)_2CHOCHF]^+$, 151 (29.1) $[CF_3CHCF_3]^+$, 113 (4.1) $[CF_3CHCF/CF_2CHCF_2]^+$, 101 (28.5) $[CF_3CHF]^+$, 82 (8.3) $[CF_3CH]^+$, 69 (100.0) $[CF_3]^+$.

$(CF_3)_2CHOCF_2CFHCF_2OCH(CF_3)_2$: 397 (4.2) $[M-CF_3]^+$, 347 (14.1) $[M-CF_3-CF_2]^+$, 249 (25.3) $[(CF_3)_2CHOCF_2CHF]^+$, 199 (17.0) $[(CF_3)_2CHOCHF]^+$, 151 (42.9) $[CF_3CHCF_3]^+$, 132 (2.3) $[CF_3CHCF_2]^+$, 113 (8.6) $[CF_3CHCF/CF_2CHCF_2]^+$, 101 (6.4) $[CF_3CHF]^+$, 69 (100.0) $[CF_3]^+$.

CF_3CHFCF_3: 151 (25.5) $[M-F]^+$, 82 (30.3) $[CF_3CH]^+$, 69 (100.0) $[CF_3]^+$, 44 (21.6) $[CFCH]^+$.

4.5 REFERENCES

1. Amii, H.; Uneyama, K. C-F Bond Activation in Organic Synthesis. *Chem. Rev.* **2009,** *109*, 2119-2183.

2. Shen, Q.; Huang, Y.; Liu, C.; Xiao, J. C.; Chen, Q.; Guo, Y. Review of recent advances in CF bond activation of aliphatic fluorides. *J. Fluorine Chem.* **2015,** *179*, 14-22.

3. (a) Dunitz, J. D. Organic fluorine: odd man out. *ChemBioChem* **2004,** *5*, 614-21; (b) Dunitz, J. D.; Gavezzotti, A.; Schweizer, W. B. Molecular Shape and Intermolecular Liaison: Hydrocarbons and Fluorocarbons. *Helv. Chim. Acta* **2003,** *86*, 4073-4092; (c) Lemal, D. M. Perspective on Fluorocarbon Chemistry. *J. Org. Chem.* **2004,** *69*, 1-11.

4. (a) Doi, R.; Kikushima, K.; Ohashi, M.; Ogoshi, S. Synthesis, characterization, and unique catalytic activities of a fluorinated nickel enolate. *J. Am. Chem. Soc.* **2015,** *137*, 3276-82; (b) Guijarro, D.; Martínez, P.; Yus, M. Reductive defluorination of fluoroalkanes. *Tetrahedron* **2003,** *59*, 1237-1244; (c) Kuehnel, M. F.; Holstein, P.; Kliche, M.; Kruger, J.; Matthies, S.; Nitsch, D.; Schutt, J.; Sparenberg, M.; Lentz, D. Titanium-catalyzed vinylic and allylic C-F bond activation-scope, limitations and mechanistic insight. *Chem. Eur. J.* **2012,** *18*, 10701-10714; (d) Dordevic, N.; Tay, M. Q.; Muthaiah, S.; Ganguly, R.; Dimic, D.; Vidovic, D. C-F bond activation by transient phosphenium dications. *Inorg. Chem.* **2015,** *54*, 4180-2; (e) Unzner, T. A.; Magauer, T. Carbon–fluorine bond

activation for the synthesis of functionalized molecules. *Tetrahedron Lett.* **2015,** *56,* 877-883; (f) Raza, A. L.; Braun, T. Consecutive C–F bond activation and C–F bond formation of heteroaromatics at rhodium: the peculiar role of $FSi(OEt)_3$. *Chem. Sci.* **2015,** *6,* 4255-4260.

5. (a) Caputo, C. B.; Stephan, D. W. Activation of Alkyl C–F Bonds by $B(C_6F_5)_3$: Stoichiometric and Catalytic Transformations. *Organometallics* **2012,** *31,* 27-30; (b) Stahl, T.; Klare, H. F.; Oestreich, M. $C(sp^3)$-F bond activation of CF3-substituted anilines with catalytically generated silicon cations: spectroscopic evidence for a hydride-bridged Ru-S dimer in the catalytic cycle. *J. Am. Chem. Soc.* **2013,** *135,* 1248-1251.

6. (a) Nova, A.; Mas-Ballesté, R.; Lledós, A. Breaking C–F Bonds via Nucleophilic Attack of Coordinated Ligands: Transformations from C–F to C–X Bonds (X= H, N, O, S). *Organometallics* **2012,** *31,* 1245-1256; (b) Tobisu, M.; Xu, T.; Shimasaki, T.; Chatani, N., Nickel-catalyzed Suzuki-Miyaura reaction of aryl fluorides. *J. Am. Chem. Soc.* **2011,** *133,* 19505-19511.

7. Stahl, T.; Klare, H. F. T.; Oestreich, M. Main-Group Lewis Acids for C−F Bond Activation. *ACS Catal.* **2013,** *3*, 1578−1587.

8. (a) Bieniarz, C.; Ramakrishna, K. V. Synthetic Method for Fluoromethylation of Halogenated Alcohols. U.S. Patent 6,303,831 B1, Oct. 16, 2001; (b) Khrimian, A. P.; Jones, B. M. Production of Fluoromethyl 2,2,2-Trifluoro-1-(Trifluoromethyl) Ethyl Ether. U.S. Patent 6,469,219 B1, Oct. 22, 2002; (c) Bieniarz, C.; Chang, S. H.; Cromack, K. R.; Huang, S. L.; Kawai, T.; Kobayashi, M.; Loffredo, D.;

Raghavan, R.; Speicher, E. R.; Stelmach, H. A. Fluoroether Compositions and Methods for Inhibiting Their Degradation in the Presence of a Lewis Acid. U.S. Patent 6,677,492 B2, Jan. 13, 2004; (d) Rozov, L. A.; Lessor, R. A. Process for Recovery of 1,1,1,3,3,3-Hexafluoroisopropanol from the Waste Stream of Sevoflurane Synthesis. U.S. Patent 6,987,204 B2, Jan. 17, 2006; (e) Pacheco, O.; Teixeira, A. C.; Lima, E. L.; Bockelmann, M. A. Process for the Preparation of Chloromethyl-2,2,2-Trifluoro-1-(Trifluoromethyl) Ethyl Ether. U.S. Patent 8,039,678 B2, Oct. 18, 2011.

9. Yang, X.; Sun, H.; Zhang, S.; Li, X. Nickel-catalyzed C–F bond activation and alkylation of polyfluoroaryl imines. *J. Organomet. Chem.* **2013,** *723*, 36-42.

10. Klabunde, K. J.; Low, J. Y. F.; Key, M. S. Metal atom reactions with fluorocarbons. II. Defluorination by calcium atoms. *J. Fluorine Chem.* **1972,** *2*, 207-209.

11. Dear, R. E. A.; Gilbert, E. E. Polyhaloethers from the Reaction of Fluoroalcohols and Haloolefins. *J. Chem. Eng. Data.* **1969**, 14, 493-497.

12. (a) Shirota, N.; Okazoe, T. Kashiwagi, K. Polycarbonate Manufacturing Method and Polycarbonate. U.S. Patent Appl. 20160032046 A1, Feb. 4, 2016; (b) Okazoe, T.; Okamoto, H.; Tajima, K.; Nagasaki, Y. Process of Producing Diphenyl Carbonate. WO 2010001870 A1, Jan. 7, 2010; (c) Newallis, P. E.; Otto, J. A.; Pasquale, L. Fluoroalcohol Carbonates. U.S. Patent 3,359,296 A, Dec. 19, 1967.

CHAPTER FIVE

POTENTIAL MONOMER FOR AMORPHOUS FLUOROPOLYMER AND POLYMERIZATION ATTEMPTS

5.1 INTRODUCTION

Not only are the small molecules of HFEs attractive, the fluoropolyethers have also been developed as low temperature fluids, coating materials, sealants etc.[1] The flexibility of fluoropolyethers is largely improved by the introduction of ether linkages in the structure. Another special type of perfluoropolymers with ether linkages exists called amorphous fluoropolymers, which have outstanding properties.

The class of amorphous fluoropolyethers usually consists of a cyclic unit and a linear unit on the backbone of the molecular chain, which has comparable thermal and chemical stability to other fluoropolymers such as PTFE, ETFE, PFA, PCTFE, and PVDF. In addition, these polymers have unique properties like intrinsic micro-porosity, transparency at UV range, low refractive index, reasonable solubility in fluorinated organic solvents (e.g., perfluorohexane, perfluorobenzene, perfluorooctane) at room temperature, and low dielectric constant. Such properties of the materials make them suitable for many applications such as gas separation, microlithography, fiber cladding, anti-reflective coating, and hydrophobic coating or mixing.[2]

The first class of amorphous fluoropolymers was developed in the 1970's-1980's by DuPont and was called Teflon® AF,[3] which is a copolymer of TFE and perfluoro-2,2-dimethyl-1,3-dioxole (PDD).[4] Asahi Glass also prepared Cytop®[5] at the same time, and

Solvay Solexis patented Hyflon® AD in the 1990's (see **Error! Reference source not found.**). [6]

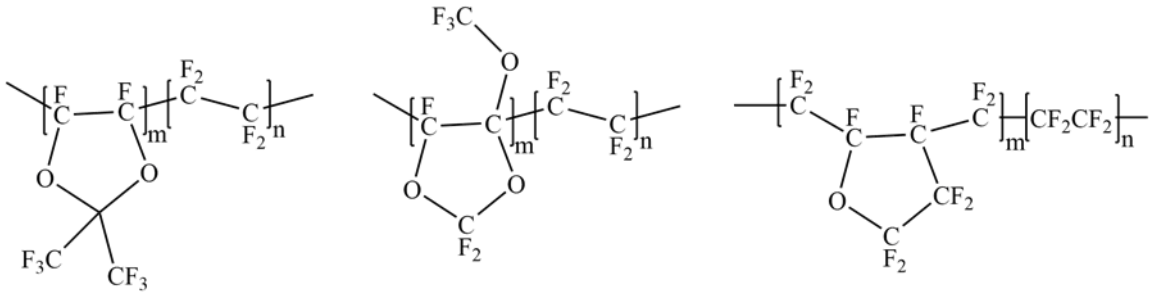

Figure 5.1. Commercial amorphous fluoropolymers.

To enrich and further develop the family of amorphous fluoropolymer, as well as reduce the environmental impact of solvent usage in the polymerization, many more monomers and new synthesis methods have been studied. Okamoto and his coworkers synthesized several new perfluoro dioxolanes as shown in Figure 5.2 and their polymers.[7]

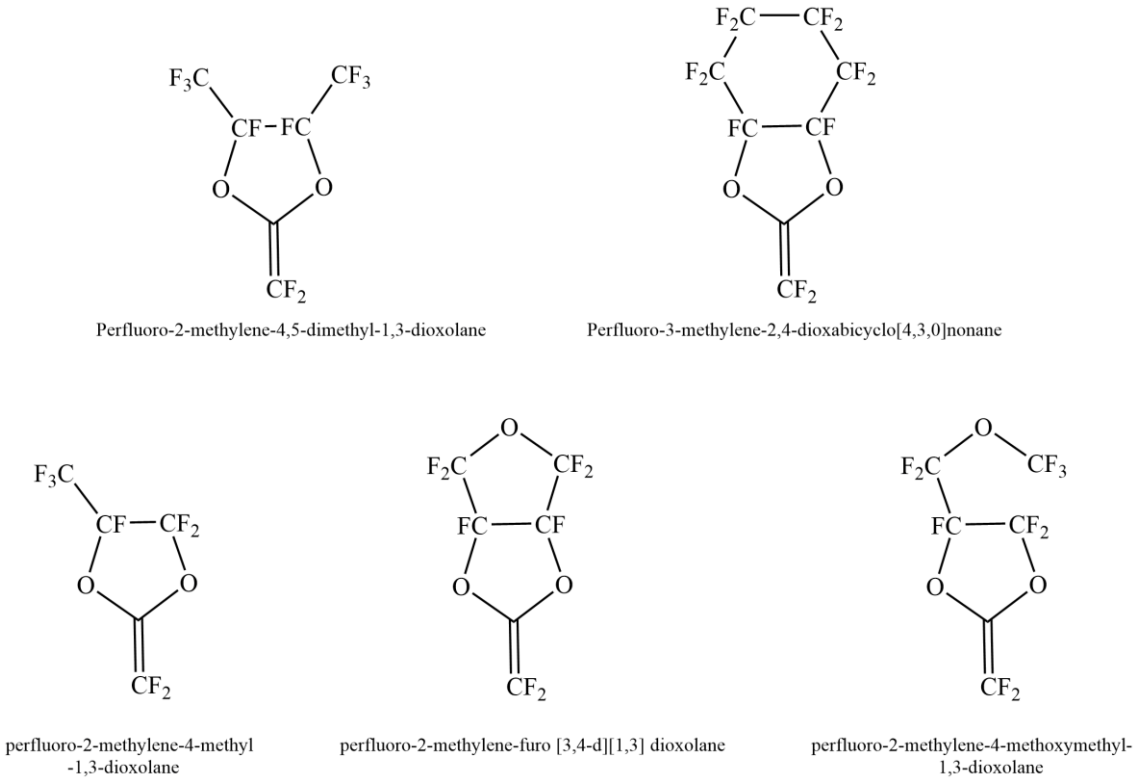

Figure 5.2. New perfluoro dixolane monomers for amorphous fluoropolymers.

The perfluoro dioxoles were studied mostly by DuPont, as first developed the materials, and new synthetic routes to such monomers were also developed by Navarrini.[8] To reduce the cost of the polymerization in organic solvent and the corresponding environmental effects, supercritical CO_2 was used in the polymerization as an environmentally friendly solvent.[9]

Even though such polymers have excellent properties, they have fatal drawbacks because they are extremely expensive to synthesize and their solubility is very limited, as they only dissolve in fluorinated solvents, which are also quite expensive to use. To improve the solubility of amorphous fluoropolymers, hydrocarbon cyclic units were

introduced into the structure. The resulting copolymers can also be dissolved in regular organics.[10] Currently, partially fluorinated amorphous fluoropolymers are still under development. Another type of amorphous fluoropolymer that stands out is perfluorocyclobutane polymer (PFCB) that is made from aromatic trifluorovinyl ether monomers by thermal cyclopolymerization.[11]

In this work, 2,2,5,5-tetrafluoro-2,5-dihydrofuran (M1) is used as a monomer to be copolymerized with several fluorinated olefins, and better solubility of the resulting materials is expected.

5.2 RESULTS AND DISCUSSION

The monomer M1 was initially synthesized (Scheme 5.1) for another branch of chemistry; however, the ring structure would be more valuable if it can be added to polymeric chains to obtain amorphous polymers having competitive thermal and chemical properties when compared to the aforementioned commercial products (**Error! Reference source not found.**). At the same time, the two protons on M1 can improve the solubility of the amorphous fluoropolymer in regular organic solvents, which is one of the biggest drawbacks of the current commercial products.

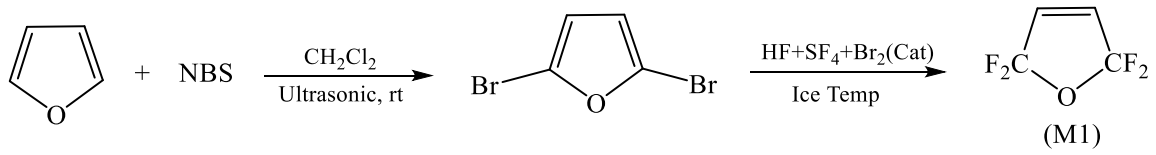

Scheme 5.1. Synthesis of M1

Initially, several regularly used and available radical initiators in laboratory stock, including azobisisobutyronitrile (AIBN), benzoyl peroxide (BPO) and bis(pentafluoropropionyl) peroxide (3P), were used as radical initiators in attempted homopolymerizations and copolymerizations of M1 with tetrafluoroethylene (CF_2=CF_2, TFE) without success. Later on UV radiation was applied to a sample of M1 in a quartz vessel in the presence of lab air, and some clear crystals were collected from the vessel. The crystals were sent directly to the X-ray diffraction laboratory for single crystal analysis, and those crystals turned out to be the cyclized dimer of M1 (tricyclic diether) as shown by the structure shown in Figure 5.3. In ^{19}F NMR spectrum of the tricyclic diether, the two fluorine atoms of CF_2 group are not equivalent and give an AB pattern shown in Figure 5.4.

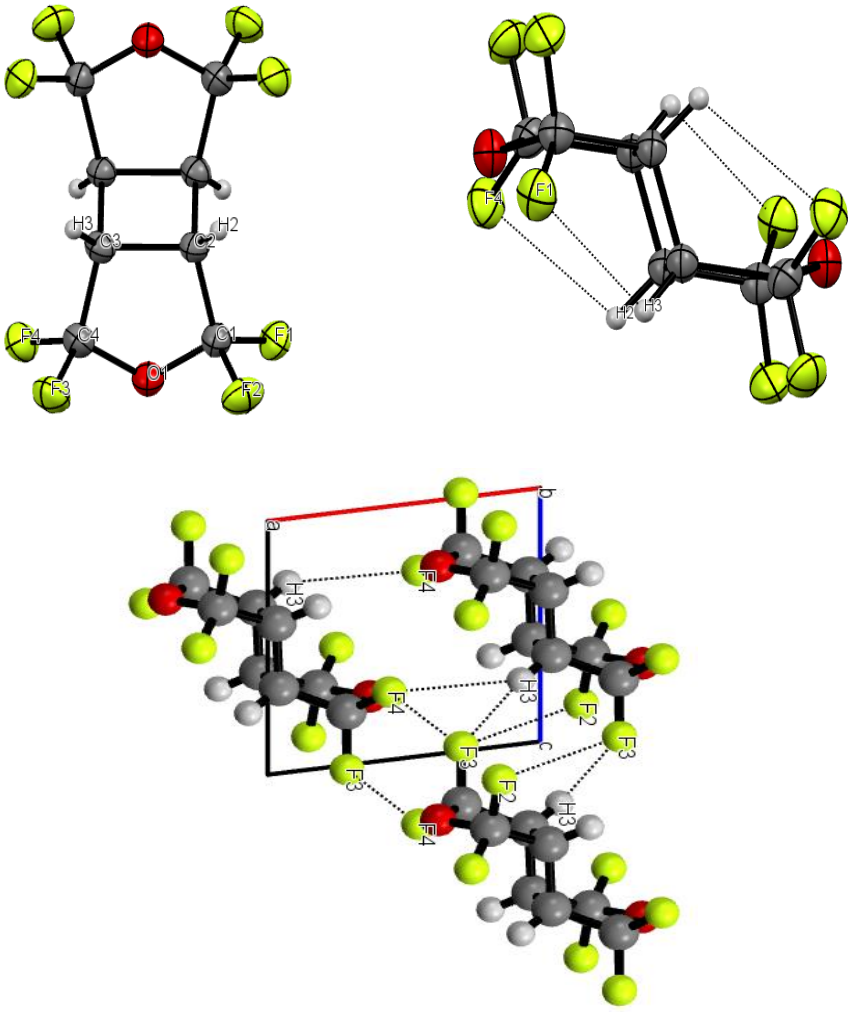

Figure 5.3. Crystal structure of tricyclic diether.

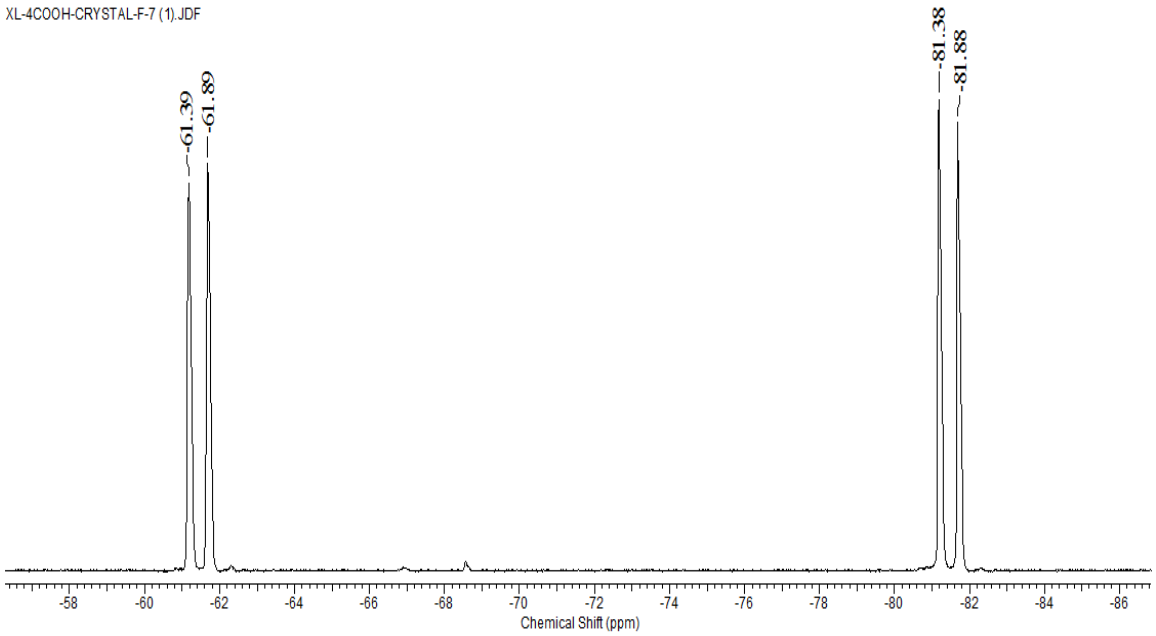

Figure 5.4. ^{19}F NMR spectrum of tricyclic diether.

UV radiation was then used in the copolymerization of M1 with TFE in the same quartz flask. About 95 wt% of the monomers was consumed during the reaction over four days and a rubbery transparent material [poly(Poly(M1-co-TFE))] accompanied by some white material (polytetrafluoroethylene, PTFE) was recovered after the solvent was vacuum transferred away. Following the same synthetic method, M1 was copolymerized with hexafluoropropene ($CF_3CF=CF_2$, HFP) giving a yield of 80 wt% and trifluorovinylsulfur pentafluoride ($SF_5CF=CF_2$, MSF_5) with a yield of 19 wt% respectively under UV radiation at room temperature. The product of copolymerization of M1 and HFP (Poly(M1-co-HFP)) appeared to be a hard brittle transparent layer after the solvent was removed. The material collected from the copolymerization of M1 and MSF_5 was also

transparent; however, it was light brown in color, which might be from bromine from residual precursor of the MSF_5 synthesis.

The mass weight yield of each copolymer follows the reverse order of the size of the fluorinated substituted group, which is TFE > HFP >MSF_5, perhaps leaving the sizes of F, CF_3, and SF_5 as a key factor in the copolymerization. The bulkier the substituent group on the trifluoroethylenic fragment is, the more difficult it is to be copolymerized with M1. M1 is itself a bulky five-membered ring, and the steric effects from both monomers might make it difficult to form a polymeric chain.

The van der Waals radii of a fluorine atom (1.47 Å) is slightly larger than that of hydrogen (1.20 Å).[12] The SF_5 and CF_3 groups are often compared with each other in terms of volume and electronegativity. The volume of a SF_5 group (49.2 cm^3/mol) is comparable to that of an isobutyl group, while a CF_3 group (20.49 cm^3/mol) is much smaller.[13] The substitution of CF_3 with SF_5 often give better or enhanced properties and activity or selectivity in pharmaceutical development.[14] SF_5-containing polymers are still under development, and an example of one of the initial studies was carried by Ameduri and coworkers in 2007.[15] Due to the difficulty of synthesizing SF_5-containing monomers, the development of such materials is quite slow.

Before an analysis of the thermal properties of the new materials, a structural determination of each product was carried out. The structure of each product was presumed to be a random copolymer with M1 as shown in Figure 5.5. Samples of Poly(M1-*co*-TFE), Poly(M1-*co*-HFP), and Poly(M1-*co*-MSF_5) were dissolved in acetone-d_6 and the resulting solutions were analyzed by ^{19}F NMR spectroscopy as shown in Section 5.2.3. ATR-IR,

SEM/EDX, TGA, and TGA/MS were taken on each product to further confirm the proposed structures. The copolymers Poly(M1-*co*-TFE) and Poly(M1-*co*-HFP) were fairly well analyzed, while Poly(M1-co-MSF5) was analyzed by only NMR spectroscopy and ATR-IR spectroscopy due to the small quantity of the sample (see Sections 5.2.3-5.2.4). Thus, thermal analysis and molecular weight (MW) measurement were mainly focused on Poly(M1-*co*-TFE) and Poly(M1-*co*-HFP).

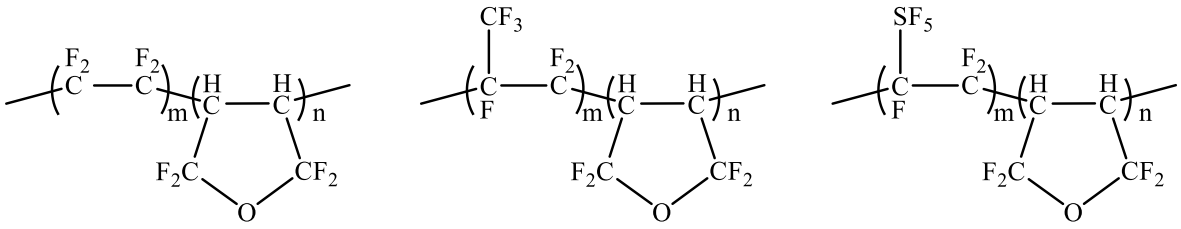

Figure 5.5. Proposed structure of M1 copolymers.

5.2.1 Synthesis of M1

The precursor for synthesizing monomer M1 and M1 itself were synthesized by following the synthetic methods reported in literature (Scheme 5.1).[16] The products were analyzed by multinuclear NMR spectroscopy, ATR-IR spectroscopy, UV/vis and gas chromatography/mass spectrometry (Figure 5.6-5.12). The precursor 2,5-dibromofuran has a singlet at 6.30 ppm in its ^{1}H NMR spectrum as shown in Figure 5.6, and it gives two singlet in the ^{13}C NMR spectrum with proton decoupling at 121.77 ppm and 114.16 ppm as shown in Figure 5.7, which agrees with the reported values.[16a]

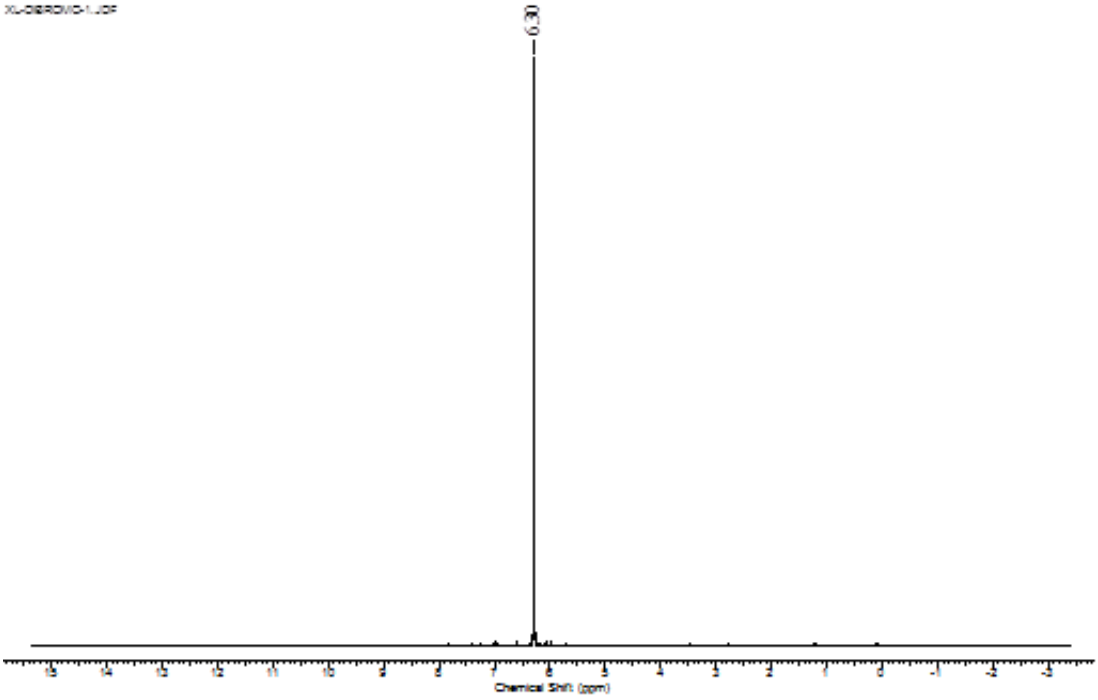

Figure 5.6. ^{1}H NMR spectrum of 2,5-dibromo-dihydrofuran in $CDCl_3$.

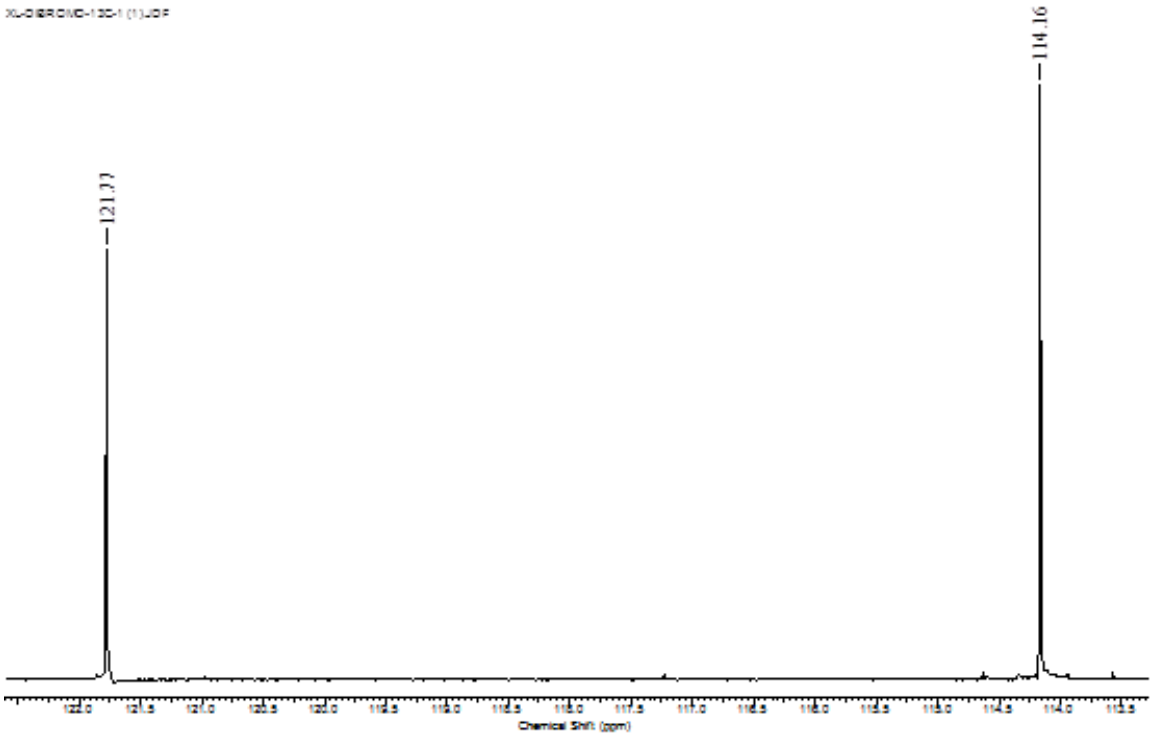

Figure 5.7. ^{13}C NMR spectrum of 2,5-dibromo-dihydrofuran with proton decoupling in $CDCl_3$.

In the ^{1}H NMR spectrum of M1, a singlet is seen at 6.49 ppm, and in the ^{19}F NMR spectrum, the compound gives a singlet at -73.12 ppm. Couplings between H and F or F and F are not observed in these two spectra (see Figure 5.8 and Figure 5.9). The ^{1}H and ^{19}F NMR spectroscopic results of both 2,5-dibromofuran and M1 agree with the reported chemical shifts.[16] The ^{13}C NMR of M1 was not reported before, and the CF_2 carbon is split into a big triplet of triplets at 127.92 ppm with a J_{CF} coupling constant 256.5 Hz, which is expected. The carbon peak of the CH unit at 130.75 ppm is split into a triplet by the adjacent CF_2 fluorine atoms, where the coupling constant is $^{2}J_{CF}$ = 31.1 Hz.

The ^{13}C spectrum of M1 was also collected with just ^{19}F decoupling as shown in Figure 5. 11, in order to have a better understanding of the structure of the molecule. The CH carbon peak at 130.74 ppm is split into a doublet of doublets with a coupling constant J_{CH} = 185.7 Hz, and $^{2}J_{CH}$ = 2.9 Hz. The signals for CF_2 carbon at 127.78 ppm is split by the protons with coupling constants of $^{2}J_{CH}$ = 8.3 Hz, and $^{3}J_{CH}$ = 1.4 Hz.

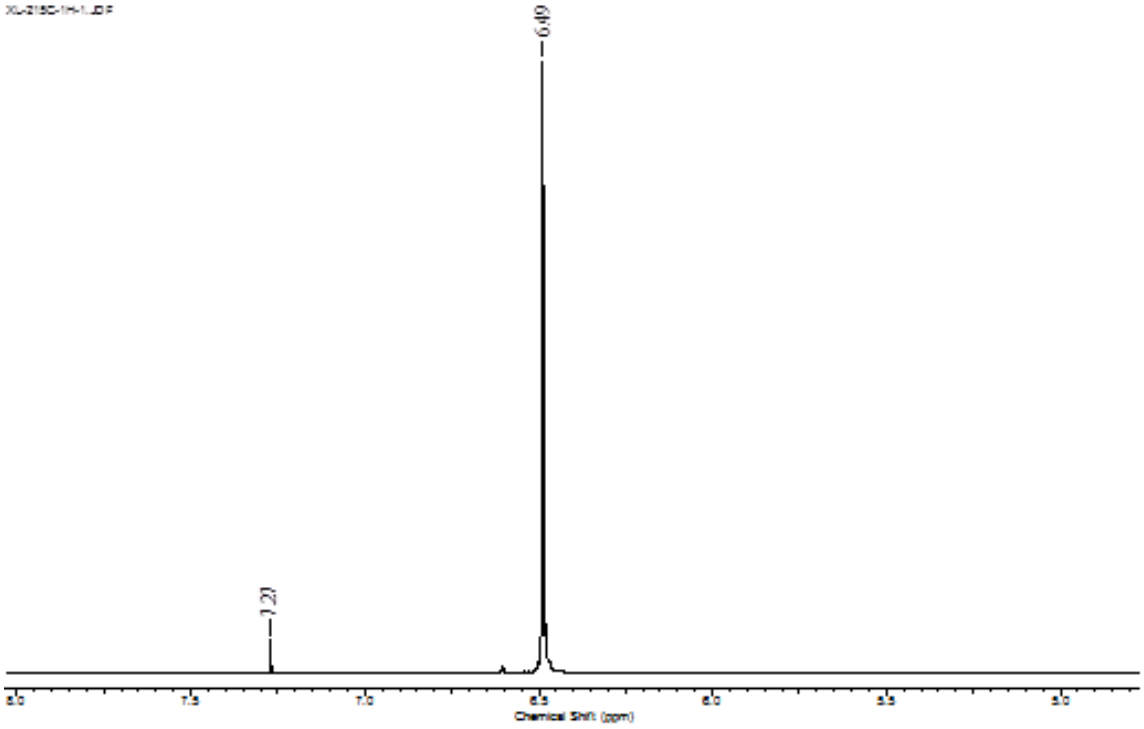

Figure 5.8. ^{1}H NMR spectrum of M1 in $CDCl_3$.

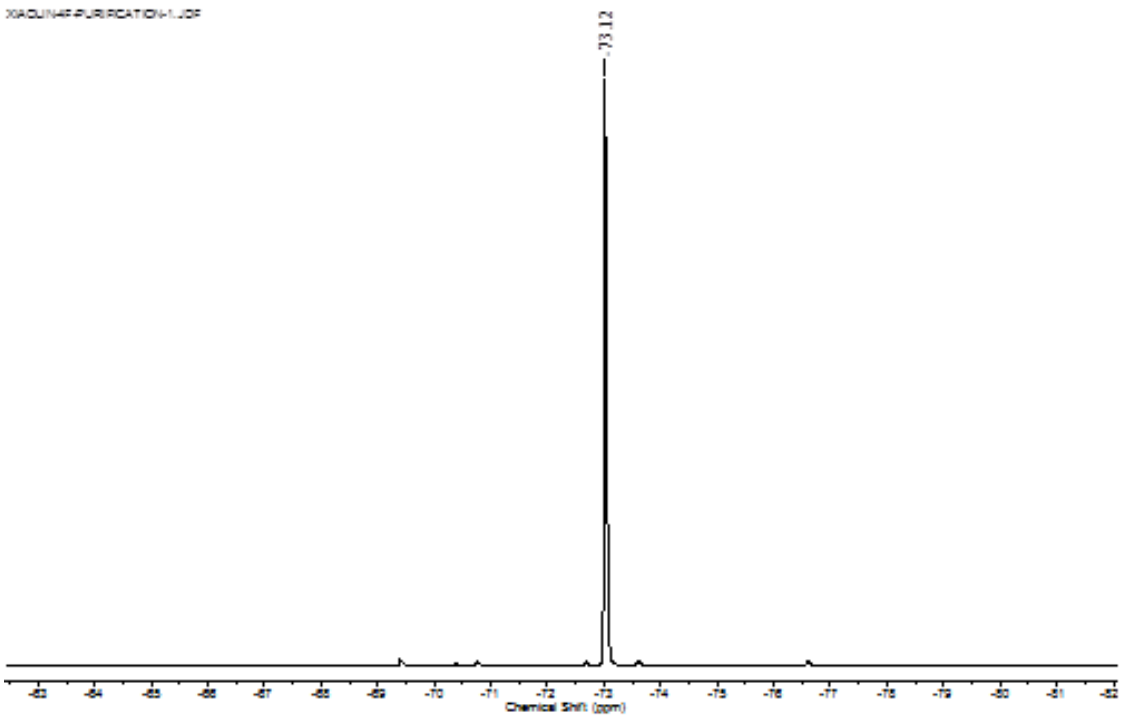

Figure 5.9. ^{19}F NMR spectrum of M1 in $CDCl_3$ with internal standard $CFCl_3$ at 0.00 ppm.

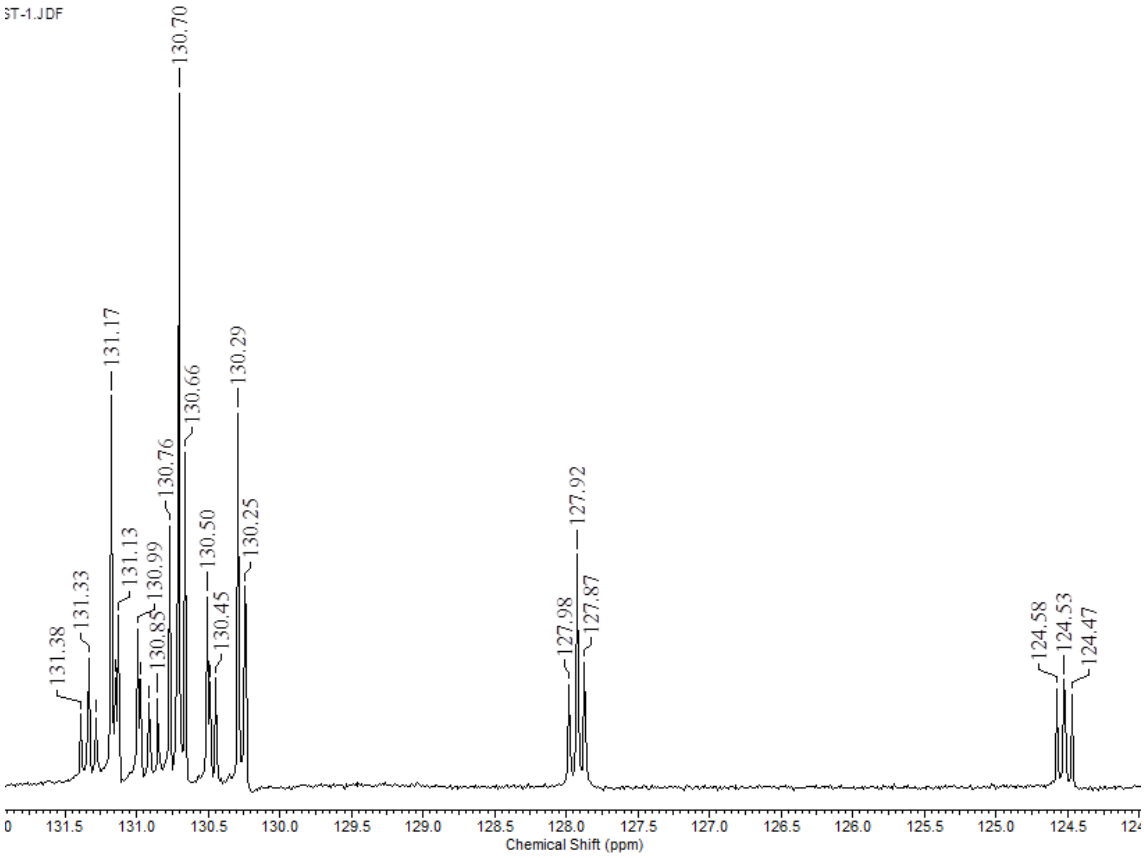

Figure 5.10. ^{13}C NMR spectrum of M1 with proton decoupling in $CDCl_3$.

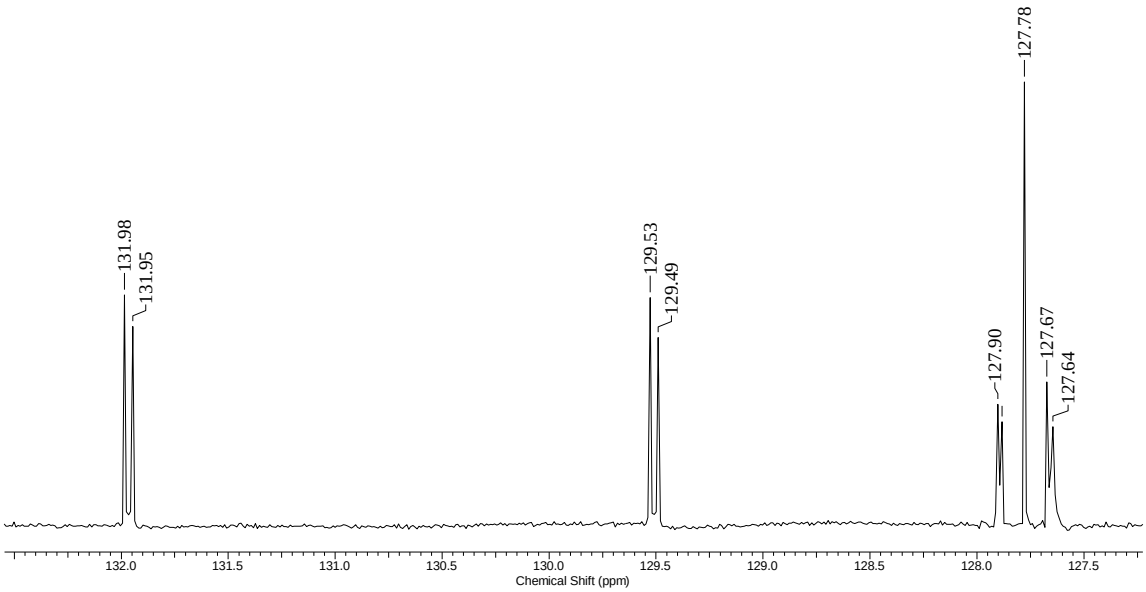

Figure 5. 11. ^{13}C NMR spectrum of M1 with ^{19}F decoupling in $CDCl_3$.

The ATR-IR information of M1 was collected on a diamond crystal, and the C-H bands are at 3127.97 cm^{-1} (w), 1361.50 cm^{-1} (m), 1332.57 cm^{-1} (s) and 846 cm^{-1} (m); the C=C stretch is at 1644.98 cm^{-1} (w); and the C-F stretch is at 1097.30 cm^{-1} (s) as shown in Figure 5.12.[29]

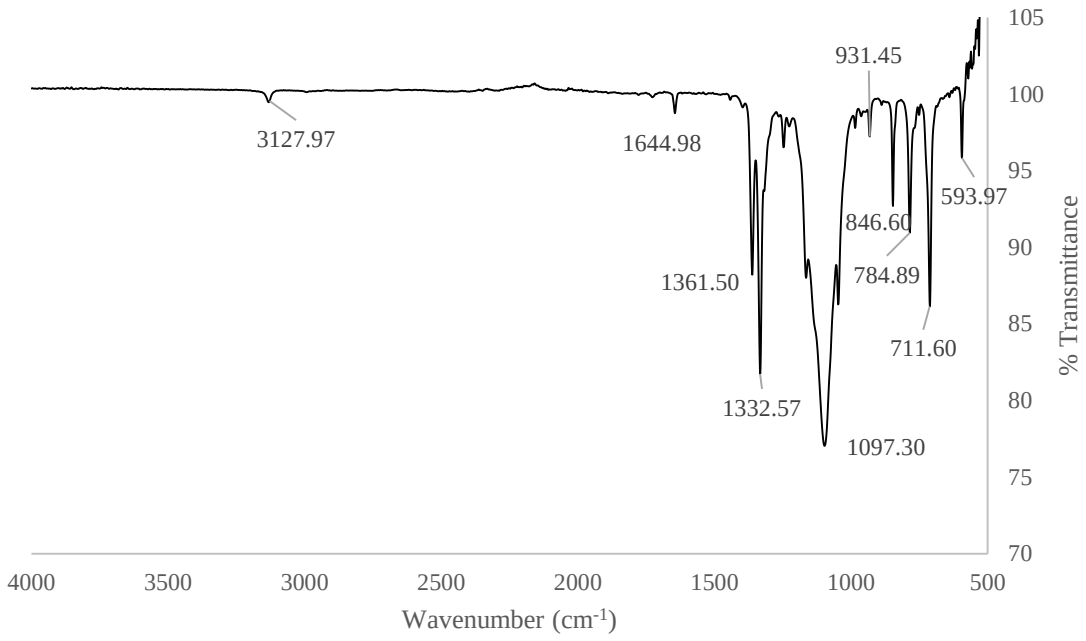

Figure 5.12. ATR-IR spectrum of M1.

It was observed that M1 has a UV absorption below 250 nm in acetonitrile solution as shown in Figure 5.13, which made it difficult to find a suitable photoinitiator in order to speed up the photopolymerization in the desired UV range.

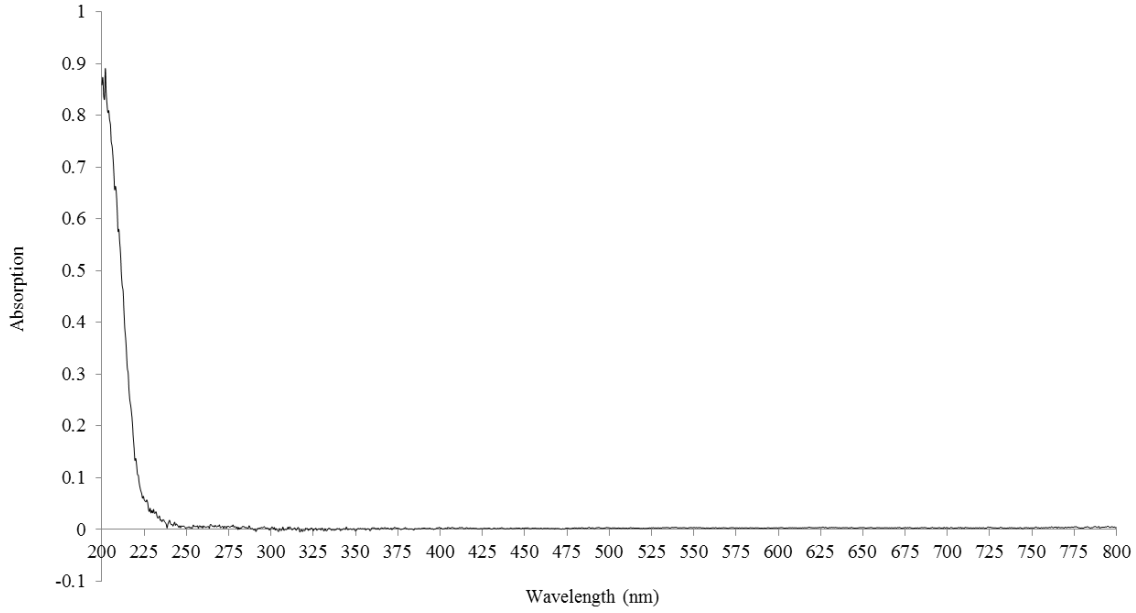

Figure 5.13. UV absorption spectrum of M1 in acetonitrile.

5.2.2 Crystal structure of tricyclic diether

This dimer was synthesized before by Pustovit,[17] and the same reaction was also performed in our laboratory in order to confirm the identity of the product by using NMR spectroscopy (Figure 5.4) and single crystal X-ray diffraction (Table 5.1). The current product gave an identical NMR spectral data to what was published before, and now the structure of this material is confirmed by single crystal X-ray analysis.

Table 5.1. Crystallographic Data of the Tricyclic Diether

Empirical formula	C4 H2 F4 O
Formula weight	142.06
Temperature	203(2) K
Wavelength	0.71073 Å

Crystal system, space group	Triclinic, P-1
Unit cell dimensions	a = 5.7468(11) Å b = 6.4934(13) Å c = 6.6785(13) Å alpha = 62.08(3)° beta = 80.37(3)°
Volume	217.01(7) A^3
Z, Calculated density	2, 2.174 Mg/m^3
Absorption coefficient	0.263 mm^{-1}
F(000)	140
Crystal size	0.41 x 0.18 x 0.10 mm
Theta range for data collection	3.48 to 25.24 deg
Limiting indices	-6<=h<=6, -7<=k<=7, -8<=l<=6
Reflections collected / unique	1845 / 778 [R(int) = 0.0273]
Completeness to theta = 25.24	99.2 %
Max. and min. transmission	0.9741 and 0.8997
Refinement method	Full-matrix least-squares on F^2
Data / restraints / parameters	778 / 0 / 83
Goodness-of-fit on F^2	1.296
Final R indices [I>2sigma(I)]	R1 = 0.0491, wR2 = 0.1274
R indices (all data)	R1 = 0.0578, wR2 = 0.1324
Extinction coefficient	0.14(2)
Largest diff. peak and hole	0.291 and -0.365 $e \cdot A^{-3}$

In the crystal structure of the tricyclic diether, one $C_4H_2F_4O$ unit connects to another $C_4H_2F_4O$ unit to form a $C_8H_4F_8O_2$ molecule sharing a central four-membered ring (C2-C3-C2-C3). These larger molecules then pack into a long-range structure by C-H---F hydrogen bonding. Meanwhile short F---F contacts (shorter than 3 Å) are also observed (see Table 5.2).

Table 5.2. Short Contact Distances Involving Fluorine Atom in the Tricyclic Diether

Interaction	Hydrogen/halogen bond distance (Å)
H2---F4	2.487
H3---F1	2.437
F2---F3	2.932

Fluorine as the most electronegative element has the least polarizability of the three lone pairs of electrons, and this is the main reason for the long debating of H-bonding and XB involving fluorine atoms.[18] The H···F interaction has been widely accepted as a type of hydrogen bonding now.[19] Both computational and experimental research has been done to prove that fluorine can be polarized and function as a halogen bonding donor to form C-F···X (X = F, Cl, Br, I) under some circumstances.[18b, 19b, 19c, 20] Short contacts involving fluorine atoms are not actually that rare, as we have observed these same interactions in other crystal structures of fluorinated molecules, which will be discussed in details in Chapters Six and Seven.

5.2.3 NMR spectroscopy of the copolymers

We were able to obtain ^{19}F NMR spectra on each sample in acetone-d_6. In Poly(M1-*co*-TFE), there are -OCF_2-, and -CF_2CF_2- fluorine atoms. The ^{19}F chemical shifts of -OCF_2- fluorine atoms are generally between -60 ppm and -80 ppm, while the signals for -CF_2CF_2- fluorine atoms show up around -120 ppm, as shown in Figure 5.14. The signals for all of the fluorine atoms in the ^{19}F NMR chemical shifts of the copolymers appear in the expected ranges. Integration of the spectrum was not applied due to the strong background noise, and the composition of the material was further investigated with EDX.

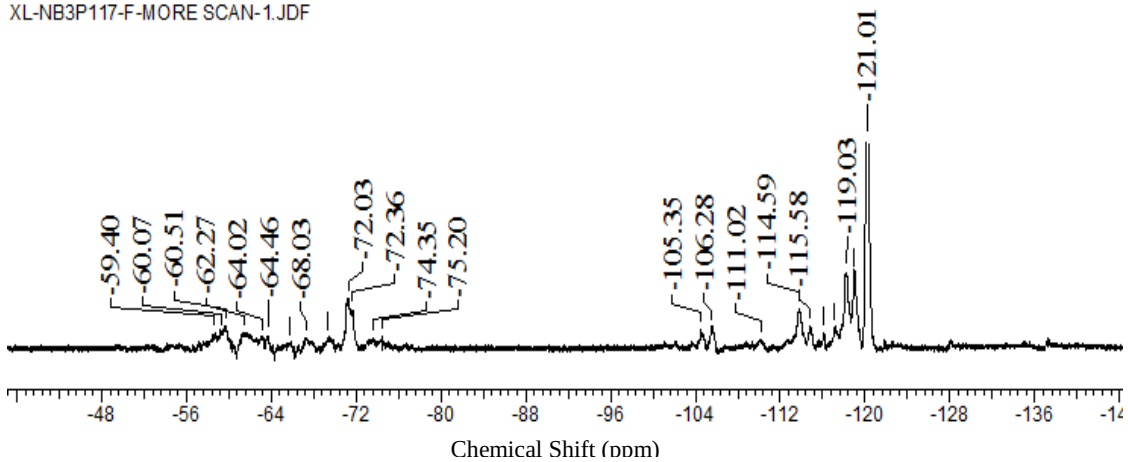

Figure 5.14. ^{19}F NMR of Poly(M1-*co*-TFE) in acetone-d6 with internal standard $CFCl_3$ at 0.00 ppm.

In Poly(M1-*co*-HFP), there are $-CF_3$, $-OCF_2$, -CF-, and $-CF_2$- fluorine atoms, and they resonate around -80 ppm, -70 ppm, -120 ppm, and -184 ppm, respectively (see Figure 5.15). The peak at -163.51 ppm is from SiF_4 generated during the reaction, which also indicates possible HF elimination when the material dissolves in the NMR solvent. When glass meets HF, HF combines with SiO_2 to form SiF_4.[21] The integration was not applied for the aforementioned reason, and the composition of the material was again further studied by EDX.

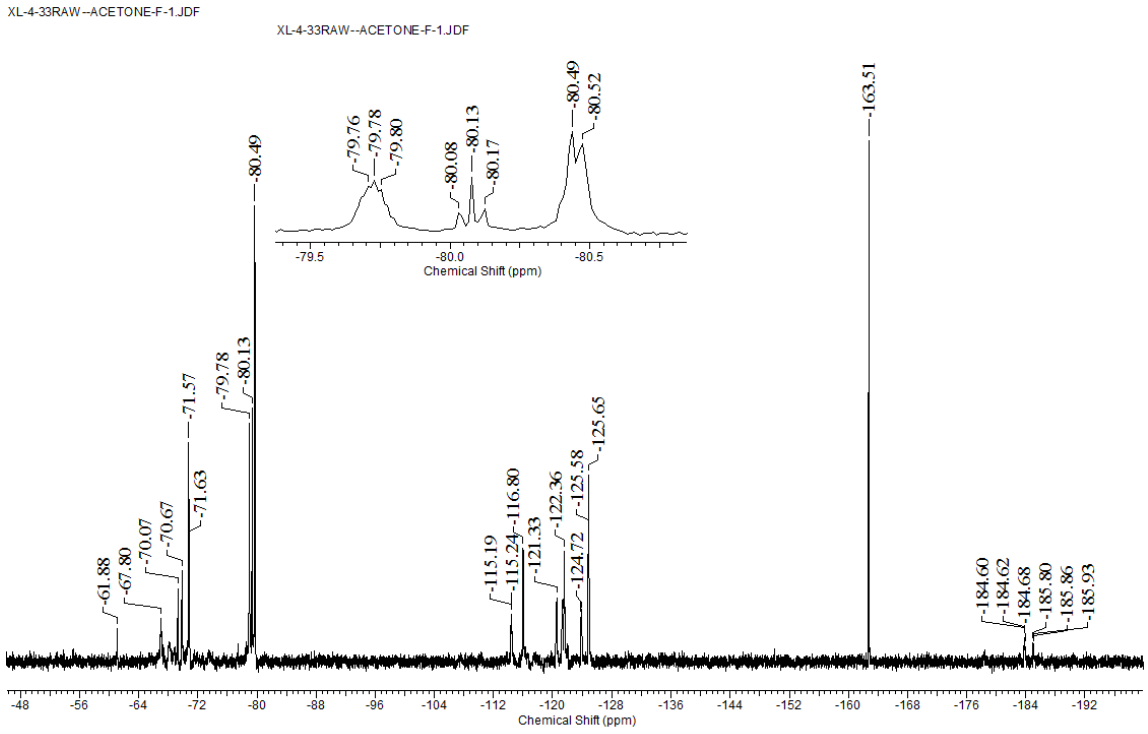

Figure 5.15. ^{19}F NMR spectrum of Poly(M1-*co*-HFP) in acetone-d6 with internal standard $CFCl_3$ at 0.00 ppm.

Poly(M1-*co*-HFP) has a solubility of about 15wt% in FC-72, which has a main component of C_6F_{14}. Since FC-72 is a perfluorocarbon solvent, ^1H NMR spectrum of the polymer was obtained with a capillary containing D_2O for solvent lock. The interference of ^{19}F and ^{13}C signals is sever, so no useful data was collected from the ^{19}F and ^{13}C spectra taken in FC-72. The protons on the polymeric chain are expected to have a chemical shift around 6 ppm in ^1H NMR spectrum. The peak at 4.75 ppm belongs to D_2O, which is contained in a capillary. The other peaks are quite broad, and the two major regions have a nearly 1:1 ratio by integration as shown in Figure 5.16.

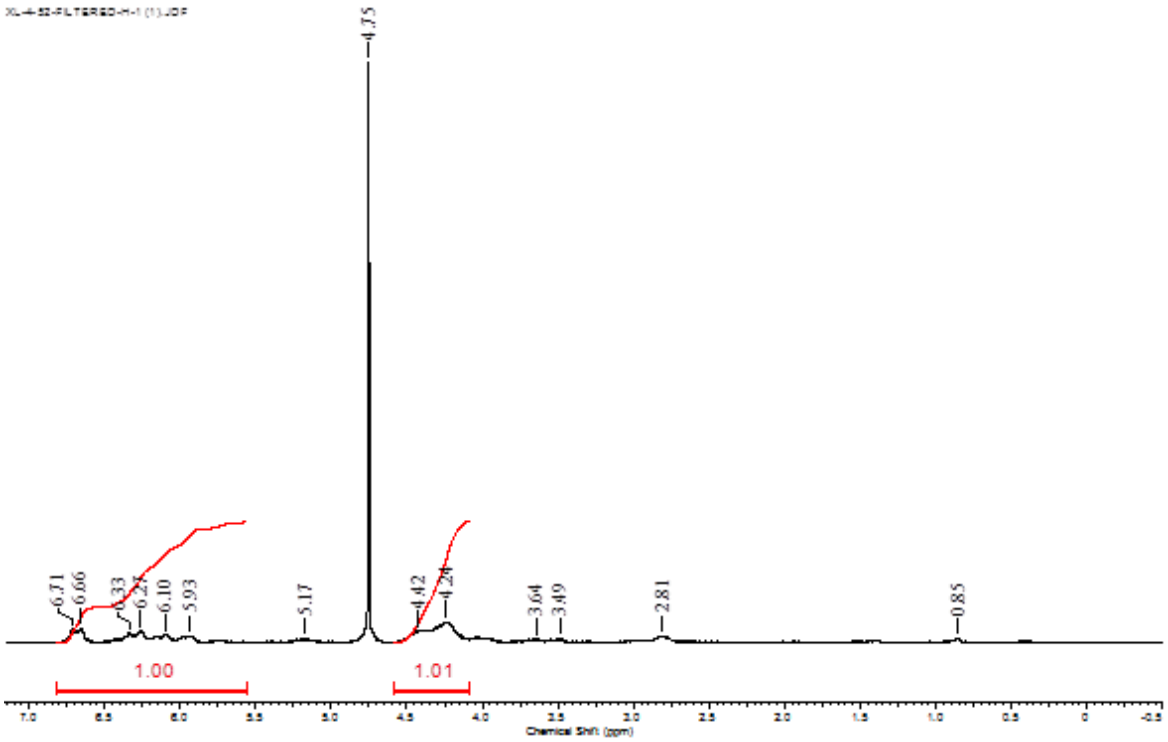

Figure 5.16. ^{1}H NMR spectrum of Poly(M1-*co*-HFP) in FC-72, external standard D_2O at 4.75 ppm.

In the ^{19}F NMR spectrum of Poly(M1-co-MSF5) shown in Figure 5.17, the fluorine signals the of SF_5 group appear in the positive region from 40 ppm to 120 ppm, which are quite distinguishable from the other fluorine signals. The fluorine signals of OCF_2 from the cyclic unit, CF_2 on the backbone, and CF showed up in the expected regions of -54 ppm to -78 ppm, -89 ppm to -131 ppm, and -149 ppm to -151 ppm, respectively. From the integration, the ratio of M1 to MSF_5 in the material is about 1:2.

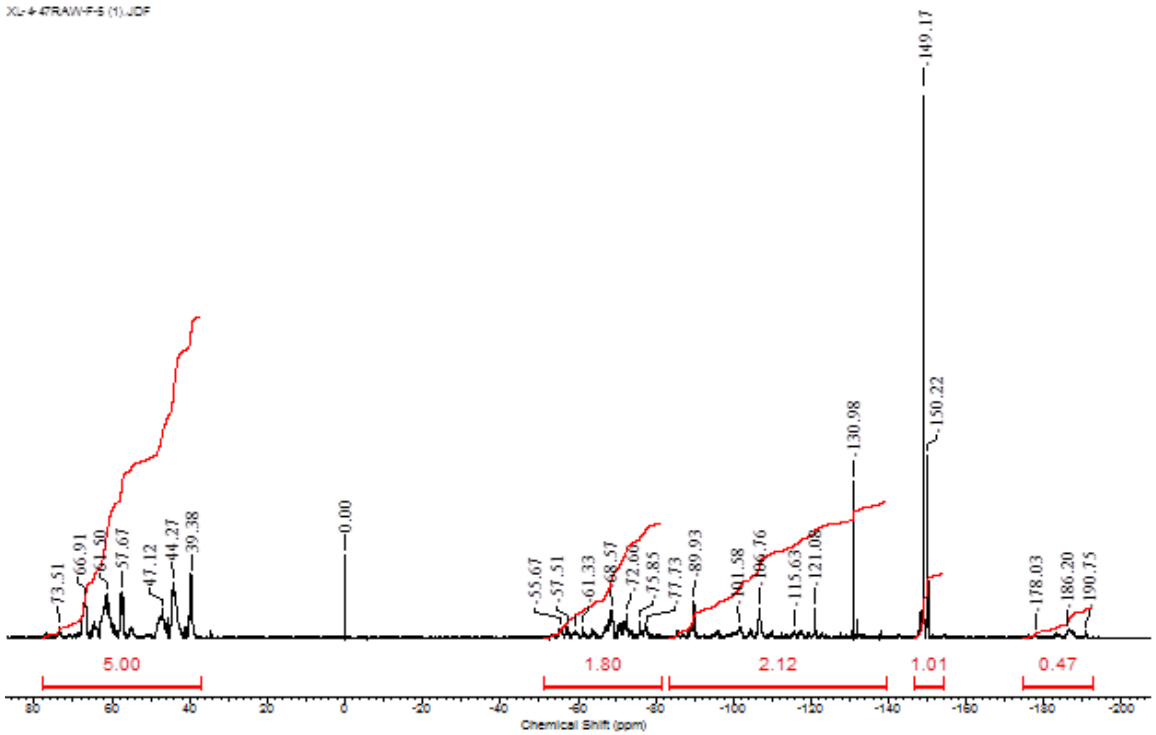

Figure 5.17. ^{19}F NMR spectrum of Poly(M1-*co*-MSF_5).

5.2.4 ATR-IR of the copolymers

Each copolymer of M1 was analyzed by ATR-IR spectroscopy. The samples were exposed in the air during the analysis. In the spectrum of Poly(M1-*co*-TFE) (Figure 5.18), the peaks that showed up between 1000 and 1400 cm^{-1} are assigned to the C-F stretches.[22] The weak band at 2999 cm^{-1} is the C-H stretch. The band at 2353 cm^{-1} is residue CO_2 from the air because the instrument is exposed to the air, and no protection from a nitrogen purge exist. The oxirane is located around 1200-1300 cm^{-1} and 700 to 900 cm^{-1}, which is overlapped with C-F stretching bands.[3, 23]

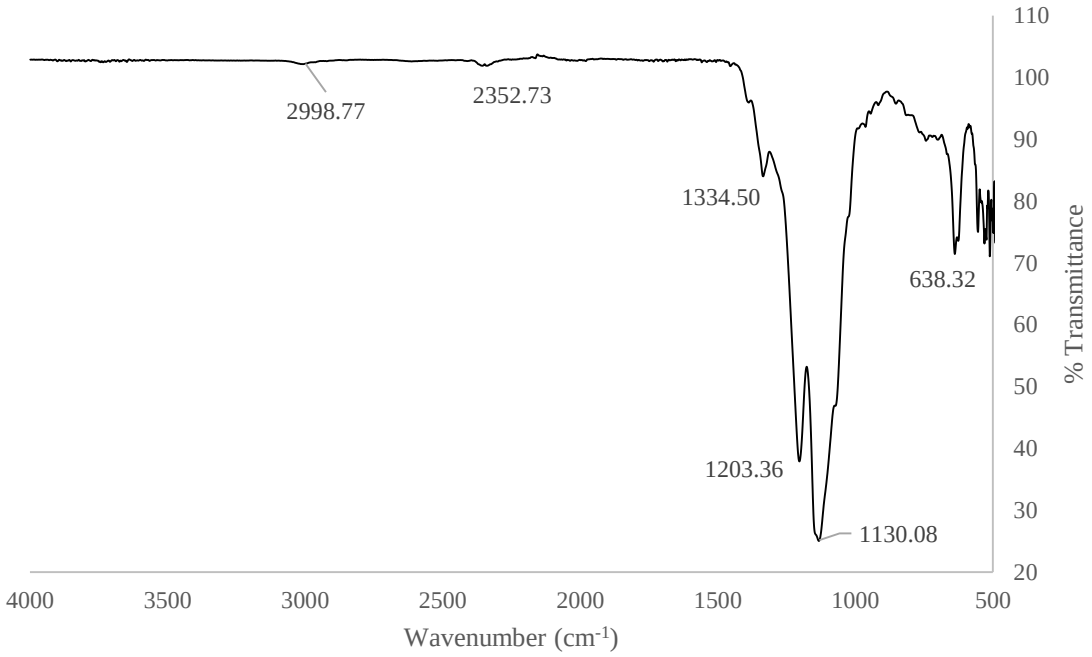

Figure 5.18. ATR-IR spectrum of Poly(M1-*co*-TFE) before evacuation at 145 °C.

A Comparison of the ATR-IR spectra of Poly(M1-*co*-TFE) before and after evacuation at elevated temperature, reveals that the shape of the CF_2 bands changed, which probably means that the sample had experienced decomposition or rearrangement of the structure at much lower temperature than the decomposition temperature 269 °C (see Figure 5.19).

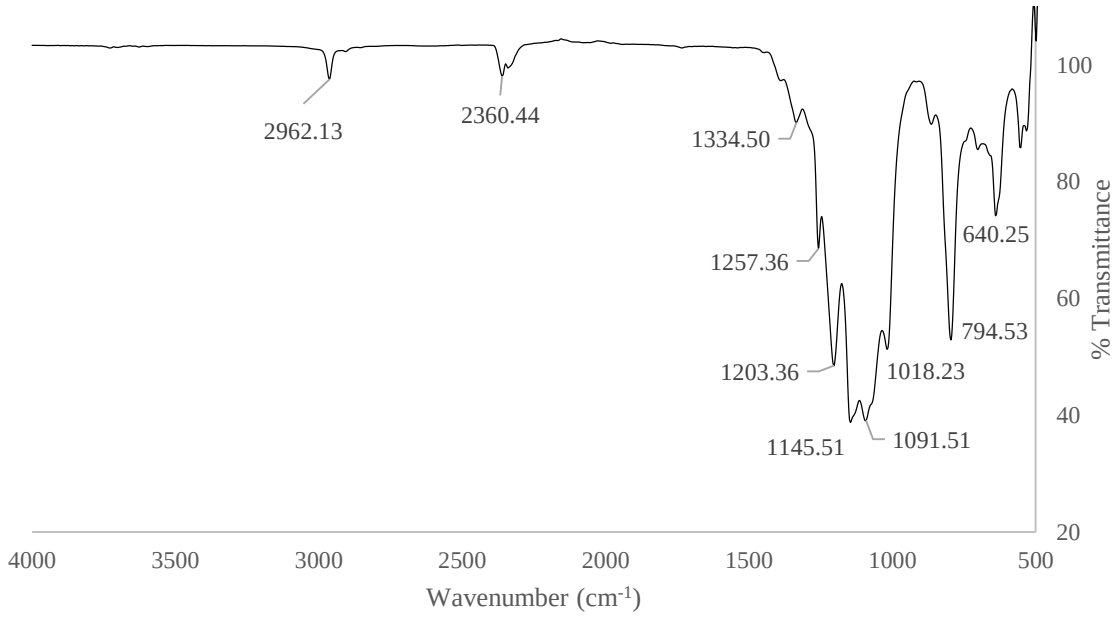

Figure 5.19. ATR-IR spectrum of Poly(M1-*co*-TFE) after evacuation at 145 °C.

After the sample had been in contact with acetone (used to rinse the material off of the ATR crystal), a band appeared at 1682 cm^{-1} that might possibly belong to a C=C absorption (see Figure 5.20). It is very likely that a small amount of HF was eliminated from the structure to form a C=C bond.[24] Another possible explanation is some carbonyl group C=O being generated on the fluorocarbon segments due to the friction during sample handling, which is discussed by Junk and coworkers in a study of the tribology of PTFE.[25]

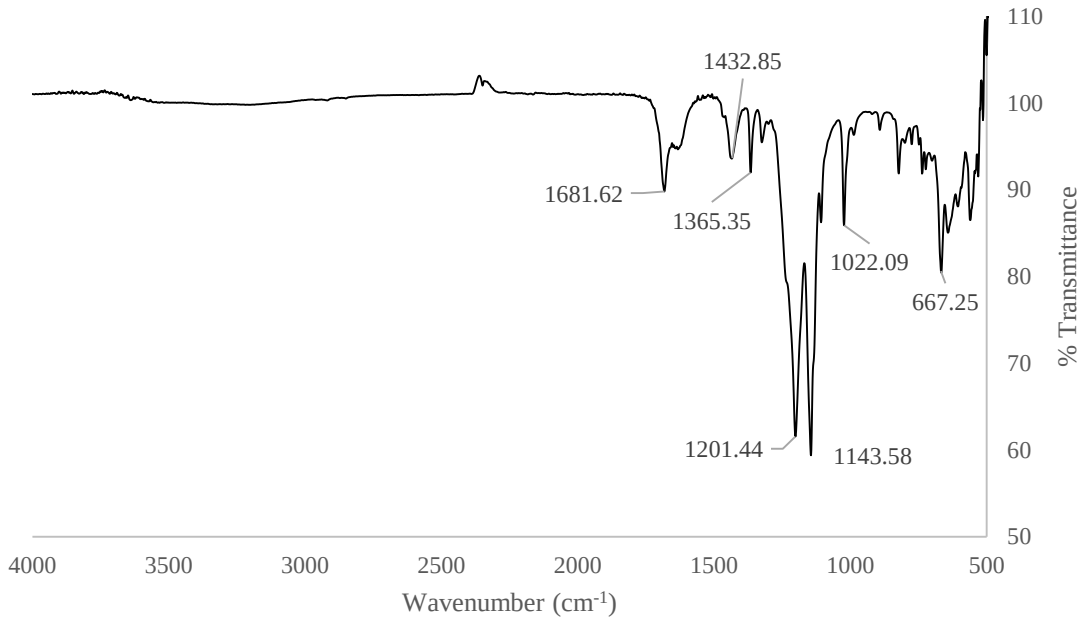

Figure 5.20. ATR-IR spectrum of Poly(M1-*co*-TFE) with new vibration at 1681.62 cm^{-1}.

The ATR-IR spectrum of poly(M1-*co*-HFP) (see Figure 5.21) is very similar with that of Poly(M1-*co*-TFE). The C-F stretching bands are located between 1000 cm^{-1} and 1400 cm^{-1} and overlap with the oxirane band. The band of 729 cm^{-1} is assigned to oxirane.[23] The C-H stretching band in the IR spectrum is extremely weak, and it is difficult to tell it apart from the baseline, even though strong ^{1}H signals appear in the ^{1}H NMR spectrum of poly(M1-*co*-HFP). The same phenomena of suppressed C-H vibrational bands were observed in both poly(M1-*co*-TFE) and poly(M1-*co*-MSF_5) (see Figure 5.18 and Figure 5.22).

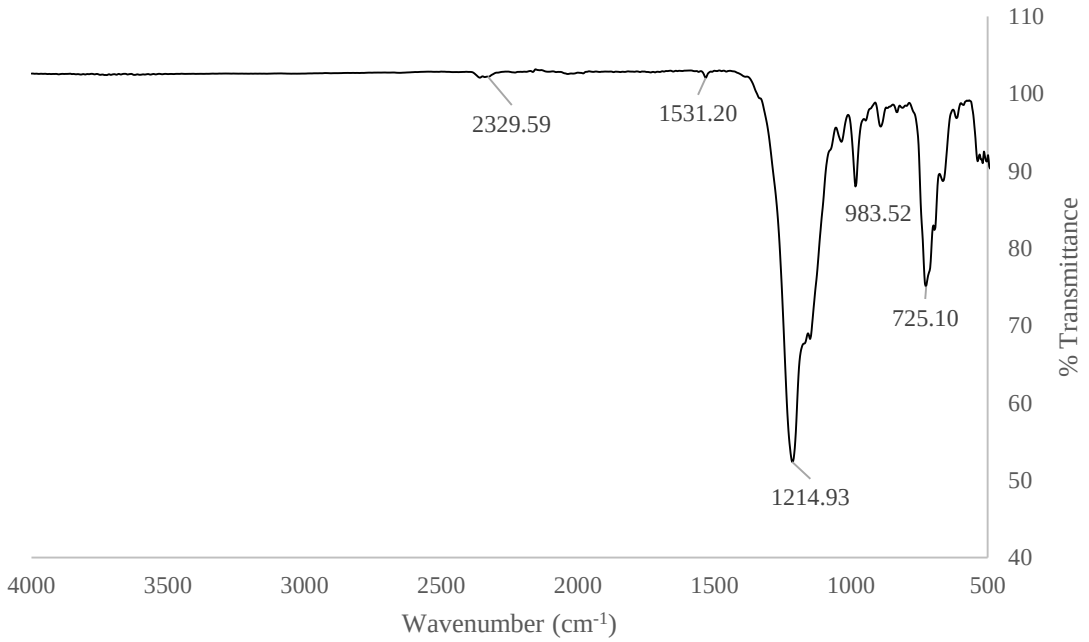

Figure 5.21. ART-IR Spectrum of Poly(M1-*co*-HFP).

In the ATR-IR spectrum of poly(M1-*co*-MSF_5) (see Figure 5.22), the large absorption 879 cm^{-1} is the S-F stretching band. The wide band between 1000 cm^{-1} and 1300 cm^{-1} are assigned to C-F stretches. The peak at 1782 cm^{-1} is the C=C stretch band, which might be caused by HF elimination. The C-H vibrational band at 2992.98 cm^{-1} is very weak, but it is often overwhelmed when a material is highly fluorinated.

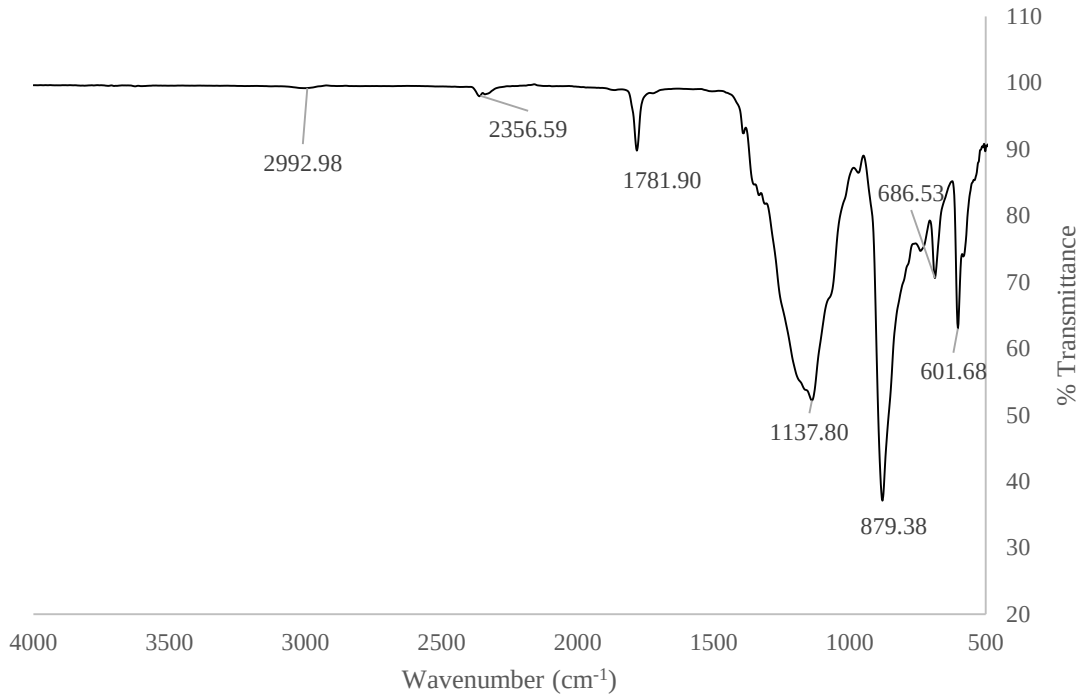

Figure 5.22. ATR-IR Spectrum of Poly(M1-*co*-MSF_5).

The intensity of a C-H vibration band is believed to be related to the acidity of the proton according to several studies. According to Leach, an increase of positive charge on the carbon atoms can result in an increased CH acidity, higher IR band intensity, as well as increased energy of hydrogen bond formation.[26]. However, an increase in intensity of CH band is not always true when induction is the only effect by an electron withdrawing substituent on a CH moiety and a backdonation of electron density is not available.[27]

In the copolymers of M1, the CH carbon is adjacent to highly electron withdrawing CF and CF_2 groups in the structure, which should cause an increased acidity of the protons by induction. Electron backdonation from fluorine atoms is not applied in this case, which results in a much reduced intensity of the CH bands in the IR spectra.

In the ATR-IR spectra of all three materials, whenever a C-H stretching band is present, the C=C band disappears, and vise versa. This result gives more insight on the structural change that might be going on during the operation of the materials, i.e., being in contact with organics may cause HF elimination from the structure. It was also observed that when a fresh sample of the material came into contact with acetone, a small amount of smoke was generated, and the quartz vessel was etched after a few reactions. In terms of relative stability when being in contact with organics, poly(M1-*co*-HFP) was the most stable product since change in color of either the material itself or the solvent was not observed. Freshly prepared poly(M1-*co*-TFE) appears to be a mixture of white solid (PTFE) and transparent, colorless material, and this material turns yellow after being dissolved in acetone or DMF.

5.2.5 SEM/EDX of poly(M1-co-TFE) and poly(M1-co-HFP)

A ground powder sample of poly(M1-*co*-TFE) and poly(M1-*co*-HFP) were analyzed with SEM/EDX TM 3000, respectively. The calculation of the composition is based on the ratio of fluorine to oxygen. Poly(M1-*co*-MSF_5) was not suitable for this analysis due to it being a viscous material. The appearances of poly(M1-*co*-TFE) and poly(M1-*co*-HFP) are quite different in that poly(M1-*co*-TFE) has some texture and less sharp edges, while poly(M1-*co*-HFP) has very sharp and clean edges as well as a smooth surface as shown in Figure 5.23 and Figure 5.25, respectively.

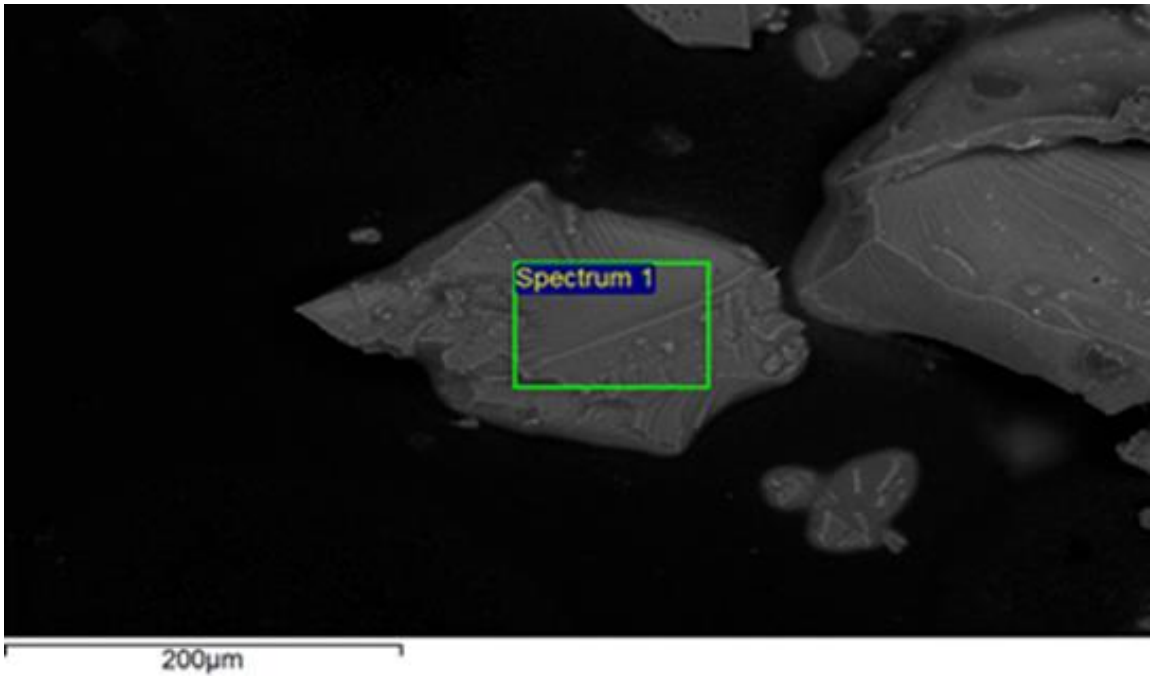

Figure 5.23. SEM of Poly(M1-*co*-TFE).

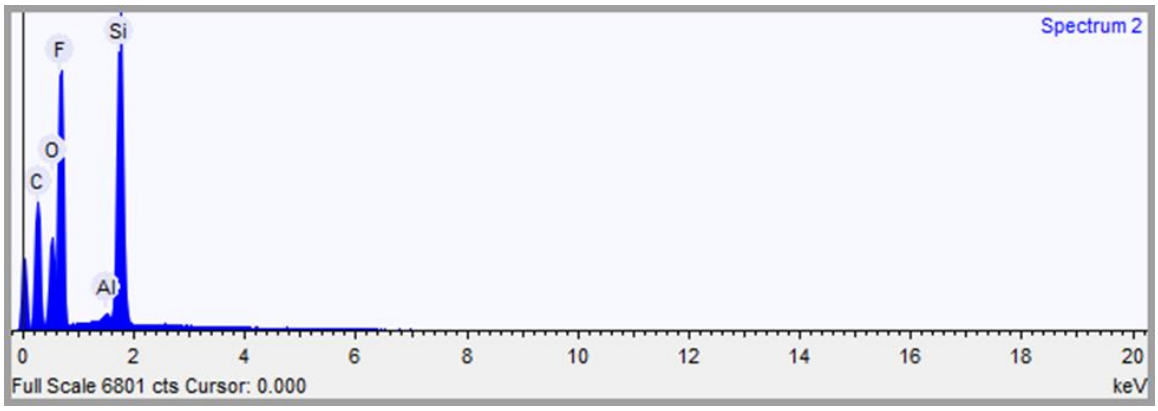

Figure 5.24. EDX of Poly(M1-*co*-TFE).

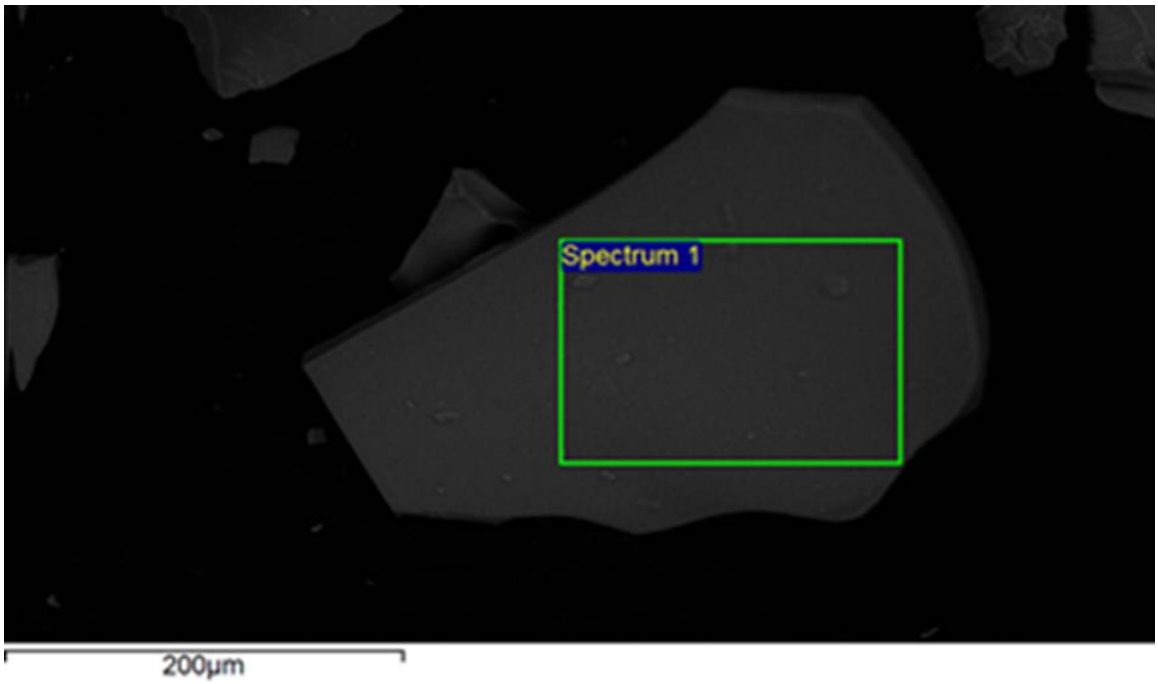

Figure 5.25. SEM of Poly(M1-*co*-HFP).

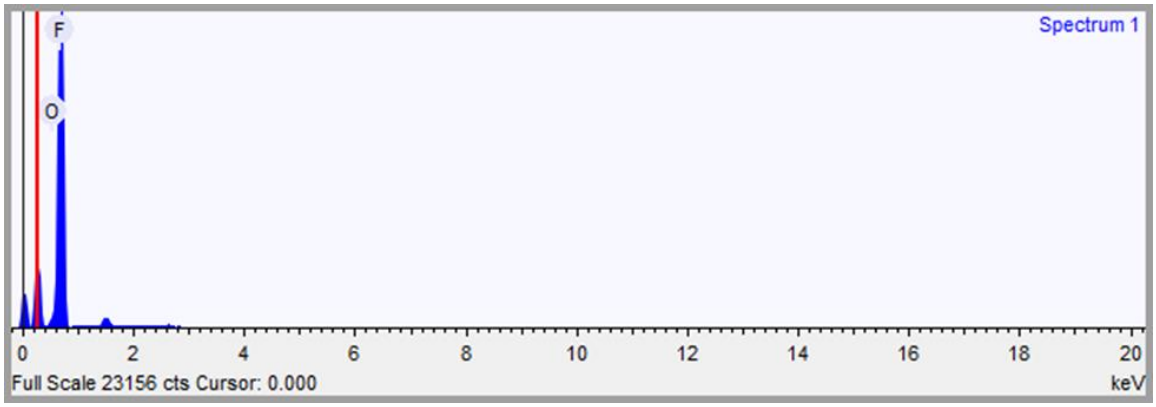

Figure 5.26. EDX of Poly(M1-*co*-HFP).

According to the calculated oxygen to fluorine elemental ratio in poly(M1-*co*-TFE), m = 1~5 n, where m is the number of TFE unit and n is the number of M1 unit (see Figure 5.5, Figure 5.24 and Table 5.3). The atomic % of carbon was neglected because the

sample was prepared on carbon tape, which will most certainly affect the analysis of carbon. The same calculation was applied to poly(M1-*co*-HFP), and m = 1~7n, where m is the number of HFP unit and n is the number of M1 unit (see Figure 5.5, Figure 5.26 and Table 5.4). The atomic % of carbon was also ignored because the sample was prepared on carbon tape, which will definitely interfere with the analysis of this element in the material.

Table 5.3. Atomic % for Oxygen and Fluorine in Poly(M1-*co*-TFE)

Atomic % / Sample	O	F
1	7.3	92.3
2	3.9	96.1
3	4.8	95.2
4	9.3	90.7
5	6.7	93.3
6	13.7	34.7
7	8.5	37.4
8	2.9	56.7
9	2.6	56.6
10	4	51.2
11	7.7	39.7
12	5.5	44.9

Table 5.4. Atomic % for Oxygen and Fluorine in Poly(M1-*co*-HFP)

Atomic % / Sample	O	F
1	3.2	96.8
2	11.1	88.9
3	2.0	98
4	5.4	94.6
5	9.8	90.2
6	7.8	92.2
7	2.6	97.4

5.2.6 TGA and TGA/MS of Poly(M1-co-TFE) and Poly(M1-co-HFP)

The decomposition temperature of poly(M1-*co*-TFE) is about 269 °C, while the decomposition temperature of poly(M1-*co*-HFP) is only about 130 °C (Figure 5.27). The thermal stabilities of these materials are not as good as expected, thus, they would not be competitive with commercial amorphous fluoropolymers.

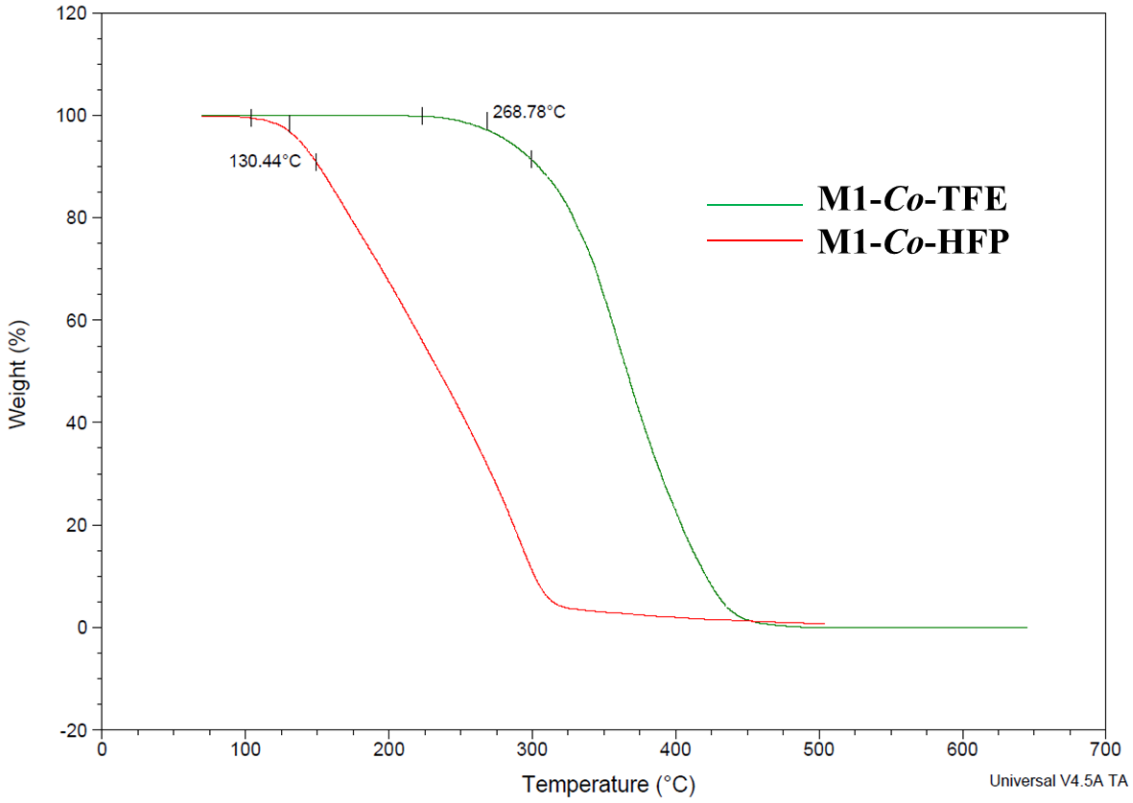

Figure 5.27. TGA of Poly(M1-*co*-TFE) and Poly(M1-*co*-HFP).

In order to investigate the decomposition of those polymers and obtain further evidence of the proposed structures, TGA/MS experiments were carried out, and selective

cations were monitored (see **Error! Reference source not found.** and **Error! Reference source not found.**). Unfortunately, the detector was not able to pick up signals from the poly(M1-*co*-MSF_5).

Report 3. TGA-MS of Poly(M1-co-TFE)

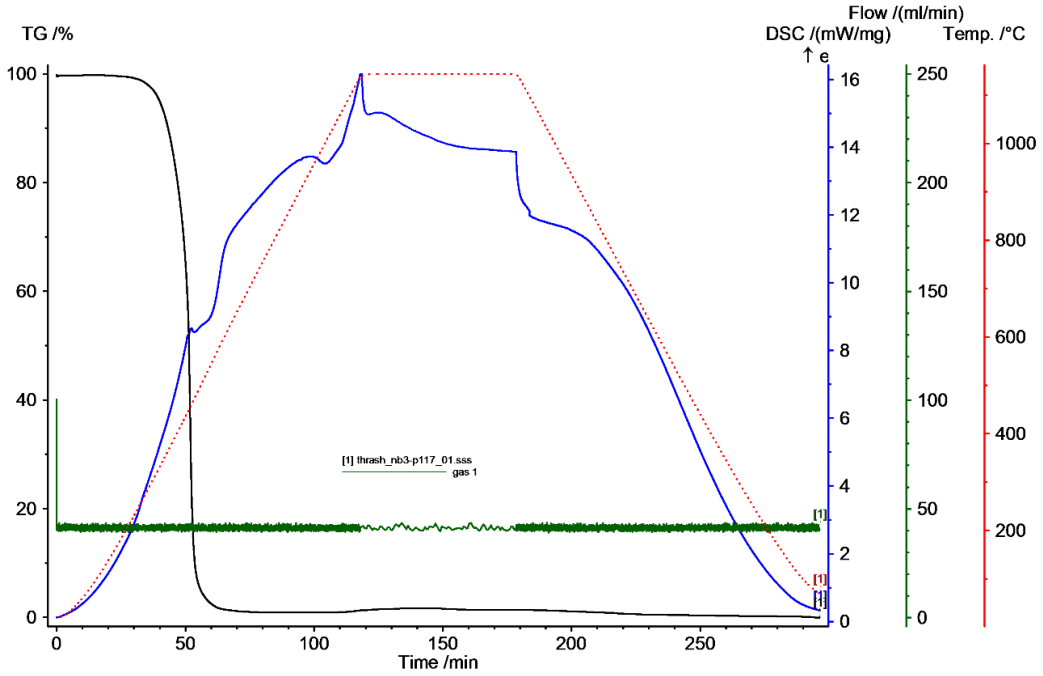

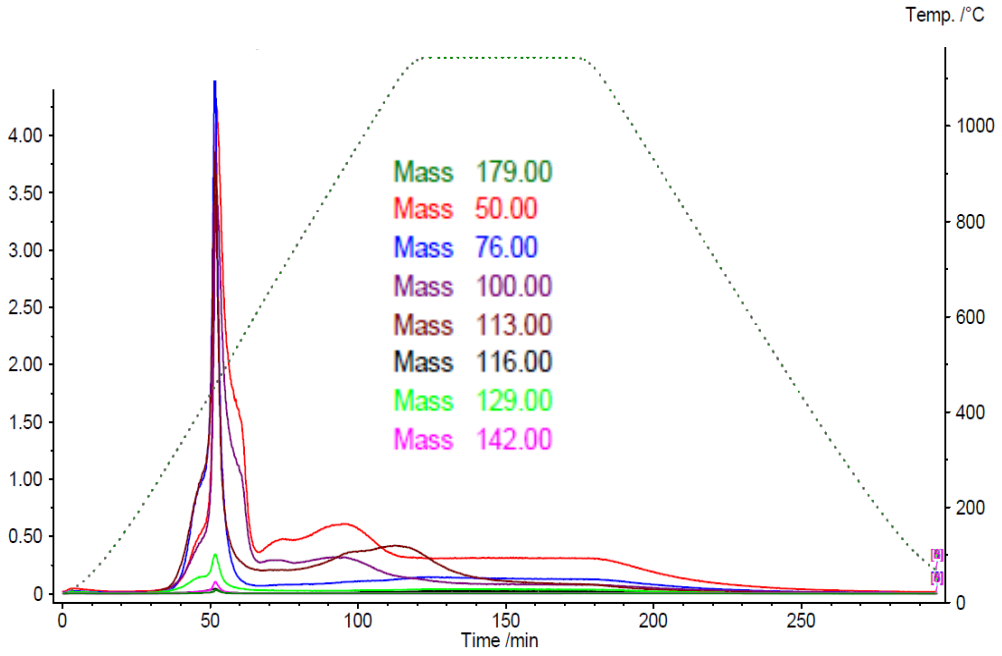

Report 4. TGA-MS of Poly(M1-co-HFP)

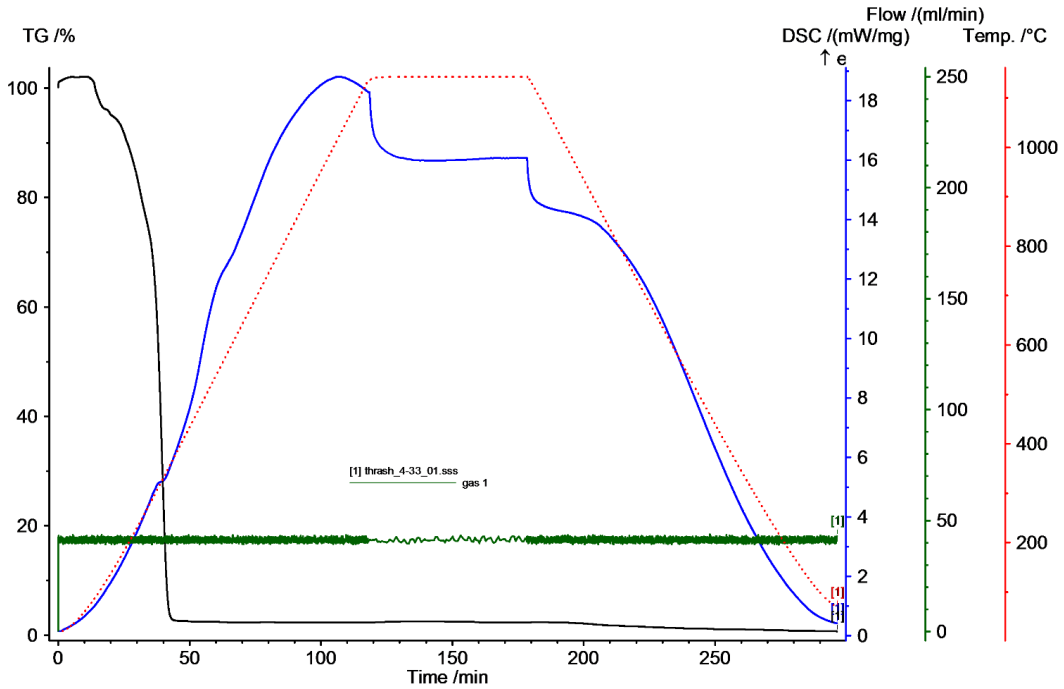

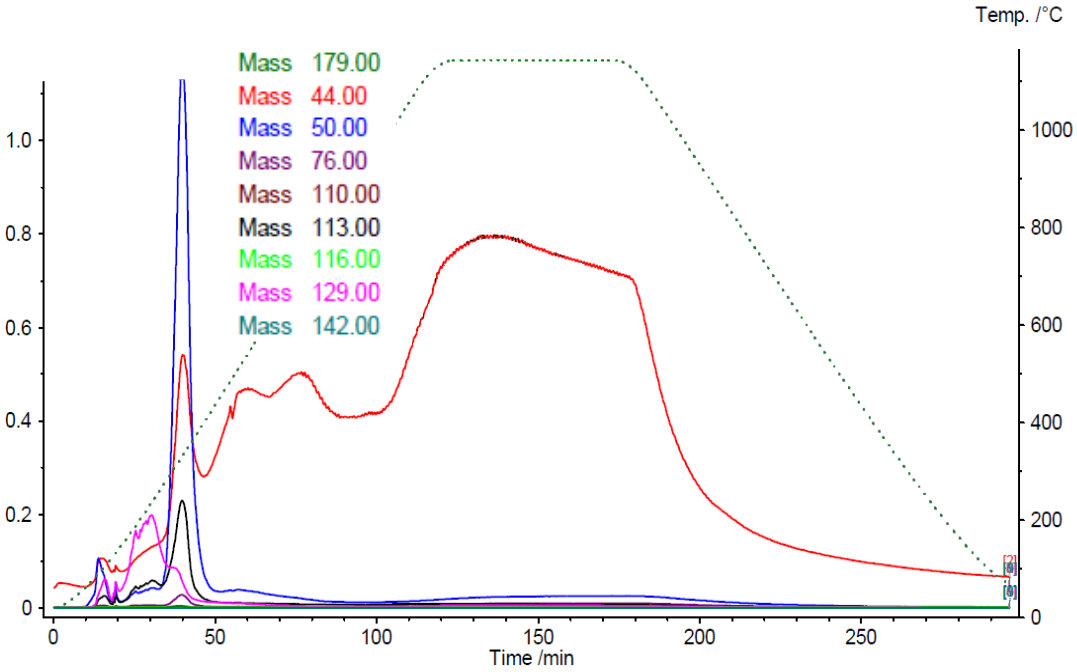

The cations expected for poly(M1-*co*-TFE) were all detected (see **Error! R eference source not found.**): CF_2^+ (50), CF_2CHCH^+ (76), $CF_2CF_2^+$ (100), $CF_2CHCF_2^+$ (113), $CF_2OCF_2^+$ (116), $CF_2CHCF_2O^+$ (129), $M1^+$ (142), $CF_2CHCF_2OCF_2^+$ (179). Among these fragments, $CF_2CHCF_2^+$ (113), $CF_2CHCF_2O^+$ (129), and $CF_2CHCF_2OCF_2^+$ (179) were from a combined structure of TFE and M1, which proves that M1 and TFE were combined in the structure.

Similarly, the cations selected for poly(M1-*co*-HFP) were all detected as well (see **Error! Reference source not found.**): $CFCH^+$ (44), CF_2^+ (50), CF_2CHCH^+ (76), $CFCHCF_2O^+$ (110), $CF_2CHCF_2^+/CF_3CFCH^+$ (113), $CF_2OCF_2^+$ (116), $CF_2CHCF_2O^+$ (129), $M1^+$ (142), $CF_2CHCF_2OCF_2^+$ (179). Among these fragments, $CFCH^+$ (44), CF_2^+ (50), CF_2CHCH^+ (76), $CF_2OCF_2^+$ (116), and $M1^+$ (142) can be from each of the monomers, while each of the ions $CFCHCF_2O^+$ (110), $CF_2CHCF_2^+/CF_3CFCH^+$ (113), $CF_2CHCF_2O^+$ (129), and $CF_2CHCF_2OCF_2^+$ (179) are from a combined structure of HFP and M1.

Both results support the proposed structures of poly(M1-*co*-TFE) and poly(M1-*co*-HFP). Meanwhile, the decompositions of both copolymers occurred abruptly once each sample reached its decomposition temperature, and the majority of all the ions were detected at the same time, which means the molecular chains break down all together instead of step-by-step. Especially in the decomposition of poly(M1-*co*-HFP), the $CFCH^+$ (44) ion was detected ahead of the other ions, and $CFCH^+$ is either only from M1 or from two adjacent units, which indicates the direct cleavage of the backbone. In poly(M1-*co*-

TFE), the ion CF_2^+ (50) was detected first, which is either from the ring structure or the backbone.

5.2.7 Molecular Weight of Poly(M1-co-TFE) and Poly(M1-co-HFP)

The molecular weights of both materials were measured by using static light scattering (SLS) technique. Several solvents were used to prepare the solutions of the materials. The solvent acetone was the best choice in terms of solubility, however, it did not give consistent readings in refractive index measurement due to the volatility of the solvent and HF eliminated of poly(M1-*co*-TFE) was observed in acetone. THF was another solvent that Poly(M1-*co*-TFE) had reasonable solubility in for SLS measurement; however, it was excluded for the same problem of high volatility. DMF was selected as the solvent for both materials due to its high boiling point and good ability to dissolve the materials. A much slower color change of poly(M1-*co*-TFE) DMF solution than that of acetone was observed over a week, therefore, the samples should be freshly prepared for the measurement.

The molecular weight determination of both poly(M1-*co*-TFE) and poly(M1-*co*-HFP) by using SLS technique were plotted and calculated with ASTRA 5.3.5 software (Figure 5.28). The molecular weight of poly(M1-*co*-TFE) was found to be $(7.1\pm1.5)10^{+5}$ g/mol, while a value of $(3.2\pm0.9)10^{+6}$ g/mol was found for Poly(M1-co-HFP); both measurements were done in DMF (Table 5.5) at room temperature 20 °C (Report 5 and Report 6).

Table 5.5. SLS Measurement of Poly(M1-*co*-TFE) and Poly(M1-*co*-HFP)

Sample	Solvent	Refractive index increment dn/dc (mL/g)	Mw (g/mol)	Rms radius (nm)
Poly(M1-	DMF	0.564	$(7.1\pm1.5)10^{+}$	198±28
Poly(M1-	DMF	-0.918	$(3.2\pm0.9)10^{+}$	225±37

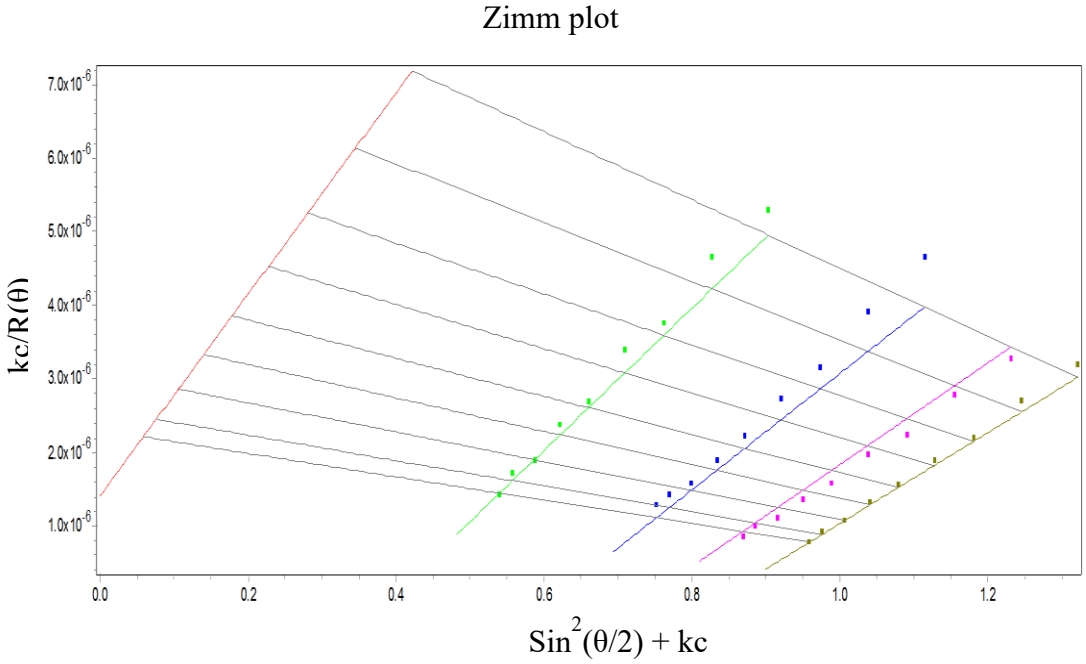

Figure 5.28. Zimm plot of SLS from poly(M1-*co*-TFE) solution in DMF.

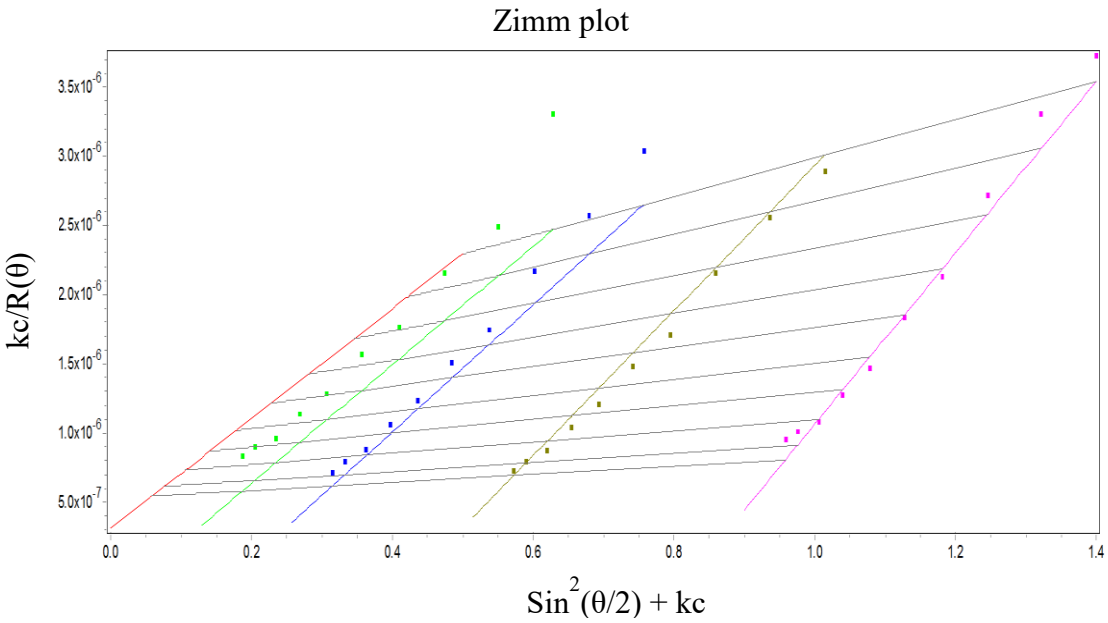

Figure 5.29. Zimm plot of SLS from poly(M1-*co*-HFP) solution in DMF.

Report 5. SLS measurement of poly(M1-co-TFE)

ASTRA 5.3.4 Detailed Report for XL-M1CoTFE-DMF 0.8-2.0

Processing Operator: Mingzhe Jiang

Collection Operator: kitchenslab

Collection Astra Version: 5.3.4.14

CONFIGURATION

Instrument Type: DAWN HELEOS

Cell type: Scintillation vial

Laser wavelength: 659.0 nm

Calibration constant: 2.8288e-5 1/(V cm)

Collection interval: 2.000 sec

Detector	Scattering angle	Gain	Normalization coefficient
1	22.5°	n/a	0.726
2	28.0°	n/a	1.081
3	32.0°	n/a	0.844
4	38.0°	n/a	1.019
5	44.0°	n/a	1.436
6	50.0°	n/a	0.531
7	57.0°	n/a	0.678
8	64.0°	n/a	0.730

9	72.0°	n/a	0.806
10	81.0°	n/a	0.928
11	90.0°	n/a	1.000
12	n/a	n/a	1.000
13	108.0°	n/a	0.868
14	117.0°	n/a	0.842
15	126.0°	n/a	0.748
16	134.0°	n/a	0.680
17	141.0°	n/a	1.894
18	147.0°	n/a	1.679

Solvent: DMF

Refractive index: 1.431

PROCESSING

Processing time: Monday March 28, 2016 09:04 PM @tzres.dll,-111

Collection time: Tuesday March 22, 2016 07:51 PM @tzres.dll,-111

Fit method / model: Zimm

dn/dc: 0.564 mL/g

Concentration fit degree: 1

Angle fit degree: 1

Percent to keep: 25 %

Detectors used: 2 3 4 5 6 7 8 9 10

Peaks used: 2 3 5 6

Peak	Begin (min)	End (min)	c (g/mL)	FOM
Peak 2	18.395	22.298	1.07e-4	0.38
Peak 3	24.848	28.210	1.54e-4	0.54
Peak 5	38.103	41.774	2.00e-4	0.71
Peak 6	30.336	33.543	1.80e-4	0.64

Baselines:

Series	Endpoints	Type
detector 1	(0.000, 0.000) -- (0.000, 0.000)	no baseline set
detector 2	(0.000, 0.000) -- (0.000, 0.000)	no baseline set
detector 3	(0.000, 0.000) -- (0.000, 0.000)	no baseline set
detector 4	(0.000, 0.000) -- (0.000, 0.000)	no baseline set
detector 5	(0.000, 0.000) -- (0.000, 0.000)	no baseline set
detector 6	(0.000, 0.000) -- (0.000, 0.000)	no baseline set
detector 7	(0.000, 0.000) -- (0.000, 0.000)	no baseline set
detector 8	(0.000, 0.000) -- (0.000, 0.000)	no baseline set
detector 9	(0.000, 0.000) -- (0.000, 0.000)	no baseline set
detector 10	(0.000, 0.000) -- (0.000, 0.000)	no baseline set
detector 11	(0.931, 0.076) -- (4.601, 0.076)	manual x, auto y
detector 13	(0.000, 0.000) -- (0.000, 0.000)	no baseline set
detector 14	(0.000, 0.000) -- (0.000, 0.000)	no baseline set
detector 15	(0.000, 0.000) -- (0.000, 0.000)	no baseline set
detector 16	(0.000, 0.000) -- (0.000, 0.000)	no baseline set

detector 17 (0.000, 0.000) -- (0.000, 0.000) no baseline set

detector 18 (0.000, 0.000) -- (0.000, 0.000) no baseline set

Results

Molar mass (Mw): (7.099±1.463)e+5 g/mol

rms radius (Rz): 198.1±28.4 nm

2nd virial coefficient: (-2.489±0.767)e-3 mol mL/g²

Report 6. SLS measurement of poly(M1-co-HFP)

ASTRA 5.3.4 Detailed Report for XL-M1CoHFP-DMF serial 0.05-0.7

Processing Operator: Mingzhe Jiang

Collection Operator: kitchenslab

Collection Astra Version: 5.3.4.14

CONFIGURATION

Instrument Type: DAWN HELEOS

Cell type: Scintillation vial

Laser wavelength: 659.0 nm

Calibration constant: 2.8288e-5 1/(V cm)

Collection interval: 2.000 sec

Detector	Scattering angle	Gain	Normalization coefficient
1	22.5°	n/a	0.728
2	28.0°	n/a	1.082
3	32.0°	n/a	0.843
4	38.0°	n/a	1.017
5	44.0°	n/a	1.434
6	50.0°	n/a	0.530
7	57.0°	n/a	0.677
8	64.0°	n/a	0.729

9	72.0°	n/a	0.805
10	81.0°	n/a	0.926
11	90.0°	n/a	1.000
12	n/a	n/a	1.000
13	108.0°	n/a	0.869
14	117.0°	n/a	0.842
15	126.0°	n/a	0.748
16	134.0°	n/a	0.681
17	141.0°	n/a	1.895
18	147.0°	n/a	1.680

Solvent: DMF

Refractive index: 1.431

PROCESSING

Processing time: Thursday March 31, 2016 01:24 PM @tzres.dll,-111

Collection time: Friday March 25, 2016 04:03 PM @tzres.dll,-111

Fit method / model: Zimm

dn/dc: 0.918 mL/g

Concentration fit degree: 1

Angle fit degree: 1

Percent to keep: 25 %

Detectors used: 2 3 4 5 6 7 8 9 10

Peaks used: 2 3 4 6

Peak	Begin (min)	End (min)	c (g/mL)	FOM
Peak 2	10.950	13.755	1.00e-5	0.07
Peak 3	15.880	18.794	2.00e-5	0.13
Peak 4	21.600	24.732	4.00e-5	0.26
Peak 6	33.612	36.908	7.00e-5	0.46

Baselines:

Series	Endpoints	Type
detector 1	(0.000, 0.000) -- (0.000, 0.000)	no baseline set
detector 2	(0.000, 0.000) -- (0.000, 0.000)	no baseline set
detector 3	(0.000, 0.000) -- (0.000, 0.000)	no baseline set
detector 4	(0.000, 0.000) -- (0.000, 0.000)	no baseline set
detector 5	(0.000, 0.000) -- (0.000, 0.000)	no baseline set
detector 6	(0.000, 0.000) -- (0.000, 0.000)	no baseline set
detector 7	(0.000, 0.000) -- (0.000, 0.000)	no baseline set
detector 8	(0.000, 0.000) -- (0.000, 0.000)	no baseline set
detector 9	(0.000, 0.000) -- (0.000, 0.000)	no baseline set
detector 10	(0.000, 0.000) -- (0.000, 0.000)	no baseline set
detector 11	(0.967, 0.095) -- (4.306, 0.091)	manual x, auto y
detector 13	(0.000, 0.000) -- (0.000, 0.000)	no baseline set
detector 14	(0.000, 0.000) -- (0.000, 0.000)	no baseline set
detector 15	(0.000, 0.000) -- (0.000, 0.000)	no baseline set
detector 16	(0.000, 0.000) -- (0.000, 0.000)	no baseline set

detector 17 (0.000, 0.000) -- (0.000, 0.000) no baseline set

detector 18 (0.000, 0.000) -- (0.000, 0.000) no baseline set

RESULTS

Molar mass (Mw): (3.169±0.942)e+6 g/mol

rms radius (Rz): 224.6±36.5 nm

2nd virial coefficient: (1.044±0.854)e-3 mol mL/g²

The measurement with gel permeation chromatography (GPC) was not successful due to the limited solubility of the materials in THF, which is the solvent used on our GPC instrument. Poly(M1-co-TFE) has a solubility between 0.2 mg/mL and 0.3 mg/mL in THF, while poly(M1-co-HFP) has a solubility less than 0.1 mg/mL in THF, which makes it very difficult to detect. A broad negative peak did appear in each GPC graphs of poly(M1-co-TFE). The negative peak was assigned at 3815 g/mol (Figure 5.30 and Table 5.6). Evidently, the material of higher Mw was not dissolved in the solvent. If the solute or polymer has a refractive index that is very different from the solvent, some fraction of the solution can give a negative peak on the RI detector.[28]

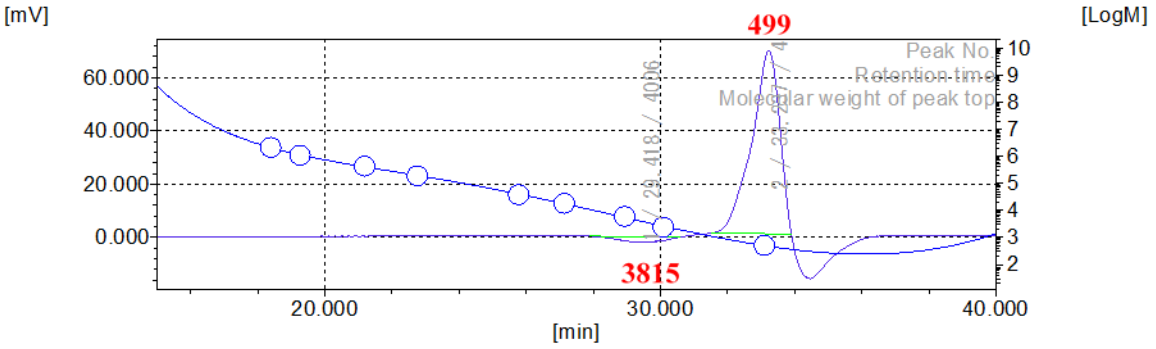

Figure 5.30. GPC of Poly(M1-co-TFE).

Table 5.6. Elution Time and Molecular Weight of Poly(M1-*co*-TFE)

Peak 1		[min]	[mV]	Mn	3,815
	Peak start	27.867	0.454	Mw	4,322
	Peak top	29.418	-1.776	Mz	4,904
	Peak end	30.610	0.231		
Peak 2				Mn	499
	Peak start	31.525	1.570	Mw	516
	Peak top	33.237	70.205	Mz	536
	Peak end	33.902	1.305		

The GPC data of poly(M1-*co*-HFP) did not give any information on molecular weight due to the extremely low solubility of the material in THF. Another technique that could be used for the measurement of molecular weight is matrix-assisted laser desorption/ionization-time of flight (MALDI-TOF) mass spectrometry; however, the range of the instrument is only up to 500,000 Da, which is not a valid range for poly(M1-*co*-TFE) and poly(M1-*co*-HFP) according to the SLS measurement results (see Table 5.5). MALDI-TOF has not been a perfluoroalkane material friendly technique or sometimes it is hard to obtain useful information most of the time. Most of the time it is applied to partially fluorinated materials such as VDF oligomers or low fluorinated materials.[30]

5.3 CONCLUSIONS AND FUTURE WORK

The copolymerization of M1 with TFE and HFP were quite successful, but MSF_5 did not give a good yield of the product. The characterization of poly(M1-*co*-MSF_5) was not sufficient due to the lack of material. More starting material will be synthesized in the future, and a larger scale reaction can be carried out in order to obtain enough material for the characterization. An electron donor acceptor mechanism was proposed and alternating

copolymers of M1 with each perfluoroolefin were expected; however, both NMR spectroscopic integration and EDX studies were not supportive of this result. TGA/MS results reveal that the decomposition of CH sites on the backbone is the reason why the decomposition is so abrupt at the decomposition temperature. We were currently not able to identify the end groups of the materials currently and that would be useful information to have in term of being able to further improve the design and properties of these materials. The molecular weight of both Poly(M1-co-TFE) and Poly(M1-co-HFP) is desirable. The molecular weights of both poly(M1-*co*-HFP) and poly(M1-*co*-TFE), as determined by SLS, were desirable. The molecular weight of poly(M1-*co*-HFP) is very high according to the SLS measurement; however, the thermal stability is not excellent for a material of such high molecular weight. Further study on the structure modification should be done in order to improve the thermal stability of the material.

5.4 EXPERIMENTAL

5.4.1 Instrumentation

NMR spectroscopic data was collected on a multinuclear JOEL ECX-300 Spectrometer. The frequency is 300 MHz for ^{1}H, 75.57 MHz for ^{13}C, and 282.78 MHz for ^{19}F respectively. Multiplicities are as follows: s (singlet), d (doublet), t (triplet), m (multiplet), dd (doublet of doublet), td (triplet of doublet), tt (triplet of triplet), tm (triplet of multiplet). The internal standard of ^{19}F NMR spectroscopy is CCl_3F (0.00 ppm); GC/MS data was collected from SHIMADZU GCMS-QP5000; SEM/EDX data was collected on a Hitachi TM 3000 tabletop Scanning Electron Microscope; ATR-IR spectra were collected on a Thermo Scientific Nicolet iS5 diamond ATR spectrometer; GPC data was collected

on a TOSOH EcoSec HLC-8320GPC; and a Shimadzu UV-2501PC Spectrophotometer was used to record UV/vis spectra. SLS data was collected on a Wyatt Dawn Heleos-II instrument at 659.0 nm. Refractive index (RI) was measure with ATAGO® Pocket Refractometer (range: 1.3306 ~ 1.5284). TGA was measured on a TA Q500 instrument.

TGA/MS method: Range: 20.0-1200.0/-10.0-10.0 K/min; atmosphere: Helium; Crucible: DSC/TGA pan Al_2O_3.

TGA method: Ramp from room temperature up to 500 °C for Poly(M1-co-HFP) and 650 C for Poly(M1-co-TFE) at a rate of 10.0 °C/min under nitrogen protection.

SLS method: Laser wavelength: 659.0 nm; fit method: Zimm; normalization: the instrument was normalized with 200,000 g/mol polystyrene in DMF at room temperature.

5.4.2 Materials

N-Bromosuccinimide (NBS) was purchased from Sigma Aldrich; dichloromethane (CH_2Cl_2) was purchased from Sigma Aldrich; furan was purchased from TCI, hexafluoropropene (HFP) was purchased from PCR; FC-72 was purchased from 3M Company (3M); acetonitrile was purchased from Mallinckrodt Baker. Tetrahydrofuran (THF) was purchased from VWR; potassium hydroxide (KOH) was purchased from Sigma Aldrich; dimethyl formamide (DMF) was purchased from Alfa Aesar. Tetrafluoroethylene (TFE, stabilized with limonene) and MSF_5 were available in laboratory stock, and TFE was passed through a silica gel scrubber in order to get rid of residual limonene before use. $CDCl_3$ was purchased from Cambridge Isotope Laboratories, Inc.. Polystyrene standard 200,000 g/mol was purchased from PSS Polymer Standards Service GmbH. Polystyrene

standards PStQuick mix C and PStQuick mix D for GPC calibration were purchased from Tosoh Corporation.

5.4.3 Synthesis of 2,5-dibromo-dihydrofuran.

An amount of 89 g (0.5 mol) NBS was mixed with 17 g (0.25 mol) furan in 300 mL dichloromethane at room temperature in a 1-L one-necked flask. The reaction was complete after 4 hrs sonication at room temperature. The reaction mixture was filtered through a frit filter funnel to remove any undissolved solid byproduct. Then most dichloromethane was removed by blowing house nitrogen through the bulk solution first, and the remaining mixture was distilled under house vacuum. A viscous light yellow liquid was collected at 83 °C, giving a yield of 70% of the compound[16a].

NMR spectroscopy of 2,5-dibromo-dihydrofuran:

^{1}H NMR chemical shift: 6.30 ppm (s).

^{13}C NMR chemical shifts: 121.77 ppm (s), 114.16 ppm (s).

5.4.4 Synthesis of 2,2,5,5-tetrafluoro-2,5-dihydrofuran, M1

An amount of 20.0 g (1 mol) of anhydrous HF was condensed into a 500-mL stainless steel cylinder, and 40.0 g (0.37 mol) of SF_4 gas was condensed into the cylinder on the vacuum line. The cylinder was warmed up and kept on a shaker overnight. An amount of 29.4 g (0.13 mol) of 2, 5-dibromo-dihydrofuran was transferred into the cylinder that had been cooled with liquid nitrogen. The reaction cylinder was then kept at ice temperature for 18-24 h. thereafter, the gas phase of reaction mixture was released through a caustic scrubber. The remaining volatile materials were transferred into a cylinder containing excess amount of 15 wt% KOH solution, and after the second cylinder was

warmed up to room temperature, the solution was poured into a flask, and M1 was distilled out at 63-64 °C. The yield of M1 was 59%.[16b]

NMR spectroscopy of M1:

^{1}H NMR chemical shift: 6.49 ppm (s).

^{19}F NMR chemical shift: -73.12 ppm (s).

^{13}C NMR chemical shifts with ^{1}H decoupling:

127.97 ppm (tt, J_{CF} = 256.5 Hz, $^{4}J_{CF}$ = 4.0 Hz), 130.75 ppm (tm, $^{2}J_{CF}$ = 31.1 Hz).

^{13}C NMR chemical shifts with ^{19}F decoupling:

127.78 ppm (dd, $^{2}J_{CH}$ = 8.3 Hz, $^{3}J_{CH}$ = 1.4 Hz), 130.74 ppm (dd, J_{CH} = 185.7 Hz, $^{2}J_{CH}$ = 2.9 Hz).

UV absorption of M1 is in the area below 250 nm.

IR absorption of M1[29]:

C-H stretch: 3127.97 cm^{-1} (w), 1361.50 cm^{-1} (m), 1332.57 cm^{-1} (s) and 846 cm^{-1} (m).

C=C stretch: 1644.98 cm^{-1} (w).

C-F: 1097.30 cm^{-1} (s).

Mass spectrum of M1, m/z (relative intensity, %):

142 (5.8) $[M]^{+}$, 123 (13.4) $[M\text{-}F]^{+}$, 95 (82.8) $[CF_3C_2H_2]^{+}$, 82 (0.2) $[CF_3CH]^{+}$, 76 (3.4) $[C_3H_2F_2]^{+}$, 69 (33.7) $[CCHCHCF]^{+}$, 51 (9.2) $[CF_2H]^{+}$, 47 (12.7) $[CFO]^{+}$, 31 (5.7) $[CF]^{+}$, 20 (2.5) $[HF]^{+}$.

5.4.5 Synthesis of the tricyclic diether.

To a 500-mL quartz flask, 1.0 g (7.0 mmol) M1 compound was added， and the starting material was degassed on a vacuum line by several freeze, pump, thaw cycles. The

flask was then pressurized to 1 atm with dry air, and the contents of the flask were irradiated with a UV lamp having three exchangeable wavelengths (254 nm, 300 nm, and 350 nm) for 12 hrs.

Some colorless crystals were collected directly from the reactor and analyzed with single crystal X-Ray and NMR spectroscopy, and the results were in agreement with the work of Pustovit.[17]

NMR spectroscopy of tricyclic diether:

^{19}F NMR chemical shifts: -61.64 ppm, -81.63 ppm (AB pattern, $^{2}J_{FF}$ = 141.4 Hz)

5.4.6 Photocopolymerization of tetrafluorohydrofuran with TFE, poly(M1-co-TFE)

To an 800 mL evacuated quartz flask equipped with a magnetic stir bar, 4.8 g FC-72 solvent, 0.61 g (6.1 mmol) TFE and 0.61 g (4.3 mmol) M1 were condensed on the vacuum line at liquid nitrogen temperature. The flask was installed in a UV reactor equipped with a cooling fan at the bottom and 8 lamps around the internal wall generating 254nm (principle wavelength), 300nm, and 350 nm lights. The UV reactor was positioned on top of a stir plate. The lights, stirring and cooling fan were turned on with a stream of house air to cool down the chamber, the reaction was stopped in 4 days.

$$monomer\ consumption = \frac{mass\ of\ remaining\ solid\ material \times 100}{mass\ of\ total\ monomers\ input}\ \% \qquad (5.1)$$

After the reaction was stopped, the solvent and unreacted monomers were transferred out of the quartz vessel in order to measure the monomer taken up after the reaction. The products were evacuated on the vacuum line at 120 °C for 24 hrs to remove any volatile or low Mw products. The monomer consumption (eq 5.1) was up to 95%.

5.4.7 Photocopolymerization of tetrafluorohydrofuran with HFP, poly(M1-co-HFP)

To an 800- mL evacuated quartz flask equipped with a magnetic stir bar, 5.4 g FC-72 solvent, 1.2 g (12.0 mmol) HFP and 0.44 g (3.1 mmol) M1 were condensed on the vacuum line at liquid nitrogen temperature. The flask was installed in the UV reactor used in the aforementioned copolymerization. The UV reactor was sat on top of a stir plate. The lights, stirring and cooling fan were turned on with a stream of house cool air, the reaction was stopped in 7 days. After the reaction was ceased, the solvent and unreacted monomers are transferred out of the quartz vessel in order to measure the monomer taken up during the reaction. The yielding products were evacuated on the vacuum line at room temperature for 24 hrs to remove any volatile or low Mw products. The monomer consumption (eq 5.1) was up to 80 %.

5.4.8 Photocopolymerization of tetrafluorohydrofuran with MSF_5, poly(M1-co-MSF_5)

To an 800 mL evacuated quartz flask equipped with a magnetic stir bar, 7.9 g FC-72 solvent, 0.6 g (2.9 mmol) MSF_5 and 0.3 g (2.2 mmol) M1 were condensed on the vacuum line at liquid nitrogen temperature. The flask was installed in the UV reactor used in the aforementioned copolymerization. The UV reactor was sat on top of a stir plate. The lights, stirring and cooling fan were turned on with a stream of house cool air, the reaction was stopped in 2 days. After the reaction was ceased, the solvent and unreacted monomers are transferred out of the quartz vessel in order to measure the monomer taken up during the reaction. The yielding products were evacuated on the vacuum line at room temperature for 24 hrs to remove any volatile or low Mw products. The monomer consumption (eq 5.1) was 19 %.

5.4.9 SEM/EDX of poly(M1-co-TFE) and poly(M1-co-HFP)

The powdery portion of each material was carefully scattered on a sample holder, which was covered with a layer of dark carbon tape. The sample holder was then installed in the vacuum chamber of the instrument. Multiple specimens were taken on each sample in order to calculate the composition of the material.

5.4.10 TGA and TGA/MS of poly(M1-co-TFE) and poly(M1-co-HFP)

The samples were analyzed by using the method described in instrumentation section. The cations selected for Poly(M1-co-TFE) were: CF_2^+ (50), CF_2CHCH^+ (76), $CF_2CF_2^+$ (100), $CF_2CHCF_2^+$ (113), $CF_2OCF_2^+$ (116), $CF_2CHCF_2O^+$ (129), $M1^+$ (142), $CF_2CHCF_2OCF_2^+$ (179).

The cations selected for Poly(M1-co-HFP) were: $CFCH^+$ (44), CF_2^+ (50), CF_2CHCH^+ (76), $CFCHCF_2O^+$ (110), $CF_2CHCF_2^+/CF_3CFCH^+$ (113), $CF_2OCF_2^+$ (116), $CF_2CHCF_2O^+$ (129), $M1^+$ (142), $CF_2CHCF_2OCF_2^+$ (179).

5.4.11 GPC and SLS of poly(M1-co-TFE) and poly(M1-co-HFP)

The SLS samples were prepared with DMF in multiple concentrations in Scintillation vials, and the measurement was normalized by using 2000,000 g/mol polystyrene standard. The refractive indexes of both poly(M1-*co*-TFE) and poly(M1-*co*-HFP) solutions were measure with ATAGO® Pocket Refractometer at room temperature. The concentrations of the poly(M1-*co*-TFE) solutions were 1.07×10^{-4} M, 1.54×10^{-4} M, 1.80×10^{-4} M and 2.00×10^{-4} M. The concentrations of the solutions were 1.00×10^{-5} M,

2.00×10^{-5} M, 4.00×10^{-5} M, and 7.00×10^{-5} M. The samples were analyzed at room temperature and the scattering was detected at 18 different angles.

For GPC measurement, a solution of a concentration 1 mg/1mL of each polymer was prepared in THF one day before the analysis. The instrument was calibrated with PStQuick mix C and PStQuick mix D polystyrene standards.

5.5 REFERENCES

1. (a) Howell, J. L.; Shtarov, A. B.; Thrasher, J. S.; Waterfeld, A.; Murata, K.; Friesen, C. M.; Pérez, E. W. Synthesis of new linear perfluoroalkyl polyethers starting from diols and tetrafluoroethylene. *Lubr. Sci.* **2010,** *23*, 61-80; (b) Hanford, W. E.; Rigby, G. W. Polyfluoro Organic Ethers and the Preparation. U.S. Patent 2,469,274, Oct. 15, 1946; (c) Koshikawa, H.; Tarumi, Y.; Shiono, M. Perfluoroether elastomer for wide fluid and temperature capabilities. *Sealing Tech.* **2006,** *2006*, 7-12; (d) Woo, E. J.; Lehman, G. K. Perfluoroether Release Coatings for Organic Photoreceptors. U.S. Patent 5,723,242, Mar. 3, 1998; (e) Jones, W. R. J.; Bierschenk, T. R.; Juhlke, T. J.; Kawa, H.; Lagow, R. J. The Preparation of New Perfluoro Ether Fluids Exhibiting Excellent Thermal-Oxidative Stabilities. *Ind. Eng. Chem. Res.* **1988,** *27*, 1497-1502.
2. (a) Prabhakar, R. S.; Freeman, B. D.; Roman, I. Gas and Vapor Sorption and Permeation in Poly(2,2,4-trifluoro-5-trifluoromethoxy-1,3-dioxole-co-tetrafluoroethylene). *Macromolecules* **2004,** *37*, 7688-7697; (b) Jesorka, A.; Shaali, M. Lithographic Pattern Development Process for Amorphous Fluoropolymer. U.S. Patent Appl. 20140065551 A1, Mar. 6, 2014; (c) Khang, D.; Lee, H. H. Sub-100

nm Patterning with an Amorphous Fluoropolymer Mold. *Langmuir* **2004,** *20*, 2445-2448.

3. Hung, M.-H.; Resnick, P. R. Thermal Rearrangement of Fluorinated Dioxoles. *J. Am. Chem. Soc.* **1990,** *112*, 9672-9674.

4. (a) Teng, H. Overview of the Development of the Fluoropolymer Industry. *Appl. Sci.* **2012,** *2*, 496-512; (b) Resnick, P. R. Polymers of Fluorinated Dioxoles. U.S. Patent 3,978,030, Aug. 31, 1976; (c) Squire, E. N. Perfluorodioxole and Its Polymers. U.S. Patent 4,399,264 A, Aug. 16, 1983; (d) Squire, E. N. Perfluorodioxole and Its Polymers. U.S. Patent 4,558,141, Dec. 10, 1985.

5. Ino, T.; Shinohara, T.; Sakane, Y. Process for Molding Amorphous Perfluororesin and Optical Elements. EP Patent 2,199,051A1, Jun. 23, 2010.

6. Navarrini, W.; Tortelli, V.; Colaianna, P.; Abusleme, J. A. Perfluorodioxoles, the Preparation Process Thereof, and Homopolymers and Copolymers Therefrom. U.S. Patent 5,646,223 A, Jul. 8, 1997.

7. (a) Liu, W.; Koike, Y.; Okamoto, Y. Synthesis and Radical Polymerization of Perfluoro-2-methylene-1,3-dioxolanes. *Macromolecules* **2005,** *38*, 9466-9473; (b) Yang, Y.; Mikeš, F.; Yang, L.; Liu, W.; Koike, Y.; Okamoto, Y. Investigation of homopolymerization rate of perfluoro-4,5-substituted-2-methylene-1,3-dioxolane derivatives and properties of the polymers. *J. Fluorine Chem.* **2006,** *127*, 277-281.

8. (a) Navarrini, W.; Bragante, L. Process for the Dehalogenation of 1,3-Dioxolanes. U.S. Patent 5,245,054 A, Sep. 14, 1993; (b) Navarrini, W.; Fontana, S. Process for Preparing 1,3-Dioxoles. U.S. Patent 5,296,617 A, Mar. 22, 1994; (c) Russo, A.;

Navarrini, W. Perfluoro-4-methyl-1,3-dioxole: a new monomer for high-Tg amorphous fluoropolymers. *J. Fluorine Chem.* **2004,** *125*, 73-78; (d) Avataneo, M.; Navarrini, W.; De Patto, U.; Marchionni, G. Novel perfluoropolyethers containing 2,2,4-trifluoro-5-trifluoromethoxy-1,3-dioxole blocks: synthesis and characterization. *J. Fluorine Chem.* **2009,** *130*, 933-937.

9. (a) Romack, T. J.; DeSimone, J. M. Synthesis of Tetrafluoroethylene-Based, Nonaqueous Fluoropolymers in Supercritical Carbon Dioxide. *Macromolecules* **1995,** *28*, 8429-8431; (b) Kendall, J. L.; Canelas, D. A.; Young, J. L.; DeSimone, J. M. Polymerizations in Supercritical Carbon Dioxide. *Chem. Rev.* **1999,** *99*, 543-563; (c) Michel, U.; Resnick, P.; Kipp, B.; DeSimone, J. M. Copolymerization of Tetrafluoroethylene and 2,2-Bis(trifluoromethyl)-4,5-difluoro-1,3-dioxole in Supercritical Carbon Dioxide. *Macromolecules* **2003,** *36*, 7107-7113; (d) Wood, C. D.; Michel, U.; Rolland, J. P.; DeSimone, J. M. New fluoropolymer materials. *J. Fluorine Chem.* **2004,** *125*, 1671-1676.

10. Feiring, A. E.; Crawford, M. K.; Farnham, W. B.; Feldman, J.; French, R. H.; Junk, C. P.; Leffew, K. W.; Petrov, V. A.; Qiu, W.; Schadt, F. L., III; Tran, H. V.; Zumsteg, F. C. New Amorphous Fluoropolymers of Tetrafluoroethylene with Fluorinated and Non-Fluorinated Tricyclononenes. Semiconductor Photoresists for Imaging at 157 and 193 nm. *Macromolecules* **2006,** *39*, 3252-3261.

11. Smith, D. W. Jr.; Babb, D. A.; Shah, H. V.; Hoeglund, A.; Traiphol, R.; Perahia, D.; Boone, H. W.; Langhoff, C.; Radler, M. Perfluorocyclobutane (PFCB) polyaryl ethers: verstatile coatings materials. *J. Fluorine Chem.* **2000,** *104*, 109-117.

12. Bondi, A. Van der Waals Volumes and Radii. *J. Phys. Chem.* **1964,** *68*, 441-451.

13. (a) Altomonte, S.; Zanda, M. Synthetic chemistry and biological activity of pentafluorosulphanyl (SF_5) organic molecules. *J. Fluorine Chem.* **2012,** *143*, 57-93; (b) Savoie, P. R.; Welch, J. T. Preparation and utility of organic pentafluorosulfanyl-containing compounds. *Chem. Rev.* **2015,** *115*, 1130-1190.

14. Iida, N.; Tanaka, K.; Tokunaga, E.; Mori, S.; Saito, N.; Shibata, N. Synthesis of Phthalocyanines with a Pentafluorosulfanyl Substituent at Peripheral Positions. *Chemistry Open* **2015,** *4*, 698-702.

15. Boyer, C.; Ameduri, B.; Boutevin, B.; Dolbier, W. R.; Winter, R.; Gard, G. Radical Terpolymerization of 1,1,2-Trifluoro-2-pentafluorosulfanylethylene and Pentafluorosulfanylethylene in the Presence of Vinylidene Fluoride and Hexafluoropropylene by Iodine Transfer Polymerization. *Macromolecules* **2008,** *41*, 1254-1263.

16. (a) Arsenyan, P.; Paegle, E.; Belyakov, S. A Novel Method for the Bromination of Thiophenes. *Tetrahedron Lett.* **2010,** *51*, 205-208; (b) Kunshenko, B. V.; Motnyak, L. A.; Neizvestnaya, T. A.; Il'nitskii, S. O.; Yagupol'skii, L. M. Reaction of 2,5-Dibromofuran with the SF_4-HF-Br_2 System. *Zh. Organich. Khim.* **1986,** *22*, 1791-1792.

17. Pustovit, Y. M.; Ogojko, P. I.; Nazaretian, V. P. Reactions of Cycloalkanecarboxylic Acids with SF4. III. Fluorination of Cycloburane- and Cyclopentane-tetracarboxylic Acids with SF4. *J. Fluorine Chem.* **1994,** *69*, 237-240.

18. (a) Politzer, P.; Lane, P.; Concha, M. C.; Ma, Y.; Murray, J. S. An Overview of Halogen Bonding. *J. Mol. Model.* **2007,** *13*, 305-11; (b) Chopra, D. Is Organic Fluorine Really "Not" Polarizable? *Cryst. Growth & Des.* **2012,** *12*, 541-546.

19. (a) Schneider, H. Hydrogen bonds with fluorine. Studies in solution, in gas phase and by computations, conflicting conclusions from crystallographic analyses. *Chem. Sci.* **2012,** *3*, 1381; (b) Pavan, M. S.; Durga Prasad, K.; Row, T. N. Halogen Bonding in Fluorine: Experimental Charge Density Study on Intermolecular F···F and F···S Donor-acceptor Contacts. *Chem. Commun.* **2013,** *49*, 7558-7560; (c) Matta, C. F.; Castillo, N.; Boyd, R. J. Characterization of a Closed-Shell Fluorine-Fluorine Bonding Interaction in Aromatic Compounds on the Basis of the Electron Density. *J. Phys. Chem. A* **2005,** *109*, 3669-3681.

20. (a) Metrangolo, P.; Murray, J. S.; Pilati, T.; Politzer, P.; Resnati, G.; Terraneo, G. Fluorine-Centered Halogen Bonding: A Factor in Recognition Phenomena and Reactivity. *Cryst. Growth & Des.* **2011,** *11*, 4238-4246; (b) Metrangolo, P.; Murray, J. S.; Pilati, T.; Politzer, P.; Resnati, G.; Terraneo, G. The fluorine atom as a halogen bond donor, viz. a positive site. *Cryst. Eng. Comm.* **2011,** *13*, 6593; (c) Esraili, M. D.; Mohammadian-Sabet, F.; Esmailpour, P.; Solimannejad, M. Cooperativity between fluorine-centered halogen bonds: investigation of substituent effects. *J. Mol. Model* **2013,** *19*, 5625-5632; (d) Hathwar, V. R.; Row, T. N. G. Charge Density Analysis of Heterohalogen (Cl···F) and Homohalogen (F···F) Intermolecular Interactions in Molecular Crystals: Importance of the Extent of Polarizability. *Cryst. Growth & Des.* **2011,** *11*, 1338-1346; (e) Vangala, V. R.;

Nangia, A.; Lynch, V. M. Interplay of phenyl–perfluorophenyl stacking, C–H···F, C–F···π and F···F interactions in some crystalline aromatic azinesElectronic supplementary information (ESI) available: experimental powder X-ray diffraction spectra. *Chem. Commun.* **2002**, 1304-1305; (f) Chopra, D.; Row, T. N. G. Role of Organic Fluorine in Crystal Engineering. *Cryst. Eng. Comm.* **2011,** *13*, 2175-2186; (g) McAllister, L. J.; Bruce, D. W.; Karadakov, P. B. Halogen bonding interaction between fluorohalides and isocyanides. *J. Phys. Chem. A* **2011,** *115*, 11079-11086.

21. Makulski, W. ^{19}F and ^{29}Si nuclear magnetic shielding and spin–spin coupling constants in silicon tetrafluoride and hexafluorodisiloxane in the gaseous state. *J. Mol. Struct.* **2013,** *1036*, 168-173.

22. Hohorst, F. A.; Shreeve, J. M. Bis (fluoroxy) difluoromethane, $CF_2(OF)_2$. *J. Am. Chem. Soc.* **1967,** *89*, 1809-1810.

23. Silverstein, R. M.; Webster, F. X.; Kiemle, D. J. *Spectrometric Identification of Organic Compounds*. 7th ed.; John Wiley and Sons: New York, 2005. pp 121-122.

24. (a) Morino, Y.; Kuchitsu, K.; Shimanouchi, T. The Mean Amplitudes of Thermal Vibrations in Polyatomic Molecules. I. $CF_2=CF_2$ and $CH_2=CF_2$. *J. Chem. Phys.* **1952,** *20*, 726; (b) Jiang, H.; Appadoo, D.; Robertson, E.; McNaughton, D. A comparison of predicted and experimental vibrational spectra in some small fluorocarbons. *J. Comput. Chem.* **2002,** *23*, 1220-1225; (c) Ignat'eva, L. N.; Buznik, V. M. Quantum-chemical calculations of the IR absorption spectra of modified polytetrafluoroethylene forms. *Russ. J. Phys. Chem.* **2006,** *80*, 1940-1948.

25. (a) Harris, K. L.; Pitenis, A. A.; Sawyer, W. G.; Krick, B. A.; Blackman, G. S.; Kasprzak, D. J.; Junk, C. P. PTFE Tribology and the Role of Mechanochemistry in the Development of Protective Surface Films. *Macromolecules* **2015,** *48*, 3739-3745; (b) Pitenis, A. A.; Harris, K. L.; Junk, C. P.; Blackman, G. S.; Sawyer, W. G.; Krick, B. A. Ultralow Wear PTFE and Alumina Composites: It is All About Tribochemistry. *Tribol. Lett.* **2015,** *57*, 1-8; (c) Krick, B. A.; Pitenis, A. A.; Harris, K. L.; Junk, C. P.; Sawyer, W. G.; Brown, S. C.; Rosenfeld, H. D.; Kasprzak, D. J.; Johnson, R. S.; Chan, C. D.; Blackman, G. S. Ultralow wear fluoropolymer composites: Nanoscale functionality from microscale fillers. *Tribol. Int.* **2016,** *95*, 245-255.

26. Leach, J. B. The Carbaboranes, including their Metal Complexes. In *Organometallic Chemistry;* Abel, E. W.; Stone, F. G. A., Eds.; The Chemical Society: London, 1978; Vol. 7, p 75.

27. Gussonia, M.; Castiglionib, C. Infrared intensities. Use of the CH-stretching band intensity as a tool for evaluating the acidity of hydrogen atoms in hydrocarbons. *J. Mol. Struct.* **2000,** *521*, 1-18.

28. Kashiwagi, M. Water and Oil Repellent Composition and Treatment Method. U.S. Patent 7,754,836 B2, Jul. 13, 2010.

29. Ameduri, B.; Ladavie`re, C.; Delolme, F.; Boutevin, B. First MALDI-TOF Mass Spectrometry of Vinylidene Fluoride Telomers Endowed with Low Defect Chaining. *Macromolecules* **2004,** *37*, 7602-7609.

30. Billes, F.; Böhlig, H.; Ackermann, M.; Kudra, M. A vibrational spectroscopic study on furan and its hydrated derivatives. *J. Mol. Struc.: THEOCHEM* **2004,** *672*, 1-16.

CHAPTER SIX

SHORT CONTACTS INVOLVING FLUORINE AND SILVER ATOMS IN FLUOROORGANIC CARBOXYLATES CRYSTALS

6.1 INTRODUCTION

A variety of Ag---Ag contacts have been observed crystallographically in the past few decades. These interactions include not only argentophilic interactions between pairs of silver atoms, but they are also present in multinuclear units, chains, or even layers.[1] Silver (I) compounds have been used to construct various supramolecular structures, especially Ag (I) organics have shown a variety of structures of 2D or 3D networks.[2]

Silver (I) carboxylates often form oligomers and give interesting long range structures complex with donor ligands.[3] Most of the time the supramolecular isomerism have solvents in the structures and the solvents used can be good tools to manipulate the packing of the structures.[4] Li and Du reviewed the role of solvents in supramolecular systems in 2011.[5]

Silver trifluoroacetate is a commonly used building block in the study of Ag networks or complex formations. The presence of silver atoms often shows argentophilic phenomena and helps with supramolecular network assembly in the crystal structures.[6] Lots of work has been done regarding organosilver (I) frameworks, and interestingly the single crystal structure of silver trifluoroacetae has long been left without being properly solved. In 1972, the single crystal of $CF_3C(O)OAg$ was solved, and unfortunately a more detailed report was not filed.[7] We revised the work and prepared a specimen for single crystal X-ray analysis.

We report herein the preparation of two silver perfluoroacetates and the growth of crystals from different solvents. The disilver perfluoro-oxodiacetate compound coordinated with different solvent to give two different structures. In the structures, a number of Ag---O, Ag---Ag, F---F and F---O short contacts and solid-state 3D network structures were observed.

6.2 RESULTS AND DISCUSSION

During our work with 2,2,5,5-tetrafluoro-2,5-dihydrofuran (see Scheme 6.1, Figure 6.1, and Figure 6.2), we were able to obtain crystals of good quality for single crystal X-ray analysis. Both perfluoro-oxodiacetic acid (POA) and its corresponding silver acetate disilver perfluoro-oxodiacetate from water (DPO-H_2O) were analyzed at first. In the structures, several interesting short contacts involving fluorine and silver were observed.

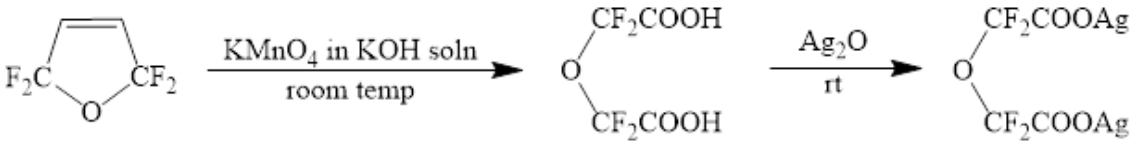

Scheme 6.1. Synthesis of perfluoro-oxodiacetic acid and disilver perfluoro-oxodiacetate

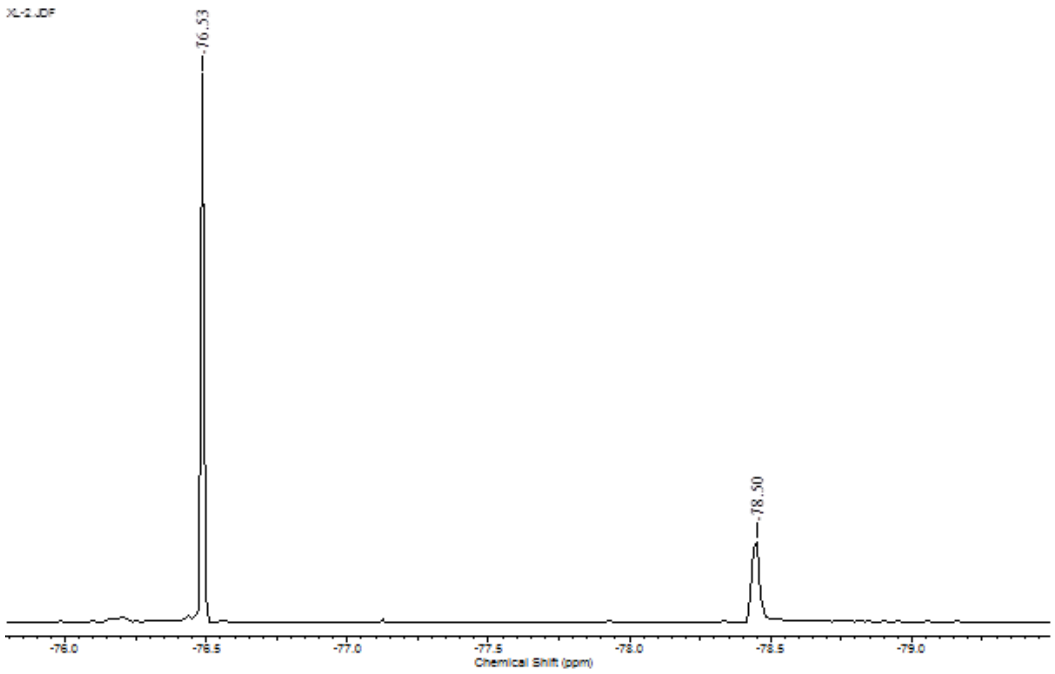

Figure 6.1. ^{19}F NMR spectrum of POA in D_2O. Internal standard: CF_3COOH: -78.50 ppm.

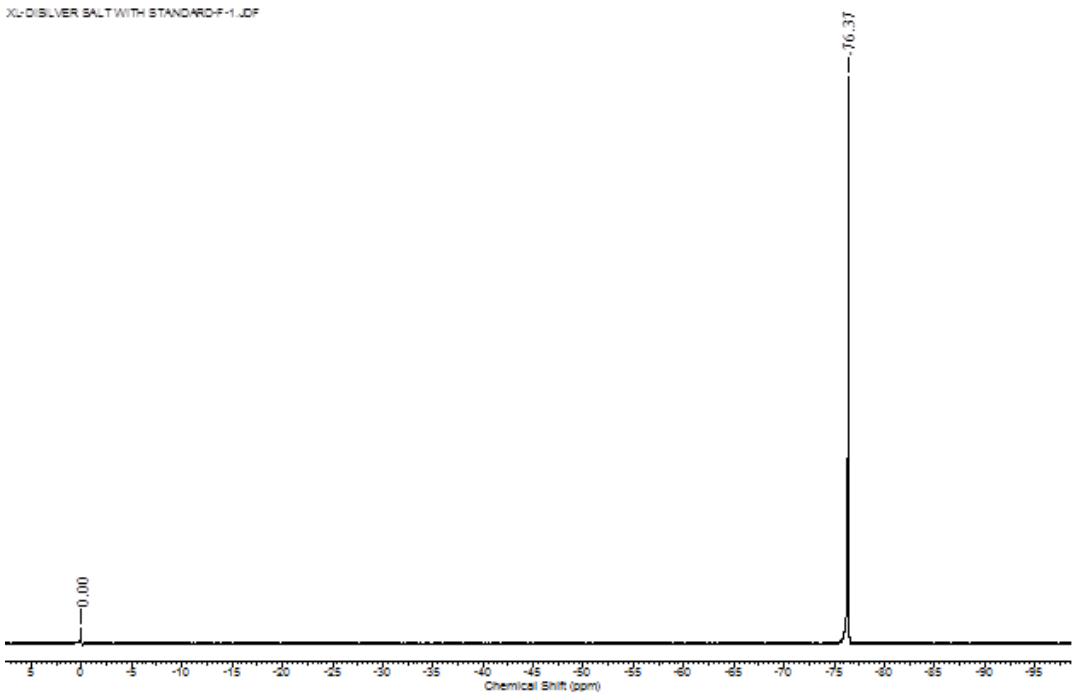

Figure 6.2. ^{19}F NMR spectrum of DPO in D_2O. Internal standard: CCl_3F: 0.00 ppm.

Another crystal of disilver perfluoro-oxodiacetate from THF (DPO-THF) was obtained and it was discovered that the structure of DPO-THF is very different from that of DPO-H_2O. The solvent plays a key role in the arrangement, and several other organic solvents such as acetone, diethyl ether, etc. were used. However, no crystals were obtained from them.

In both silver acetate structures, Ag---Ag short contacts, which are known as argentophilic phenomena were observed. In order to have a good comparison of the structures, silver trifluoroacetate (STA) was selected as a reference. The entire data package of the single crystal structure of STA was found not to be available in literatures,[7] therefore, a sample of STA was prepared in our lab and analyzed by single crystal X-ray crystallography in order to obtain more detailed information.

6.2.1 Crystal structure of silver trifluoroacetate (STA)

The silver trifluoroacetate molecule forms a nice dimer (see Figure 6.3), and each Ag1-O1 and Ag1-O2 bond coordinates with additional Ag and O atoms to form a four-membered rings around/outside the dimer (see Figure 6.4). The structure of silver trifluoroacetate is used as a comparison to the following perfluoro silver carboxylates compounds.

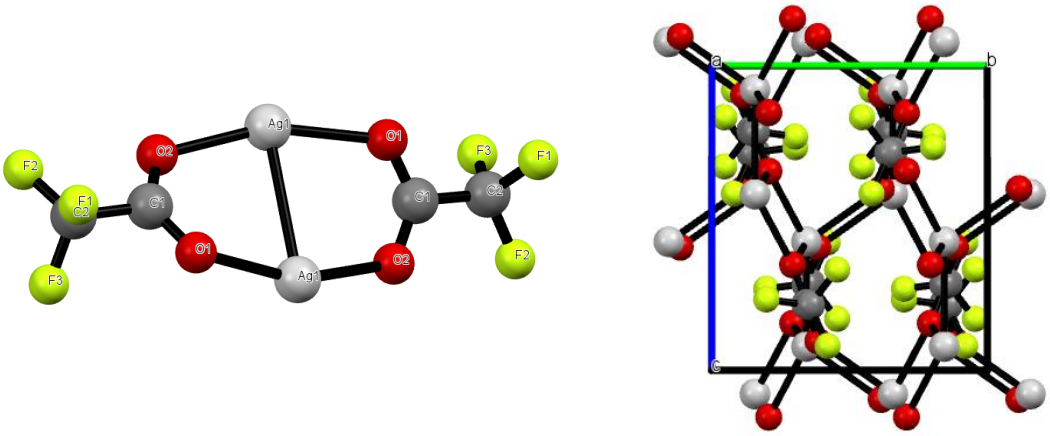

Figure 6.3. Crystal structure and packing of trifluoroacetate. Color code: Yellow-Fluorine, Grey-Carbon, Red-Oxygen, White-Silver.

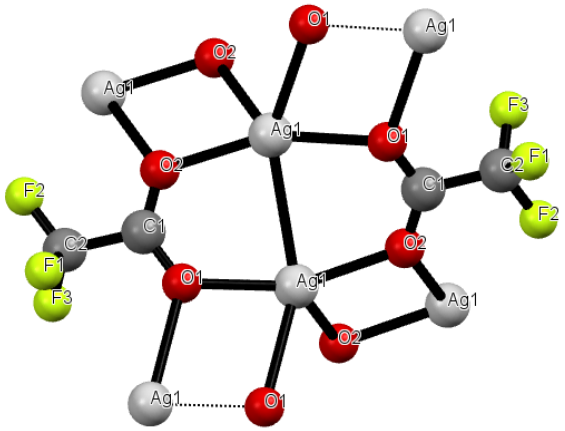

Figure 6.4. Ag---O ring coordinates around the dimer.

In the structure of STA, several F---F, F---O, Ag---Ag, and Ag---O short contacts were observed (see Table 6.1). If the distance between the two atoms from different molecules or spaced by at least three bonds is shorter than the sum of van der Waals radii, we consider it as a short contact. A thorough study on the van der Waals Radii of elements has been published.[8] The van der Waals radii of H, F, O, and Ag are 1.20 Å, 1.47 Å, 1.52 Å, and 1.72 Å, respectively, as reported by Bondi.[9] The sum of the van der Waals radii of fluorine and oxygen would be about 2.99 Å. The distances of O---F contacts in this structure is between 2.646 Å and 2.983 Å, which are shorter than 2.99 Å. The F---F contacts here are also shorter than the sum of the van der Waals radii of two fluorine atoms or 2.94 Å.

Table 6.1. Short Contacts Involve in F or Ag atoms in STA

Interaction	Hydrogen/halogen bond distance, Å	Angle, °	Type
F1---F1	2.731(4)	∠C2-F1⋯F1 = 113.79 (2)	Cis, I
F1---F2	2.927(3)	∠C2-F1⋯F2 = 93.83(2) ∠C2-F2⋯F1 = 124.65(2)	L, II
F1---O2	2.916(4)		
F2---O1	2.983(4)		
O1---F1	2.802(5)		
O1---F3	2.749(4)		
O2---F2	2.646(4)		
Ag1---Ag1	2.9431(4)		
Ag1---O2	2.234(3)		
Ag1---O1	2.541(2)		

If the C-F bond length of which the fluorine atoms is involved in short contacts is longer than the C-F bond not involved in any contacts, it would be a strong proof that the C-F bond can be elongated by the attraction of the contacts.

In the structure of STA, the bond lengths of three C-F bond are nearly the same or the difference is in the range of error, and it cannot be taken as direct evidence of F---F short contacts. Attention must be paid that each F atom here is involved in some short interactions with another atom, and forces could be balanced out and this might be the reason why all three C-F bonds are of the same length (see Table 6.2). For Ag---Ag, the contact in this structure is 2.943 Å, which is much shorter than the sum of the van der Waals radii at 3.44 Å, and the silver carboxylates compounds often have this type of argentophilic phenomena. The C=O double bond character is delocalized in that both C-O bonds are basically the same that C1-O1 = 1.252 Å, and C1-O2 = 1.245 Å.

Table 6.2. Selected C-F Bond Length in STA

Bond	Bond length, Å
F(1)-C(2)	1.341(4)
F(2)-C(2)	1.334(4)
F(3)-C(2)	1.336(4)

6.2.2 Crystal structure of perfluoro-oxodiacetic acid (POA)

In the first crystal structure that we had (see Figure 6.5), both H---O bonding and H---F bonding were observed (see Table 6.3). Meanwhile O---F interactions are observed providing 3-dimensional connectivity of molecules in the long-range structure. All of the fluorine interactions involve F1, and anything involving F2 is at a distance greater than 3 Å, which is not being considered as short contacts. The double bond character of -C(O)O group is present in this structure in that C2=O2 is 1.210 Å and C2-O3 is 1.291 Å.

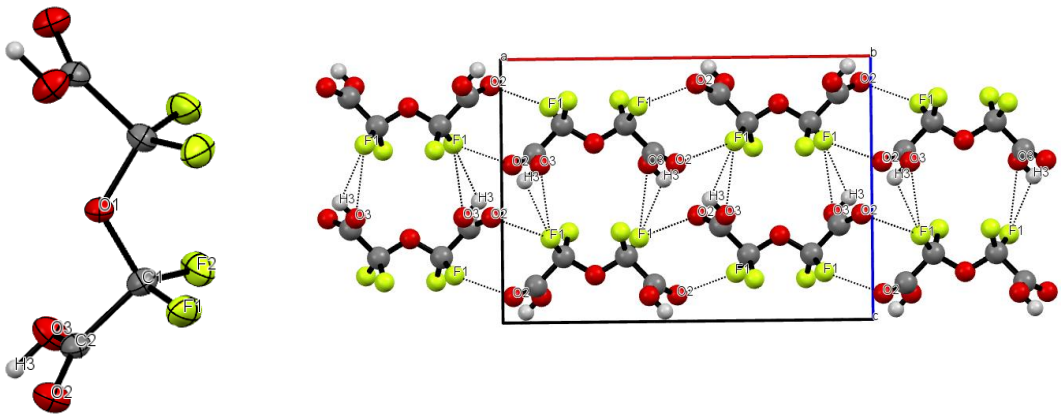

Figure 6.5. Crystal structure of perfluoro-oxodiacetic acid.

Table 6.3. Short Contacts of POA

Interaction	Hydrogen/halogen bond distance, Å
O2---F1	2.936(2)
O3---F1	2.999(2)
H3---F1	2.731
H3---O2	1.854

6.2.3 Crystal structure of disilver perfluoro-oxodiacetate with H_2O (DPO-H_2O)

The structure of DPO-H_2O was a surprise that it is a complicated three dimensional solid state structure with OOC-CF_2-O-CF_2-COO bridges between silver atoms. Instead of the proposed structure $AgOOCCF_2OCF_2COOAg$, each oxygen atom coordinates with a silver atom (see Figure 6.6).

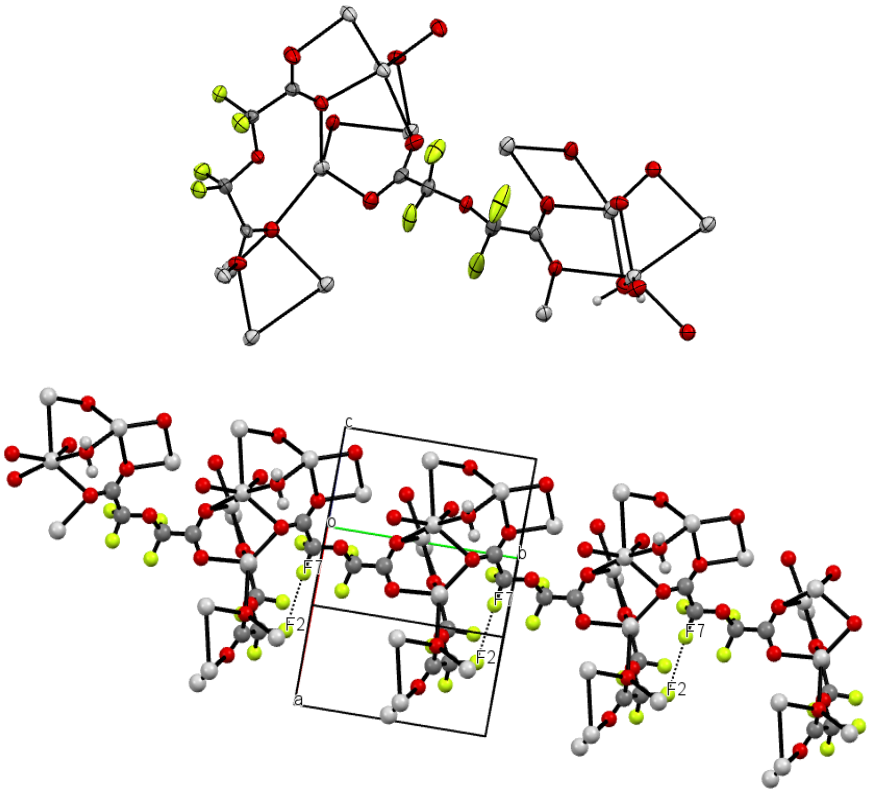

Figure 6.6. Crystal structure of DPO-H_2O.

The C-O bond distances in the fluoroacetate group are essentially identical, so the double bond character expected to be seen (observed in perfluoro-oxodiacetic acid structure) is delocalized over both oxygen atoms. This is not surprising since both oxygen atoms support bonds to silver.

An additional oxygen atom that only acts as a bridge between two silver atoms and is not a part of the organic portion of the structure also exist, and it is identified as the oxygen from H_2O (3350 cm^{-1}, 1600 cm^{-1}) used in crystal growth according to the ATR-IR analysis on the crystal (see Figure 6.7).

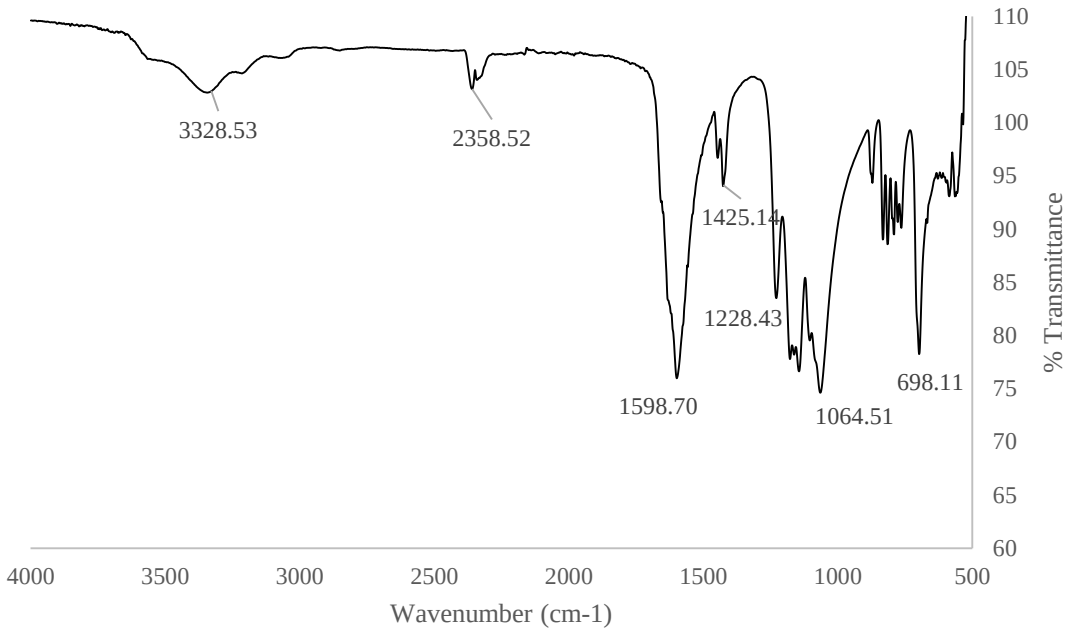

Figure 6.7. ATR-IR of DPO-H_2O.

Silver is notorious for having distorted, or unusual coordination, and we see a bit of that here. Both some very short (2.2 Å), and some fairly long (2.6-2.7 Å) Ag-O distances exist, but nothing that is unheard of for silver. A couple instances of "argentophilic" interactions were also observed, where there are short Ag-Ag contact distances (2.8-3.0 Å). Considering these interactions improves the local geometries of a couple of the Ag atoms that would be distorted if we only considered the Ag-O bonds (see Table 6.4).

Table 6.4. Short Contacts Involved in F or Ag in the Structure of DPO-H_2O

Interaction	Hydrogen/halogen bond distance, Å	Angle, °	Type
F7---F2	2.866(6)	∠C2-F2···F7 = 110.6 (3) ∠C7-F7···F2 = 150.4 (4)	L, II
F5---F3	2.989(5)	∠C3-F3···F5 = 107.9 (2) ∠C6-F5···F3 = 97.0 (3)	Trans, I
F5---H11A	2.090		
F8---O5	2.909(4)		
O10---F7	2.613(6)		
O7---F6	2.718(5)		
O1---F2	2.816(5)		
O2---F1	2.628(4)		
O4---F3	2.687(4)		
O4---F4	2.854(4)		
Ag2---Ag2	2.8174(8)		
Ag3---Ag3	2.9750(9)		
Ag1---Ag3	3.354(1)		

Two F---F contacts that are shorter than 3 Å were observed, and F7---F2 is also considered as a type II halogen-halogen bonding because the bond angles are ∠C7-F7---F2 = 150.41° (close to 180°) and ∠C2-F2---F7 = 110.58° (close to 90°). The electron density contour map of the F7---F2 area shows some suspicious distortion (see Figure 6.8).

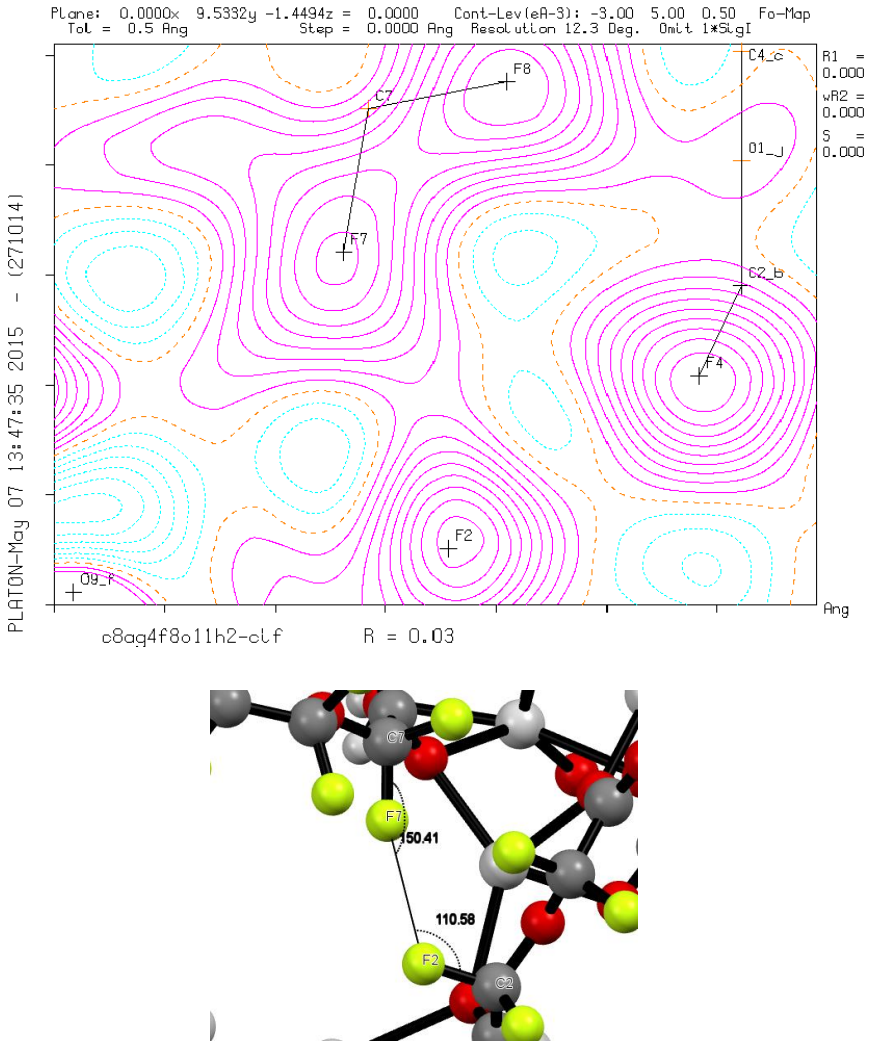

Figure 6.8. Electron density contour map of C2---F7 in DPO-H_2O.

The water molecule plays a key role in the structural arrangement in terms of Ag---O contacts. The Ag---O contacts forms several kinds of ring systems (see Figure 6.9). There are even larger ring systems of 8 or 10 members or even larger bridged by H_2O molecules. No Ag atoms clusters were observed in this structure. Compare with the –COO group in STA, the C-O bonds in DPO-H_2O have the same character and nearly the same

lengths between 1.241 Å and 1.260 Å, and both silver carboxylates dimerize to a large ring system between two molecules regardless the presence of H_2O molecules in the system.

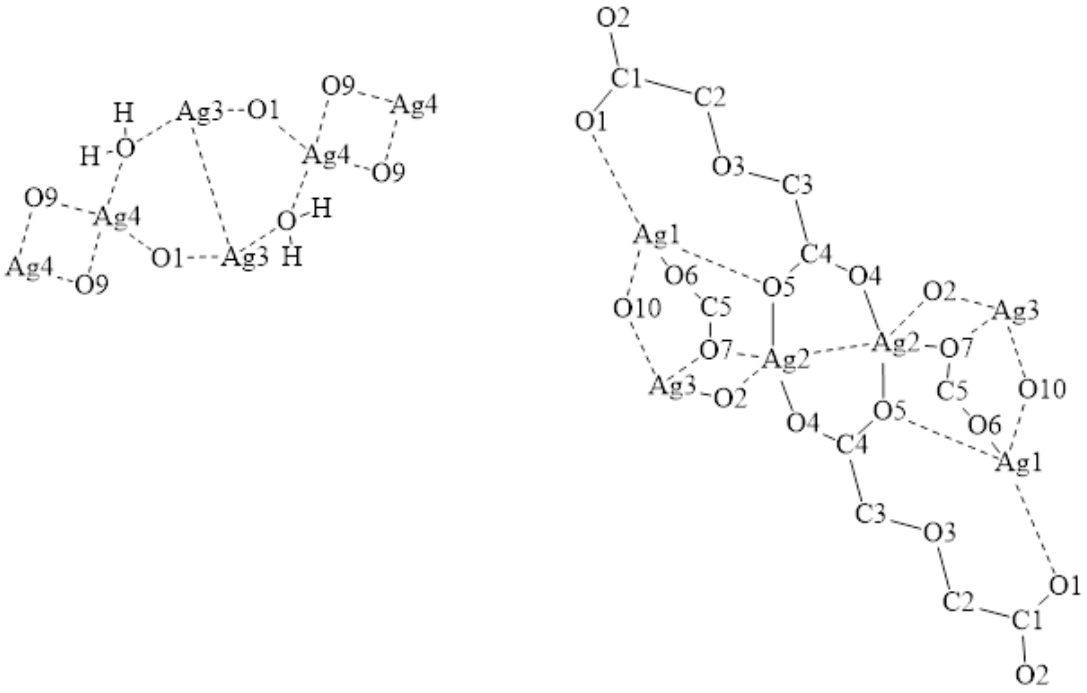

Figure 6.9. Ag---O ring systems in DPO-H_2O.

In terms of the F---F short contacts, an indirect evidence of the attraction between fluorine atoms is the bond length of the fluorine atoms with the same carbon as discussed above for STA C-F bonds. In the structure of DPO-H_2O, a stronger proof exists from the following point of view. For instance, F2 in involved in a short contact with F7, the bond length of C2-F2 is 1.347 (5) Å and C2-F1 = 1.338 (5) Å. F2 is involved in an interaction with F7, and the C2-F2 distance is about 0.01 Å longer than that of C2-F1, which is not involved in any short distance contacts. However, 0.01 Å is about on the edge of error range, and both F2 and F7 are involved in other short distance interactions at the same time.

The distance C7-F7 = 1.347 (5) Å and C7-F8 = 1.341 (7) Å (see Table 6.5) are basically the same length. Thus, it is hard to decide if it is the attraction between F atoms or F and O atoms. The distance C3-F3 is about 0.015 Å longer than C3-F4, which is a noticeable difference; however, both F3 and F4 are also involved in F---O interactions.

Table 6.5. Selected C-F Bond Length in DPO-H_2O

Bond	Bond length Å
C(2)-F(1)	1.338(5)
C(2)-F(2)	1.347(5)
C(3)-F(4)	1.347(5)
C(3)-F(3)	1.362(5)
F(5)-C(6)	1.340(6)
F(6)-C(6)	1.342(6)
C(7)-F(7)	1.347(6)
F(8)-C(7)	1.341(7)

6.2.4 Crystal structure of disilver perfluoro-oxodiacetate with tetrahydrofuran (DPO-THF)

The structure of DPO-THF is even more complicated, as both oxygen atoms on the –C(O)O group coordinate with Ag atoms, and each oxygen atom can coordinate with more than one Ag atoms. The C-O bonds of the –C(O)O group are also essentially identical but slightly shorter than the C-O bond in DPO-H2O structure (see Figure 6.10).

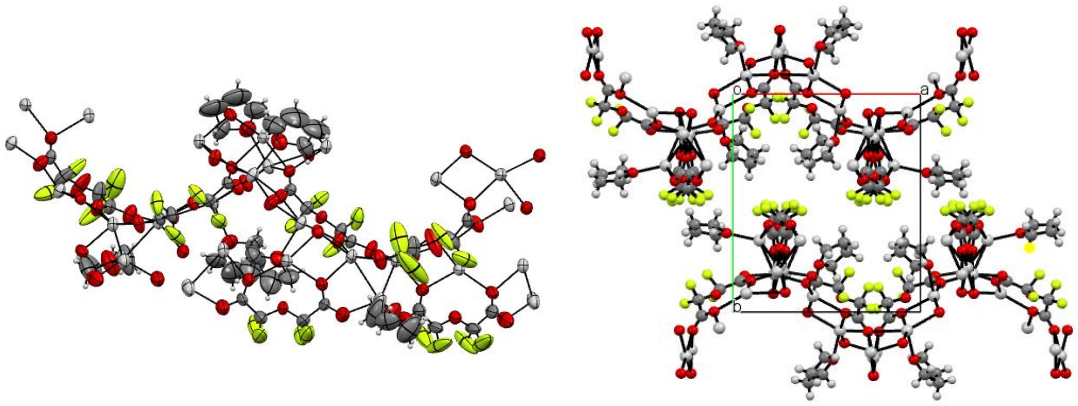

Figure 6.10. Crystal structure and packing of DPO-THF.

Table 6.6. Crystallography Data

	STA	POA	DPO-H_2O	DPO-THF
Empirical	$C_4Ag_2F_6O_4$	$C_4H_2F_4O_5$	$C_8Ag_4F_8O_{11}$	$C_{24}H_{24}Ag_6F_{12}O_{18}$
FW, g/mol	441.78	206.06	855.56	1475.65
system	monoclinic	Orthorhombic	Triclinic	Monoclinic
dimension mm	0.12 x 0.18 x 0.22	0.60 x 0.54 x 0.22	0.34 x 0.26 x 0.18	0.18 x 0.30 x 0.37
space group	C 1 2/c 1	Pccn	P-1	P 1 2/n 1
T, K	100(2)	200	293	293
a, Å	12.2379(11)	13.623 (3)	8.4803 (17)	12.8278 (11)
b, Å	7.7246(7)	5.0101 (10)	9.5477 (19)	15.4387 (12)
c, Å	9.9625(7)	9.6941(19)	11.034 (2)	20.7288 (15)
β, °	121.043(4)	90	107.49	93.752 (4)
V, $Å^3$	806.90(12)	661.7 (2)	842.7 (3)	4096.4 (6)
θ range	3.28 to 33.16	2.99 – 25.25	2.53 – 25.25	2.24 – 25.15
Index ranges	-18<=h<=18, -11<=k<=11, -14<=l<=14	-16<=h<=16, -6<=k<=4, -11<=l<=11	-10<=h<=10, -11<=k<=11, -12<=l<=13	-15<=h<=15, -18<=k<=18, -24<=l<=24

No. Of reflections collected	8551	4494	6780	34211
μ (Mo Kα), mm^{-1}	4.960	0.251	4.723	2.935
d_{calc}, $mg.m^{-3}$	3.637	2.068	3.372	2.393
data/restraints/parameters	1427 / 0 / 74	594 / 0 / 61	3022 / 0 / 281	7325 / 37 / 543
final R [$I > 2\sigma(I)$] R1,wR2	R_1 = 0.0244, wR_2 = 0.0805	R_1 = 0.0373, wR_2 = 0.0969	R_1 = 0.0275, wR_2 = 0.0687	R_1 = 0.0626, wR_2 = 0.1632
final R (All data) R1, wR2	R_1 = 0.0252, wR_2 = 0.0810	R_1 = 0.0398, wR_2 = 0.0999	R_1 = 0.0300, wR_2 = 0.0707	R_1 = 0.0792, wR_2 = 0.1770
GOF	1.152	1.097	1.082	1.160
largest diff. peak/hole, e/ $Å^3$	1.834/-1.380	0.209/-0.243	0.972/-0.881	2.071/-1.027

There are several Ag---O contacts ranging from 2.187-2.881 Å (see Table 6.7). And in both DPO-H_2O and DPO-THF structures, there are several 4-, 6-, 8-, 12-membered ring structures formed by placing Ag and O atoms alternatively. In DPO-THF there is a silver atom cluster (see Figure 6.11) that consists of three Ag atoms forming a triangle (Ag1---Ag2 = 2.963 Å, Ag2---Ag3 = 3.003 Å, Ag3---Ag1 = 3.037 Å).

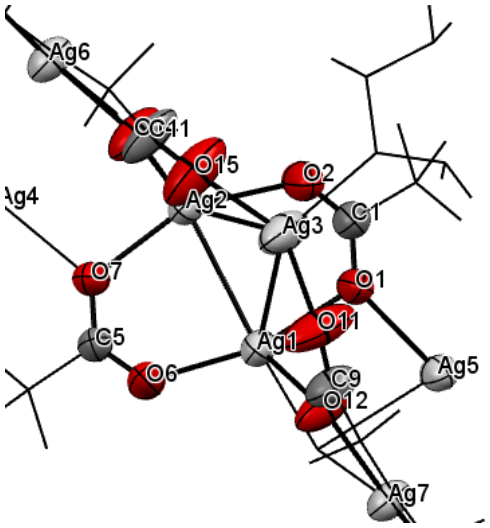

Figure 6.11. Ag atoms cluster in DPO-THF.

The atoms Ag1 and Ag2 both coordinate with four oxygen atoms and Ag3 coordinates with the two oxygen atoms from different -C(O)O- groups and the third oxygen from the THF solvent molecule. This triangle cluster bridges four -C(O)O- groups from four molecules (see Figure 6.11). No Ag clusters were observed in STA and DPO-H_2O structures. Besides the Ag---Ag and Ag---O interactions, the F---F interactions are quite short in this structure, e.g., F7---F1 = 2.788 (10) Å and F5---F3 = 2.748 (10) Å (see Table 6.7).

Table 6.7. Short Contacts in DPO-THF

Interaction	Hydrogen/halogen bond distance Å	Angle, °	Type
F7---F1	2.788(10)	∠C2-F1⋯F7=153.0 (1) ∠C7-F7⋯F1=142.4 (6)	Cis, I
F5---F3	2.748(10)	∠C3-F3⋯F5=158.5 (8) ∠C6-F5⋯F3=145.9 (7)	Cis, I

O10---F7	2.588(9)		
O4---F3	2.596(10)		
O5---F4	2.74(1)		
O15---F11	2.718(10)		
O15---F12	2.66(1)		
O11---F9	2.59(1)		
O11---F10	2.84(2)		
Ag6---Ag4	3.380(1)		
Ag7---Ag5	3.280(1)		
Ag1---Ag2	2.963(1)		
Ag1---Ag3	3.037(1)		
Ag2---Ag3	3.003(1)		

Among the fluorine atoms, which are involved in F---F short contact, only F3 and F7 are involved in other interactions with oxygen atoms, and F1 and F5 are only involved in F---F contacts. This offers a good chance to study if the C-F bond length is affected by the F---F interaction (Table 6.8). On carbon atom C2, the C2-F1 distance is about 0.15 Å shorter than that of C2-F2, while the C2-F2 is 1.42 Å, which is slightly longer than an average C-F bond length,[10] and the C6-F5 distance is about 0.01 Å longer than C6-F6 bond distance; however, this is in the error range. It seems that the F---F interaction of F1---F7 is more likely to be a repelling force instead of an attraction between two atoms. The C7-F7 distance is also about 0.05 Å shorter than that of C7-F8. In the contact of F1---F7, both the C1-F1 and C7-F7 bonds are shorter than the C1-F2 and C7-F8 bonds, which are not involved in any short distance contacts. Neither F1 nor F7 donated electrons to the contact, and this might not be considered as an example of halogen bonding in the end.

Table 6.8. Selected C-F Bond Length in DPO-THF

Bond	Bond length Å
C(2)-F(1)	1.265(19)
C(2)-F(2)	1.42(2)
C(3)-F(3)	1.325(14)
C(3)-F(4)	1.36(2)
C(6)-F(5)	1.338(14)
C(6)-F(6)	1.323(14)
C(7)-F(7)	1.317(12)
C(7)-F(8)	1.352(12)

6.3 CONCLUSION

In the structure of all three silver fluoroacetate structures, the Ag---Ag argentophilic phenomena was observed. The double bond character of -COO- group is delocalized and both C-O bonds are essentially identical in the structures of the acetates. The solvent plays an important role in the structure of DPO-H_2O and DPO-THF. Various long range or cyclic Ag---O 3-dimensional networks bridged by the solvent molecules were formed. A silver atoms cluster consisting of three silver atoms was observed in the structure DPO-THF.

Solvent is a very useful tool to modify the assembly of the silver acetate molecules. Several different organic solvents were also attempted to prepare crystals from DPO; however, the more polar the solvent is, the more difficult to form single crystals that are suitable for structural analysis. Short F---F and F---O contact distances were also observed in all the crystal structures. Whether short contacts between fluorine atoms are attractive or examples of real halogen bonding or not is under debating. The C-F bond length in which the fluorine atom is involved with F---F short contacts can be a secondary evidence of the attractive character of F---F contacts; however, the elongation of the contacted C-F

bond is not significant enough to decide if such an interaction is attractive or repulsive between two fluorine atoms in the contact.

6.4 EXPERIMENTAL

6.4.1 Materials

The starting material 2,2,5,5-tetrafluoro-2,5-dihydrofuran is synthesized following the method reported by Kunshenko.[11] KMnO4 and silver(I) oxide were purchased from Alfa Aesar; KOH, H_2SO_4 and diethyl ether were purchased from VWR; THF was purchased from BDH; silver trifluoroacetate was purchased from Sigma-Aldrich. All the materials purchased were used directly as received without further purification.

6.4.2 Instrumentation

NMR spectroscopic data was collected on multinuclear JOEL ECX-300 Spectrometer. The frequency is 282.78 MHz for ^{19}F NMR spectroscopy. Multiplicities are as follows: s (singlet). The internal standard of ^{19}F NMR spectroscopy is CCl_3F (0.00 ppm, s) or CF_3COOH (-78.50 ppm, s); single crystal-X-ray data were collected on a Bruker D8 Venture instrument. The structures were solved and refined by using full-matrix least-squares on F^2 method with Bruker SHELXTL-2014 Software Package. ATR-IR spectra were collected on a Thermo Scientific Nicolet iS5 diamond ATR spectrometer.

6.4.3 Crystal growth

Crystal of POA and DPO-H_2O were obtained directly from evaporating solvent from the reaction. Crystal DPO-THF was prepared with solvent evaporation method from dry disilver perfluoro-oxodiaetate solution in dry THF. Crystals of silver trifluoroacetate

crystal were prepared via the solvent evaporation method from a diethyl ether solution of silver trifluoroacetate.

6.4.4 Synthesis of perfluoro-oxodiacetic acid, POA

An amount of 9.7 g (62 mmol) $KMnO_4$ and an amount of 6.9 g (123 mmol) KOH are dissolved in 100 mL DI water at room temperature. To the above solution, 4.4 g (31 mmol) 2,2,5,5-tetrafluoro-2,5-dihydrofuran are added dropwise at room temperature with stirring. The reaction is stopped in 12 hrs. The reaction mxture is acidified with 50% H_2SO_4, and the solution is extracted with diethyl ether. The solvent is removed on the vacuum line by trap-to-trap distillation. The starting material 2,2,5,5-tetrafluoro-2,5-dihydrofuran is converted quantitatively.

NMR Chemical Shifts of POA:

^{19}F NMR chemical shift: δ = -76.53 ppm (s).

6.4.5 Synthesis of disilver perfluoro-oxodiaetate, DPO

An amount of 1 g (4.9 mmol) perfluoro-oxodiacetic acid compound is dissolved in 50 mL DI water. To the above solution, 2.3 g (10 mmol) Ag_2O powder is added slowly with stirring at room temperature. The reaction is stopped after no more of the black Ag_2O powder appears to be dissolving in the solution. The rest of the powder is filtered out, and a colorless solution is obtained. The water is removed by distillation yielding a white crystalline material. A sample of the crystalline material was analyzed by single crystal X-ray. The white crystal was dissolved in dimethoxyethane (glyme), and the solution was dried over activated molecular sieves to remove water. The solvent was transferred away on a vacuum line leaving DPO as a dry powdery solid in the flask. The flask was stored in

a dry box for further use. A small portion of the dry DPO was dissolved in dry THF, and the solvent was slowly evaporated away at room temperature, yielding DPO-THF crystals. This crystal was also analyzed by single crystal X-ray diffraction.

NMR Chemical Shifts of DPO:

^{19}F NMR chemical shift: δ = -76.37 ppm (s).

6.5 REFERENCES

1. Schmidbaur, H.; Schier, A. Argentophilic interactions. *Angew. Chem. Int. Ed.* **2015,** *54*, 746-784.

2. (a) Hau, S. C.; Tam, D. Y.; Mak, T. C. Organosilver(I) framework assembly with trifluoroacetate and enediyne-functionalized alicycles. *Acta Crystallogr., Sect. B: Struct. Sci.* **2014,** *70*, 37-46; (b) Crundwell, G.; Cantalupo, S.; Foss, P. D. C.; McBurney, B.; Kopp, K.; Westcott, B. L.; Updegraff Iii, J.; Zeller, M.; Hunter, A. D. Molecular and electronic structure of several 2,3-dithienylquinoxalines and their 2:1 complexes with silver(I) nitrate. *Open J. Inorg. Chem.* **2014,** *04*, 10-17; (c) Li, B.; Zang, S. Q.; Ji, C.; Hou, H. W.; Mak, T. C. W. Syntheses, Structures, and Properties of Silver–Organic Frameworks Constructed with 1,1′-Biphenyl-2,2′,6,6′-tetracarboxylic Acid. *Cryst. Growth Des.* **2012,** *12*, 1443-1451; (d) Serpe, A.; Artizzu, F.; Marchiò, L.; Mercuri, M. L.; Pilia, L.; Deplano, P. Argentophilic Interactions in Mono-, Di-, and Polymeric Ag(I) Complexes withN,N′-Dimethyl-piperazine-2,3-dithione and Iodide. *Cryst. Growth Des.* **2011,** *11*, 1278-1286.

3. Djordjevic, B.; Schuster, O.; Schmidbaur, H. A Cyclic Hexamer of Silver Trifluoroacetate Supported by Four Triphenylphosphine Sulfide Template Molecules. *Inorg. Chem.* **2005,** *44*, 673-676.

4. Yin, P.; Zhang, J.; Li, Z.; Qin, Y.; Cheng, J.; Zhang, L.; Lin, Q.; Yao, Y. Supramolecular Isomerism and Various Chain/Layer Substructures in Silver(I) Compounds: Syntheses, Structures, and Luminescent Properties. *Cryst. Growth Des.* **2009,** *9*, 4884-4896.

5. Li, C. P.; Du, M. Role of solvents in coordination supramolecular systems. *Chem. Commun.* **2011,** *47*, 5958-72.

6. (a) Sun, D.; Cao, R.; Bi, W.; Weng, J.; Hong, M.; Liang, Y. Syntheses and characterizations of a series of silver-carboxylate polymers. *Inorg. Chim. Acta* **2004,** *357*, 991-1001; (b) Whitcomb, D. R.; Rajeswaran, M. Designing silver carboxylate polymers: Crystal structures of silver-acetyl-benzoate and silver-1,2-benzenedicarboxylate monomethyl ester. *Polyhedron* **2006,** *25*, 1747-1752; (c) Effendy; Marchetti, F.; Pettinari, C.; Pettinari, R.; Skelton, B. W.; White, A. H. Synthesis and structural characterization of adducts of silver(I) carboxylate salts AgX (X=CF_3COO, CH_3COO) with ER_3 (E=P, As; R=Ph, cy, o-tolyl) and oligodentate aromatic bases derivative of 2,2′-bipyridyl, L, AgX:PR3:L (1:1:1). *Inorg. Chim. Acta* **2007,** *360*, 1451-1465; (d) Whitcomb, D. R.; Rajeswaran, M. Unusual silver coordination by mono-carboxylate utilization of a poly-carboxylate anion, solid-state structures of silver-tetrachlorophthalate with phthalazine and amine ligands. *Inorg. Chim. Acta* **2008,** *361*, 1357-1362; (e) Chen, H. T.; Lin, H.

L.; Chen, I. G.; Kuo, C. Conducting silver networks based on electrospun poly(methyl methacrylate) and silver trifluoroacetate. *Appl. Mater. Interfaces* **2015,** *7*, 9479-85.

7. Griffin, R. G. Single Crystal Study of the ^{19}F Shielding Tensors of a Trifluoromethyl Group. *J. Chem. Phys.* **1972,** *57*, 2147.

8. Batsanov, S. S. Van der Waals Radii of Elements. *Inorg. Mater.* **2001,** *37*, 871–885.

9. Bondi, A. Van der Waals Volumes and Radii. *J. Phys. Chem.* **1964,** *68*, 441-451.

10. Hayd, H.; Savin, H.; Stoll, A.; Preuss, H. Influence of Substituents on Bond Lengths. *J. Mol. Struct.: Theochem* **1988,** *165*, 87-97.

11. Kunshenko, B. V.; Motnyak, L. A.; Neizvestnaya, T. A.; Il'nitskii, S. O.; Yagupol'skii, L. M. Reaction of 2,5-Dibromofuran with the SF_4-HF-Br_2 System. *Zh. Organich. Khim.* **1986,** *22*, 1791-1792.

CHAPTER SEVEN

HALOGEN BONDINGS IN PERFLUORINATED DISULFONYL DICHLORIDE COMPOUNDS

7.1 INTRODUCTION

Desiraju, et al. recommended a definition of the halogen bonding (XB) in 2013, and it states that: '*A halogen bond occurs when there is evidence of a net attractive interaction between an electrophilic region associated with a halogen atom in a molecular entity and a nucleophilic region in another, or the same, molecular entity.*'[1]

The reason why XB attracts more and more attention from scientists is the growing wide range of applications in pharmaceutical chemistry and self-assembling materials,[2] especially when fluorine is introduced into the organic molecules, the structures and the chemical and biological properties can be significantly altered when compared to those of non-fluorinated molecules.[3] Fluorine is known as the most electronegative element, and it is the least polarizable. Whether it can be a XB donor or not has long been debated.[4] In the case of H---F contacts, it has been widely accepted as a type of hydrogen bonding;[5] however, in XB, several theories exist to explain the mechanism of XB, among which σ-hole theory is most often used. The halogen atom X acts as electrophilic XB donor to the nucleophile XB acceptor (Lewis base), and on the outmost side of the halogen along the axis there exists a positive electrostatic potential area, which is termed as a σ-hole.[6] The electrostatic potential is considered as the driving force of the XB formation along with some contributions from inductive and dispersive interactions.[7]

The X···O, X···N, X···S, X···Se interactions were discussed long ago, where X =F, Cl, Br, I. It has been shown that they are electrostatic in nature.[8] The halogen-halogen (X···X) bonding is classified as a special type of halogen bonding. The nature of X···X has been believed to be specific attractive forces, however, the debating never stopped.[9] In dihalogens (X_a···X_a) or hetero-halogens (X_a···X_b) bonding, one halogen atom acts as a halogen bonding donor having a positive electrostatic potential area or σ-hole interacting with the electron rich area on the other halogen atom as a halogen bonding acceptor.[10] Generally the more polarizable the halogen is, the stronger the halogen bonding is, therefore the strength of XB increases in the order F < Cl < Br < I. In the case of fluorine, the interaction is very weak compared to other XBs.[4a, 11]

In terms of the geometry of X···X, the interaction is very weak but highly directional. There are mainly two types, type I and type II contacts (see Error! Reference s ource not found.).[8b, 12] The cause of the geometries has been believed to be due to their chemical differences,[13] and these interactions have been studied experimentally along with some computational work based on strong analogies between XB and corresponding hydrogen bonding.[5b, 7]

Type I: $\theta_1 \approx \theta_2$

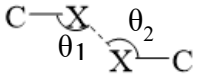

trans geometry

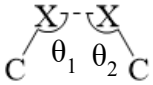

cis geometry

Type II: $\theta_1 \approx 180°$, $\theta_2 \approx 90°$

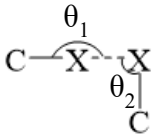

L geometry

Figure 7.1. Type I and type II halogen---halogen bonding.

Two perfluorinated disulfonyl dichloride compounds were synthesized for fuel cell applications. Crystals of good quality were obtained and analyzed by single crystal X-ray diffraction, and short distance F---F and Cl---O interactions were observed in the structures.

7.2 RESULTS AND DISCUSSION

7.2.1 Synthesis of the compound

The deiodo-sulfination reaction was discovered by Huang in 1980s[14] and it has been a very useful method in the synthesis of fluorinated sulfonyl fluorides. Two bissulfonyl chloride compounds perfluoro-1,4-butanedisulfonyl dichloride (C4) and perfluoro-1,6-hexanedisulfonyl dichloride (C6) were synthesized from the corresponding diiodide compounds in our laboratory by following the synthetic method reported by Qiu and Burton.[15] The products were identified by NMR spectroscopy, and the spectra are shown in Figure 7.2-7.5. The results agreed with the reported data.[15]

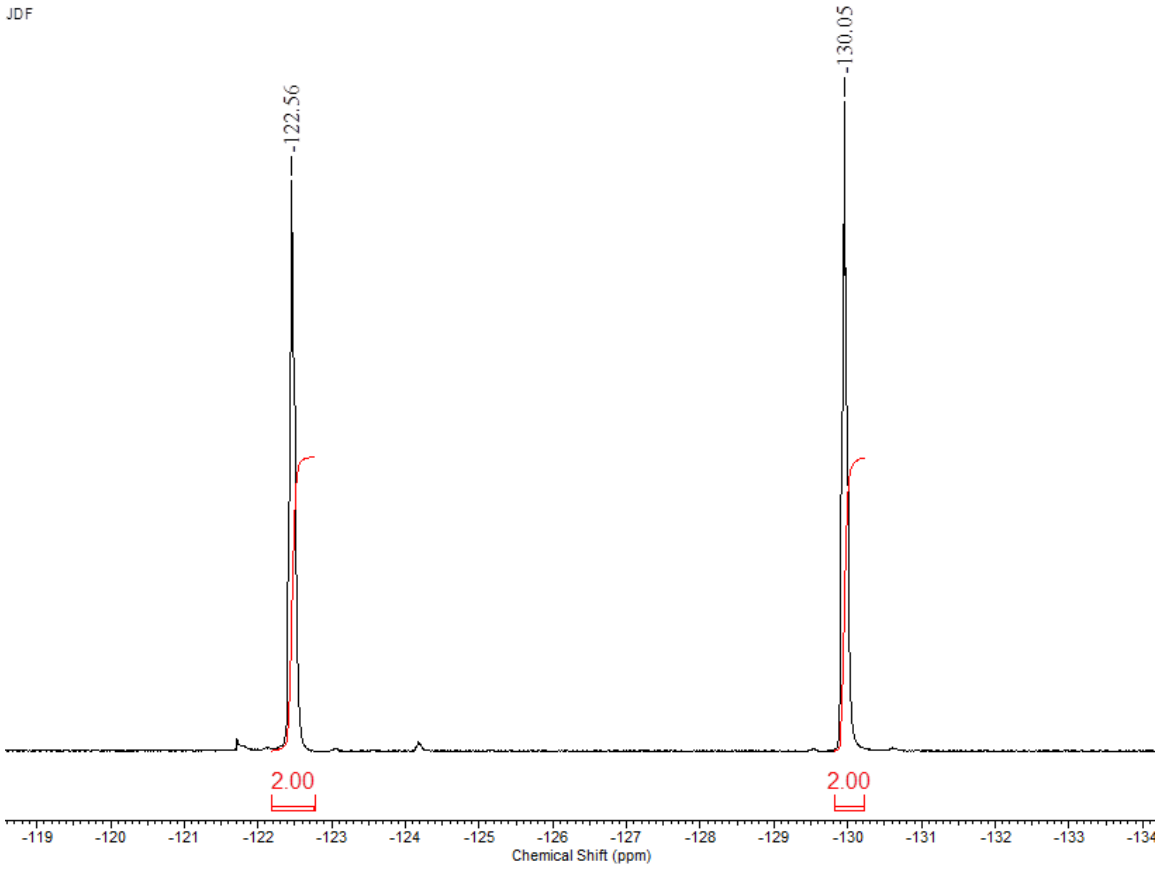

Figure 7.2. ^{19}F NMR spectrum of $NaSO_2CF_2CF_2CF_2CF_2SO_2Na$.

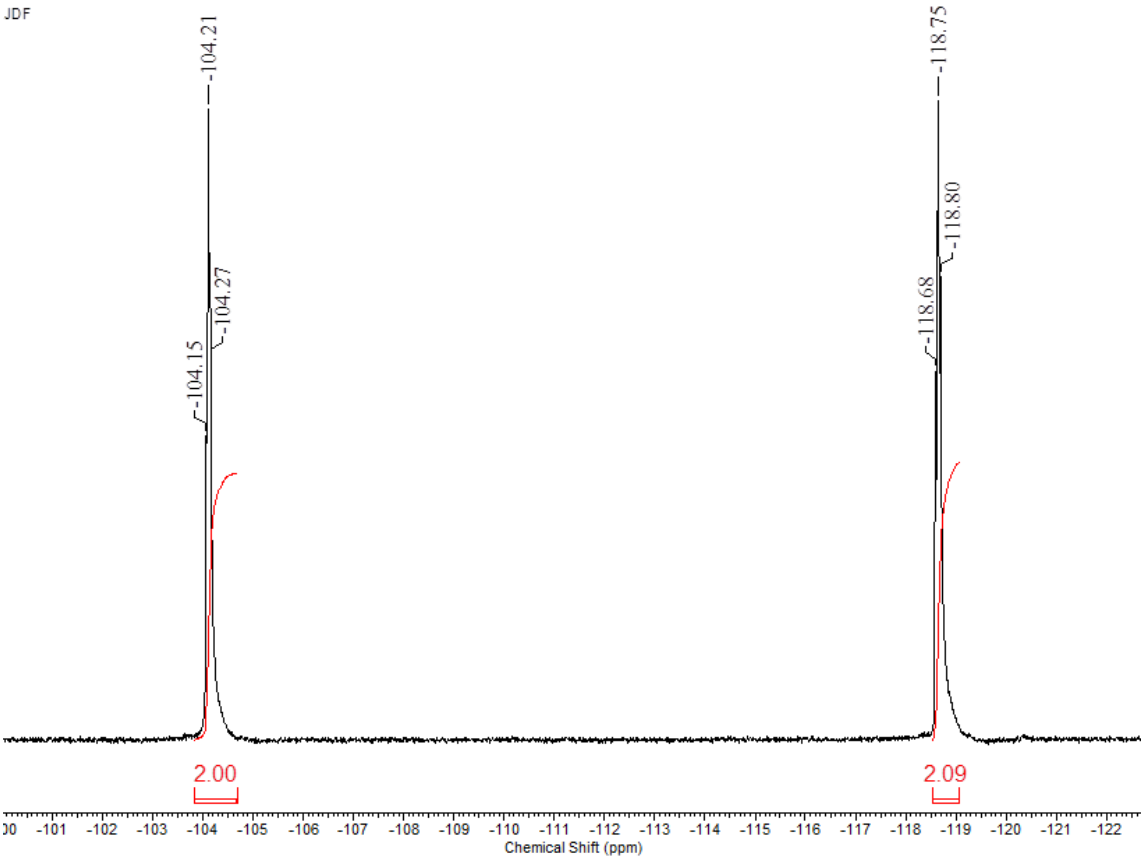

Figure 7.3. ^{19}F NMR spectrum of $ClSO_2CF_2CF_2CF_2CF_2SO_2Cl$ (C4).

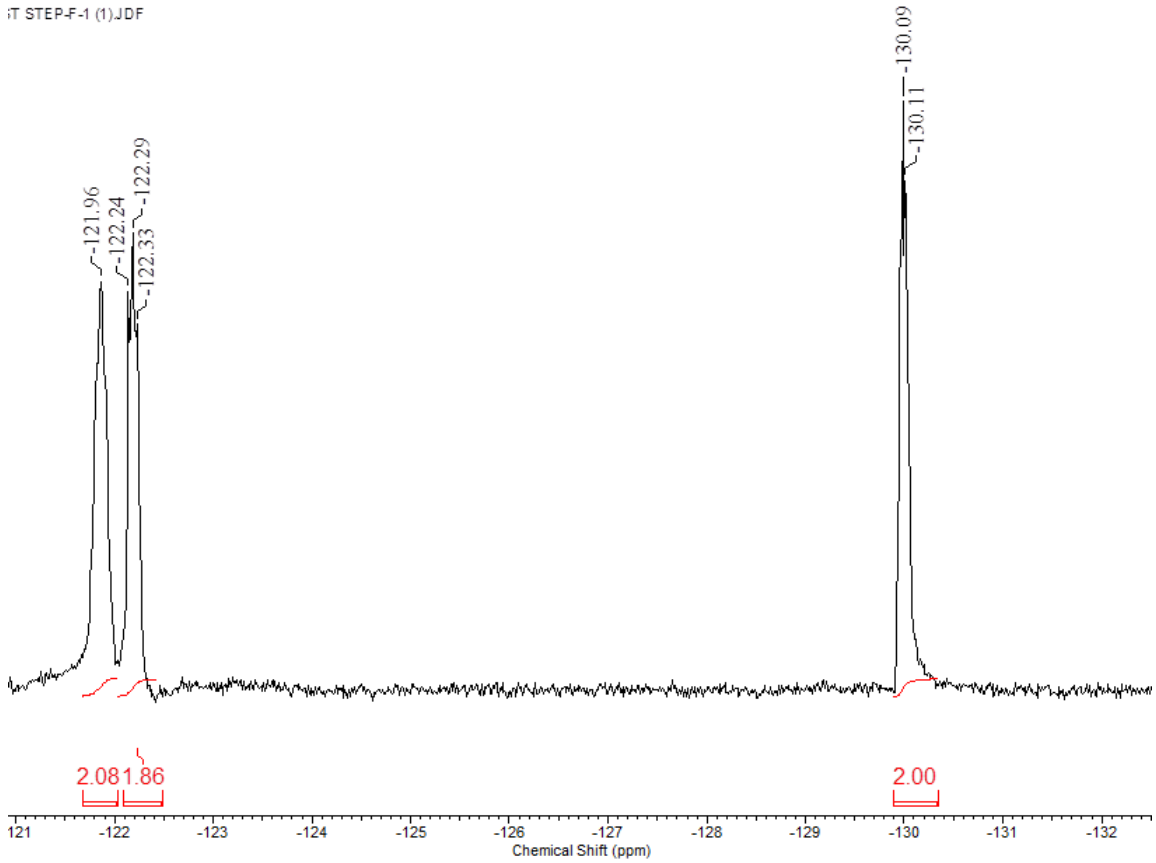

Figure 7.4. ^{19}F NMR of $NaSO_2CF_2CF_2CF_2CF_2CF_2CF_2SO_2Na$.

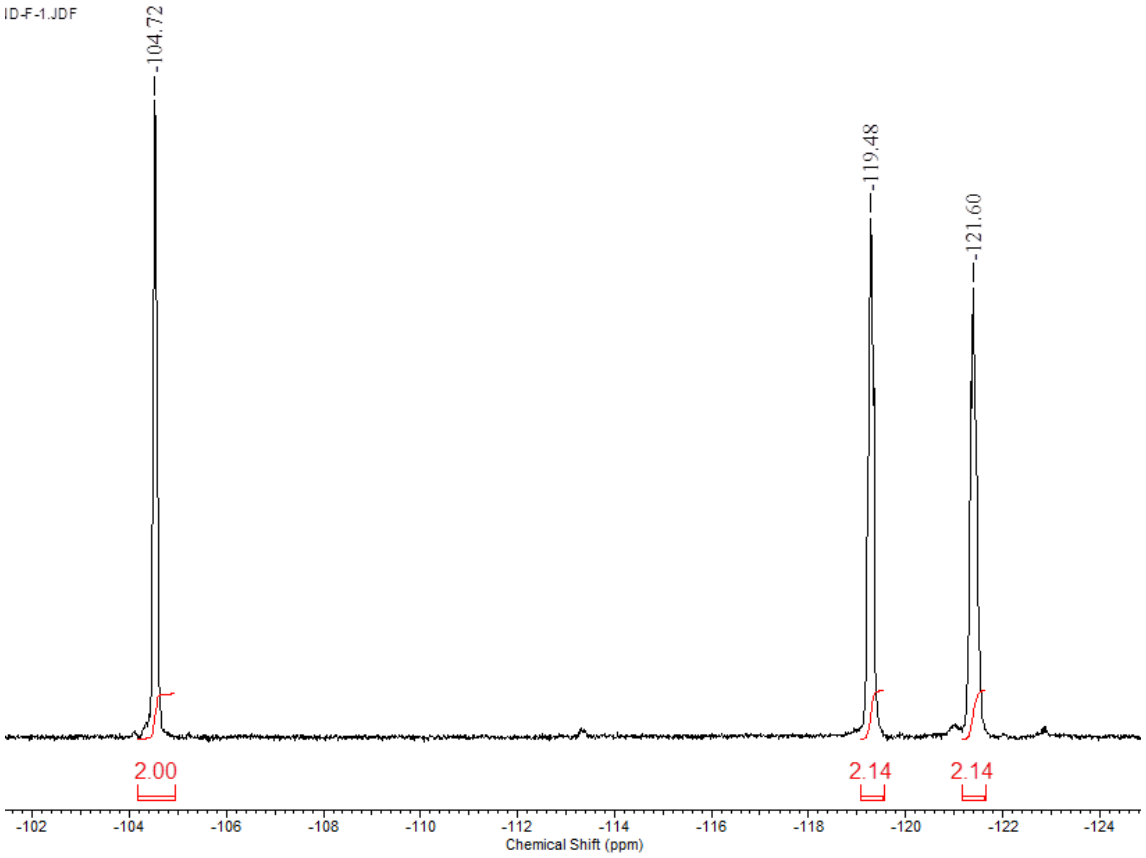

Figure 7.5. ^{19}F NMR spectrum of $ClSO_2CF_2CF_2CF_2CF_2CF_2SO_2Cl$ (C6).

7.2.2 Crystallization

After the compounds were synthesized, they were dissolved in chloroform, and two needle-shaped crystals of acceptable quality were obtained after the solvent was slowly evaporated in a refrigerator held at 4 °C. All the crystals were analyzed in X-ray laboratory, and both are monoclinic crystal systems (see Table 7.1).

Table 7.1. Crystallography Data

	C4	C6
Chemical formula	$C_4Cl_2F_8O_4S_2$	$C_6Cl_2F_{12}O_4S_2$
FW, g/mol	399.06	499.08
Temperature, K	293(2)	100(2)
Wavelength, Å	0.71073	0.71073
Crystal size, mm	0.38 x 0.30 x 0.07	0.021 x 0.242 x 0.268
Crystal system	monoclinic	monoclinic
Space group	P2(1)/c	P 1 21/c 1
Unit cell dimensions	a = 5.4994(11) Å	a = 5.3148(7) Å
	b = 19.724(4) Å	b = 24.007(3) Å
	c = 6.2190(12) Å	c = 5.8975(8) Å
	α = 90°	α = 90°
	β = 114.28(3)	β = 111.669(3)°
	γ = 90°	γ = 90°
Volume, $Å^3$	614.9(2)	699.30(16)
Z	2	2
Density (calculated), g/cm^3	2.155	2.370
Absorption coefficient,	0.978	0.926
F(000)	388	484

7.2.3 Crystal structure of perfluoro-1,4-butanedisulfonyl dichloride, $ClSO_2C_4F_8SO_2Cl$ (C4)

Some halogen bondings exist in the crystal structure of C4 that stabilizes the molecules in its long-range packing arrangement in this structure (see Figure 7.6). Namely, a Cl1-O1 interaction at 3.226 Å and a F1-F1 interaction at 2.705 Å (see Table 7.2) can be seen, and both interactions are less than the sum of their van der Waals radii (Cl-O = 3.27 Å; F-F = 2.94 Å). The bond angles for F1---F1 interactions are the same 154.84° (5) (type I, trans), and the Cl1---O1 bonds have different angles that ∠S1-Cl1---O1 = 160.37° (2) and ∠S1-O1---Cl1 = 136.37° (4). The Cl---O contacts angles are fairly close, and they have

a trans geometry. Most of the time, the F---F contacts we observed are type I bondings. Previously, a type II F---F contact had been observed in our laboratory in the crystal structure of DPO-H_2O, as reported in Chapter 6.

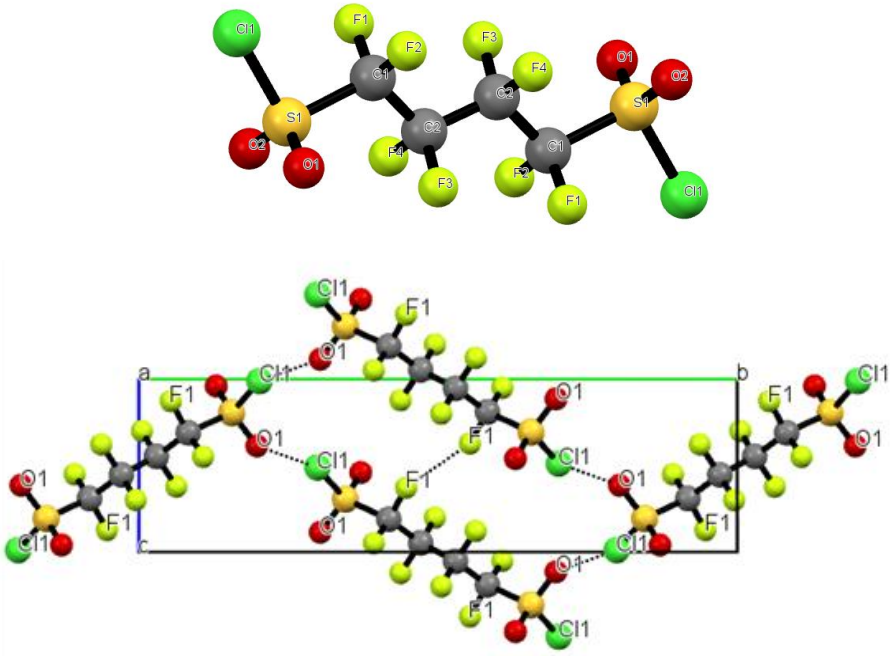

Figure 7.6. Crystal structure of 1,1,2,2,3,3,4,4-octafluoro-1,4-butanedisulfonyl dichloride (C4).

It is found that the C-F bond length of the contacted F atom is nearly equal to the length of the other C-F on the same carbon in this structure. More specifically, F1 is the contacted atom, where C1-F1 = 1.316 (8) Å and C1-F2 = 1.318 (1) Å. If the contacted C-F bond is longer than the non-contacted C-F bond on the same CF2 group, it can be a strong evidence of attraction between fluorine atoms. Since C1-F1 and C1-F2 are of nearly the same bond lengths, it is hard to tell if any attraction exists between the two fluorine atoms.

For the bonds involved in the O---Cl interactions, O1 is the contacted atom, where S1=O1 = 1.415 (7) Å, S1=O2 = 1.404 (1) Å. S1=O1 is about 0.01 Å longer than S1-O2 bond, which is a considerable difference (see Table 7.3). It is very likely that the Cl---O contact is a real halogen bonding where one atom is donating electrons to another, according to the definition given at the beginning of the introduction. The S-Cl bond length is in a normal range, and S1-O1 bond is elongated, which is an indirect evidence that O atom is the electron donor and Cl plays the role of electron acceptor or attracting electrons in this case.

Table 7.2. Contact Distances and Angles of C4 and C6

Crystal	Interaction	Halogen bond	Angle (°)	Type
C4	F1---F1	2.706(8)	∠C1-F1---F1 = 154.84(5)	Trans, I
	Cl1---O1	3.226(7)	∠S1-Cl1---O1 = 160.37(2) ∠S1-O1---Cl1 = 136.37(4)	
C6	F3---F1	2.8813	∠C1-F1---F3 = 149.85(4) ∠C2-F3---F1 = 144.90(4)	Trans, I
	F1---F5	2.7448	∠C1-F1---F5 = 152.63(4) ∠C3-F5---F1 = 152.41(4)	Trans, I
	Cl1---O1	3.2364	∠S1-Cl1---O1 = 113.46(1) ∠S1-O1---Cl1 = 121.50(3)	
	Cl1---O2	3.2146	∠S1-Cl1---O2 = 154.32(1) ∠S1-O2---Cl1 = 130.37(3)	

Table 7.3. Selected Bond Length in C4 and C6.

Crystal	Bond	Bond length Å
C4	C1-F1	1.316(8)
	C1-F2	1.319(1)
	S1=O1	1.415(7)
	S1=O2	1.404(1)
	S1-Cl1	1.991(3)
C6	C1-F1	1.336(7)
	C1-F2	1.319(1)
	C2-F3	1.331(7)
	C2-F4	1.336(9)
	C3-F5	1.352(7)
	C3-F6	1.332(1)
	S1=O1	1.417(7)
	S1=O2	1.419(5)
	S1-Cl1	2.000(2)

7.2.4 Crystal structure of perfluoro-1,6-hexanedisulfonyl dichloride, $ClSO_2C_6F_{12}SO_2Cl$ (C6)

This structure is very similar with that of C4, and halogen bonding is also stabilizing this structure in the long range packing (Figure 7.7). Both oxygen atoms are in contact with a chlorine atom from two other molecules, meanwhile one fluorine atom on a number of the CF_2 groups is in contact with another fluorine atom from the neighbor molecule.

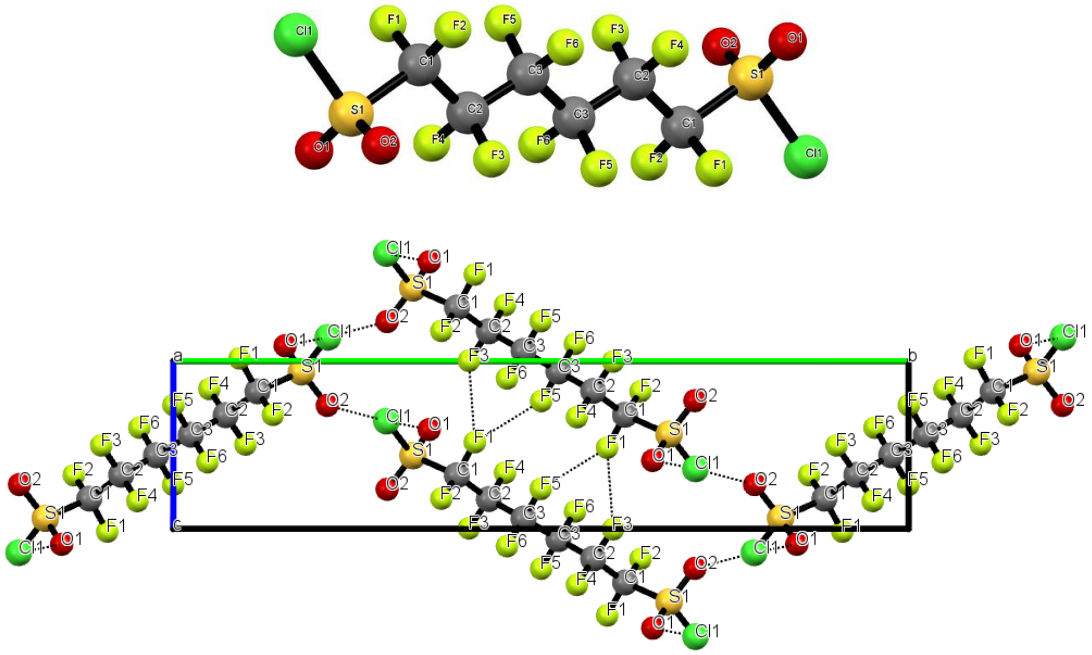

Figure 7.7. Crystal structure and packing of C6.

In the structure of C4, the S1-Cl1 bond is 1.991(3) Å, and the same bond is 2.000(1) Å in C6, which is of very minimal difference. Both S=O bonds in C6 [1.417 (7) Å and 1.419 (5) Å] are of similar length with S1=O1 [1.415 (7) Å] in C4. The S1=O2 bond in C4 is 0.01 Å shorter than the other three S=O bonds, which are involved in Cl---O interactions. This is a further evidence of the elongation of S=O bond by a Cl atom to form a halogen bond.

Both F---F short contacts are type I bonding judging from the bond angles, e.g., ∠C1-F1---F3 = 149.85(4)° ≈ ∠C2-F3---F1 = 144.90(4)°, and ∠C1-F1---F5 = 152.63(4)° ≈ ∠C3-F5---F1 = 152.41(4)° (see Table 7.2). The bond length of each C-F bond that is involved in a F---F short contact versus the C-F bond length that is not involved on the

same CF_2 group are compared, and the contacted C-F bond is elongated and has longer bond length than the non-contacted C-F bond. The bond C1-F1 = 1.336 Å and C1-F2 = 1.319 Å. Thus, the bond C1-F1 is elongated by about 0.017 Å. The C2-F3 and C2-F4 bonds are of similar lengths. The bond C3-F5 = 1.352 Å and it is about 0.02 Å longer than the bond C3-C6 being equal to 1.332 Å. Both the C1-F1 and C3-F5 bonds are elongated and F1---F5 are in contact at the same time. Judging from this scenario, F1---F5 has a sort of attractive force that elongates the C-F bond lengths. The F3---F1, F1---F5 short contacts along with the Cl---O contacts form a network force between molecules that results in the long-range packing structure shown in Figure 7.7.

If one takes the plane of the paper as XY coordination plane, the Z axis is more or less along the carbon chain direction. Aliphatic hydrocarbon chains have a planar zigzag conformation,[18] while on the contrary, aliphatic fluorocarbon (CF_2) carbon chains were discovered to have a helical twist.[19] However, the CF_2 chains of C4 and C6 have a conformation like aliphatic hydrocarbon chains (see Figure 7.8).

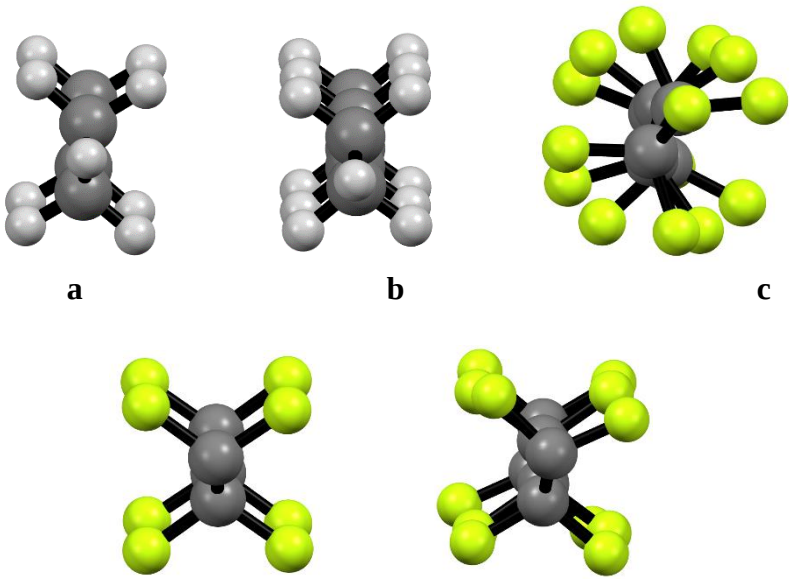

Figure 7.8. a. n-butane;[18] b. n-hexane;[18] c. n-perfluorohexane;[20] d. CF_2 chain of C4; e. CF_2 chain of C6.

This zipper shaped network formed by Cl---O contacts and F---F contacts (Figure 7.7) is believed to be responsible for the unusual zigzag and nearly planar conformation of the CF2 chains in crystal structures. The torsion angles around the C-C bonds in **c**, **d,** and **e** were measured (see Figure 7.8). Since n-butane and n-hexane have zigzag planar conformation, the torsional angles of the C-C bonds are all 180°. The four CF_2 groups of C4 have a torsion angel of 180.0°, and they are in the same planar. In the structure of C6, the four carbon atoms in the middle are in the same planar while the two carbon atoms on the end are slightly twisted, since the torsion of C2-C3-C3-C2 is equal to 180.0°, C1-C2-C3-C3 is equal to -174.5°, and C3-C3-C2-C1 is equal to 174.4°. These six carbons are nearly planar, which is a lot less twisted than the carbon atoms in n-perfluorohexane. In n-perfluorohexane, the torsion of the C-C bonds are C1-C2-C3-C4 = 167.5°, C2-C3-C4-C5 = 159.9°, and C3-C4-C5-C6 = 167.5°.

Table 7.4. Torsion in C4, C6, and n-Perfluorohexane

Crystal	Atoms	Torsion, °
C4	C1-C2-C2-C1	180.0(6)
C6	C1-C2-C3-C3	-174.5(6)
	C2-C3-C3-C2	-180.0(6)
	C3-C3-C2-C1	174.4(6)
n-perfluorohexane	C1-C2-C3-C4	167.5(1)
	C2-C3-C4-C5	159.9(1)
	C3-C4-C5-C6	167.5(1)
$I(CF_2)_6I$[1]	C1-C2-C3-C3	177.3(6)
	C2-C3-C3-C2	-180.0(5)
	C3-C3-C2-C1	-177.3(6)

A similar CF_2 chain conformation with that of C6 is observed in one of the structures of a complexes of $I(CF_2)_6I$ reported by Metrangolo et al. in that the four CF_2 carbons in the middle of the perfluorocarbon chain are located in one plane, while the two CF_2 groups on both ends slight are slightly twisted out of the plane (see **Error! Reference s ource not found.**). However, the CF_2 chain of $I(CF_2)_8I$ has a helical conformation like what is found in PTFE.[21]

7.3 CONCLUSIONS

The fluorocarbons in C4 and C6 tend to segregate from the $–SO_2Cl$ groups in C4 and C6, and this is often observed in other heteroatom fluorocarbon molecules. The Cl---O and F---F interactions somehow balance out to form an interlocking network in the long range and stabilize the structures. Both Cl---O and F---F short contacts are very likely to be based on attractions between the atoms. The distances are all shorter than the sum of van der Waal's radii, and all of the bonds involved in short contact distances have a

significant elongation. The conformation of the CF_2 chains appeared not to be helical in all scenarios. The cause of such a conformation needs to be studied further, and perhaps more single crystal structures of $I(CF_2)_mI$ or $ClSO_2(CF_2)_mSO_2Cl$ (m is a positive integer) derivatives need to be solved along with computational modeling in terms of carrying this study forward.

7.4 EXPERIMENTAL

7.4.1 Materials

1,1,2,2,3,3,4,4-octafluoro-1,4-diiodo-butane ($ICF_2CF_2CF_2CF_2I$) and 1,1,2,2,3,3,4,4,5,5,6,6-decfluoro-1,6-diiodo-hexane ($ICF_2CF_2CF_2CF_2CF_2CF_2I$) were purchased from SynQuest; NaS_2O_4 and $NaHCO_3$ were purchased from Sigma-Aldrich; acetonitrile was purchased from Mallinckrodt Baker; chloroform was purchased from Alfa Aesar. The NMR solvent $CDCl_3$ was purchased from Cambridge Isotope Laboratories, Inc..

7.4.2 Instrumentation

NMR spectroscopic data was collected on a multinuclear JOEL ECX-300 Spectrometer. The frequency is 282.78 MHz for ^{19}F. Multiplicities are as follows: s (singlet), t (triplet). The internal standard of ^{19}F NMR spectroscopy is CF_3Cl (0.00 ppm). Single crystal X-Ray data was collected on a Bruker D8 Venture instrument. The structures were solved and refined by using full-matrix least-squares on F^2 method with Bruker SHELXTL-2014 Software Package.

7.4.3 Synthesis of $NaSO_2C_4F_8SO_2Na$

To a 500 mL three-necked flask equipped with a magnetic stir bar, 100 mL acetonitrile, 150 mL DI water, 34.8 g (0.2 mol) $Na_2S_2O_4$ and 33.6 g (0.4 mol) $NaHCO_3$ were added and mixed. An amount of 45.4 g (0.1 mol) $ICF_2CF_2CF_2CF_2I$ was added drop wise to the above mixture at 40-45 C° with stirring. ^{19}F NMR spectroscopy was taken on the reaction mixture to ensure the completion of the reaction.

^{19}F NMR chemical shifts:

$NaSO_2CF_2{}^aCF_2{}^bCF_2CF_2SO_2Na$: δ_a = -122.56 ppm (s), δ_b = -130.05 ppm (s).

7.4.4 Synthesis of $ClSO_2C_4F_8SO_2Cl$ (C4)

Enough water was added to the above reaction mixture to fully dissolve all the salts. A condenser cooled to -50 ~ -60 °C was placed on one of the three necks of the reaction flask. The reaction mixture was cooled to ice temperature and chlorine gas was passed through the mixture with stirring. The bulk solution turned bright yellow, and a white solid precipitated. The chlorine gas was stopped when no more white solid was observed to be precipitating. The white solid was filtered out and dissolved in dichloromethane. The dichloromethane solution was washed with water two times, and the bottom layer was separated and dried over Na_2SO_4. The solvent was then evaporated, giving the white solid as the desired product. The yield was 79%.

^{19}F NMR chemical shifts:

$ClSO_2CF_2{}^aCF_2{}^bCF_2CF_2SO_2Cl$: δ_a = -104.21 ppm (t, $^3J_{FF}$ = 16.8 Hz), δ_b = -118.8 ppm (t, $^3J_{FF}$ = 16.8 Hz).

7.4.5 Synthesis of $NaSO_2C_6F_{12}SO_2Na$

To a three necked flask, 20 mL acetonitrile, 40 mL DI water, 7.4 g (0.036 mol) $Na_2S_2O_4$, and 4.54 g (0.054 mol) NaHCO3 were added and mixed with stirring at 45 °C. An amount of 5.0 g (0.01 mol) $ICF_2CF_2CF_2CF_2CF_2CF_2I$ was dissolved in 15 mL acetonitrile and the solution was added to the above mixture drop wise over 30 min. The ^{19}F NMR spectrum was taken on the reaction mixture to ensure the completion of the reaction.

^{19}F NMR chemical shifts:

$NaSO_2CF_2{}^aCF_2{}^bCF_2{}^cCF_2CF_2CF_2SO_2Na$: δ_a = -121.96 ppm (s), δ_b = -122.29 ppm (t, $^3J_{FF}$ = 13.2 Hz), δ_c = -130.09 ppm (t, $^3J_{FF}$ = 6.6 Hz).

7.4.6 Synthesis of $ClSO_2C_6F_{12}SO_2Cl$ (C6)

Enough water was added to the above reaction mixture to fully dissolve all the salts. A condenser cooled to -50 ~ -60 °C was placed on one of the three necks. The reaction bulk was cooled to ice temperature and chlorine gas was passed through the mixture with stirring. The bulk solution turned bright yellow and a white solid was precipitated. The chlorine gas was stopped when no more white solid was observed to be precipitating. The white solid was filtered out and dissolved in dichloromethane. The dichloromethane solution was washed with water twice, and the bottom layer was separated and dried through Na_2SO_4. The solvent was then evaporated, giving the white solid as the desired product. The yield was 65%.

^{19}F NMR chemical shifts:

$ClSO_2CF_2{}^aCF_2{}^bCF_2{}^cCF_2CF_2CF_2SO_2Cl$: δ_a = -104.72 ppm (s), δ_b = -119.48 ppm (s), δ_c = -121.60 ppm (s).

7.5 REFERENCES

1. Desiraju, G. R.; Ho, P. S.; Kloo, L.; Legon, A. C.; Marquardt, R.; Metrangolo, P.; Politzer, P.; Resnati, G.; Rissanen, K. Definition of the Halogen Bond. *Pure Appl. Chem.* **2013,** *85*, 1711-1713.
2. Wang, C.; Danovich, D.; Mo, Y.; Shaik, S. On The Nature of the Halogen Bond. *J. Chem. Theory Comput.* **2014,** *10*, 3726-3737.
3. Dunitz, J. D.; Gavezzotti, A.; Schweizer, W. B. Molecular Shape and Intermolecular Liaison: Hydrocarbons and Fluorocarbons. *Helv. Chim. Acta* **2003,** *86*, 4073-4092.
4. (a) Nayak, S. K.; Reddy, M. K.; Row, T. N. G.; Chopra, D. Role of Hetero-Halogen (F···X, X = Cl, Br, and I) or Homo-Halogen (X···X, X = F, Cl, Br, and I) Interactions in Substituted Benzanilides. *Cryst. Growth Des.* **2011,** *11*, 1578-1596; (b) Chopra, D.; Row, T. N. G. Role of Organic Fluorine in Crystal Engineering. *Cryst. Eng. Comm.* **2011,** *13*, 2175.
5. (a) Metrangolo, P.; Murray, J. S.; Pilati, T.; Politzer, P.; Resnati, G.; Terraneo, G. The fluorine atom as a halogen bond donor, viz. a positive site. *Cryst. Eng. Comm.* **2011,** *13*, 6593; (b) Metrangolo, P.; Murray, J. S.; Pilati, T.; Politzer, P.; Resnati, G.; Terraneo, G. Fluorine-Centered Halogen Bonding: A Factor in Recognition Phenomena and Reactivity. *Cryst. Growth Des.* **2011,** *11*, 4238-4246; (c) Chopra, D. Is Organic Fluorine Really "Not" Polarizable? *Cryst. Growth Des.* **2012,** *12*, 541-546.

6. (a) Schneider, H. Hydrogen bonds with fluorine. Studies in solution, in gas phase and by computations, conflicting conclusions from crystallographic analyses. *Chem. Sci.* **2012,** *3*, 1381; (b) Wolters, L. P.; Bickelhaupt, F. M. Halogen Bonding versus Hydrogen Bonding: A Molecular Orbital Perspective. *Chemistry Open* **2012,** *1*, 96-105.

7. (a) Pavan, M. S.; Durga Prasad, K.; Row, T. N. Halogen Bonding in Fluorine: Experimental Charge Density Study on Intermolecular F...F and F...S Donor-acceptor Contacts. *Chem. Commun.* **2013,** *49*, 7558-7560; (b) Clark, T.; Hennemann, M.; Murray, J. S.; Politzer, P. Halogen bonding: the sigma-hole. Proceedings of "Modeling interactions in biomolecules II", Prague, September 5th-9th, 2005. *J. Mol. Model.* **2007,** *13*, 291-296.

8. Stone, A. J. Are halogen bonded structures electrostatically driven? *J. Am. Chem. Soc.* **2013,** *135*, 7005-7009.

9. (a) Awwadi, F. F.; Willett, R. D.; Peterson, K. A.; Twamley, B. The Nature of Halogen···Halogen Synthons: Crystallographic and Theoretical Studies. *Chem. Eur. J.* **2006,** *12*, 8952 - 8960; (b) Bent, H. A. Structural Chemistry of Donor-acceptor Interactions. *Chem. Rev.* **1968,** *68*, 587-648; (c) Politzer, P.; Murray, J. S.; Clark, T. Halogen bonding: an electrostatically-driven highly directional noncovalent interaction. *Phys. Chem. Chem. Phys.* **2010,** *12*, 7748-7757.

10. (a) Hathwar, V. R.; Row, T. N. G. Nature of Cl···Cl Intermolecular Interactions via Experimental and Theoretical Charge Density Analysis: Correlation of Polar Flattening Effects with Geometry. *J. Phys. Chem. A* **2010,** *114*, 13434-13441; (b)

Desiraju, G. R.; Parthasarathy, R. The Nature of Halogen-Halogen Interactions: Are Short Halogen Contacts Due to Specific Attractive Forces or Due to Close Packing of Nonspherical Atoms? *J. Am. Chem. Soc.* **1989,** *111*, 8725-8726; (c) Yang, M. K. Optical properties of Teflon® AF amorphous fluoropolymers. *J. Micro/Nanolith. MEMS MOEMS* **2008,** *7*, 033010-1-033010-9.

11. Dikundwar, A. G.; Row, T. N. G. Evidence for the "Amphoteric" Nature of Fluorine in Halogen Bonds: An Instance of Cl···F Contact. *Cryst. Growth Des.* **2012,** *12*, 1713-1716.

12. (a) Donald, K. J.; Wittmaack, B. K.; Crigger, C. Tuning σ-Holes Charge Redistribution in the Heavy (Group 14) Analogues of Simple and Mixed Halomethanes Can Impose Strong Propensities for Halogen Bonding. *J. Phys. Chem. A* **2010,** *114*, 7213–7222; (b) Politzer, P.; Lane, P.; Concha, M. C.; Ma, Y.; Murray, J. S. An Overview of Halogen Bonding. *J. Mol. Model.* **2007,** *13*, 305-311.

13. Ramasubbu, N.; Parthasarathy, R.; Murray-RustI, P. Angular Preferences of Intermolecular Forces around Halogen Centers: Preferred Directions of Approach of Electrophiles and Nucleophiles around the Carbon-Halogen Bondla. *J. Am. Chem. Soc.* **1985,** *108*, 4308-4314.

14. Metrangolo, P.; Resnati, G. Type II halogen...halogen contacts are halogen bonds. *IUCrJ* **2014,** *1*, 5-7.

15. (a) Huang, W. Y.; Huang, B. N.; Hu, C. M. Study on Deiodo-Sulfination. Part I. Studies on the Deiodo-Sulfination of Perfluoroalkyl Iodides. *J. Fluorine Chem.* **1983,** *23*, 193-204; (b) Huang, W. Y.; Huang, B. N.; Hu, C. M. Studies on Deiodo-

Sulfination Part. II. the Reactions of Perfluoroalkanesulfinates with Halogen and Halogen Acids and A New Method for the Synthesis of Perfluorosulfonic Acid. *J. Fluorine Chem.* **1983,** *23*, 229-240.

16. Qiu, W.; Burton, D. J. A Useful Synthesis of w-iodoperfluoroalkanesulfonyl Fluorides and Perfluoroalkane-a,w-bis-sulfonyl Fluorides. *J. Fluorine Chem.* **1993,** *60*, 93-100.

17. Boese, R.; Weiss, H. C.; Blaser, D. The Melting Point Alternation in the Short Chain n-Alkanes: Single-Crystal X-Ray Analyses of Propane at 30 K and of n-Butane to n-Nonane at 90 K. *Angew. Chem. Int. Ed.* **1999,** *38*, 988-992.

18. (a) Bunn, C. W.; Howells, E. R. Structures of Molecules and Crystals of Fluorocarbons. *Nature* **1954,** *174*, 549-551; (b) Bunn, C. W.; Cobbold, A. J.; Palmer, R. P. The Fine Structure of Polytetrafluoroethylene. *J. Polymer Sci.* **1958,** *28*, 365-376.

19. Dunitz, J. D.; Gavezzotti, A.; Schweizer, W. B. Molecular Shape and Intermolecular Liaison: Hydrocarbons and Fluorocarbons. *Helv. Chim. Acta* **2003,** *86*, 4073-4092.

20. Metrangolo, P.; Carcenac, Y.; Lahtinen, M.; Pilati, T.; Rissanen, K.; Vij, A.; Resnati, G. Nonporous Organic Solids Capable of Dynamically Resolving Mixtures of Diiodoperfluoroalkanes. *Science* **2009,** *323*, 1461-1464.